University of Warsaw
Faculty of Physics
Institute of theoretical physics

Doctoral Thesis

Refined Topological Vertex and Supersymmetric Gauge Theories

Shi Cheng

Advisor: Prof. Dr Hab. Piotr Sułkowski

October, 2021

Abstract

This thesis focuses on open topological string theory on Calabi-Yau threefolds without compact four-cycles. We first review relevant aspects of topological string theories and gauge theories. Then we use the refined topological vertex formalism to compute refined open topological string amplitudes. We find that the refined geometric transition, or in other words, Higgsing, is the key step in this computation. We find there are different types of refined open topological branes, and the corresponding refined Ooguri-Vafa formulas encode refined open BPS invariants. Moreover, we discuss a quiver structure of refined open topological string amplitudes on toric Calabi-Yau threefolds. In order to physically understand this quiver structure, we study the corresponding 3d $\mathcal{N} = 2$ gauge theories and find quivers encode actually effective mixed Chern-Simons levels of the mirror dual theories. Along the way, we discuss brane webs for 3d $\mathcal{N} = 2$ theories and find quiver structure also for nonabelian theories.

Acknowledgments

I would like to express my deepest gratitude for my supervisor, Piotr Sułkowski, for his support in the past three years, his patience and encouragement when I came across difficulties. He motivated and trained me to conduct research with passion and confidence. I am also grateful to my previous advisor, Sung-Soo Kim, for introducing me to gauge theory and teaching me physics and research skills, which influenced deeply my way of doing research.

I would like to thank my colleagues Dimitry Noshchennko and Hélder Larraguível for many delightful discussions. Moreover, I would like to thank particularly Zhengyan Lu for friendship tracing back to the time in UCAS, and thank Yinghua Deng and Xingyue Wei for the happy time in UESTC. Last but not the least, I would like to thank my parents and sisters for unconditional love and support, and Ranran Wang for her love, which is the source of my ideas.

The research conducted during my PhD studies and presented in this thesis was supported by the TEAM programme of the Foundation for Polish Science co-financed by the European Union under the European Regional Development Fund (POIR.04.04.00-00-5C55/17-00).

To my mother

Contents

Chapter 1

Overview

The story that we are going to discuss involves many aspects of topological strings and gauge theories, including geometric engineering, M-theory/type IIB string duality, brane webs and geometric transition.

Geometric engineering enables to construct gauge theories of various dimensions from string theory compactified on Calabi-Yau manifolds [1]. In a parallel way, brane systems can also be used to construct gauge theories. In this thesis, we are only interested in 5d $\mathcal{N} = 1$ gauge theories and 3d $\mathcal{N} = 2$ gauge theories that are constructed by M-theory compactified on Calabi-Yau threefolds. The brane constructions referred to as brane webs, are in type IIB string theory. Because of M/IIB duality, these brane webs are dual to Calabi-Yau threefolds in M-theory [2]. The BPS particles of gauge theories are hence realized as M2-branes ending on M5-branes. The summation of all contributions from these M2-branes gives rise to partition functions of gauge theories.

Topological string theory is powerful enough to compute partition functions of gauge theories [3, 4, 5]. In particular, closed topological strings are related to 5d $\mathcal{N} = 1$ gauge theories and open topological strings are related to 3d $\mathcal{N} = 2$ gauge theories [6]. Topological string partition functions are interpreted as gauge theory partition functions, because BPS particles are identified with M2-brane states through geometric engineering. Topological string methods for computing string amplitudes therefore can be used to obtain the partition functions of gauge theories without addressing the difficulty of computing the path integral in the quantum field theory description. In addition, the 3d $\mathcal{N} = 2$ theories we consider are obtained by Higgsing appropriate 5d $\mathcal{N} = 1$ brane webs [6]. Higgsing could introduce D3-branes, on which a 3d $\mathcal{N} = 2$ theory lives. Generically, we get 3d-5d coupled theories with the D3-brane as the surface defect. Higgsing can also be interpreted as the geometric transition in the A-model of topological string theories.

The geometric transition is the correspondence between open topological strings and closed topological strings, which is similar to AdS/CFT correspondence, and can be reinterpreted as the large N transition [7]. Initially, open topological strings are described by the Chern-Simons theory on a three sphere S^3 on which we wrap N couples of M5-branes. This $U(N)$ Chern-Simons theory is equivalent to the closed topological strings on a two sphere S^2 inside the resolved conifold on which there is no brane but with magnetic flux around S^2 which gives

rise to the Kähler deformation. By using this geometric transition, the closed topological string partition functions are related to amplitudes of the Chern-Simons theory that are more easy to compute [8].

The topological vertex method is formulated in [9] to compute the closed topological string amplitudes of toric Calab-Yau thereefolds that are represented as toric diagrams. Toric diagrams consist of several vertices connected by lines, and each vertex denotes a $\mathbb{C}^3$ patch. By putting branes and antibranes on these external lines, vertices are glued to large toric diagrams. Toric diagrams through M-theory/IIB duality are identical to (p,q)-brane webs that engineer 5d $\mathcal{N}=1$ gauge theories in type IIB string theory [2]. If we implement the geometric transition on a two sphere S^2 in a toric diagram by tuning its Kähler parameter (volume of the two sphere) to particular values, then a Lagrangian submanifold with topology S^3 emerges, which carries D3-branes in the dual type IIB string theory. In this case we obtain 3d $\mathcal{N}=2$ theories.

The purpose of the thesis is to study the refined open topological string theory and its corresponding 3d $\mathcal{N}=2$ theories. Since the computation of refined open topological strings is missing in literature, we develop the refined topological vertex by using geometric transition (Higgsing) to compute refined open string amplitudes. Along the way, we find the relations between different types of refined open topological branes, as well as corresponding refined Ooguri-Vafa formulas. We compute the amplitudes for some strip Calabi-Yau threefolds and find they have quiver structure at refined level. In order to understand the quivers for strip Calabi-Yau threefolds we implement mirror transformations on sphere partition functions of the corresponding 3d $\mathcal{N}=2$ theories. By reading off information from effective superpotentials, we find that quivers encode effective mixed Chern-Simons levels. In this process, we consider a particular type of theories denoted by $\mathcal{T}_{A,N}$. Since toric diagrams are identical to brane webs, in the end we discuss the 3d brane webs, using vortex partition functions and quivers. We find many equivalent 3d brane webs, corresponding to different real mass deformations.

Publications

This thesis is based on the author's papers:

- S. Cheng, *3d $\mathcal{N}=2$ Brane Webs and Quivers*, arXiv:2108.03696 (submitted to Journal of High Energy Physics).
- S. Cheng and P. Sułkowski, *Refined open topological strings revisited*, arXiv:2104.00713 (submitted to PRD).
- S. Cheng, *Mirror Symmetry and Mixed Chern-Simons Levels for Abelian 3d $\mathcal{N}=2$ theories*, *Phys.Rev.D* **104**, 046011 (2021), arXiv:2010.15074.

In addition, I have another two papers involving 2d mirror symmetry, 5d gauge theories and closed topological strings:

- S. Cheng and S.-S. Kim, *Refined topological vertex for a 5d sp(n) gaugetheories with antisymmetric matter*, *Phys.Rev.D* **104**, 086004 (2021), arXiv:1809.00629.

- S. Cheng, F. J. Xu and F. Z. Yang, *Off-shell D-brane/F-theory effective superpotentials and Ooguri-Vafa invariants of several compact Calabi-Yau manifolds*, *Mod. Phys. Lett. A* **29**, no. 12, 1450061 (2014), arXiv:1303.3318.

Outline of the thesis

This thesis consists of six chapters.

In chapter 2, we give a short review of topological string theory. We discuss 2d sigma models, toric geometry, and geometric transition that relates open topological strings and closed topological strings. After that, we focus on the topological vertex method and Ooguri-Vafa formula. In this chapter the discussion on refined Ooguri-Vafa formulas and refined topological vertex for open topological strings is based on [10].

In chapter 3, we give a short introduction to 3d $\mathcal{N} = 2$ gauge theories and discuss the structure of partition functions as well as effective superpotentials [11]. We also briefly review 3d mirror symmetry and localization results. The second part of this chapter is devoted to brane constructions of gauge theories. In this chapter, we refer to some results from [11], including vortex partition functions and quivers for 3d abelian theories.

In chapter 4, we mainly discuss the computation of refined open topological string partition functions in the presence of a Lagrangian brane on strip Calabi-Yau threefolds. We also discuss the relations between different types of topological branes and their refined Ooguri-Vafa formulas. Some non-toric diagrams resulting from Hanany-Witten transitions are also discussed. This chapter is based on the paper [10].

In chapter 5, we use the 3d mirror symmetry to analyze 3d $\mathcal{N} = 2$ gauge theories engineered by strip Calabi-Yau manifolds. The quivers encoded in open topological string partition functions are shown to be the effective mixed Chern-Simons levels of the mirror dual 3d abelian gauge theories. This chapter is based on the paper [11].

In chapter 6, we discuss the correspondence between 3d brane webs and quivers. It turns out that there are many equivalent 3d brane webs related by 3d mirror symmetry. These 3d brane webs come from real mass deformations of the massless theories. We show that nonabelian theories also have quiver structure. This chapter is based on the paper [12].

In the appendix A, we summarize some useful identities.

Chapter 2

Topological string theory

Topological string theories are basically two dimensional supersymmetric sigma models coupled to 2d gravity. There are two types of topological strings called A-model and B-model, depending on different topological twists [13].

Because of geometric engineering, topological string partition functions are interpreted as gauge theory partition functions which capture contributions from BPS particles. The degeneracy numbers of these particles are closed (Gopakumar-Vafa) and open (Ooguri-Vafa) BPS invariants [3, 14]. In some cases, closed topological strings and open topological strings are related by geometric transitions [7]. The topological string partition functions on toric Calabi-Yau threefolds can be computed in the formalism of the topological vertex [9]. Because of the duality between M-theory and type IIB string theory, the toric diagrams of Calabi-Yau manifolds that engineer gauge theories through M-theory are identical with the brane webs in type IIB string theory [2]. Therefore, the topological vertex method can be used to analyze gauge theories.

In this chapter, we review topological string theories and also mention the connections to gauge theories. Firstly, we review the 2d $\mathcal{N} = (2,2)$ sigma model, which is the worldsheet description of topological strings [15], which leads to A-model and B-model after topological twist. The target spaces of topological strings are Calabi-Yau manifolds. In order to describe target spaces, we review toric geometry that is used to construct Calabi-Yau manifolds. In the second part of this chapter, we review the geometric transition between open topological strings and closed topological strings, which finally leads to the topological vertex method [9]. There are some nice introductions to topological string theories; we refer to [16, 17].

2.1 2d $\mathcal{N} = (2,2)$ sigma model

In this section, we give an introduction to the two dimensional sigma model with supersymmetry $\mathcal{N} = (2,2)$. After the topological twist, there are two types of theories, namely A-model and B-model. The relation between these two models is 2d mirror symmetry; see [13, 15, 18, 19] for more details.

2.1.1 2d $\mathcal{N} = (2,2)$ nonlinear sigma model

The definition of the 2d sigma model is similar to string theory, which is described by the map from a world-sheet Σ_g to a target space X

$$\phi : \Sigma_g \to X \,. \tag{2.1}$$

The 2d worldsheet has coordinate $z \in \mathbb{C}$ and its conjugate $\bar{z}$. We denote ∂_z by ∂_+ and $\partial_{\bar{z}}$ by ∂_-. The Lorentz symmetry is $U(1)$ that acts on the coordinates as $z \to e^{i\alpha} z$ and acts on fermonic coordinates as $\theta^\pm \to e^{\pm i\alpha}\theta^\pm$, $\bar{\theta}^\pm \to e^{\pm i\alpha}\bar{\theta}^\pm$. In the 2d nonlinear sigma model, we have the chiral superfield

$$\Phi = \phi(z,\bar{z}) + \psi_+(z,\bar{z})\theta^+ + \psi_-(z,\bar{z})\theta^- + F(z,\bar{z})\theta^+\theta^- \,, \tag{2.2}$$

satisfying $\overline{D}_\pm \Phi = 0$.

To begin with, we show generators and commutators of the supersymmetry algebra. There are Hamiltonian and momentum operator

$$H = -i(\partial_+ - \partial_-) \,, \quad P = -i(\partial_+ + \partial_-) \,, \tag{2.3}$$

Lorentz rotation operator

$$M = 2z\partial_+ - 2\bar{z}\partial_- + \theta^+ \frac{d}{d\theta^+} - \theta^- \frac{d}{d\theta^-} + \bar{\theta}^+ \frac{d}{d\bar{\theta}^+} - \bar{\theta}^- \frac{d}{d\bar{\theta}^-} \,, \tag{2.4}$$

and

$$Q_\pm = \frac{\partial}{\partial\theta^\pm} + i\bar{\theta}^\pm \partial_\pm \,, \quad \overline{Q}_\pm = -\frac{\partial}{\partial\theta^\pm} - i\bar{\theta}^\pm \partial_\pm \,, \tag{2.5}$$

$$D_\pm = \frac{\partial}{\partial\theta^\pm} - i\bar{\theta}^\pm \partial_\pm \,, \quad \overline{D}_\pm = -\frac{\partial}{\partial\theta^\pm} + i\bar{\theta}^\pm \partial_\pm \,, \tag{2.6}$$

where $Q_\pm$ and $\overline{Q}_\pm$ are supersymmetry generators, transforming as spin $\frac{1}{2}$ fermions under the Lorentz group. The commutators between them are

$$\{Q_\pm, \overline{Q}_\pm\} = -2i\partial_\pm = P \pm H \,, \tag{2.7}$$

$$\{Q_\pm, \overline{D}_\pm\} = \quad 2i\partial_\pm = -P \mp H \tag{2.8}$$

$$[M, Q_\pm] = \mp Q_\pm \,, \quad [M, \overline{Q}_\pm] = \mp \overline{Q}_\pm \,, \tag{2.9}$$

$$[M, D_\pm] = \mp D_\pm \,, \quad [M, \overline{D}_\pm] = \mp \overline{D}_\pm \,, \tag{2.10}$$

$$[M, H] = -2P \,, \quad [M, P] = -2H \,. \tag{2.11}$$

In addition, there are R-symmetries acting on variables, which can be recombined into the

vector symmetry $U(1)_V$ and axial symmetry $U(1)_A$

$$U(1)_V: \quad (\theta^+, \overline{\theta}^+) \to (e^{-i\alpha}\theta^+, e^{i\alpha}\overline{\theta}^+)\,, \qquad (\theta^-, \overline{\theta}^-) \to (e^{-i\alpha}\theta^-, e^{i\alpha}\overline{\theta}^-)\,, \tag{2.12}$$

$$U(1)_A: \quad (\theta^+, \overline{\theta}^+) \to (e^{-i\alpha}\theta^+, e^{i\alpha}\overline{\theta}^+)\,, \qquad (\theta^-, \overline{\theta}^-) \to (e^{-i\alpha}\theta^-, e^{i\alpha}\overline{\theta}^-)\,, \tag{2.13}$$

with generators

$$F_V = -\theta^+\frac{d}{d\theta^+} - \theta^-\frac{d}{d\theta^-} + \bar{\theta}^+\frac{d}{d\bar{\theta}^+} + \bar{\theta}^-\frac{d}{d\bar{\theta}^-}\,, \tag{2.14}$$

$$F_A = -\theta^+\frac{d}{d\theta^+} + \theta^-\frac{d}{d\theta^-} + \bar{\theta}^+\frac{d}{d\bar{\theta}^+} - \bar{\theta}^-\frac{d}{d\bar{\theta}^-}\,. \tag{2.15}$$

The associated commutators are

$$[F_V\,, Q_\pm] = Q_\pm\,, \quad [F_V\,, \overline{Q}_\pm] = -\overline{Q}_\pm\,, \quad [F_A\,, Q_\pm] = \pm Q_\pm\,, \quad [F_A\,, \overline{Q}_\pm] = \mp\overline{Q}_\pm\,. \tag{2.16}$$

In addition, the chiral superfield carries charges (q_V, q_A) under R-symmetries.

In the following, we show the Lagrangian description of 2d nonlinear sigma model. The Lagrangian is given by a Kähler potential

$$S_D = \int d^2z d^4\theta\, K(\Phi_i, \overline{\Phi}_i)\,, \tag{2.17}$$

where is also called D-term, and the measure is $d^2zd^4\theta = dzd\bar{z}d\theta^+d\theta^-d\bar{\theta}^+d\bar{\theta}^-$. One could also include the F-term

$$S_F = \int d^2z d^2\theta\, W(\Phi_i)|_{\bar{\theta}^\pm=0}\,. \tag{2.18}$$

In this thesis, we do not consider this F-term. The bosonic part of the action is

$$S_\phi = -\int d^2z g_{i\bar{j}}\eta^{\alpha\beta}\partial_\alpha\phi^i\partial_\beta\overline{\phi}^{\bar{j}}\,, \tag{2.19}$$

where ϕ is the scalar in Φ, and the spacetime metric $g_{i\bar{j}}$ is given by

$$g_{i\bar{j}} = \frac{d^2K}{d\phi^i d\overline{\phi}^{\bar{j}}}\,. \tag{2.20}$$

Therefore, the target space is a Kähler manifold. The worldsheet metric $\eta^{\alpha\beta}$ can be fixed by conformal transformation

$$\eta^{+-} = \eta^{-+} = 2\,, \quad \eta^{++} = \eta^{--} = 0\,. \tag{2.21}$$

If we add the fermonic part, then the D-term Lagrangian reads

$$\mathcal{L} = g_{i\bar{j}}(\partial_z\phi^i\partial_{\bar{z}}\phi^{\bar{j}} + \partial\bar{z}\phi^i\partial z\phi^{\bar{j}}) + iB_{i\bar{j}}(\partial_z\phi^i\partial_{\bar{z}}\phi^{\bar{j}} - \partial\bar{z}\phi^i\partial z\phi^{\bar{j}}) \tag{2.22}$$

$$+ig_{i\bar{j}}\overline{\psi}^{\bar{j}}_- D_+\psi^i_+ + ig_{i\bar{j}}\overline{\psi}^{\bar{j}}_- D_-\psi^i_+ - R_{i\bar{j}k\bar{l}}\psi^i_+\psi^k_-\overline{\psi}^{\bar{j}}_+\overline{\psi}^{\bar{l}}_-\,, \tag{2.23}$$

where

$$R_{i\bar{j}k\bar{l}} = g^{m\bar{n}} g_{m\bar{j},\bar{l}} g_{\bar{n}i,k} - g_{i\bar{j},k\bar{l}}\,, \tag{2.24}$$

$$D_\pm \psi^i = \partial_\pm \psi^i + \Gamma^i_{jk} \partial_\pm \phi^j \psi^k\,, \tag{2.25}$$

$$\Gamma^i_{jk} = g^{i\bar{l}} g_{\bar{l}j,k}\,, \tag{2.26}$$

and the field $B_{i\bar{j}}$ is an anti-symmetric $(1,1)$-form that can be added without breaking supersymmetry. Fermionic fields are sections of bundles on the worldsheet

$$\psi^i_+ \in \Gamma(K^{1/2} \otimes \phi^* T^{1,0} X)\,, \qquad \psi^{\bar{i}}_+ \in \Gamma(K^{1/2} \otimes \phi^* T^{0,1} X)\,, \tag{2.27}$$

$$\psi^i_- \in \Gamma(\overline{K}^{1/2} \otimes \psi^* T^{1,0} X)\,, \qquad \psi^{\bar{i}}_- \in \Gamma(\overline{K}^{1/2} \otimes \phi^* T^{0,1} X)\,, \tag{2.28}$$

where K is the canonical bundle on the target space X and we split the tangent bundle into holomorphic and antiholomorphic parts $TX = T^{1,0}X \oplus T^{0,1}X$. The fermions ψ^i_+ and ψ^i_- are the left and the right moving modes respectively. The supersymmetry variation is

$$\delta = \epsilon_+ Q_+ + \epsilon_- Q_- + \tilde{\epsilon}_+ \overline{Q}_+ + \tilde{\epsilon}_- \overline{Q}_-\,, \tag{2.29}$$

which transforms various fields as follows

$$\delta\phi^i = i\epsilon_- \psi^i_+ + i\epsilon_+ \psi^i_-\,, \tag{2.30}$$

$$\delta\phi^{\bar{i}} = i\tilde{\epsilon}_- \psi^i_+ + i\tilde{\epsilon}_+ \psi^i_-\,, \tag{2.31}$$

$$\delta\psi^i_+ = -\tilde{\epsilon}_- \partial_z \phi^i - i\epsilon_+ \psi^j_- \Gamma^i_{jk} \psi^k_+\,, \tag{2.32}$$

$$\delta\psi^{\bar{i}}_+ = -\epsilon_- \partial_z \phi^{\bar{i}} - i\tilde{\epsilon}_+ \psi^{\bar{j}}_- \Gamma^{\bar{i}}_{\bar{j}\bar{k}} \psi^{\bar{k}}_+\,, \tag{2.33}$$

$$\delta\psi^i_- = -\tilde{\epsilon}_+ \partial_{\bar{z}} \phi^i - i\epsilon_- \psi^j_+ \Gamma^i_{jk} \psi^k_-\,, \tag{2.34}$$

$$\delta\psi^{\bar{i}}_- = -\epsilon_+ \partial_{\bar{z}} \phi^{\bar{i}} - i\tilde{\epsilon}_- \psi^{\bar{j}}_+ \Gamma^{\bar{i}}_{\bar{j}\bar{k}} \psi^{\bar{k}}_-\,, \tag{2.35}$$

where fermonic parameters $\epsilon_-, \tilde{\epsilon}_-$ are sections of $K^{-1/2}$, and $\epsilon_+, \tilde{\epsilon}_+$ are sections of $\overline{K}^{-1/2}$.

2.1.2 A-model and B-model

The supersymmetry cannot be preserved on the worldsheet with genus $g \neq 1$. In order to have convariant spinors on the whole worldsheet of genus g, we need to change the transformations of fields such that the supersymmetry transformation becomes a scalar on the worldsheet. One way is to use the topological twist, which redefines a new Lorentz generator by combining it with R-symmetry generators

$$M_A = M - F_V\,, \quad M_B = M - F_A \tag{2.36}$$

Then we have commutators

$$[M_A\,, Q_+ + \overline{Q}_-] = 0\,, \quad [M_A\,, Q_-] = 0\,, \qquad [M_A\,, \overline{Q}_+] = 0\,, \tag{2.37}$$

$$[M_B\,, Q_+ + Q_-] = 0\,, \quad [M_B\,, \overline{Q} + -] = 0\,, \quad [M_B\,, \overline{Q}_-] = 0\,. \tag{2.38}$$

After the topological twist, the operator $Q_A := \overline{Q}_+ + Q_-$ becomes a scalar for M_A, and $Q_B := \overline{Q}_+ + \overline{Q}_-$ becomes a scalar for M_B. These twisted operators can exist on Riemann surfaces with any genus. We have two kinds of twists, for which the associated R-symmetries are different:

$$\text{A-twist: } U(1)_V\,, \qquad \text{B-twist: } U(1)_A\,. \tag{2.39}$$

If the R-symmetry is $U(1)_V$, then the target space is a Kähler manifold, while if the R-symmetry is $U(1)_A$, the target space is not only a Kähler manifold but is also a Calabi-Yau manifold such that $U(1)_A$ is anomalous [13]. Therefore, there are two types of theories called A-model and B-model accordingly.

A-model

In the A-twist, the bundles for fields are changed, and we have

$$\chi^i = \psi^i_+ \in \Gamma(\phi^* T^{1,0} X) \tag{2.40}$$

$$\chi^{\bar{i}} = \psi^{\bar{i}}_- \in \Gamma(\phi^* T^{0,1} X) \tag{2.41}$$

$$\psi^{\bar{i}}_z = \psi^{\bar{i}}_+ \in \Gamma(K \otimes \phi^* T^{0,1} X) \tag{2.42}$$

$$\psi^i_{\bar{z}} = \psi^i_- \in \Gamma(\overline{K} \otimes \phi^* T^{0,1} X)\,. \tag{2.43}$$

Note that χ^i and $\chi^{\bar{i}}$ become scalars on the worldsheet once we set $\epsilon_- = \tilde{\epsilon}_+ = \epsilon$ and $\tilde{\epsilon}_- = \epsilon_+ = 0$, then the supersymmetry variation is

$$\delta = \epsilon Q_A = \epsilon(Q_- + \overline{Q}_+)\,, \quad \delta^2 = 0\,. \tag{2.44}$$

The variations of scalars ϕ^i reduce to

$$\delta\phi^i = i\epsilon\chi^i\,, \quad \delta\phi^{\bar{i}} = i\epsilon\chi^{\bar{i}}, \tag{2.45}$$

and the variations of other fields are zero. In the A-model, there is an interesting correspondence between supersymmetry operator and differential operator

$$Q_A \leftrightarrow d = \partial + \overline{\partial}\,, \quad \chi^i \leftrightarrow dx^i\,, \quad \chi^{\bar{i}} \leftrightarrow d\overline{x}^{\bar{i}}\,, \tag{2.46}$$

where x^i and $\overline{x}^{\bar{i}}$ are local coordinates on X and d is de Rham differential. The action in this twist degenerates to

$$S = i \int_\Sigma \{Q_A, V\} - 2\pi\phi^*(B + iJ)\,, \tag{2.47}$$

where $V = 2\pi g_{i\bar{j}}(\psi_z^{\bar{j}}\overline{\partial}\phi^i + \partial\phi^{\bar{j}}\psi_{\bar{z}}^i)$, and $B + iJ \in H^2(X, \mathbb{C})$ is the complexified Kähler form. Note that the A-model does not depend on the complex structure.

The infinite dimensional space of all maps $\phi : \Sigma \to X$ localizes at saddle points of $V = 0$, which are finite dimensional if we perform path integral:

$$Z = \int \mathcal{D}\phi\mathcal{D}\psi\mathcal{D}\chi\ e^{-S} = \sum_{\beta\in H_2(X,\mathbb{Z})} e^{-2\pi i t_\beta} \int_{\text{fixed }\beta} d\phi d\psi d\chi\ e^{-i\int\{Q_A,V\}}\,. \tag{2.48}$$

At saddle points $V = 0$, we have $\overline{\partial}\phi^i = 0$ and fields ϕ^i become holomorphic. These holomorphic maps are worldsheet instantons. If we consider a genus $g \neq 0$ Riemann surface, then the A-model becomes trivial because of ghost number conservation constraints [13]. In this case, to obtain nontrivial theory the worldsheet gravity needs to be included, namely including all metrics on Σ_g in the path integral. This is the topological string theory we discuss. Note that the target space of A-model is a Kähler manifold. If we couple A-model with 2d gravity, then the target space should be a Calabi-Yau manifold. Before discussing that, let us first review the B-model.

B-model

The B-model has a different setting in comparison with the A-model. We have fields

$$\psi_\pm^{\bar{j}} \in \Gamma(\phi^* T^{0,1}X)\,, \tag{2.49}$$
$$\psi_+^j \in \Gamma(K \otimes \phi^* T^{1,0}X)\,, \tag{2.50}$$
$$\psi_-^j \in \Gamma(\overline{K} \otimes \phi^* T^{1,0}X)\,, \tag{2.51}$$

and define scalars

$$\eta^{\bar{j}} = \psi_+^{\bar{j}} + \psi_-^{\bar{j}}\,, \quad \theta_j = g_{i\bar{k}}(\psi_+^{\bar{k}} - \psi_-^{\bar{k}})\,. \tag{2.52}$$

If we set $\epsilon_\pm = 0$ and $\tilde{\epsilon}_\pm = \epsilon$, then the supersymmetry variation is

$$\delta = \epsilon Q_B = \epsilon(\overline{Q}_- + \overline{Q}_+)\,, \delta^2 = 0\,. \tag{2.53}$$

There is a correspondence

$$\eta^{\bar{i}} \leftrightarrow d\bar{x}^{\bar{i}}\,, \quad \theta_i \leftrightarrow \frac{\partial}{\partial x^i}\,, \quad Q_B \leftrightarrow \overline{\partial}\,. \tag{2.54}$$

The action for the B-model is

$$S = i \int \{Q, V\} + U \,, \tag{2.55}$$

where

$$V = g_{i\bar{k}} \left(\rho_z^j \overline{\partial} \phi^{\bar{k}} + \rho_{\bar{z}}^j \partial \phi^{\bar{k}} \right) \,, \tag{2.56}$$

$$U = \left(-\theta_j D \rho^j - \frac{i}{2} R_{j\bar{j}k\bar{k}} \right) \rho^j \wedge \rho^k \eta^{\bar{j}} \theta_l g^{l\bar{k}} \,. \tag{2.57}$$

Here U only depends on the complex structure of the target space Y.

At the saddle point $V = 0$, we have $\partial \phi^{\bar{k}} = 0$ and $\overline{\partial} \phi^{\bar{k}} = 0$, so fields ϕ^k map to points in the Calabi-Yau manifold Y. Hence correlation functions are classical integrals. There is no worldsheet instanton correction in the B-model. The target space of B-model should be a Calabi-Yau manifold to be free of $U(1)_A$ anomaly. There is a unique holomorphic $(3,0)$-form Ω on the target space Y. The complex structure deformations in B-model are elements in $H^{2,1}(Y)$.

2.1.3 2d $\mathcal{N} = (2,2)$ linear sigma model

A more general theory is the linear sigma model discussed in [15], which probes the global moduli space, while the nonlinear sigma model can only probe the large parameter regime. In this subsection, we review the 2d linear sigma model and discuss in particular its moduli space.

We can add the vector multiplet

$$\begin{aligned} V =& (A_0 - A_1)\theta^- \overline{\theta}^- + (A_0 + A_1)\theta^+ \overline{\theta}^+ - \sigma \theta^- \overline{\theta}^+ - \sigma \theta^+ \overline{\theta}^- + i\theta^- \theta^+ (\overline{\theta}^- \overline{\lambda}_- + \overline{\theta}^+ \overline{\lambda}_+) \\ &+ i\overline{\theta}^- \overline{\theta}^+ (\theta^- \lambda_- + \theta^+ \lambda_+) + \theta^- \theta^+ \overline{\theta}^+ \overline{\theta}^- D \end{aligned} \tag{2.58}$$

and write down the Lagrangian

$$\begin{aligned} \mathcal{L} &= \mathcal{L}_{kin} + \mathcal{L}_{gauge} + \mathcal{L}_W + \mathcal{L}_{FI} = \\ &= \int d^4\theta \Phi^\dagger e^{q \cdot V} \Phi - \int d^4\theta \frac{1}{2g^2} \Sigma^\dagger \Sigma + \int d^2\theta \mathcal{W}(\Phi) + \frac{1}{2} \left(-t \int d^2\vartheta \; \Sigma + c.c. \right) \,, \end{aligned} \tag{2.59}$$

where the field strength is $\Sigma = \overline{D}_+ D_- V$ and the Fayet-Iliopoulos parameter is $t = r - i\vartheta$.

We consider the theory with a gauge group $U(1)$ as an example. Its Lagrangian can be expanded as

$$\mathcal{L} = -\frac{1}{2g^2} (|\partial_\mu \sigma|^2 + F_{01}^2) - |D_\mu \phi|^2 - U(\sigma, \phi) + \vartheta F_{0,1} + \text{fermions} \,, \tag{2.60}$$

where the scalar potential is

$$U(\sigma,\phi)=\frac{1}{2g^2}D^2+\sum_i|F_i|^2+|q_i\sigma|^2|\phi_i|^2\,. \tag{2.61}$$

The D-term and F-term are

$$D=-g^2\left(\sum_i q_i|\phi_i|^2-r\right)\,,\quad F_i=\frac{\partial\mathcal{W}}{\partial\phi_i}\,. \tag{2.62}$$

The vacua moduli space is defined by $U(\sigma,\phi)=0$ [15]. We assume $r>0$ and $\sigma=0$; then the Coulomb branch moduli space $\mathcal{M}_C$ can be obtained by the D-term after modding out the $U(1)$ gauge group:

$$\mathcal{M}_C=\Big\{\sum_{i=1}^{N}q_i|\phi_i|^2=r\Big\}/U(1)\,. \tag{2.63}$$

This is a toric Cabi-Yau manifold by definition. This moduli space is identified with the target space of topological string theory. Note that the R-symmetry $U(1)_A$ is anomaly free only if $\sum_i q_i=0$; otherwise the measure in the path integral is not invariant. This condition is the Calabi-Yau condition [15].

We can also consider the effective theory of the linear sigma model by integrating out matter fields

$$e^{iS_{\text{eff}}(\Sigma)}=\int\mathcal{D}\Phi e^{iS(\Sigma,\Phi)}\,. \tag{2.64}$$

The effective Lagrangian is

$$\mathcal{L}_{\text{eff}}=\int d^4\theta K_{\text{eff}}(\Sigma,\overline{\Sigma})+\frac{1}{2}\left(\int d^2\vartheta^2\widetilde{\mathcal{W}}_{\text{eff}}(\Sigma)+c.c\right)\,, \tag{2.65}$$

and the scalar potential is

$$U_{\text{eff}}(\sigma)=-\left(\frac{\partial K_{\text{eff}}}{\partial\sigma\partial\sigma^\dagger}\right)^{-1}\left|\frac{\widetilde{\mathcal{W}}_{\text{eff}}}{\partial\sigma}\right|^2\,, \tag{2.66}$$

which gives rise to the vacuum equation

$$\exp\left(\frac{\widetilde{\mathcal{W}}_{\text{eff}}}{\partial\sigma}\right)=1\,. \tag{2.67}$$

This equation is also called Bethe equation in the Bethe/gauge correspondence [20]

2.1.4 2d mirror symmetry

A-model and B-model are related by the famous mirror symmetry [13, 21]. In this subsection, we give a short review on this duality. Note that the mirror symmetry corresponds to the

T-duality between type IIA and type IIB string theories.

The Calabi-Yau manifold X has complex structure parameters and Kähler deformation parameters as follows:

$$\text{complex structure moduli: } h^{2,1} = \dim H^{2,1}(X)\,, \qquad \text{Kähler moduli: } h^{1,1} = \dim H^{1,1}(X)\,. \tag{2.68}$$

Two mirror dual manifolds (X, Y) are target spaces of A-model and B-model respectively, satisfying

$$h^{1,1}(X) = H^{2,1}(Y)\,, \quad h^{2,1}(X) = H^{1,1}(Y)\,. \tag{2.69}$$

In the A-model moduli parameters are Kähler parameters in the Calabi-Yau manifold X

$$t_I = \int_{\beta_I} B + iJ\,, \quad I = 1, \ldots, h^{1,1}(X)\,, \tag{2.70}$$

where $\beta_I \in H_2(X)$ and J is the Kähler form. In the B-model, moduli parameters are complex structure parameters of the Calabi-Yau manifold Y:

$$z_I = \int_{\alpha_I} \Omega\,, \quad I = 1, \ldots, h^{2,1}(Y)\,, \tag{2.71}$$

where $\alpha_I \in H_3(Y)$. In order to connect A-model and B-model, we need to construct the mirror maps between these parameters, which is defined as

$$t_I = \frac{\int_{\alpha_I} \Omega}{\int_{\alpha_0} \Omega} = \frac{1}{2\pi i} \left(\log z_I + \cdots\right)\,, \quad I = 1, \ldots, h^{2,1}(Y)\,,\ \alpha_I \in H_3(Y)\,, \tag{2.72}$$

where Ω is the unique $(3,0)$-form on Y. In the symplectic basis $(\alpha_{I_1}, \beta^{I_2})$, the unique three-form can be written as

$$\Omega = X^{I_1} \alpha_{I_1} + F_{I_2} \beta^{I_2}\,. \tag{2.73}$$

The mirror symmetry can also be extended to open topological strings, which needs the presence of D-branes [22]. Then one obtains the open-closed mirror symmetry; see [23, 18, 24]. D-branes are boundaries of open strings from the worldsheet perspective. In the A-model, open strings should end on a Lagrangian submanifold L in the Calabi-Yau manifold X. The Lagrangian is defined as the submanifold that the dimension of L is a half of X and the Kähler form ω vanishes when it is restricted to L. Such L is a real section of X, and open topological strings ending on such a manifold L preserve a half of the supersymmetry. On the other hand, the B-model admits Dp-branes of even dimensions, and supermymmetric branes should wrap holomorphic submanifolds. In particular, for the mirror Calabi-Yau pair (X, Y) with a Lagrangian $L \subset X$ and a holomorphic curve $\mathcal{C} \subset Y$, D6-branes wrapping $R^4 \times L$ are

mirror dual to D5-branes wrapping $R^4 \times \mathcal{C}$. Hence the open-closed mirror pair is

$$(X, L) \overset{\text{mirror}}{\longleftrightarrow} (Y, \mathcal{C}) \,. \tag{2.74}$$

2.1.5 Topological string theory

Topological string theory is defined as a 2d $\mathcal{N} = (2, 2)$ nonlinear sigma model with maps from worldsheets to a target space $\phi : \Sigma \to X$ and then couples to 2d gravity. In order for the 2d theory to be superconformal, the target space needs to be a Kähler manifold that satisfies the Calabi-Yau condition $c_1(TX) = 0$. After topological twist, this theory becomes anomaly free and topological. The partition function sums over all maps $\phi : \Sigma \to X$

$$\int \mathcal{D}\phi \mathcal{D}g e^{-\int_\Sigma \mathcal{L}(\phi)} \,, \tag{2.75}$$

where g is the metric on Σ. This path integral is an integral over the complex structure parameters on Σ. Moreover, we need to define the free energy for the Riemann surface of any genus. The free energy is the integral over the moduli space $\mathcal{M}_g$ of the Riemann surface with genus g. For genus $g = 0$, the moduli space is a point, and for $g = 1$, the moduli space is the fundamental domain for torus. For higher genus $g > 1$, free energy is

$$\mathcal{F}_g = \int_{\overline{\mathcal{M}}_g} [dm d\overline{m}] \Big\langle \prod_{a=1}^{3g-3} \left(\int_\Sigma \mu_a G^- \right) \left(\int_\Sigma \mu_{\bar{a}} \overline{G}^- \right) \Big\rangle_{\Sigma_g} \,. \tag{2.76}$$

For more details on this worldsheet description of topological string, see [25, 19].

In string theory, worldsheets of any genus need to be summed up to get a complete string partition functions. Similarly, in topological string theories, we should to sum up all genus contributions and get the free energy

$$\mathcal{F} = \sum_{g=0}^{\infty} \mathcal{F}_g g_s^{2g-2} \,, \tag{2.77}$$

where g_s is the string coupling and the free energy is defined through the topological string partition function

$$\mathcal{F} = \log Z \,. \tag{2.78}$$

2.2 Toric Calabi-Yau threefolds

In this section we give a brief introduction to toric Calabi-Yau manifolds. Toric geometry is important in our context as it represents Calabi-Yau threefolds in terms of toric diagrams, which through the duality between M-theory and IIB string theory, are identical to 5-brane webs in type IIB string theory, and D3-branes on 5-brane webs correspond to Lagrangian submanifolds [2, 24]. In this section, we first give the definition of Calabi-Yau manifolds and then discuss toric diagrams. For a nice introduction to toric geometry, see [26].

Calabi-Yau manifolds. The target space of topological string theory should be Calabi-Yau manifold X, satisfying the following properties:

- X is a complex manifold with a metric g satisfying $g_{ij} = g_{\bar{i}\bar{j}} = 0$.
- X is a Kähler manifold. Namely, there is a real function $K(z, \bar{z})$ such that $g_{i\bar{j}} = \partial_i \partial_{\bar{j}} K$, and the Kähler form is $\omega = g_{i\bar{j}} dz_i \wedge d\bar{z}_j$ satisfying $d\omega = 0$.
- X has a holomorphic n-form $\Omega = f(z_1, \ldots, z_n) dz_1 \wedge \cdots \wedge dz_n$. This is equivalent to the Calabi-Yau condition $c_1(TX) = 0$, where TX is the tangent bundle of X.

Typical examples of one dimensional Calabi-Yau manifolds are complex plane $\mathbb{C}$ and torus T^2. Two dimensional Calabi-Yau manifolds are $K3$ surfaces which are defined as hypersurfaces in $\mathbb{P}^3$. Note that the complex projective space $\mathbb{P}^n$ is not a Calabi-Yau manifold. In this thesis, we focus on non-compact Calabi-Yau three dimensional complex manifolds (also called Calabi-Yau threefolds), which are considered as fiber bundles, for instance

$$\mathcal{O}(-3) \to \mathbb{P}^2 \,, \ \mathcal{O}(-2,-2) \to \mathbb{P}^1 \times \mathbb{P}^1 \,, \ \mathcal{O}(-1) \oplus \mathcal{O}(-1) \to \mathbb{P}^1 \,.$$

2.2.1 Toric diagrams

Toric geometry has been used in many aspects of string theory for constructing Calabi-Yau manifolds and brane webs. In the following, we give a short introduction to toric diagrams.

Toric geometry represents Calabi-Yau manifolds in terms of toric diagrams. Toric geometry can be understood by considering $\mathbb{C}^3$ as building blocks. The n-complex dimensional manifold $\mathbb{C}^n$ has complex coordinates $(z_1, \ldots, z_n)$. We write $z_i = |z_i| e^{i\theta_i}$ and then use angular coordinates $(|z_1|^2, \ldots, |z_n|^2, \theta_1, \ldots, \theta_n)$. Then the Kähler form can be written as $\omega = \sum_i dz_i \wedge d\bar{z}_i = \sum_i d|z_i|^2 \wedge d\theta_i$. Angular coordinates $(\theta_1, \ldots, \theta_n)$ parameterize n-dimensional torus $T^n = S^1 \times \cdots \times S^1$, and $|z_i|$ is the radius for i-th circle S^1. The space $\mathbb{C}^n$ can be factorized as $\mathbb{C}^n = \mathcal{O}^{n+} \times T^n$ where $\mathcal{O}^{n+}$ denotes the special locus defined as $\{|z_i|^2 \geqslant 0\}$, which looks like a frame, as shown in Figure 2.1. The frame in Figure 2.1 is known as the toric diagram.

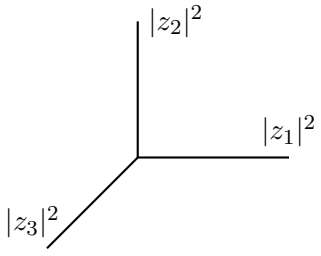

Figure 2.1: The frame of special locus for $\mathbb{C}^3$, which is known as the toric diagram if we project the frame to a plane.

Since $z_i = |z_i| e^{i\theta_i}$, when $|z_i| = 0$, the circle S^1 parameterized by θ_i shrinks. Therefore, on closed surfaces (divisors) of the toric diagram, there is a circle S^1 that shrinks and a torus T^2 is left. On edges of toric diagrams, a circle S^1 is left and two-cycles $S^1 \times S^1$ shrink. On the bulk of toric diagrams, no cycle shrinks and $T^3 = S^1 \times S^1 \times S^1$ is left. In particular, at each

vertex of toric diagrams all circles shrink. We illustrate the toric diagram of $\mathbb{C}^3$ in Figure 2.1. Similarly, we can describe projective spaces such as $\mathbb{P}^n$, which satisfies $|z_1|^2 + \cdots + |z_{n+1}|^2 = r$ and the identification $(z_1, \ldots, z_{n+1}) \sim (e^{i\theta} z_1, \ldots, e^{i\theta} z_{n+1})$.

Each compact (noncompact) polygon in a toric diagram is called a divisor, and corresponds to a compact (noncompact) four-cycle. The compact divisors give rise to vector multiplets, while noncompact divisors give rise to hypermultiplets in the geometric engineering of 5d $\mathcal{N} = 1$ gauge theories, see e.g. [27]. Each internal line corresponds to a two-cycle $\mathbb{P}^1$, and each external line corresponds to a disk $\mathbb{C}$. A typical example is $\mathcal{O}(-2,-2) \to \mathbb{P}^1 \times \mathbb{P}^1$ illustrated in Figure 2.2, in which the compact divisor represents a four-cycle $\mathbb{P}^1 \times \mathbb{P}^1$, and there are two independent compact two-sphere $\mathbb{P}^1$.

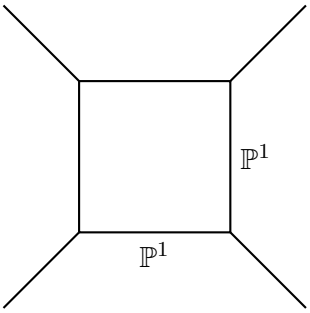

Figure 2.2: This toric diagram is for the geometry $\mathcal{O}(-2,-2) \to \mathbb{P}^1 \times \mathbb{P}^1$. This manifold contains one compact divisor, four noncompact divisors, four compact two-spheres $\mathbb{P}^1$, and four disks $\mathbb{R}_+ \times S^1$.

Resolved conifold. Conifold geometry is particularly useful in toric diagrams, because it relates to the geometric transition in topological strings and hypermultiplets in gauge theries. The toric diagram for the geometry $\mathcal{O}(-1) \oplus \mathcal{O}(-1) \to \mathbb{P}^1$ is shown in Figure 2.3. This Calabi-Yau threefold is called resolved conifold[1]. Sometimes, we also call it local conifold in this thesis for convenience. The local conifold plays an important role, as it gives rise to BPS particle in M-theory if we wrap M2-brane on it, or gives rise to hypermultiplets in brane constructions of gauge theories. In addition, conifold geometry can undergo a geometric transition in the A-model.

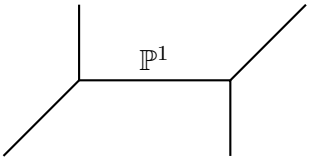

Figure 2.3: Resolved conifold (local conifold).

Geometrically, the conifold is a singular manifold in $\mathbb{C}^4$ with coordinates (x, y, z, t), defined by a polynomial equation

$$xy - zt = 0\,, \tag{2.79}$$

[1]The $\mathbb{P}^1$ is a two-sphere introduced by blowing up the conifold singularity. Note that the conifold itself is a singularity which is the limit that this two-sphere $\mathbb{P}^1$ shrinks.

which can be deformed by turning on a complex structure parameter

$$xy - zt = \mu\,. \tag{2.80}$$

Then one can change variables to write (2.80) as

$$x_1^2 + x_2^2 + x_3^2 + x_4^2 = r\,, \tag{2.81}$$

whose real part is a three-sphere S^3. The full geometry including the fiber is a cotangent bundle T^*S^3. On the other hand, the conifold singularity can also be resolved by blowing up the singularity by introducing a two-sphere $\mathbb{P}^1$ at the singular point. These two ways of resolutions are illustrated in Figure 2.4.

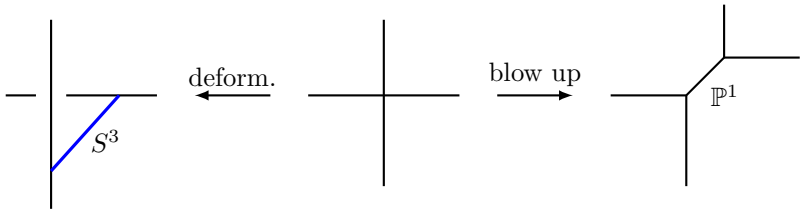

Figure 2.4: The $\mathbb{P}^1$ in the resolved conifold can be wrapped by M2-branes. These two different resolutions are connected by the geometric transition. The three-sphere S^3 in the left diagram carries a Chern-Simons theory, while the $\mathbb{P}^1$ in the right diagram carries closed topological strings [7].

Recall that the volume of $\mathbb{P}^1$ in the resolved conifold is given by

$$t = \mathrm{vol}(\mathbb{P}^1) = \int_{\mathbb{P}^1} J + iB\,. \tag{2.82}$$

When $t \to 0$, the $\mathbb{P}^1$ shrinks to a point. The resolved conifold is obtained by turning on the Kähler parameter for $\mathbb{P}^1$.

2.2.2 Lagrangian submanifolds

Lagrangian submanifolds are boundaries of open topological strings. The toric geometry construction of these submanifolds is discussed in [24]. In the following, we give a short introduction to such submanifolds. If some branes wrap Lagrangian submanifolds, then these branes are called Lagrangian branes or Aganagic-Vafa branes [24]. In type IIB string theory, wrapping D3-branes on Lagrangian submanifolds give rise to 3d $\mathcal{N} = 2$ theories.

The Lagrangian submanifold in toric geometry is a real slice of the Calabi-Yau manifold. For instance, $\mathbb{R}^3 \subset \mathbb{C}^3$ with fixed θ_i is a Lagrangian submanifold. Generically, the Lagrangian submanifold is a n-dimensional real space parametrized by $|z_i|^2$ and Kähler forms vanish on it $\omega|_L = 0$. On toric diagrams, we only consider Lagrangian submanifolds that have topology $\mathbb{C} \times S^1$. Lagrangian submanifolds are represented as additional lines attached to some edges on toric diagrams. For instance, we can find Lagrangian submanifolds in $\mathcal{O}(-2) \oplus \mathcal{O}(0) \to \mathbb{P}^1$. As illustrated in Figure 2.5, blue lines stretching in the bulk denote Lagrangian submanifolds.

The slopes of these lines correspondes to the charges of Lagrangian branes.

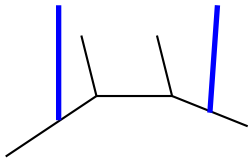

Figure 2.5: The Calabi-Yau threefold $\mathcal{O}(-2)\oplus\mathcal{O}(0) \to \mathbb{P}^1$ with some Lagrangian submanifolds denoted by blue lines.

2.2.3 D-terms and brane webs

In this section, we use algebraic polynomials to define toric diagrams, and discuss relations between toric diagrams and brane webs.

As we discussed in subsection 2.1.3, the D-term in the 2d linear sigma model gives rise to a toric geometry construction of Calabi-Yau manifolds. The target space of A-model is the Coulomb moduli space $\mathcal{M}_C$ of a 2d $\mathcal{N} = (2,2)$ linear sigma model. We assume that there are $N_c + 3$ chiral multiplets Φ_i whose lowest components are scalar fields z_i [2]. Then D-terms give rise to a toric Calabi-Yau threefold X in the A-model, defined by linear equations:

$$X: \quad \sum_i q_i^A |z_i|^2 = t^A\,, \quad A = 1, \ldots, N_c\,, \tag{2.83}$$

where q_i^A are charges for coordinates z_i under the gauge group $U(1)^{N_c}$ and satisfy $\sum_i q_i^A = 0$ which is known as the Calabi-Yau condition; see e.g. [28], and t^A are complexified Kähler parameters. The action of the gauge group $U(1)^{N_c}$ on coordinate z_i is

$$z_i \to \exp\left(i q_i^A \theta_A\right) z_i\,. \tag{2.84}$$

Note that the Lagrangian submanifold can also be defined by (2.83) with an additional charge vector q_i^L satisfying $\sum_i q_i^L = 0$. Because of this property, both open topological strings and closed topological strings can be considered by toric geometry.

Let us go to the relations between toric diagrams and brane webs. Recall that a toric Calabi-Yau threefold is fiber bundle with the torus T^2 as the fiber and a complex two dimensional manifold as the base. Since the M-theory/IIB duality argues that the M-theory compactified on torus T^2 is dual to the type IIB string theory compactified on a cycle S^1. It is natural to relate the toric Calabi-Yau manifolds X in M-theory and brane webs in type IIB string theory [2]. It turns out that the toric diagrams as the degeneration locus of torus are mapped to the (p,q)-brane webs in type IIB string theory. For example, the brane web in Figure 2.2 gives rise to a pure 5d $\mathcal{N} = 1$ theory with a gauge group $SU(2)$, and the resolved conifold in Figure 2.3 gives rise to a theory with a gauge group $U(1)$.

Note that at each vertex of the brane web, there are three edges. Because of charge

[2] These scalar fields are denoted by ϕ^i in previous sections. Here we denote then by z_i as they are coordinates for toric Calabi-Yau manifolds.

conservation, the sum of charges for three edges is zero:

$$\sum_{i=1}^{3} p_i = 0\,, \quad \sum_{i=1}^{3} q_i = 0\,, \tag{2.85}$$

which is equivalent to the Calab-Yau condition for the corresponding toric diagrams [29]. In addition, the $SL(2,\mathbb{Z})$ symmetry of the toric diagrams is the $SL(2,\mathbb{Z})$ symmetry in type IIB string theory. This symmetry can be used to change the slope of toric diagrams, namely the charges of 5-branes. More explicitly, we can use this $SL(2,\mathbb{Z})$ transformation to change the electric charges of the whole brane web in the way:

$$(1,0) \to (1,0)\,, \quad (p,1) \to (p+n,1)\,, \tag{2.86}$$

and change the magnetic charges in another way:

$$(0,1) \to (0,1)\,, \quad (1,q) \to (1,q+n)\,, \tag{2.87}$$

where n can be any integer. These two ways of changing charges can be implemented on brane webs one after another, leading to equivalent brane webs. In particular, the S-operator in $SL(2,\mathbb{Z})$ is the S-duality in type IIB string theory, which rotates toric diagrams (brane webs) by a 90 degree.

2.3 Open topological string theory

Open and closed topological strings are combined with each other and developed together; hence it is hard to distinguish them and discuss one type of topological strings independent of the other one. We prefer to start from the open-closed duality which arises from Chern-Simons theory and geometric transition [7]. In this section, we also discuss Gopakumar Vafa formula and Ooguri-Vafa formula that encode BPS invariants [5, 30, 14, 6, 10]. In the end, we give a review of the refined topological vertex, which is the main tool that we will use in this thesis.

The A-model admits D-branes of odd dimensions inside Calabi-Yau manifolds. The open topological strings have boundaries ending on D-branes wrapping Lagrangian submanifolds. A key example is the deformed conifold, namely, the cotangent bundle T^*S^3. We wrap N D-branes on the base S^3. In this way, we obtain a topological field theory with a gauge group $U(N)$. In [31], Witten found that open topological string theory in this case is Chern-Simons theory. In this section we show how Chern-Simons theory is crucially related to topological strings.

2.3.1 Geometric transition

We can analyze Chern-Simons theory instead of the open topological string theory. The geometric transition makes the story complete by connecting open topological strings to closed topological strings [7].

To begin with, the Chern-Simons theory on a three-sphere S^3 has action

$$S = \frac{k}{4\pi} \int_{S^3} \mathrm{Tr} \left(A \wedge dA + \frac{2}{3} A \wedge A \wedge A \right) . \tag{2.88}$$

In order for it to be gauge invariant, the Chern-Simons level k should be integer. The path integral of the partition function of Chern-Simons theory is

$$Z = \int DA e^{iS[A]} . \tag{2.89}$$

In the A-model, geometric transition states that the Chern-Simons theory on S^3 with a gauge group $U(N)$ and a level k is equivalent to the closed topological string theory on resolved conifold $\mathcal{O}(-1) \oplus \mathcal{O}(-1) \to \mathbb{P}^1$, with the identification of parameters

$$g_s = \frac{2\pi}{k+N} , \qquad t = \frac{2\pi i N}{k+N} = i g_s N , \tag{2.90}$$

where g_s is the string coupling, t is the Kähler parameter of $\mathbb{P}^1$. In addition, the $U(N)$ Chern-Simons theory is constructed by wrapping N D-branes on S^3. It can be checked that the 't-Hooft expansion of the Chern-Simons partition function on S^3 is exactly equal to the closed A-model amplitude on S^2 to all genus [7], with $N g_s = \lambda$ as the 't-Hooft coupling.

Recall that the Chern-Simons theory on S^3 describes the open topological strings of the A-model. Hence the geometric transition is an open-closed duality, connecting open topological strings and closed topological strings.

2.3.2 Chern-Simons correlation functions

One can use Chern-Simons theory to compute topological string partition functions for generic Calabi-Yau manifolds. In this subsection, we given a review on the computation, following [14, 8].

We start from the Ooguri-Vafa construction of knots in M-theory [14]. As we have discussed above, N overlapped branes wrapping on the base S^3 of deformed conifold T^*S^3 are described by Chern-Simons theory. We can probe the dynamics on these branes by another stack of M overlapped branes which wrap a Lagrangian submanifold L_K and intersect the base S^3 along a knot K

$$L_K \cap S^3 = K .$$

Note that L_K is along the fiber of tangent bundle T^*S^3.

This Ooguri-Vafa brane system describes the Chern-Simons theory with the gauge group $U(N) \times U(M)$. There are two types of Wilson loops along the knot

$$U = \mathcal{P} e^{\oint_K A} \in U(N) , \quad V = \mathcal{P} e^{\oint_K \tilde{A}} \in U(M) , \tag{2.91}$$

where A and $\tilde{A}$ are gauge fields on these two stacks of branes respectively. In M-theory, the open strings connecting these two stacks of branes are lifted to M2-branes with two boundaries,

which in this case have the topology of annulus. In [14, 8], it is derived that M2-branes lead to the annulus amplitude

$$\mathcal{O}(U,V;r) = \exp\Big[-\mathrm{Tr}\,\log\left(1 - e^{-r}U\otimes V^{-1}\right)\Big] \tag{2.92}$$

$$= \exp\Big[\sum_{n=1}^{\infty}\frac{e^{-rn}}{n}\mathrm{Tr}U^n\ \mathrm{Tr}V^{-n}\Big]\,, \tag{2.93}$$

where r is the length of this annulus and n is the winding number. The Chern-Simons path integrals for generic toric geometries can be computed by using this annulus operator.

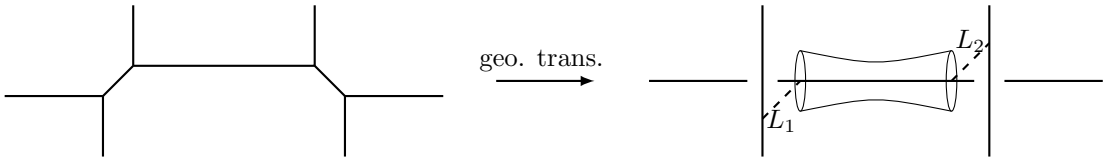

Figure 2.6: After geometric transitions, the amplitude of closed topological strings become the correlation function of Chern-Simons theory. In this example, the boundaries of M2-branes ending on Lagrangian submanifolds L_1 and L_2 are unknots S^1.

The procedure of computing topological string amplitudes is the following. Firstly, one needs to implement geometric transitions on some resolved conifolds and get Lagrangian submanifolds L_i which are three-spheres S^3. On each of these three-spheres we wrap M5-branes to get a gauge group, and the M2-branes connecting two stacks of M5-branes contribute to the annulus operator $\mathcal{O}(V_i,V_j)$. Finally, by taking all annulus operators into account, one ends up with topological string amplitudes. We use an example to illustrate. The strip Calabi-Yau threefold described by the left toric diagram in Figure 2.6 captures the closed string amplitude of the A-model, which is transformed into the correlation function of Chern-Simons theory:

$$Z^{\text{closed top.}} = \langle\mathcal{O}(V_1,V_2;r)\rangle = \int \mathcal{D}A_1\mathcal{D}A_2 e^{S_{CS}(A_1)+S_{CS}(A_2)}\exp\Big[\sum_{n=1}^{\infty}\frac{e^{-rn}}{n}\mathrm{Tr}V_1^n\ \mathrm{Tr}V_2^{-n}\Big]\,. \tag{2.94}$$

Moreover, by using the Frobenius formula

$$\mathrm{Tr}_{\vec{k}}V := \prod_{j=1}^{\infty}(\mathrm{Tr}V^j)^{k_j} = \sum_R \chi_R(\vec{k})\mathrm{Tr}_R V\,, \tag{2.95}$$

where $\chi_R(\vec{k})$ is the character of the symmetric group $S_{|R|}$, the annuls operator can be rewritten in terms of Young diagram R

$$\mathcal{O}(V_1,V_2) = \sum_R \mathrm{Tr}_R V_1 e^{-|R|r}\mathrm{Tr}_R V_2^{-1}\,, \tag{2.96}$$

where V_i is the homolomy of the gauge field on the Lagrangian submanifold L_i. By gluing the annulus operators, one can compute the path integrals of correlation functions for more

complicated toric diagrams

$$Z^{\text{top.string}} = \int \prod_i^n \mathcal{D}A_i e^{\sum_i S_{CS}(A_i)} \mathcal{O}(V_1, V_2; r_1)\mathcal{O}(V_2, V_3; r_2)\dots\mathcal{O}(V_n, V_1, r_n)\,, \tag{2.97}$$

which can be represented as the summation over Young diagrams

$$Z^{\text{top. string}} = \sum_{R_1,R_2,\dots,R_n} \langle \overline{R}_1|V_{L_2}e^{-|R_2|r_2}R_2\rangle\langle \overline{R}_2|V_{L_3}e^{-|R_3|r_2}R_3\rangle\cdots\langle \overline{R}_n|V_{L_1}e^{-|R_1|r_1}R_1\rangle\,, \tag{2.98}$$

where $V_{L_i} \in SL(2,\mathbb{Z})$ are the operators transferring the Wilson loop V_{i+1} to the Wilson loop V_i. In particular, the amplitude for the Hopf link $K_1 \cup K_2$ is

$$W_{R_1,R_2} = \langle \text{Tr}_{R_1} V_1 \text{Tr}_{R_2} V_2\rangle\,. \tag{2.99}$$

If one of Young diagrams is empty, we get the correlation function for a single unknot

$$W_R(K) = \langle \text{Tr}_R V\rangle = s_R(Q)\,, \tag{2.100}$$

where $s_R(Q)$ is a Schur function. More explicitly, the Wilson loop of the unknot in representation R is

$$W_R = \frac{S_{0R}}{S_{00}} = \dim_q R\,, \tag{2.101}$$

and for the Hopf link

$$W_{R_1R_2} = q^{|R_1||R_2|/N}\frac{S^{-1}_{R_1R_2}}{S_{00}}\,. \tag{2.102}$$

One can represent Wilson loops in terms of Kähler parameters, using

$$\text{Tr}U^n = -i\frac{e^{nt/2} - e^{-nt/2}}{q^{n/2} - q^{-n/2}}\,. \tag{2.103}$$

Then the annulus amplitude (2.92) is

$$\langle \mathcal{O}(U,V)\rangle_{S^3} = \exp\Big[-i\sum_{n=1}^{\infty}\frac{e^{nt/2} - e^{-nt/2}}{n(q^{n/2} - q^{-n/2})}\text{Tr}V^{-n}\Big]\,, \tag{2.104}$$

where two components $e^{nt/2}$ and $e^{-nt/2}$ correspond to two disks that are the two hemispheres of $\mathbb{P}^1$ in the resolved conifold.

2.4 Topological string invariants

Topological string theories have a target space interpretation in M-theory. The M-theory compactified on Calabi-Yau threefolds through geometric engineering gives rise to supersymmetric gauge theories. Therefore, topological string partition functions are interpreted as gauge the-

ory partition functions. In this section, we first discuss the refinement of gauge theories and then discuss Gopakumar-Vafa formula and Ooguri-Vafa formula that encode degeneracy numbers of BPS particles.

Ω-background in gauge theories

In 4d and 5d, supersymmetric gague theories depend on two parameters ϵ_1 and ϵ_2, which are Ω-deformation parameters [32, 33]. The Ω-deformations are interpreted as the rotation symmetry $SO(4)$ acting on spacetime $\mathbb{R}^4$. This rotation symmetry is generated by a vector field on $\mathbb{R}^4$. The metric is deformed

$$ds^2 = g_{ij}\left(dx^i i + V^i dx^i\right)\left(dx^j + V^j dx^j\right), \tag{2.105}$$

and the vector field is

$$V = V^i \frac{\partial}{\partial x^i} = \Omega^j_j x^j \frac{\partial}{\partial x^i}, \tag{2.106}$$

where

$$\Omega^{ij} = \begin{pmatrix} 0 & \epsilon_1 & 0 & 0 \\ -\epsilon_1 & 0 & 0 & 0 \\ 0 & 0 & 0 & \epsilon_2 \\ 0 & 0 & -\epsilon_2 & 0 \end{pmatrix}. \tag{2.107}$$

If we regard the spacetime as two complex planes $\mathbb{R}^4 = \mathbb{C}_1 \times \mathbb{C}_2$, then V can be written as

$$V = i\epsilon_1 \left(z_1 \frac{\partial}{\partial z_1} - \overline{z}_1 \frac{\partial}{\overline{z}_1}\right) + i\epsilon_2 \left(z_2 \frac{\partial}{\partial z_2} - \overline{z}_2 \frac{\partial}{\overline{z}_2}\right). \tag{2.108}$$

Moreover, V is a Killing vector field acting on the moduli space of k-instantons $\mathcal{M}_k^+$. By adding this deformation, the integral over moduli space are localized to fixed points. For instance, the k-instanton partition function

$$Z_k = \int_{\mathcal{M}_k^+} 1 = \sum_{\text{fixed points}} \frac{1}{\det(\cdots)}. \tag{2.109}$$

These fixed points are labeled by Young diagrams [32]. The Ω-deformations are introduced as a method to perform localization, but immediately it is realized that the Ω-deformation is the graviphoton field strength [32, 33].

2.4.1 Gopakumar-Vafa formula

The topological string theories can also be refined. There are refined formulas for topological partition functions, which sum up all the contributions of BPS particles. Let us first discuss the geometric engineering of these BPS particles and then discuss the Gopakumar-Vafa formula. For details of this construction, see e.g. [30].

The topological string amplitudes can be interpreted as partition functions of 5d $\mathcal{N} = 1$ gauge theories which are engineered by the M-theory compactified on noncompact Calabi-Yau

threefolds X. The BPS particles in 5d gauge theories are engineered as M2-branes wrapped on holomorphic curves $\beta \in H_2(X,\mathbb{Z})$. The masses of these BPS particles are the areas of holomorphic curves $T_\beta = \int_\beta \omega$, where $\omega = J + iB$ is the complexified Kähler form on X. These BPS particles are charged under the little group $SO(4) = SU(2)_L \times SU(2)_R$ and hence are classified by spins (j_L, j_R). In addition, M2-branes have momentums along the circle S^1 direction. Therefore, the mass of the M2-brane with momentum n is given by $T_\beta + 2\pi i n/g_s$. Because of the M-theory/IIB-string duality, BPS particles given by M2-branes carry electric and magnetic charges, and hence correspond to (p,q)-strings in brane webs

$$\text{M2-branes} \leftrightarrow (p,q)\text{-strings}\,. \tag{2.110}$$

On the Coulomb branch the gauge group is broken to $U(1)^{N_c}$, which can also be interpreted via the Calabi-Yau geometry X. Each $U(1)_i$ corresponds to a compact divisor $D_i \subset X$, and gauge fields come from the three-form $C_{11}^{(3)}$ in M-theory

$$C_{11}^{(3)} = \sum_{i=1}^{N_c} A_\mu^{(i)} \wedge \omega^{(i)}\,, \tag{2.111}$$

by wrapping a M2-brane on a curve β

$$\sum_{i=1}^{N_c} A_\mu^{(i)} \int_\beta \omega^{(i)} = \sum_{i=1}^{N_c} A_\mu^{(i)}\ (D_i \cdot \beta)\,, \tag{2.112}$$

where the term $D_i \cdot \beta$ (intersection number) is the electric charge for the BPS particle.

Moreover, we can get 4d $\mathcal{N}=2$ theories by shrinking the circle S^1 in the 5d spacetime $\mathbb{R}^4 \times S^1$. There is a graviphoton field strength

$$F = \epsilon_1 dx^1 \wedge dx^2 + \epsilon_2 dx^3 \wedge dx^4\,, \tag{2.113}$$

which can be interpreted as the field V in (2.108). In 5d gauge theories, BPS particles go around the circle S^1 and are charged under this field strength F. The Ω-deformation leads to refined partition functions of 5d theories and 4d theories [32, 33]; there should exist a refinement of topological strings. The original topological string theory is the unrefined topological string theory that defined at the unrefined limit $\epsilon_1 + \epsilon_2 = 0$. Because of geometric engineering discussed above, we have the equivalence between partition functions in this limit[3]

$$Z^{\text{top.}}(g_s) = Z^{\text{Nek.}}(\epsilon_1,\epsilon_2)|_{g_s=\epsilon_2=-\epsilon_1}\,. \tag{2.114}$$

However, unrefined partition functions do not capture the full rotation symmetry on $\mathbb{R}^4_{\epsilon_1,\epsilon_2}$, so we prefer to refine it.

Let us go back to M-theory and discuss how the Ω-deformation rotates the spacetime coordinates. In our context, the M-theory compactified on Calabi-Yau threefold X has the

[3]Note that the gauge theroy partition functions for 5d $\mathcal{N}=1$ theories and 4d $\mathcal{N}=2$ theories are usually called Nekrasov partition functions.

spacetime $TN \times S^1$, where TN is the Taub-NUT space similar to $\mathbb{C}_1 \times \mathbb{C}_2$ and has two complex coordinates z_1 and z_2. The Taub-NUT is twisted along the S^1. If we go around the S^1, complex coordinates rotate by

$$(z_1, z_2) \to (qz_1, t^{-1}z_2)\,, \tag{2.115}$$

where $q = e^{i\epsilon_1}$ and $t = e^{-i\epsilon_2}$. In order to preserve supersymmetry we need $\epsilon_1 + \epsilon_2 = 0$, namely the unrefined limit $q = t$. The refinement of topological string is obtained by relaxing this constraint on $\epsilon_{1,2}$. However, in order to preserve supersymmetry, we need R-symmetry $U(1)_R$ acting on X. Since the M-theory partition function is the same as the A-model topological string partition function on X, the refined M-theory partition function defines the refined topological strings.

The refined M-theory partition function has a very nice formula. As discussed in [30], the summation of contributions of BPS particles gives rise to the free energy:

$$\mathcal{F} = \sum_{\beta\in H_2(X,\mathbb{Z})} \sum_{n\in\mathbb{Z}} \sum_{j_L,j_R} N_\beta^{(j_L,j_R)} \int_\varepsilon^\infty \frac{ds}{s} \frac{\mathrm{Tr}_{(j_L,j_R)}(-1)^{\sigma_L+\sigma_R} e^{-sT_\beta - 2\pi i n} e^{-2s(\sigma_L\epsilon_+ + \sigma_R\epsilon_-)}}{(2\sinh(s\epsilon_1/2))(-2\sinh(s\epsilon_2/2))}\,, \tag{2.116}$$

where $N_\beta^{(j_L,j_R)}$ is the number of BPS particles. The refined closed topological string partition functions $Z = \exp(\mathcal{F})$ take form

$$Z^{\text{closed}}(Q,q,t) = \prod_{\beta\in H_2(X,\mathbb{Z})} \prod_{j_L,j_R} \prod_{k_L=-j_L}^{j_L} \prod_{k_R=-j_R}^{j_R} \prod_{m_{1,2}=1}^{\infty} \left(1 - t^{k_L+k_R+m_1-\frac{1}{2}} q^{k_L-k_R+m_2-\frac{1}{2}} Q_\beta\right)^{(-1)^{2j_L+2j_R+1} N_\beta^{(j_L,j_R)}}\,, \tag{2.117}$$

where the parameters $\sqrt{qt}$ and $\sqrt{\frac{t}{q}}$ are fugacities for $SU(2)_L$ and $SU(2)_R$, and $Q_\beta = e^{-\int_\beta \omega}$. One can write (2.117) in another form

$$\begin{aligned} &Z^{\text{closed}}(Q,q,t) \\ &= \exp\left(\sum_{\beta\in H_2(X,\mathbb{Z})} \sum_{n=1}^{\infty} \sum_{j_L,j_R} \frac{(-1)^{2j_L+2j_R} N_\beta^{(j_L,j_R)} \chi_{j_L}((qt)^n) \chi_{j_R}\left(\left(\frac{t}{q}\right)^n\right)}{n(t^{n/2}-t^{-n/2})(q^{n/2}-q^{-n/2})} Q_\beta^n\right) \qquad (2.118) \\ &= \mathrm{PE}\left[\sum_{\beta\in H_2(X,\mathbb{Z})} \sum_{j_L,j_R} \frac{(-1)^{2j_L+2j_R} N_\beta^{(j_L,j_R)} \chi_{j_L}((qt)) \chi_{j_R}\left(\left(\frac{t}{q}\right)\right)}{n(t^{1/2}-t^{-1/2})(q^{1/2}-q^{-1/2})} Q_\beta\right], \qquad (2.119) \end{aligned}$$

where $\chi_j(x) := x^{-j} + x^{-j+1} + \cdots + x^j$. This formula is called Gopakumar-Vafa (GV) formula [30]. The integers $N_\beta^{(j_L,j_R)}$ are called Gopakumar-Vafa invariants or closed BPS invariants.

2.4.2 Ooguri-Vafa formula

Open topological strings are also related to gauge theories through geometric engineering. In this subsection, we discuss the Ooguri-Vafa formula encoding open BPS invariants.

The topological branes in the A-model can be lifted to M5-branes wrapping the Lagrangian submanifold $L \subset X$ and the spacetime $\mathbb{R}^2 \times S^1 \subset TN \times S^1$. These branes preserve a half of supersymmetry. Hence the theory on Lagrangian branes has four supercharges and turns out to be a 3d $\mathcal{N} = 2$ theory on the spacetime $\mathbb{R}^2 \times S^1$. In M-theory interpretation, M2-branes wrap holomorphic disks in X and end on L. These M2-branes engineer vortex particles in 3d $\mathcal{N} = 2$ theories.

As we have discussed in section 2.3.2, the annulus amplitude (2.104) is engineered by the M2-branes stretching between two stacks of M5-branes. In [14], it is found that by using Schwinger computation and summing up all particles with the representation P on the boundary, one can get a unrefined formula for the open topological string free energy:

$$\mathcal{F}(t, V) = i \sum_{n=1}^{\infty} \sum_{\beta \in H_2(X,L,\mathbb{Z})} \sum_{P,j} \frac{N^j_{\beta,P} q^{nj}}{n(q^{n/2} - q^{-n/2})} Q^n_\beta \, \mathrm{Tr}_P V^n \,, \tag{2.120}$$

where P is the Young diagram on the Lagrangian brane. This formula is called unrefined Ooguri-Vafa (OV) formula. The unrefined Ooguri-Vafa invariants $N^j_{\beta,P}$ are the degeneracy numbers of open BPS particles, which can be positive or negative integers.

In the Ω-background, there are two types of Lagrangian branes, depending on which $\mathbb{C}$ of TN the M5 brane wraps [34]:

$$q\text{-brane}: \quad L \times \mathbb{C}_q \times S^1 \,, \qquad \bar{t}\text{-brane}: \quad L \times \mathbb{C}_{\bar{t}} \times S^1 \,. \tag{2.121}$$

The refined open topological strings are charged under the rotation symmetry $SO(2)$ on $\mathbb{R}^2$ and the R-symmetry $U(1)_R$. There are refined open Gopakumar-Vafa formulas e.g. [6, 10]. The t-brane partition function takes form

$$\begin{aligned} Z^{\text{open}}(Q, q, t) &= \exp\left[\sum_{\beta \in H_2(X,L,\mathbb{Z})} \sum_{j,r \in \mathbb{Z}/2} \sum_{n=1}^{\infty} \frac{(-1)^{2j+2r} q^{nj} \left(\frac{t}{q}\right)^{n\,r} N^{(j,r)}_\beta}{n\left(q^{\frac{n}{2}} - q^{-\frac{n}{2}}\right)} Q^n_\beta \right] \\ &= \mathrm{PE}\left[\sum_{\beta \in H_2(X,L,\mathbb{Z})} \sum_{j,r \in \mathbb{Z}/2} \frac{(-1)^{2j+2r} q^j \left(\frac{t}{q}\right)^{r} N^{(j,r)}_\beta}{\left(q^{\frac{1}{2}} - q^{-\frac{1}{2}}\right)} Q_\beta \right], \end{aligned} \tag{2.122}$$

where refined Ooguri-Vafa invariants $N^{(j,r)}_\beta$ are degeneracy numbers of vortex particles. The variables $e^{-R\,T_\beta}$ is the Kähler parameter for the relative two-cycle $\beta \in H_2(X, L, \mathbb{Z})$, and T_β is area of the M2-brane wrapping β, and R is the radius of S^1. We will discuss the relations between different types of refined open topological branes (Lagrangian branes) in chapter 4.

In addition, the free energy of open topological strings with multiple boundaries takes form

$$\mathcal{F}(t,V)=\sum_{g=0}^{\infty}\sum_{n_i=1}^{\infty}g_s^{2g-2+h}\mathcal{F}_{g,n_1,\cdots,n_h}(t)\mathrm{Tr}V_1^{n_1}\cdots\mathrm{Tr}V_h^{n_h}\,. \tag{2.123}$$

Here $\mathcal{F}_{g,n_1,\cdots,n_h}(t)$ is the amplitude for open topological strings with genus g and h boundaries, and V_i is the holonomy along the i-th boundary.

2.5 Topological vertex formalism

We have discussed that Chern-Simons amplitudes are equal to topological string amplitudes due to the geometric transition. Using the Chern-Simons theory, one can compute the topological string amplitudes associated to generic toric Calabi-Yau threefolds. This method was further generalized to the topological vertex method [9], which also has a refined version because of the Ω-deformations, computing the refined topological string amplitudes. Topological vertex is a powerful method in the A-model, which enables to compute even the amplitudes of non-toric diagrams, see e.g. [35, 36]. It can be viewed as a reformulation of the localization method used in supersymmetric gauge theories. In this section, we first mention unrefined topological vertex, and then focus on the computation details of the refined topological vertex.

2.5.1 Unrefined topological vertex

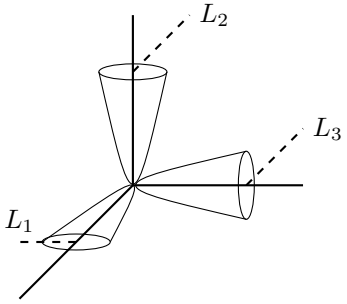

Figure 2.7: The building block for toric diagrams is $\mathbb{C}^3$, on which we can attach Lagrangian branes.

The idea of topological vertex is simple. One can put brane/anti-brane pairs to a generic toric diagram, which chop off the Calabi-Yau to building blocks $\mathbb{C}^3$ shown in Figure 2.7. Computing the open topological string amplitude on $\mathbb{C}^3$ defines the cubic topological vertex amplitude

$$C_{R_1,R_2,R_3}(q)=\sum_{R,Q_1,Q_2}N_{Q_1R}^{R_1}N_{Q_3^TR}^{R_3^T}q^{\kappa_{R_2}/2+\kappa_{R_3}/2}\frac{W_{R_2^TQ_1}(q)W_{R_2Q_3^T}(q)}{W_{R_2}(q)}\,, \tag{2.124}$$

where $N_{R_1R_2}^{R_2}$ is the tensor product coefficients. Then one can glue these cubic vertices to get the full topological string amplitude. In this thesis, we only use refined topological vertex.

Since it reduces to unrefined topological vertex in the limit $q = t$, we only briefly discuss unrefined topological vertex.

2.5.2 Refined topological vertex

The refined topological string amplitudes can be computed by using refined topological vertex [30, 37], which is also related to refined Chern-Simons theory [34]. Refined topological vertex has been developed into a computational method, so in the following we only discuss how to implement it on toric diagrams. This section follows the notation in [10].

The first step is the assignment of Ω-deformation parameters q, t and preferred directions. Recall that the structure of a toric Calabi-Yau manifold can be encoded in a toric diagram, which consists of trivalent vertices connected by edges (internal lines) and some edges (external lines) extend from vertices to infinity. In the refined setting we also need to have preferred directions, which are not unique but lead to the same result. The preferred direction is denoted by $||$ assigned on parallel lines on toric diagrams, and each vertex should be associated with one $||$ on one of its connected lines, and other two legs should be assigned with parameters q and t respectively. Note that the assignment of q and t does not play a role in the computation of closed topological string amplitudes. Namely, two possible choices of such an assignment yield the same refined closed string partition functions.

Having made the above choices, we assign to all edges of a toric diagram their directions (represented by arrows, see e.g. Figure 2.8 and 2.9), and to edges around each vertex we assign Young diagrams $(\mu, \nu, \lambda, \ldots)$ (for outgoing arrows) or their transpose $(\mu^T, \nu^T, \lambda^T, \ldots)$ (for incoming arrows), as well as framing numbers. Here we change the notation for Young diagrams from R_i to $\mu \cdots$, following the convention in literature. Furthermore, to internal edges we assign Kähler parameters $Q_\bullet$, where $\bullet$ in the subscript stands for an appropriate label of a given leg. Then, each vertex with edges labeled by Young diagrams (μ, ν, λ), contributes to a topological vertex amplitude defined as

$$C_{\lambda\mu\nu}(t,q) = q^{\frac{||\mu||^2+||\nu||^2}{2}} t^{-\frac{||\mu^T||^2}{2}} \tilde{Z}_\nu(t,q) \sum_\eta \left(\frac{q}{t}\right)^{\frac{|\eta|+|\lambda|-|\mu|}{2}} s_{\lambda^T/\eta}(t^{-\rho}q^{-\nu}) s_{\mu/\eta}(q^{-\rho}t^{-\nu^T}) \,, \tag{2.125}$$

where $s_{\lambda/\eta}$ are skew Schur functions, $t^\rho = (t^{-1/2}, t^{-3/2}, t^{-5/2}, \ldots)$, and

$$\tilde{Z}_\nu(t,q) = \prod_{(i,j)\in\nu} \left(1 - q^{\nu_i - j} t^{\nu_j^T - i + 1}\right)^{-1} . \tag{2.126}$$

Parameters $q = e^{-\epsilon_2}$ and $t = e^{\epsilon_1}$ parametrize the Ω-deformation. Note that (2.125) is the refined version of (2.124). Similarly, each edge contributes to a edge factor

$$f_\nu^\bullet(t,q)^{\text{framing number}} L_\nu(Q), \qquad L_\nu(Q) = (-Q)^{|\nu|}, \tag{2.127}$$

where $f^\bullet(t,q)$ denotes either $f^p(t,q)$ for the edges along the preferred direction, or $f(t,q)$ for

other edges of non-preferred directions, such that

$$f_\nu^p(t,q) = (-1)^{|\nu|} t^{\frac{||\nu^T||^2}{2}} q^{-\frac{||\nu||^2}{2}}, \qquad f_\nu(t,q) = \left(\frac{q}{t}\right)^{-\frac{|\nu|}{2}} f_\nu^p(t,q). \tag{2.128}$$

The assignment of vertex factors and edge factors is illustrated in Figure 2.8 and Figure 2.9; in particular, pink arrows in these figures denote the ordering of diagrams μ, ν, λ at a given vertex and the ordering of arguments q and t in the function $f^\bullet(\cdot,\cdot)$. For more details see e.g. [38].

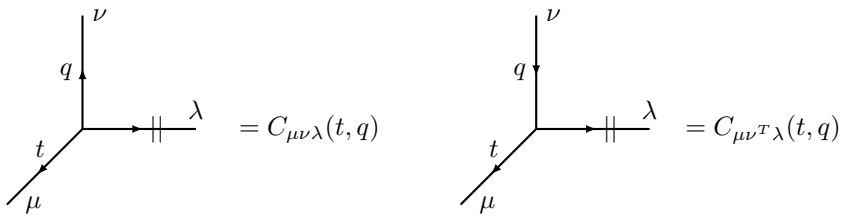

Figure 2.8: Assignment of the vertex factor. The direction of arrows on edges can be chosen arbitrarily, and the associated Young diagram is transposed if the arrow is reversed.

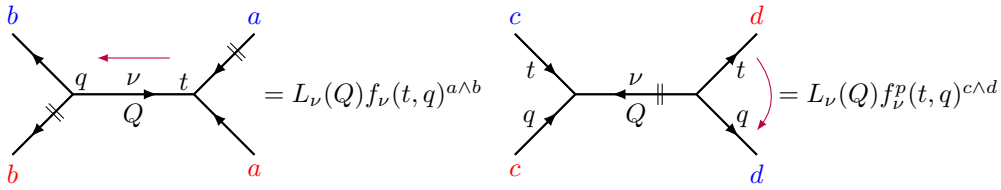

Figure 2.9: Factors assigned to an edge along a non-preferred direction (left) and preferred direction (right). The directions of external legs are specified by vectors a, b, c, d, whose cross products are denoted by a wedge $\wedge$. Consistency conditions impose that the value $a \wedge b$ is the same for both blue and red a and b, and similarly $c \wedge d$ is the same for both blue and red c and d.

Finally, the topological string partition function schematically takes form

$$Z^{\text{top}} = \sum_{\mu_\bullet} \prod (\text{edge factor}) \cdot \prod (\text{vertex factor}) \,. \tag{2.129}$$

After summing over Young diagrams along non-preferred directions and many contractions of Schur functions through Cauchy identities, the above expression generically reduces to

$$Z^{\text{top}}(Q_\bullet, t, q) \;\; = \;\; Z^M \cdot Z^{\text{sum}} \,, \tag{2.130}$$

where Z^M is a product of MacMahon functions

$$Z^M = \prod M^{\pm}(Q_\bullet, t, q) \,, \tag{2.131}$$

and Z^{sum} is the sum over Young diagrams along preferred directions, which has the following

structure

$$Z^{\rm sum} = \sum_{\mu_\bullet,\ \nu_\bullet} Q_\bullet^{|\mu_\bullet|} \prod_{\mu_\bullet} ||\tilde{Z}_{\mu_\bullet}(t,q)||^2 \frac{\prod N_{\nu_\bullet}^{\rm half,-}(Q_\bullet, t^{-1}, q^{-1}) N_{\mu_\bullet\nu_\bullet}(Q_\bullet, t^{-1}, q^{-1})}{\prod N_{\mu_\bullet\nu_\bullet}(Q_\bullet, t^{-1}, q^{-1})}\,, \tag{2.132}$$

where $||\tilde{Z}_\mu(t,q)||^2 = \tilde{Z}_{\mu^T}(t,q)\tilde{Z}_\mu(q,t)$, and $N_{\mu\nu}(Q;t,q)$ is called the Nekrasov factor

$$N_{\mu\nu}(Q;t,q) = \prod_{i,j=1}^{\infty} \frac{1 - Q\ q^{\nu_i - j}\ t^{\mu_j^T - i + 1}}{1 - Q\ q^{-j}\ t^{-i+1}}\,, \tag{2.133}$$

and half-Nekrasov factors are defined by

$$N_\nu^{\rm half,-}(Q;t,q) = N_{\nu\emptyset}\left(Q\sqrt{\frac{q}{t}}, t, q\right), \qquad N_\nu^{\rm half,+}(Q;t,q) = N_{\emptyset\nu}\left(Q\sqrt{\frac{q}{t}}, t, q\right). \tag{2.134}$$

Note that Z^M is an overall factor in $Z^{\rm top}$ and it can be obtained by setting Young diagrams along preferred directions to $\emptyset$, i.e. $Z^M = Z^{\rm top}|_{\mu_i=\emptyset}$.

There may be extra closed string contributions that should be removed by hand, which are the closed strings stretching between parallel external lines in toric diagrams. These strings are not charged under the gauge symmetry, and do not satisfy closed Gopakumar-Vafa formula. More details on such extra closed states can be found in [39, 40, 41, 36].

In the above, we have summarized the formalism of refined topological vertex, following the notation in [36]. To implement computations, we use the Mathematica notebook *schur-cancellation.nb* [42].

Lagrangian brane

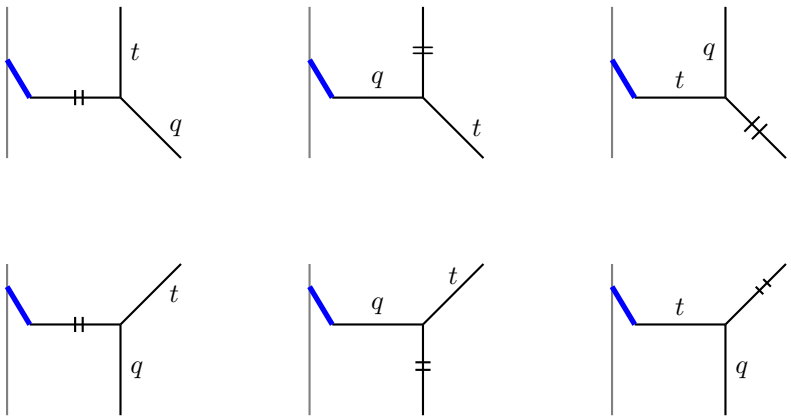

Figure 2.10: Choices of preferred direction together with a standard assignment of q and t at the vertex to which a topological brane (Lagrangian brane) is attached. These are the assignments that we appreciate. The assignment of q and t in the rest of a toric diagram (for simplicity not shown in this figure) follows uniquely from the above choices. The vertical line in gray comes from the geometric transitions that produce the open topological branes. We will discuss this in section **??**.

We emphasize that in the presence of open topological branes, the assignment of (q,t)

becomes important [10]. If we change the assignment, we would get a different refined open topological string amplitude. We summarize all possible standard assignments in Figure 2.10. The assignment of the rest of toric diagrams can be determined accordingly. We note that it is possible to exchange the parameters $q \leftrightarrow t$ and get another six assignments. We refer to opposite assignments of q and t as alternative assignments; for these opposite choices, definitions of topological brane types and refined open BPS states must be appropriately adjusted [10].

Refined open topological string partition functions are also independent of preferred directions. We find these standard assignments by matching the open topological string partition functions assigned with different preferred directions. By computing specific examples, we find the threes cases in the top row of Figure 2.10 are equivalent. In addition, the open topological string amplitudes are invariant under flop transitions of closed Kähler parameters. By using this property, we relate the diagrams in the top and bottom rows of Figure 2.10.

Chapter 3

Gauge theory and brane webs

3d $\mathcal{N}=2$ gauge theories have nice properties, such as 3d mirror symmetry [43] and various other dualities [44, 45, 46, 47]. We mainly consider the 3d gauge theories constructed by Higgsing 5d $\mathcal{N}=1$ gauge theories [6, 48]. We have discussed the corresponding M-theory interpretation in chapter 2, i.e. the geometric engineering using Calabi-Yau three-manifolds. On the other hand, these gauge theories can also be constructed through brane webs in type IIB string theory [27, 29, 49, 50, 51, 52]. In this chapter, we review field theory descriptions for 3d gauge theories and brane constructions. This chapter contains some results from [11].

3.1 3d gauge theories

In this section, we give a short introduction to 3d gauge theories from the aspects of vector and hyper multiplets, Lagrangians and moduli spaces; see e.g. [44, 45]. In particular, we discuss the relations between effective superpotentials and holomorphic disk potentials encoded in open topological string amplitudes [11].

3.1.1 Lagrangian description

3d $\mathcal{N}=2$ theories have four supercharges with the algebra

$$\{Q_\alpha, Q_\beta\} = \{\bar{Q}_\alpha, \bar{Q}_\beta\} = 0, \quad \{Q_\alpha, \bar{Q}_\beta\} = 2\gamma^\mu_{\alpha\beta} P_\mu + 2i\epsilon_{\alpha\beta} Z\,, \quad \alpha,\beta = 1,2\,, \mu = 0,1,2\,, \tag{3.1}$$

where $\gamma^\mu = (-\mathbf{1}, \sigma^1, \sigma^3)$ are chosen to be real and symmetric, and Z is the real central charge corresponding to the momentum P_3 in dimension reduction from 4d $\mathcal{N}=1$ theories. Note that supercharge Q_α and $\bar{Q}_\alpha$ are complex, and the automorphism of this algebra is R-symmetry $U(1)_R$.

The multiplets in 3d $\mathcal{N}=2$ theories come from the dimensional reduction of the 4d $\mathcal{N}=1$ superfields; see [44] for a nice introduction. 3d $\mathcal{N}=2$ gauge theories contain the vector multiplet $V=(A_\mu, \sigma, \lambda, D)$ in the adjoint representation and the chiral multiplet $Q=(\phi, \psi, F)$, in which σ is a real adjoint scalar field and ϕ is a complex scalar, λ and ϕ are two-component Dirac fermions, D and F are auxiliary fields. Chiral multiplets could compose a holomorphic function $\mathcal{W}(Q_i)$ called superpotential describing the interaction between chiral

multiplets. More explicitly, the chiral multiplet

$$Q_i = \phi_i + \theta\psi_i + \theta^2 F_i \tag{3.2}$$

and vector multiplets

$$V_a = -i\theta\bar{\theta}\sigma_a - \theta\gamma^\mu\bar{\theta}A^a_\mu + i\theta^2\bar{\lambda}_a - i\bar{\theta}^2\theta\lambda_a + \frac{1}{2}\theta^2\bar{\theta}^2\, D_a\,, \quad a = 1\,, \ldots\,, \mathrm{rank}(G)\,, \tag{3.3}$$

which satisfy $V_a = V_a^\dagger$, and a goes from one to the rank of the gauge group G. The superspace derivatives are

$$D_\alpha = \frac{\partial}{\partial\theta^\alpha} + i\gamma^\mu_{\alpha\beta}\partial_\mu\,, \quad \bar{D}_\alpha = -\frac{\partial}{\partial\bar{\theta}^\alpha} - i\theta^\beta\gamma^\mu_{\beta\alpha}\partial_\mu\,. \tag{3.4}$$

The gauge field strength is in the linear multiplet defined as

$$\Sigma_a := -\frac{i}{2}\epsilon^{\alpha\beta}\bar{D}_\alpha D_\beta V_a = \sigma_a + \theta\bar{\lambda}_a + \bar{\theta}\lambda_a + \frac{1}{2}\theta\gamma^\mu\bar{\theta}F_a^{\nu\rho}\epsilon_{\mu\nu\rho} + i\theta\bar{\theta}D_a + \frac{i}{2}\bar{\theta}^2\theta\gamma^\mu\partial_\mu\bar{\lambda}_a + \frac{1}{4}\theta^2\bar{\theta}^2\partial^2\sigma_a\,, \tag{3.5}$$

which satisfies $D^2\Sigma_a = \bar{D}^2\Sigma_a = 0$. The linear multiplet is the current superfield for the $U(1)_J$ topological symmetry, which is associated with each gauge node $U(N_c)$ and has a conserved current

$$j_J = \frac{1}{2\pi} * \mathrm{Tr}F\,. \tag{3.6}$$

3d $\mathcal{N} = 2$ gague theories have Lagrangian descriptions, which contains kinetic term, Chern-Simons term and Fayet-Iliopoulos term. Depending on gauge groups and matter multiplets, Lagrangians for different theories are slightly different. In the following, we illustrate Lagrangian and moduli space by reviewing two typical theories that have been discussed in [45, 53].

$U(N_c) + N_f\mathbf{F}$

This theory has a gauge group $U(N_c)$ and N_f hypermultiplets. We quote the discussion of this theory from [45]. This theory has global symmetries $SU(N_f) \times SU(N_{af}) \times U(1)_A \times U(1)_T \times U(1)_R$. The Lagrangian for this theory is

$$\mathcal{L} = \int d^4\theta \left(+\frac{1}{g^2}\Sigma^2 + \frac{k}{4\pi}\Sigma V + \frac{\xi}{2\pi}V \right) + \sum_i \int d^4\,\theta Q_i^\dagger e^{q_i V + i m_i\theta\bar{\theta}} Q_i\,, \tag{3.7}$$

where the second term is the Chern-Simons term and the third term is the Fayet-Iliopoulos term. We denote the hypermultiplet Q_i by $\mathbf{F}$, which has charges q_i under the gauge symmetry and m_i is its real mass parameter.

After expanding the superfield in Chern-Simons term, one can obtain

$$\mathcal{L}_{CS} = \frac{k}{4\pi}\mathrm{Tr}\Big[AdA + \frac{2}{3}A^3 + \big(2D\sigma - \bar{\lambda}\lambda\big)\Big]\,. \tag{3.8}$$

The interaction between $U(1)_T$ topological symmetry and the $U(1)$ factor of $U(N_c)$ gives rise to the term

$$\mathcal{L}_{FI} = \frac{1}{2\pi}D\xi\,, \tag{3.9}$$

where the Fayet-Iliopoulos (FI) parameter ξ can be viewed as the real scalar of a background vector multiplet for the $U(1)_T$ topological symmetry.

In the case of abelian theory $N_c = 1$, after integrating out auxiliary fields, one gets the scalar potential:

$$U = g^2\Big(\sum_i q_i|\phi_i|^2 - \xi - k\sigma\Big)^2 + \sum_i (q_i\sigma + m_i)^2|\phi_i|^2\,, \tag{3.10}$$

where ϕ_i is the complex scalar in the chiral multiplet Q_i that carries charge q_i and real mass m_i, and σ is the real scalar in the vector multiplet. There are one loop quantum corrections to Fayet-Iliopoulos parameter ξ and Chern-Simons level k; therefore effective parameters read

$$\xi^{\text{eff}} = \xi + \frac{1}{2}\sum_i q_i m_i\ \mathrm{sign}(m_i + q_i\sigma)\,, \tag{3.11}$$

$$k^{\text{eff}} = k + \frac{1}{2}\sum_i q_i^2\ \mathrm{sign}(m_i + q_i\sigma)\,. \tag{3.12}$$

The vacua are given by the solutions of $U = 0$, so we have

$$\sum_i 2\pi q_i|\phi_i|^2 - \xi^{\text{eff}} - k^{\text{eff}}\sigma = 0\,,\quad (m_i + q_i\sigma)\phi_i = 0\,. \tag{3.13}$$

The Higgs vacuum $\mathcal{M}_H$ is given by the solutions with nonzero vacuum expectation value $\langle\phi_i\rangle \neq 0$ which requires $m_i + q_i\sigma = 0$. Higgs branch consists of discrete points $\{\sigma = m_i/q_i\}$. The Coulomb branch $\mathcal{M}_V$ is defined by $\langle\phi_i\rangle = 0$ and hence the solutions are given by $\xi^{\text{eff}} = k^{\text{eff}} = 0$. There may also other branches; see [45].

$U(1)^{N_c} + N_f\mathbf{F}$

This theory has a gauge group $U(1)^{N_c}$ and N_f hypermultiplets. This abelian theory has been discussed in [53]. Its special case is the $\mathcal{T}_{A,N}$ theory that we will use for considering mirror transformation in chapter 5. This abelian theory has a gauge group $U(1)^{N_c}$, vector multiplets $V_a\,(a = 1,\cdots,N_c)$ and chiral superfields $Q_i\,(i = 1,\cdots,N)$. There are N_c linear superfields $\Sigma_a = \epsilon^{\alpha\beta}\bar{D}_\alpha D_\beta V_a$ and hence the topological groups are $U(1)_J^{N_c}$. In the following, we quote the discussion on this theory from [53].

The Lagrangian of this theory contains terms

$$\mathcal{L} = \mathcal{L}_{kin} + \mathcal{L}_{FI} + \mathcal{L}_{CS} + \mathcal{L}_{W} \,. \tag{3.14}$$

The kinetic term for vector multiplets and chiral multiplets reads

$$\mathcal{L}_{kin} = \int d^4\theta \, \sum_{a=1}^{N_c} \frac{1}{g_a^2} \Sigma_a^2 + \sum_{i=1}^{N_f} Q_i^\dagger \, e^{\sum_{a=1}^{N_c} q_i^a V_a} Q_i \,, \tag{3.15}$$

where the g_a is the a-th gauge coupling that has dimension $(\text{mass})^{1/2}$ and q_i^a is the charge of the i-th chiral multiplet under the a-th gauge group.

A real mass parameter can be turned on for each chiral multiplet, which can be interpreted as weakly gauging the flavor symmetry of the theory and giving a vacuum expectation value (VEV) to the scalar in the background vector multiplet. Namely

$$\int d^4\theta \, \sum_{i=1}^{N_f} Q_i^\dagger \, e^{m_i \theta\bar{\theta}} Q_i \,. \tag{3.16}$$

Note that there are only $N_f - N_c$ independent real mass parameters, and the remaining N_c parameters are set to zero by shifting scalars σ_a. The 3d superpotential is the gauge invariant monomial of chiral superfields Q_i

$$\mathcal{L}_W = \int d^2\theta \, \mathcal{W}(Q_i) + h.c. \tag{3.17}$$

In addition, Fayet-Iliopoulos parameters ξ_a have the dimension of mass, whose Lagrangian term is

$$\mathcal{L}_{FI} = \sum_{a=1}^{N_c} \xi_a \int d^4\theta \, V_a \,. \tag{3.18}$$

The mixed Chern-Simons levels k_{ab} have dimension zero, whose Lagrangian term is

$$\mathcal{L}_{CS} = \sum_{a,b=1}^{N_c} k_{ab} \int d^4\theta \, \Sigma_a V_b \,. \tag{3.19}$$

After integrating out auxiliary fields D_i and F_i, one can obtain the scalar potential

$$U = \sum_{a=1}^{N_c} g_a^2 \left(\sum_{i=1}^{N_f} q_i^a |\phi_i|^2 - \sum_{i=1}^{N_c} k_{ab}\sigma_b - \xi_a \right)^2 + \sum_{i=1}^{N_f} (q_i^a \sigma_a + m_i)|\phi_i|^2 + \sum_{i=1}^{N_f} \left| \frac{\partial \mathcal{W}}{\partial \phi_i} \right|^2 . \tag{3.20}$$

In the case $\mathcal{W} = 0$, the effective Chern-Simons term is obtained by integrating out the charged

fermions:

$$k_{ab}^{\text{eff}} = k_{ab} + \frac{1}{2}\sum_{i=1}^{N_f} q_i^a q_j^b \text{sign}(q_i \cdot \sigma + m_i)\,. \tag{3.21}$$

Note that the theory with $k_{ab}^{\text{eff}} \in \mathbb{Z}$ is free of the parity anomaly [44]. The effective Fayet-Iliopoulos parameters read

$$\xi_a^{\text{eff}} = \xi_a + \sum_{b=1}^{N_c} k_{ab}^{\text{eff}}\sigma_b + \frac{1}{2}\sum_{i=1}^{N_f} q_i^a m_i \text{ sign}(q_i \cdot \sigma + m_i)\,. \tag{3.22}$$

Similarly, the Higgs branch $\mathcal{M}_H$ consists of discrete points $\{q_i^a\sigma_a + m_i = 0\}$.

Vortex particles

Vortex particles are BPS states on the Higgs branch. Let us analyze the theory $U(1) + N_f\mathbf{F}$ to illustrate; see e.g. [45]. We first define new supercharges $Q_\pm$

$$Q_\pm = \frac{1}{2}(Q_1 \pm iQ_2)\,, \tag{3.23}$$

then the algebra (3.1) is written as

$$\{Q_\pm\,, \overline{Q}_\pm\} = \pm iP_1 + P_2\,, \quad \{Q_\pm\,, \overline{Q}_\mp\} = P^0 \pm Z\,. \tag{3.24}$$

We assume the coordinates on the 3d spacetime are (t, x, y). Then supersymmetry transformations on the vector multiplet read

$$\begin{aligned}
\{Q_-\,\lambda_-\} &= F_{\bar{z}t} + \partial_{\bar{z}}\sigma\,,\\
\{Q_+, \lambda_+\} &= F_{zt} - \partial_z\sigma\,,\\
\{Q_-, \lambda_+\} &= F_{z\bar{z}} + \partial_t\sigma - iD\,,\\
\{Q_+, \lambda_-\} &= F_{z\bar{z}} + \partial_t\sigma + iD\,,
\end{aligned} \tag{3.25}$$

where the field strength $F_{z\bar{z}} = iF_{xy}$, $z = x + iy$, and $\lambda_\pm = \lambda_1 \pm i\lambda_2$. One can get the transformations for complex conjugation of these fields by replacing $Q_\pm \to \overline{Q}_\mp\,, \overline{\lambda}_\pm \to \lambda_\mp\,, z \to \bar{z}$. The supersymmetric variation of the chiral multiplet Q_i with a charge q_i and a real mass $m_i = 0$ are

$$\begin{aligned}
\{\overline{Q}_+, \psi_{i+}\} &= D_z\phi_i\,,\\
\{\overline{Q}_-, \psi_{i-}\} &= D_{\bar{z}}\phi_i\,,\\
\{\overline{Q}_+, \psi_{i-}\} &= iD_t\phi_i + q_i\sigma\phi_i\\
\{\overline{Q}_-, \psi_{i+}\} &= -iD_t\phi_i + q_i\phi_i\,,\\
\{Q_-, \psi_{i+}\} &= F_i\,,\\
\{Q_+, \psi_{i-}\} &= F_i\,,
\end{aligned} \tag{3.26}$$

where $D_\mu \to \partial_\mu - iq_i A_\mu$ and $D_z := \frac{1}{2}(D_x - iD_y)$.

The half-BPS state is defined as the state that has a central charge $Z > 0$ and is annihilated by Q_- and its complex conjugate $\overline{Q}_+$. Its anti-BPS state is given by the CPT conjugation and should be annihilated by $\overline{Q}_-$ and Q_+. We consider the BPS eqution for BPS states annihilated by Q_- and $\overline{Q}_+$, which are given by (3.25) and (3.26)

$$\begin{aligned} &\partial_t \sigma = 0\,, \quad F_{zt} + \partial_z \sigma = 0\,, \quad F_{z\bar{z}} - iD = 0\,, \\ &i\partial_t \phi_i + q_i(\sigma + A_t)\phi_i = 0\,, \quad D_z \phi_i = 0\,, \quad F_i = 0\,. \end{aligned} \tag{3.27}$$

The static configuration giving by setting $\partial_t \to 0$ and $A_t = -\sigma$, leads to the BPS equations for vortex particles

$$F_{z\bar{z}} = iD\,, \quad D_z \phi_i = 0\,, \quad F_i = 0\,, \tag{3.28}$$

where D is the D-term. Moreover, vortex particles on the Higgs branch have non-vanishing magnetic charges q_J under the topological symmetry $U(1)_J$. The fields for vortex particles take form

$$\phi = \sqrt{\frac{\xi}{2\pi}} e^{iq_J\theta} + \cdots\,, \quad A_\theta = q_J + \cdots\,, \tag{3.29}$$

where $z = x + iy = |z|e^{i\theta}$. The central charge is

$$Z = \frac{\xi_J}{2\pi} \int d^2z\, F_{z\bar{z}} = \frac{\xi_J}{2\pi} \int d^2z\, j^0_J = q_J \xi_J\,, \tag{3.30}$$

where the magnetic charge is the winding number

$$q_J = \frac{1}{2\pi} \int F = c_1(F) \in \mathbb{Z}\,. \tag{3.31}$$

Since vortex particles are BPS saturated, their charges are equal to masses $|Z| = m = q_J \xi_J$.

Surface defect

One could introduce a surface defect (surface operator) in the 5d $\mathcal{N} = 1$ gauge theory. On the surface defect lives the 3d $\mathcal{N} = 2$ theory. We consider the 3d-5d coupled theories engineered by toric diagrams (toric Calabi-Yau threefolds) with Lagrangian branes in M-theory. Gauge theory partition functions count vortex particles and instanton particles that are engineered by M2-branes. The leading terms of partition functions are propotentials that encode the information of gauge theories. In this section, we discuss these physical quantities. For a nice review on surface defects, see e.g. [6, 20]

Surface defects are similar to Wilson lines and 't Hooft lines. In this thesis, we only consider the surface defects of co-dimension two, which are half-BPS and supported on spacetime $\mathbb{R}^2 \subset \mathbb{R}^4$. Recall that the Ω-deformation acts as the rotation symmetries $SO(2)_1 \times SO(2)_2$ of $\mathbb{R}^2_{\epsilon_1} \times \mathbb{R}^2_{\epsilon_2} = \mathbb{R}^4$. The 3d theories preserve the rotation symmetry $SO(2)$ on surface defects.

Depending on which R_{ϵ_i} are located surface defects, we get two types of defects, corresponding to the q-brane and $\bar{t}$-brane discussed in (2.121).

Surface defect satisfies vortex BPS equations (3.28). The gauge field is singular nearby it

$$A_\theta = m\, d\theta + \cdots , \tag{3.32}$$

where the θ is the angular coordinate for the spacetime perpendicular to surface defect. Hence the field strength $F = 2\pi m\, \delta_{\mathsf{D}} + \cdots$. The integral along the normal direction of the surface defect D, the magnetic charge, is the vortex number

$$m = \frac{1}{2\pi}\int_{\mathsf{D}} F\,, \tag{3.33}$$

where $\mathsf{D} = \mathbb{R}^2$ in our context.

Instantons

There are non-perturbative contributions in the bulk theory, which are instantons. Instantons have origin in the topological term in the Lagrangian. In 4d theories, the Yang-Mills term reads

$$S_{YM} = \int_{\mathbb{R}^4} \frac{1}{4g^2}\mathrm{Tr} F\wedge *F + \frac{i\theta}{8\pi^2}\mathrm{Tr} F\wedge F\,, \tag{3.34}$$

where $\tau = \frac{4\pi i}{g^2} + \frac{\theta}{2\pi}$ in the coupling. If we set the self-dual field strength $F^+ = (F + *F)/2 = 0$ (instanton equation), then we get instantons with the charge (instanton number)

$$k = \frac{1}{8\pi^2}\int_{\mathbb{R}^4} \mathrm{Tr} F\wedge F \in \mathbb{Z}\,. \tag{3.35}$$

In 5d $\mathcal{N}=1$ theories, the topological term comes from 6d $(1,0)$ theories. As discussed in e.g. [54], the relevant term is

$$\int_{\mathbb{R}^6} B\wedge \mathrm{Tr}(F\wedge F)\,, \tag{3.36}$$

where B is the B-field $B_{\mu\nu}$. After the dimensional reduction on a circle $S^1 \in \mathbb{R}^6$, one gets a gauge field $A = \int_{S^1} B$, and the topological term in 5d reads

$$\int_{\mathbb{R}^5} A\wedge \mathrm{Tr}(F\wedge F) = \int_{\mathbb{R}^5} A_\mu J^\mu\,, \tag{3.37}$$

which couples the gauge field to the current $J^\mu = *\mathrm{Tr}(F\wedge F)$ of the conserved topological symmetry $U(1)_I$, satisfying $\partial_\mu J^\mu = 0$.

Since instantons are one dimensional objects in 5d theories, they are called instanton particles. Upon the compactification on S^1, the gauge coupling for the 5d theory on $\mathbb{R}^4\times S^1$ is complexified by picking up a theta angle $\theta = \oint_{S^1} A$ in the term (3.37). Then one gets the

5d gauge coupling

$$\tau_{5d} = \frac{4\pi i R}{g^2} + \frac{\theta}{2\pi}\,, \tag{3.38}$$

which contributes to the phase factor $\mathbf{q}^k$ where the instanton parameter is defined as $\mathbf{q} = e^{2\pi i \tau}$. In addition, the instanton particle has the central charge

$$Z = m_0 \int d^4x J^0 = m_0 q_J^0\,, \tag{3.39}$$

where the $U(1)_J$ charge q_J^0 is the instanton number, and m_0 is the effective gauge coupling $m_0 = 1/g_{\text{eff}}^2$. Since there are one-loop quantum corrections from hypermultiplets, we use the effective gauge coupling g_{eff}. As we have reviewed in section 2.4.1, these instanton particles are engineered by M2-branes wrapping two-cycles, whose magnetic dual objects are magnetic strings given by M5-branes wrapped on compact four-cycles in Calabi-Yau threefolds. In addition, the M-theory interpretation of 5d partition functions leads to Gopakumar-Vafa formula (2.118).

3.1.2 Prepotentials

In this subsection we review properties of prepotentials in 3d and 5d theories, which are the leading terms of free energy, as found in [55, 56] and discussed in [6].

In the presence of the surface defect, the instanton partition function of the 3d-5d coupled theory is ramified:

$$Z^{\text{inst}}_{k,m} = \oint_{\mathcal{M}_{k,m}} 1\,, \tag{3.40}$$

where $\mathcal{M}_{k,m}$ is the ramified instanton moduli space with the instanton number $k = c_2(E)$ [1] and the vortex number m. The partition function takes form

$$Z^{\text{inst}} = \sum_{k=0}^{\infty}\sum_{m=0}^{\infty} \mathbf{q}^k z^m Z^{\text{inst}}_{k,m}\,, \tag{3.41}$$

where $\mathbf{q} = e^{2\pi i\tau}$ is the instanton parameter and $z = e^{i\xi}$ relates to the Fayet-Iliopoulos parameter ξ.

The 3d partition function in the Ω-background counts vortex particles on $\mathbb{R}^2 \times S^1$. We can expand the vortex partition function and read off the leading term

$$Z^{\text{vortex}} = \exp\left(\frac{\mathcal{W}}{\hbar} + \cdots \mathcal{O}(\hbar)\right), \tag{3.42}$$

where the leading term $\mathcal{W}$ is the 3d prepotential [56]. Here, the Ω-deformation can be regarded

[1] Here E is the gauge bundle restricted on the surface defect.

as a regularization of the 2d gauge theory on $\mathbb{R}^2$,

$$\mathrm{vol}(\mathbb{R}^2) = \int_{\mathbb{R}^2} 1 = \frac{1}{\hbar}\,. \tag{3.43}$$

More explicitly, both the bulk spacetime and the surface defect are regularized by the Ω-deformation:

$$\mathrm{vol}(\mathbb{R}^2) = \int_{\mathbb{R}^2_{\epsilon_1}} 1 = \frac{1}{\epsilon_1}\,, \qquad \mathrm{vol}(\mathbb{R}^4) = \int_{\mathbb{R}^4_{\epsilon_1,\epsilon_2}} 1 = \frac{1}{\epsilon_1\epsilon_2}\,. \tag{3.44}$$

The combined partition function encodes prepotentials [48, 6]

$$Z_{\text{3d-5d}}(\epsilon_1,\epsilon_2) = \exp\left(-\frac{1}{\epsilon_1\epsilon_2}\mathcal{F} + \frac{\mathcal{W}}{\epsilon_1} + \cdots + \mathcal{O}(\epsilon_1,\epsilon_2)\right)\,, \tag{3.45}$$

where $\mathcal{F}$ is the prepotential of the bulk 5d $\mathcal{N}=1$ gauge theory and $\mathcal{W}$ is the prepotential for the 3d $\mathcal{N}=2$ theory on the surface defect. The 3d theory and the 5d bulk theory considered in this thesis can be decoupled. As the closed topological string theory corresponds to the bulk 5d theory and the open topological string theory corresponds to the 3d surface defect theory, by setting the instanton parameter $\mathbf{q}$ or the Fayet-Iliopoulos parameter to zero, we can end up with only the 3d theory or the 5d bulk theory. Namely,

$$Z^{\text{3d}}_{\mathbb{R}^2\times S^1}(z,q,t) = Z^{\text{open top.}}(Q,q,t)\,, \tag{3.46}$$

$$Z^{\text{5d}}_{\mathbb{R}^4\times S^1}(\mathbf{q},q,t) = Z^{\text{closed top.}}(Q,q,t)\,. \tag{3.47}$$

In addition, using the mirror symmetry between A-model and B-model, we can identify the prepotential with an integral over the Seiberg-Witten differential [48]

$$\mathcal{W} = \int_{p^*}^{p} \lambda_{SW}\,. \tag{3.48}$$

The Seiberg-Witten curve is the mirror curve in the B-model, which can also be interpreted as the moduli space of the surface defect. The surface defect is engineered by a D5-brane in the B-model, which mirrors to a D6-brane wrapping a Lagrangian submanifold in the A-model [28].

3.1.3 Effective superpotential

The 3d $\mathcal{N}=2$ gauge theory compactified on a circle S^1 can be viewed as a 2d $\mathcal{N}=(2,2)$ sigma models with infinite many Kaluza-Klein modes. The effective theories of 2d sigma models are described by effective superpotentials, see e.g.[15, 18, 20]. It is argued in [57, 58, 59, 60] that both vortex partition function, sphere partition function and superconformal index have the same asymptotic expansion in the semi-classical limit $\hbar \to 0$, and the leading term is the

effective superpotential

$$Z^{\text{vortex}}_{\mathbb{R}^2\times S^1}\,,\;\; Z_{S^3_b}\,,\;\; Z_{S^2\times S^1} \sim \int \prod_i d\,x_i\; e^{\frac{1}{\hbar}\widetilde{\mathcal{W}}^{\text{eff}}_{3d\,\mathcal{N}=2}(\xi_i,\,x_i)+O(\hbar)}\,. \tag{3.49}$$

Moreover, the leading term plays the role of the 3d prepotential and encodes the effective CS levels. In particular, the equivariant parameter $\hbar$ is related to the Plank constant $\hbar$:

$$Q=\frac{\log(q)}{2\pi b\,i}\,,\quad \hbar=2\pi\,i\,b^2\,,\quad q=e^{\hbar}=e^{2\pi\,i\,b^2}\,. \tag{3.50}$$

There are intricate relations between prepotentials and superpotentials. In the following part of this subsection we review the discussion in [11]. It turns out that the prepotential is the disk potential from the open topological string perspective. Refined Ooguri-Vafa formulas can be used to find the relations between various invariants at different limits.

The 3d gauge theory on the surface defect $\mathbb{R}^2_{\epsilon_1}\times S^1$ has vortex partition function on the Higgs branch. According to (3.45), this theory has a prepotential given by [55, 56, 61, 62]

$$\mathcal{W}_{\mathbb{R}^2\times S^1}=\lim_{\epsilon_1,\epsilon_2\to 0}\;\epsilon_2\log Z^{\text{vortex}}_{\mathbb{R}^2\times S^1}\,, \tag{3.51}$$

where the vortex partition function is equal to the open topological string amplitude. In addition, the prepotential and quantum integrable system are related [20, 63]. If we relate ϵ_1 to the Plank constant $\hbar$ by $\hbar=R\,\epsilon_1$, then the combination of (3.49) and (3.51) reveals the relation between the prepotential and the effective superpotential:

$$e^{\frac{\mathcal{W}_{\mathbb{R}^2\times S^1}}{\hbar}}=\int\prod_i d\,x_i\; e^{\frac{1}{\hbar}\widetilde{\mathcal{W}}^{\text{eff}}_{3d\,\mathcal{N}=2}(k_{ij},\,\xi_i,\,x_i)}\,. \tag{3.52}$$

The prepotential and the holomorphic disk potential are also related. By using the refined Ooguri-Vafa formula in (2.122) and the definition of prepotential, we find

$$\begin{aligned}\mathcal{W}_{\mathbb{R}^2\times S^1}&=\lim_{\epsilon_1,\epsilon_2\to 0}\;\epsilon_2\log Z^{\text{vortex}}_{\mathbb{R}^2\times S^1}\\&=-\frac{1}{R}\sum_{\beta\in H_2(X,L,\mathbb{Z})}\;\sum_{j,r\in\mathbb{Z}/2}(-1)^{2j+2r}N^{(j,r)}_{\beta}\text{Li}_2\big(e^{-R\,T_\beta}\big)\,.\end{aligned} \tag{3.53}$$

Expanding the polylogarithm function $\text{Li}_2(z):=\sum_{n=1}^{\infty}\frac{z^n}{n^2}$, one can obtain

$$-R\,\mathcal{W}_{\mathbb{R}^2\times S^1}=\sum_{n=1}^{\infty}\sum_{\beta\in H_2(X,L,\mathbb{Z})}\;\sum_{j,r\in\mathbb{Z}/2}(-1)^{2j+2r}N^{(j,r)}_{\beta}\,\frac{e^{-n\,R\,T_\beta}}{n^2}\,, \tag{3.54}$$

which has the same form as the holomorphic disc potential encoding classical Ooguri-Vafa

invariants in the A-model [14, 24]

$$\mathcal{W}_{\text{open}} = \sum_{\beta\in H_2(X,L,\mathbb{Z})} N_\beta^{OV} \text{Li}_2\big(e^{-R\,T_\beta}\big) = \sum_{n=1}^{\infty} \sum_{\beta\in H_2(X,L,\mathbb{Z})} N_\beta^{OV}\, \frac{e^{-n\,R\,T_\beta}}{n^2}\,. \tag{3.55}$$

Therefore, the propotential is equivalent to the holomorphic disk potential

$$-R\,\mathcal{W}_{\mathbb{R}^2\times S^1} = \mathcal{W}_{\text{open}}\,, \tag{3.56}$$

and the classical Ooguri-Vafa invariant can be represented as the summation of refined open BPS invariants

$$N_\beta^{OV} = \sum_{j,r\in\mathbb{Z}/2} (-1)^{2j+2r} N_\beta^{(j,r)}\,. \tag{3.57}$$

Note that the disk potential is classical and can be expressed as an integral in the B-model

$$\mathcal{W}_{\text{open}} = \int \lambda_{SW} = \int \log y\, \frac{dx}{x}\,, \tag{3.58}$$

where is consistent with (3.48), and λ_{SW} is the differential one-form on the mirror curve [24, 28].

We emphasize that the prepotential $\mathcal{W}_{\mathbb{R}^2\times S^1}$ is not complete at the decompactification limit $R\to\infty$. Following the treatment in [64], we define the complete prepotential for 3d $\mathcal{N}=2$ theory in this limit

$$\mathcal{W}^{\text{complete}}_{\mathbb{R}^2\times S^1} := \lim_{R\to+\infty} \frac{1}{R}\mathcal{W}_{\mathbb{R}^2\times S^1}\,, \tag{3.59}$$

which takes form

$$\mathcal{W}^{\text{complete}}_{\mathbb{R}^2\times S^1} = -\frac{1}{2} \sum_{\beta\in H_2(X,L,\mathbb{Z})} \sum_{j,r\in\mathbb{Z}/2} (-1)^{2j+2r} N_\beta^{(j,r)}\, [\![T_\beta]\!]^2\,, \tag{3.60}$$

where we used (A.39). Furthermore, refined open BPS invariants can be resummed into different invariants in various limits. In the Nekrasov-Shatashvili limit $\epsilon\neq 0, \epsilon_2 = 0$ [56], using Gopakumar-Vafa formula (4.17) we get

$$\lim_{\epsilon_2\to 0}\ \epsilon_2 \log Z_{\mathbb{R}^2\times S^1} = -\frac{1}{R} \sum_{\beta\in H_2(X,L,\mathbb{Z})} \sum_{j,r\in\mathbb{Z}/2} (-1)^{2j+2r} N_\beta^{(j,r)} \text{Li}_2\big(t^r\, e^{-R\,T_\beta}\big)\,, \tag{3.61}$$

which implies that $N_\beta^r := \sum_{j\in\mathbb{Z}/2} (-1)^{2j} N_\beta^{(j,r)}$ are the invariants in Nekrasov-Shatashvili limit [20]. In the unrefined limit $\epsilon_1 = \epsilon_2$, refined formula (2.122) reduces to unrefined formula and we define $N_\beta^j := \sum_{r\in\mathbb{Z}/2} (-1)^{2r} N_\beta^{(j,r)}$ as the unrefined invariants.

3.1.4 3d mirror symmetry

Generically, 3d mirror symmetry is the duality between Higgs branch $\mathcal{M}_H$ and Coulomb branch $\mathcal{M}_V$ [43]. The mass parameters for hypermultiplets are mirror to the Fayet-Iliopoulos parameters for vector multiplets. This argument is correct for the 2d mirror symmetry between A-model and B-model, as well as the 3d mirror symmetry, which is one kind of electric-magnetic duality, relating different theories. The mirror symmetry in 3d $\mathcal{N}=4$ theories is interpreted as the S-duality which exchanges various branes (3.92). In 3d $\mathcal{N}=2$ theories, since mirror dual theories have equivalent partition functions, the mirror symmetry can be in principle interpreted as a transformation. In this thesis we appreciate the interpretation that 3d mirror symmetry is a functional Fourier transformation on the path integral of partition functions [65]. On the other hand, in [66, 57] it is pointed out that 3d mirror symmetry is the ST-operator in the group $SL(2,\mathbb{Z})$, such that $(ST)^3=1$.

To begin with, we consider the 3d $\mathcal{N}=4$ SQED, which has a gauge group $U(1)$ and a hypermultiplet $\mathbf{H}$. Note that each hypermultiplet in $\mathcal{N}=4$ contains two chiral multiplets in $\mathcal{N}=2$, namely $1\mathbf{H}=1\mathbf{F}+1\mathbf{AF}$. The Fayet-Iliopoulos parameter can be promoted to be a background vector multiplet V associated to the topological symmetry; then its partition function is

$$Z_{\text{SQED}}[\mathsf{V}]=\int \mathcal{D}V\mathcal{D}Q\, e^{S_{\text{kin}}(V)/g^2+S_{\text{BF}}(V,\mathsf{V})+S_{\mathbf{H}}(V,Q)}\,, \tag{3.62}$$

where $S_{\text{kin}}(V)$ and $S_{\mathbf{F}}(V,Q)$ are kinetic terms for vector multiplets and hypermultiplets. The BF coupling involves a vector multiplet V, an adjoint chiral multiplet Φ, a background linear multiplet $\mathsf{\Sigma}$ and a background chiral multiplet $\mathsf{\Phi}$:

$$S_{\text{BF}}(V,\mathsf{V})=\int d^4\theta\, V\mathsf{\Sigma}-\left(\int d^2\theta\, i\Phi\mathsf{\Phi}+c.c.\right). \tag{3.63}$$

The partition function of the free hypermultiplet is a function of a background vector multiplet V associated to the $U(1)$ global symmetry:

$$Z_{\mathbf{H}}[\mathsf{V}]=\int \mathcal{D}\,Q e^{iS_{\mathbf{H}}(\mathsf{V},Q)}\,. \tag{3.64}$$

In the infrared $g\to\infty$, the theory becomes free, and the mirror dual pair becomes

$$Z_{\text{SQED}}[\mathsf{V}]=\int \mathcal{D}V e^{S_{\text{BF}}(V,\mathsf{V})}\int \mathcal{D}Q\, e^{S_{\mathbf{H}}(V,Q)}=Z_{\mathbf{H}}[\mathsf{V}]\,, \tag{3.65}$$

which is equivalent to a transformation for the free hypermultiplet:

$$\int \mathcal{D}V e^{S_{\text{BF}}(V,\mathsf{V})}Z_{\mathbf{H}}[V]=Z_{\mathbf{H}}[\mathsf{V}]\,. \tag{3.66}$$

Therefore, in this case the mirror symmetry is interpreted as a transformation for the hyper multiplet. This mirror transformation can be used to derive other mirror pairs in literature [67].

In $\mathcal{N}=4$ language the abelian mirror pair that we discussed above is

$$U(1)+1\mathbf{H}+1\mathbf{Adj}\,,\quad \mathcal{W}=Q\tilde{Q}\Phi \quad\longleftrightarrow\quad \{q\,,\tilde{q}\}\,,\mathcal{W}=0\,, \tag{3.67}$$

which can also be represented in $\mathcal{N}=2$ language as the mirror pair between SQED and XYZ-model:

$$U(1)+1\mathbf{F}+1\mathbf{AF}\,,\quad \mathcal{W}=0 \quad\longleftrightarrow\quad \{X,Y,Z\}\,,\ \mathcal{W}=XYZ\,. \tag{3.68}$$

3.1.5 Sphere partition function

The localization is a powerful technique that could compute partition functions of theories on curved manifolds. Localization method needs to introduce an artificial potential to the Lagrangian, which does not change the path integral, but could localize the path integral to finite dimensional contour integrals [68]. The localization of 3d $\mathcal{N}=2$ gauge theories on three-sphere was developed in [69, 70]. In this section we only use their results.

To begin with, the three-sphere is defined as

$$S^3_b : b^2|z_1|^2+b^{-2}|z_2|^2=1\,,\quad z_1,z_2\in\mathbb{C}\,, \tag{3.69}$$

Note that when $b=1$, we return to the standard three-sphere S^3. On Coulomb branch, the sphere partition function only contains the perturbative part and one-loop parts from chiral multiplets and vector multiples. The higher loops contributions vanishes for supersymmetric theories. More explicitly, bare Chern-Simons level k and Fayet-Iliopoulos term ξ appear in the perturbative part

$$\exp\big(-i\,\pi\,kx^2+2\,i\,\pi\xi x\big)\,, \tag{3.70}$$

where x is the gauge transformation parameter for the gauge group $U(1)$. The one-loop contributions from the fundamental chiral multiplet $\mathbf{F}$ and antifundamental chiral multiplet $\mathbf{AF}$ are given by

$$s_b\Big(x+\frac{i\,Q}{2}+\frac{u}{2}\Big)\,,\quad s_b\Big(\frac{i\,Q}{2}-x+\frac{u}{2}\Big), \tag{3.71}$$

where $Q=b+1/b$ is the localization parameter and u is the real mass parameter. Note that chiral multiplets $\mathbf{F}$ and $\mathbf{AF}$ have charges 1 and -1 respectively under the gauge group $U(1)$. The charge q appears in the coefficient of the variable x in the one-loop contribution

$$s_b(qx+iQ/2+u/2)\,. \tag{3.72}$$

Now we use examples to illustrate. $U(1)_k+N_F\mathbf{F}$ has the sphere partition function

$$Z^{U(1)_k+N\mathbf{F}}_{S^3_b}=\int dx\,e^{-i\,\pi\,kx^2+2\,i\,\pi\xi x}\prod_{i=1}^{N_F}s_b\Big(\frac{i\,Q}{2}+x+\frac{u_i}{2}\Big)\,, \tag{3.73}$$

and $U(1)_k + N_F\,\mathbf{F} + N_{AF}\,\mathbf{AF}$ has the sphere partition function

$$Z^{U(1)_k+N_F\,\mathbf{F}+N_{AF}\,\mathbf{AF}}_{S^3_b} = \int dx\, e^{-i\,\pi\,k x^2+2\,i\,\pi\xi x} \prod_{i=1}^{N_F} s_b\Big(\frac{i\,Q}{2}+x+\frac{u_i}{2}\Big) \prod_{j=1}^{N_{AF}} s_b\Big(\frac{i\,Q}{2}-x+\frac{u_j}{2}\Big)\,. \tag{3.74}$$

The sphere partition functions for the mirror pair in (3.68) are equivalent

$$\int dx e^{-2\pi i x y} H_m(x) = s_b(m) H_{-m}(y)\,, \tag{3.75}$$

where

$$H_m(x) := s_b\left(x + i\frac{Q}{4} + \frac{m}{2}\right) s_b\left(-x + i\frac{Q}{4} + \frac{m}{2}\right)\,.$$

This is an identity that can be used to derive other mirror dual pairs [67].

3.2 Brane construction

Gauge theories can also be realized by branes via the Hanany-Witten construction [71]. There are different types of branes in string theories, carrying charges and gauge fields. Branes could overlap, intersect and cross other branes, leading to diverse brane configurations. Brane systems have successfully constructed many supersymmetric gauge theories of various dimensions from 2d to 6d. Particularly, in 5d $\mathcal{N}=1$ theories, the corresponding toric diagrams can be identical with 5d brane webs [27]. We can also have 3d brane webs by Higging 5d brane webs; see chapter 6. In this section we review basic picture of brane constructions. For a nice introduction to string theory, D-brane and brane constructions, see e.g. [72, 73, 74, 75].

3.2.1 D-branes and higher form gauge fields

Dp-brane is the brane of p-dimension, which is the source of a $(p+1)$-form gauge field in supergravity. Dp-brane has tension $T_{\mathrm{D}p} = 1/g_s l_s^{p+1}$ and along $(x^1,\ldots,x^p)$ directions. The chiralities of type IIA string theory and type IIB string theory are different. Type IIA string theory has $(1,1)$ spacetime supersymmetry, while the type IIB string theory has $(2,0)$ spacetime supersymmetry. For Dp-branes in type IIA string theory, the spacetime supersymmetries are generated by the left and the right moving worldsheet supercharges Q_L and Q_R with opposite chirality for spinors

$$\Gamma^0\cdots\Gamma^p\epsilon_L = \epsilon_L\,,\quad \Gamma^0\cdots\Gamma^p\epsilon_R = -\epsilon_R\,. \tag{3.76}$$

The Dp-branes in type IIB string theory have the same chirality

$$\Gamma^0\cdots\Gamma^p\epsilon_L = \epsilon_L\,,\quad \Gamma^0\cdots\Gamma^p\epsilon_R = \epsilon_R\,. \tag{3.77}$$

In addition, the supercharges obey $\Gamma^0\Gamma^1\cdots\Gamma^9 Q_{L,R} = Q_{L,R}$. D$p$-branes are half-BPS objects, preserving the following supercharges

$$\epsilon_L Q_L + \epsilon_R Q_R \tag{3.78}$$

with $\epsilon_L = \mp\Gamma^0\Gamma^1\cdots\Gamma^p\epsilon_R$. ϵ_L and ϵ_R are spinors that have $16+16$ independent real components. In addition, anti-Dp-branes are defined as the Dp-branes that carry opposite Ramond-Ramond charges and preserve the other half of supercharges.

The solitonic fivebrane NS5-branes are similar to D-branes, preserving a half of supersymmetries but have much heavier tension $T_{\rm NS5} = 1/g_s^2 l_s^6$. NS5-branes couple magnetically to the $B^{(2)}_{\mu\nu}$ field in the NS-NS sector[2]. NS5-brane stretches in $(x^1,\cdots,x^5)$ and preserves the supersymmetry $\epsilon_L Q_L + \epsilon_R Q_R$, where spinors $\epsilon_{L,R}$ in type IIA string theory satisfy $\epsilon_L = \Gamma^0\Gamma^1\Gamma^2\Gamma^3\Gamma^4\Gamma^5\epsilon_L\,,\ \epsilon_R = \Gamma^0\Gamma^1\Gamma^2\Gamma^3\Gamma^4\Gamma^5\epsilon_R$, while the NS5-brane in type IIB string theory satisfies $\epsilon_L = \Gamma^0\Gamma^1\Gamma^2\Gamma^3\Gamma^4\Gamma^5\epsilon_L\,,\ \epsilon_R = -\Gamma^0\Gamma^1\Gamma^2\Gamma^3\Gamma^4\Gamma^5\epsilon_R$.

Branes can be regarded as boundaries of open strings. From gauge theory perspective, branes carry electric or magnetic charges, and are sources of higher form gauge fields. Recall that in the 4d electronic-magnetic field theory, the gauge field A_μ gives rise to the field strength $F = dA$. The associated equations of motion in the presence of monopoles or electrons are

$$dF = \delta^{(3)} \to \text{magnetic monopole}\,, \tag{3.79}$$

$$d*F = \delta^{(3)} \to \text{electric object}\,. \tag{3.80}$$

In $d > 4$ dimensions, there are higher form gauge fields. If the field strength F is a n-form field, then $*F$ is a $d-n$-form field. The higher dimensional charged objects are referred as branes. The corresponding equations of motions are as follows:

$$dF^{(n)} = \delta^{(n+1)} \quad \to \text{ magnetic monopole} \to \text{ D}(d-n-2)\text{-brane}\,, \tag{3.81}$$

$$d*F^{(n)} = \delta^{(d-n+1)} \to \text{ electric object} \quad \to \text{ D}(n-2)\text{-brane}\,. \tag{3.82}$$

The electric charge and magnetic charge are given by flux integrals

$$q_e = \int_{\text{D}(n-2)} *F^{(n)}\,,\quad q_m = \int_{\text{D}(d-n-2)} F^{(n)}\,. \tag{3.83}$$

Each higher form gauge field sources two types of charged objects (branes). The NS-NS (Neveu-Schwarz) fields and Ramond-Ramond fields in string theories source the following

[2]where the NS stands for Neveu-Schwarz.

branes:

$$\begin{aligned}
&C_{11}^{(3)} \xrightarrow{e} \text{M2}\,, && C_{11}^{(3)} \xrightarrow{m} \text{M5}\,,\\
&B_{10}^{(2)} \xrightarrow{e} \text{F1}\,, && B_{10}^{(2)} \xrightarrow{m} \text{NS5}\,,\\
&C_{10}^{(0)} \xrightarrow{e} \text{D}(-1)\,, && C_{10}^{(3)} \xrightarrow{m} \text{D7}\,,\\
&C_{10}^{(1)} \xrightarrow{e} \text{D0}\,, && C_{10}^{(1)} \xrightarrow{m} \text{D6}\,,\\
&C_{10}^{(2)} \xrightarrow{e} \text{D1}\,, && C_{10}^{(2)} \xrightarrow{m} \text{D5}\,,\\
&C_{10}^{(3)} \xrightarrow{e} \text{D2}\,, && C_{10}^{(3)} \xrightarrow{m} \text{D4}\,,\\
&C_{10}^{(4)} \xrightarrow{e} \text{D3}\,, && C_{10}^{(4)} \xrightarrow{m} \text{D3}\,.
\end{aligned} \tag{3.84}$$

In particular, we remind that the B-field in NS-NS sectors of string theory is self-dual and its field strength is denoted by $H = dB$. Its equations of motion and associated branes are

$$dH = \delta^{(4)} \to \text{NS5-brane}\,, \tag{3.85}$$

$$d * H = \delta^{(8)} \to \text{F1-brane}\,, \tag{3.86}$$

where F1-brane is the fundamental string in both type IIA and type IIB string theories. The F1-brane is special as it can end on any Dp-brane and provides a gauge field A_μ on the worldvolume of branes.

3.2.2 M-branes and D-branes

The low energy effective theory of M-theory is a 11 dimensional supergravity (SUGRA) with 32 supercharges and fields:

$$\text{a metric}\ \ G_{MN}\,,\ \ \text{a higher form gauge field}\ \ C^{(3)}_{MNP}\,,\ \ \text{fermonic fields}\ \ \psi^M_\alpha\,,\ \ \alpha = 0, 1, \ldots, 32\,.$$

The three-form $C^{(3)}_{MNP}$ implies that there are branes of 2 dimensional and 5 dimensional, namely M2-brane and M5-brane, which are charged electrically and magnetically respectively. Note that there is no string in M-theory.

The type IIA supergravity is obtained by the dimensional reduction of this 11 dimensional SUGRA on a circle S^1, and has $(1, 1)$ supersymmetry. Then the metric G_{MN} gives the metric $g_{\mu\nu}$, a gauge field A_μ and a dilaton $\phi = G_{10,10}$. The antisymmetric tensor $C^{(3)}_{MNP}$ gives rise to a three-form $C_{\mu\nu\lambda}$ and a two-form $B_{\mu\nu}$. The fields $(g_{\mu\nu}, B_{\mu\nu}, \phi)$ compose the NS-NS sector; A_μ and $C_{\mu\nu\lambda}$ compose the Ramond-Ramond (RR) sector. According to (3.84), the gauge field A_μ is sourced by D0-branes and D6-brane, and the higher form gauge field $C_{\mu\nu\lambda}$ is sourced electrically by D2-brane and magnetically by D4-brane. Type IIB supergravity has $(2, 0)$ supersymmetry. The NS-NS sector contains $(g_{\mu\nu}, B_{\mu\nu}, \phi)$, and the RR sector contains $(C^{(0)}, C^{(2)}, C^{(4)})$. The 4-form $C^{(4)}$ is self dual $*dC^{(4)} = dC^{(4)}$ and couples to D3-brane.

We summarize some possible branes in M-theory, type IIA and type IIB string theories as

follows:

$$\text{M-theory: M2 , M5 ,} \tag{3.87}$$

$$\text{type IIA: D0, F1, D2, D4, D6, D8, NS5 ,} \tag{3.88}$$

$$\text{type IIB: D(-1), F1, D1, D3, D5, D7, D9, NS5 .} \tag{3.89}$$

3.2.3 T-duality and S-duality

The T-duality and S-duality are important dualities, which connect different types of strings and brane configurations. The T-duality exchanges Kaluza-Klein momentum and winding number of strings, and also changes the types of branes[3]:

$$\text{D}p\text{-brane wrapped on } x^i \longleftrightarrow \text{D(p-1)-brane at a point of } x^i , \tag{3.90}$$

$$\text{type IIA NS5-brane wrapped on } x^i \longleftrightarrow \text{type IIB NS5-brane wrapped on } x^i . \tag{3.91}$$

Note that T-duality can be implemented on any x^i direction. The T-duality is the duality between type IIA string theory and type IIB string theory. The type IIA string theory can be considered as the dimensional reduction of M-theory compactified on a circle S^1; in other words, the M-theory is strong coupling limit of the type IIA string theory. If the M2-brane wrapps this circle S^1, one gets a F1 brane. If the M2-brane does not wrap this circle, one gets a D2-brane. Similarly, if the M5-brane wraps this circle, then we get D4 brane, and if not we get a NS5-brane.

As we have discussed before, type IIB string theory is dual to the M-theory compactified on a torus T^2 with a complex structure τ and vanishing area. This M/IIB-duality transfers the the $SL(2,\mathbb{Z})$ symmetry between field $B^{(2)}$ and $C^{(2)}$ in type IIB string theory, to the symmetry acting on (p,q)-brane webs. S-duality is the S-generator in this $SL(2,\mathbb{Z})$ global symmetry, which also acts on the complex structure of the dual M-theory compactified on a torus T^2. The S-duality is a strong-weak duality $\tau \to -1/\tau$, exchanging $B^{(2)} \leftrightarrow C^{(2)}$ and the types of branes:

$$\text{F1} \leftrightarrow \text{D1} , \quad \text{D3} \leftrightarrow \text{D3} , \quad \text{NS5} \leftrightarrow \text{D5} , \quad \text{D7} \to \text{D7} . \tag{3.92}$$

The NS5-brane and D5-brane are united by S-duality and hence we call them (p,q)-branes, where p is the electric charge and q is the magnetic charge, which are charged under $B^{(2)}$ and $C^{(2)}$ respectively. The strings stretching in (p,q)-brane webs are named (p,q)-strings which dual to M2-branes in M-theory. In particular, the $(1,0)$-string is the F1-brane and the $(0,1)$-string is the D1-brane. In 5d $\mathcal{N}=1$ gauge theories, the D1-brane contributes to instanton particles, while F1-brane contributes to W-bosons.

Moreover, the type IIB string theory has a complex string coupling

$$\tau = C_{10}^{(0)} + \frac{i}{g_s} , \qquad g_s = e^{\phi} , \tag{3.93}$$

[3]We quote the following description of T-duality from [73].

where ϕ is the dilation. This gauge coupling can be regarded as the complex structure of a torus T^2. At the non-perturbative region of type IIB string theory, one can artificially add such a torus T^2 at each point of the complex three manifold to construct a fourfold. This torus as the fiber has zero volume but a varying complex structure τ over the base threefold B_3. This fiber bundle is a Calabi-Yau fourfold $X_4 : T^2 \to B_3$, on which the F-theory lives [76, 77, 78].

3.2.4 Brane intersections

Brane action

In classical physics, gauge field couples to a electric charge q_e along its worldline:

$$q_e \int A = q_e \int A_\mu \frac{\partial x^\mu}{\partial \tau} d\tau = A_\mu J^\mu \,. \tag{3.94}$$

Similarly, B-field couples to a string with charge q on its worldvolume:

$$q \int B^{(2)} = q \int B_{\mu\nu} \frac{dx^\mu}{d\sigma^1} \frac{dx^\nu}{d\sigma^2} d^2\sigma = B_{\mu\nu} J^{\mu\nu} \tag{3.95}$$

In string theory, we have many Ramond-Ramond (RR) forms. The $p+1$-form $C^{(p+1)}$ plays the role of a gauge field and should couple electrically to the world volume of the Dp-brane:

$$S_{\text{int}} = \mu_p \int_{\text{D}p\text{-brane}} C^{(p+1)} \,, \tag{3.96}$$

where μ_p is the electric charge of the brane. In addition, the electric charge and magnetic are defined as

$$\mu_p = \int_{S^{d-p-2}} *F^{(p+2)} \,, \quad \mu_{d-p-4} = \int_{S^{p+2}} F^{(p+2)} \,, \tag{3.97}$$

where $F^{(p+2)} = dC^{(p+1)}$ and $d = 10$ in string theories. Therefore, the action (3.96) gives rise to a phase

$$\exp(iS_{\text{int}}) = \exp\left(i\mu_p \int C^{(p+1)}\right) = \exp(i\mu_p \, \mu_{d-p-4}) \,. \tag{3.98}$$

Using Dirac quantization condition, one can get a constraint

$$\mu_p \cdot \mu_{d-p-4} \in 2\pi\mathbb{Z} \,.$$

If including kinetic term and Chern-Simons term to the D-brane action, we have

$$S_{\text{brane}} = \frac{1}{2} \int_{X_d} F^{(p+2)} \wedge *F^{(p+2)} + i\mu_p \int_{\text{D}p\text{-brane}} C^{(p+1)} + \int_{X_d} C^{(p_a+1)} \wedge F^{(d-p_b-2)} \wedge F^{(p_b-p_a+1)} \,, \tag{3.99}$$

where X_d is the spacetime and $d = 10$. This brane action gives rise to the equation of motion

$$d *_d F^{(p_a+2)} = \mu_{p_a} \delta^{(d-p_a-1)} + F^{(d-p_b-2)} \wedge F^{(p_b-p_a+1)} , \tag{3.100}$$

from which one can read off possible cases of coupled branes. We show some coupled brane configurations in the following

$$\begin{aligned}
\text{type IIA}: \quad & \text{F1} - \text{D2}\,, \quad \text{D0} - \text{D2}\,, \\
& \text{F1} - \text{D4}\,, \quad \text{D2} - \text{D4}\,, \\
& \text{F1} - \text{D6}\,, \quad \text{D4} - \text{D6}\,, \quad \text{D4} - \text{D6}\,, \\
& \text{D0} - \text{NS5}\,, \quad \text{D2} - \text{NS5}\,, \quad \text{D4} - \text{NS5}\,, \quad \text{D6} - \text{NS5}\,, \\
\text{type IIB}: \quad & \text{F1} - \text{D1}\,, \\
& \text{F1} - \text{D3}\,, \quad \text{D1} - \text{D3}\,, \\
& \text{D1} - \text{D5}\,, \quad \text{D3} - \text{D5}\,, \\
& \text{F1} - \text{D7}\,, \quad \text{D5} - \text{D7}\,, \\
& \text{D1} - \text{NS5}\,, \quad \text{D3} - \text{NS5}\,, \quad \text{D5} - \text{NS5}\,.
\end{aligned} \tag{3.101}$$

These coupled branes in (3.101) are important for brane construction of gauge theories. In particular, F1-branes can end on any Dp-brane, and Dp-brane could end on particular types of branes:

$$\text{D}p - \text{D}(p+2)\,, \quad \text{D}p - \text{D}(p+4)\,, \quad \text{D}p - \text{NS5}\,. \tag{3.102}$$

Branes ending on branes

The Dp-brane stretching in the $(x^1, \ldots, x^p)$ hyperplane, is located at a point in $(x^{p+1}, \ldots, x^9)$. The open string moves with Neumann boundary conditions on directions $(x^1, \ldots, x^p)$, while with Dirichlet boundary conditions on $(x^{p+1}, \ldots, x^9)$ directions. We illustrate the D-brane and an open string in Figure 3.1. The coupled branes in (3.101) are the brane configurations that

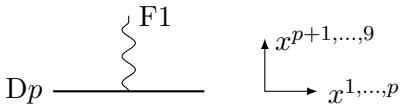

Figure 3.1: A F1-string ends on a Dp-brane.

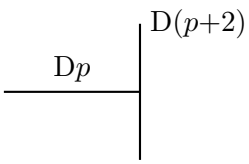

Figure 3.2: A Dp-brane ends on a D$(p+2)$-brane.

lower dimensional branes end on higher dimensional branes. We illustrate the Dp – D$(p+2)$

coupled brane in Figure 3.2.

The brane intersection in M-theory is also important. For a single M2-brane, the three-form $C^{(3)}$ lives on its worldvolume

$$\int_{\mathrm{M2}} C_{11}^{(3)} \,. \tag{3.103}$$

When a M2-brane ends on a M5-brane, we have the coupling

$$\int_{\mathrm{M5}} d^6x \; C_{11}^{(3)} \wedge H^{(3)} \tag{3.104}$$

where $H^{(3)} = dB^{(2)}$. The M2-M5 brane intersection is particularly interesting, on which there is a F1-string coupling with the two form $B^{(2)}$. We illustrate this brane configuration in Figure 3.2.4.

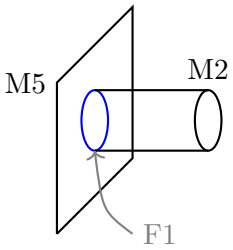

Figure 3.3: The intersection of M2-brane and M5-brane is a F1-string.

The supersymmetries on coupled brane configurations may be further broken. For the Dp-D(p+4) brane system, spinors satisfy $\epsilon_L = \Gamma^0\Gamma^1\cdots\Gamma^p\epsilon_R = \Gamma^0\Gamma^1\cdots\Gamma^{p+4}\epsilon_R$, and hence there is the constraint $\epsilon_R = \Gamma^{p+1}\cdots\Gamma^{p+4}\epsilon_R$. The total number of supercharges is broken from 32 to 8. One can relate $\mathrm{D}p-\mathrm{D}(p+4)$ to $\mathrm{D}p-\mathrm{D}(p+2)$ by compactification on a torus. This operation does not break supersymmetry as the torus is flat. Performing T-duality n-times relates $\mathrm{D}p-\mathrm{D}(p+2)$ to $\mathrm{D}(p+n)-\mathrm{D}(p+2+n)$. To reduce the number of supersymmetries from eight to four, one can add another stack of D-branes, for instance $\mathrm{D}p-\mathrm{D}(p+2)-\mathrm{D}(p+2)'$ with a relative angle between D($p+2$)-brane and D($p+2$)$'$-branes. Note that two NS5-branes with a relative angle could also break half of the supersymmetry. When this angle vanishes, the number of supersummetries recovered to eight. In order to get generic $\mathrm{D}p-\mathrm{NS5}$ brane intersection, one can begin with $\mathrm{D3}-\mathrm{D5}$, which after S-duality becomes $\mathrm{D3}-\mathrm{NS5}$; then one uses T-duality to map it to $\mathrm{D}p-\mathrm{NS5}$. The transformations between different types of brane intersectons are summarized as follows:

$$\mathrm{F1}-\mathrm{D3} \xrightarrow{S} \mathrm{D1}-\mathrm{D3} \xrightarrow{T} \mathrm{D}p-\mathrm{D}(p+2)\,, \tag{3.105}$$

$$\mathrm{D3}-\mathrm{D5} \xrightarrow{S} \mathrm{D3}-\mathrm{NS5} \xrightarrow{T} \mathrm{D}p-\mathrm{NS5}\,. \tag{3.106}$$

The corresponding brane configurations are

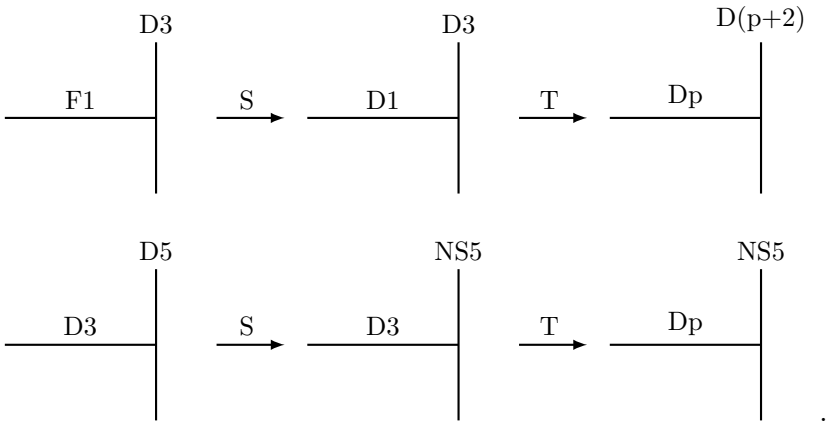

(3.107)

3.2.5 Vector multiplets and hypermultiplets

A simple brane configuration for constructing gauge theories is parallel branes. On the world-volume of N parallel Dp-branes lives a $\mathcal{N} = 4$ supersymmetric Yang-Mills theory with a gauge group $U(N)$, as illustrated in Figure 3.4. When Dp-branes are separated, the open strings

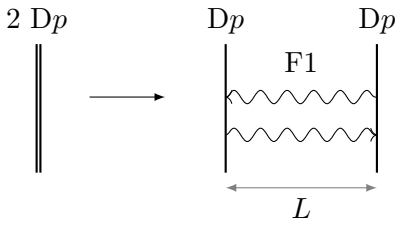

Figure 3.4: F1-strings connect parallel Dp-branes.

between parallel Dp-branes give rise to massive $W_{\pm}$-bosons and the gauge group breaks to $U(1)^N$. Inversely, when $W_{\pm}$ bosons become massless, the gauge group enhances to $U(N)$. In addition, on Dp-branes there is a gauge field $A_\mu\,, (\mu = 0, 1, \ldots, p-1)$ that comes from $B^{(2)} = dA^{(1)}$ since F1-strings end on Dp-branes, and $q - p$ scalars $(x^{p+1}, \ldots, x^9)$ describing the fluctuations of branes along transversal directions. These fields compose the bosonic part of the vector multiplet. Branes could describe Higgs mechanism. When the distance L between two parallel branes is not zero, then the gauge group $U(N)$ breaks to $U(1)^N$ with several massive W-bosons. When $L = 0$, the gauge group gets enhanced to $U(N)$. Note that there is no gauge field on the fundamental string.

The configuration that branes end on larger branes, encodes the fields in vector multiplets and hypermultiplets; hence it is very useful to construct supersymmetric gauge theories. In

the following, we discuss two basic cases $\mathrm{D}p - \mathrm{D}(p+2)$ and $\mathrm{D}p - \mathrm{NS5}$

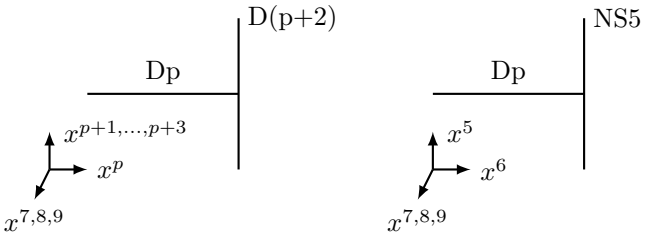

(3.108)

to identify the corresponding multiplets. Note that the gauge theory living on Dp-branes is p-dimensional.

For the $\mathrm{D}p - \mathrm{D}(p+2)$ brane configuration, the Dp-brane takes direction $(x^0, x^1, \ldots, x^p)$ and the D$(p+2)$-brane takes directions $(x^0, x^1, \ldots, x^p, x^{p+1}, x^{p+2}, x^{p+3})$. The bosonic part of the hypermultiplet contains three scalars $(x^{p+1}, x^{p+2}, x^{p+3})$ that parameterize the movement of Dp-brane along the D$(p+2)$-brane, and a gauge field $A_\mu\,(\mu = p)$ on the Dp-brane. The vector multiplet contains the $9-p$ scalars along directions $(x^{p+1}, \ldots, x^9)$ and a gauge field A_μ $(\mu = 0, 1, \ldots, p-1)$ on the Dp-brane. In particular, when $p = 3$, the S-duality exchanges NS5-brane and D5-brane; therefore in this case the hypermultiplet and vector multiplet are exchanged.

For the $\mathrm{D}p - \mathrm{NS5}$ brane configuration, the Dp-brane takes direction $(x^0, x^1, \ldots, x^{p-1}, x^6)$, and the NS5-brane takes directions $(x^0, x^1, \ldots, x^5)$. The hypermultiplet contains three scalars on (x^7, x^8, x^8) and the gauge field A_6. The vector multiplet contains $6-p$ scalars describing the movement of the boundary of Dp-brane on the NS5-brane, and the gauge field A_μ, $(\mu = 0, 1, \ldots, p-1)$ on the spacetime.

3.2.6 Hanany-Witten transitions

Hanany-Witten transition is found in [71], which is the phenomenon that when a brane cross other branes, some low dimensional branes may be created or annihilated without changing the underlying gauge theories. This process needs to follow the s-rule [71]. Hanany-Witten transition is powerful as it provide a way to manipulate brane webs, and many dualities in gauge theories can be interpreted as Hanany-Witten transitions, such as some dualities in 3d theories [46, 47].

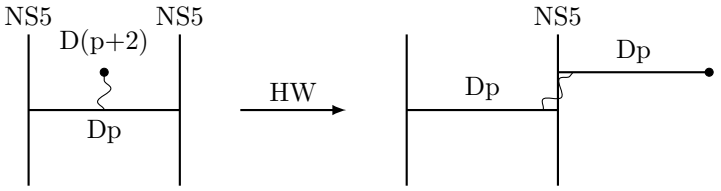

Figure 3.5: This figure illustrates the Hanany-Witten transitions of a D$(p+2)$-brane. When a flavor D$(p+2)$-brane moves to the right and crosses a NS5-brane, there should be one additional Dp-brane created. The fundamental hypermultiplet is given by the string stretching the Dp-brane and the D$(p+2)$-brane.

We follow the s-rule in order to preserve supersymmetry. If brane configurations do not follow the s-rule, then supersymmetry is broken. The s-rule is summarized as the follow: a NS5-brane and a D$(p+2)$-brane are connected by more than one Dp-brane is not supersymmetric. In other words, there can be at most one Dp-branes connecting a D$(p+2)$-brane and a NS5-brane.

The gauge coupling of the gauge theory is $1/g^2 = |t_j - t_i|$. The string stretching between a left Dp-brane and the right Dp-brane gives a hypermultiplet, whose mass parameter is the length of this string $|x_j - x_i|$. As illustrated in Figure 3.2.6, this fundamental hypermultiplet

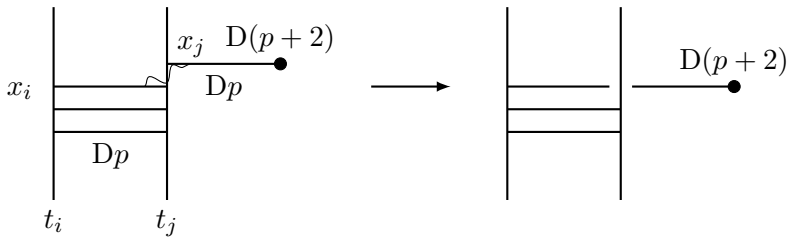

Figure 3.6: When the string becomes length zero, the Dp-branes on the two sides of NS5-brane merge into a single Dp-brane. This phenomenon is consistent with the s-rule.

becomes massless in the limit that two Dp-branes meet, where two Dp-branes join into one.

3.2.7 3d brane construction

In this subsection, we review the 3d brane webs for 3d $\mathcal{N} = 4\,, 2$ theories. We refer to [79] for more details.

In 3d $\mathcal{N} = 4$ theories, each $\mathcal{N} = 4$ hypermultiplet can be written as two $\mathcal{N} = 2$ chiral multiplets Q and $\tilde{Q}$ with charges 1 and -1 respectively. The $\mathcal{N} = 4$ vector multiplet consists a $\mathcal{N} = 2$ vector multiplet V and an adjoint chiral multiplet Φ. The R-symmetry is $SU(2)_R$ corresponding to the rotation symmetry on $x^{7,8,9}$. Vector multiplets are given by open strings connecting N_c D3-branes, and hypermultiplets are given by open strings connecting D3-brane and D5-branes sandwiching between two parallel NS5-branes. We show the brane construction for a 3d $\mathcal{N} = 4$ theory in Figure 3.7.

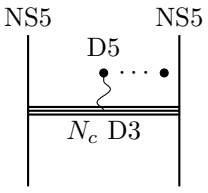

Figure 3.7: This brane system describes a 3d $\mathcal{N} = 4$ theory with a gauge group $U(N_c)$ and some hypermultiplets. The locations of these branes are shown in Table 3.1.

The 3d $\mathcal{N} = 4$ mirror symmetry is interpreted as the S-duality in (3.92) that exchange the D5-branes and NS5-branes. Hence the Coulumb branch moduli and Higgs branch moduli space are exchanged $\mathcal{M}_C \leftrightarrow \mathcal{M}_H$. The mass parameters and Fayet-Iliopoulos parameters

	0	1	2	3	4	5	6	7	8	9
NS5	–	–	–	–	–	–				
D3	–	–	–				–			
D5	–	–	–					–	–	–

Table 3.1: The common directions of these branes are $x^{0,1,2}$, which is the spacetime of 3d $\mathcal{N}=4$ theories.

are exchanged as well. In addition, the Coulomb branch is given by D-terms, and the Higgs branch is given by F-terms.

The brane system for a 3d $\mathcal{N}=2$ theories is shown in Figure 3.8, in which there is a relative angle between NS5-brane and NS5'-brane in the plane $x^{4,5}$. This angle breaks the number of supersymmetries from eight to four. The positions of branes is illustrated in Table 3.2.

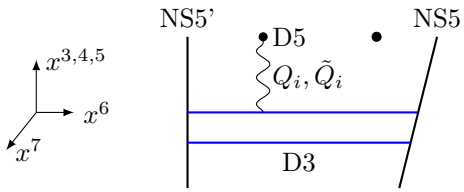

Figure 3.8: The brane web of the 3d $\mathcal{N}=2$ gauge theory with a gauge group $U(N)$ and chiral multiplets $(Q_i, \tilde{Q}_i)$.

	0	1	2	3	4	5	6	7	8	9
NS5	–	–	–	–	–	–				
NS5'	–	–	–	–					–	–
D3	–	–	–				–			
D5	–	–	–					–	–	–

Table 3.2: The directions of D3-branes, D5-branes and NS5 branes for 3d $\mathcal{N}=2$ brane webs.

Mass parameters, Fayet-Iliopoulos parameters and scalar fields are related to the relative positions of D3-banes and D5-branes. We summarize them as follows:

- x^3, the scalar fields σ_a in the vector multiplets on D3-branes.
- x^3, the position of i-th D5-brane corresponds to the real mass parameter m_i^{real}.
- $x^{4,5}$, the position of i-th D5-brane corresponds to the complex mass parameter m_i^{complex}.
- x^7, Fayet-Iliopulos (FI) parameter is the distance between NS5-barne and NS5'-brane.
- The open strings between D3-brane and i-th D5-brane give rise to a chiral multiplets Q_i and an antichiral multiplets $\tilde{Q}_i$.

In addition, there are two global symmetries $U(1)_{4,5}$ and $U(1)_{8,9}$, rotating the coordinates $x^{4,5}$ and $x^{8,9}$ respectively. We choose the global symmetry to be $U(1)_{8,9}$ as $U(1)_{4,5}$ is broken by turning on complex mass parameters. This global symmetry is the R-symmetry $U(1)_R$ in 3d

$\mathcal{N} = 2$ theories. There are Coulomb branch and Higgs branch as well, determined by D-term and F-term respectively.

3.2.8 $U(1)_k + N_F\mathbf{F} + N_{AF}\mathbf{AF}$

In this subsection, we show the 3d brane web for $U(1)_k + N_F\,\mathbf{F} + N_{AF}\,\mathbf{AF}$ in Figure 3.9, and discuss physical parameters encoded in the web. This theory is interesting, as it can be obtained by Higgsing 5d $\mathcal{N} = 1$ brane webs.

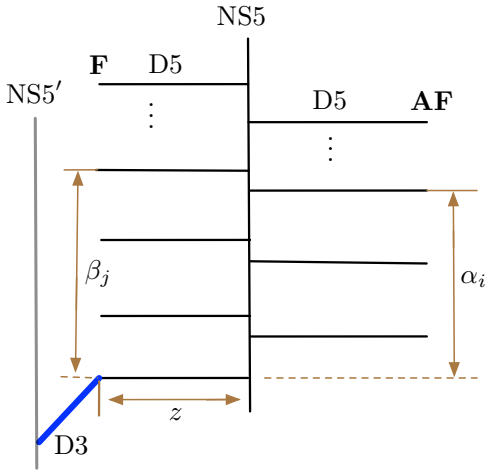

Figure 3.9: The D3-brane denoted by the blue line is perpendicular to the D5/NS5/NS5'-brane web. There is a relative angle θ between NS5-brane and NS5'-brane. This diagram is the 3d brane web for $U(1)_k + N_F\mathbf{F} + N_{AF}\mathbf{AF}$ in type IIB string theory.

This 3d brane web is dual to a toric Calabi-Yau threefold with a Lagrangian brane through M-theory/type IIB string duality. The matter content is given by open strings in this brane web. More explicitly, open strings connecting D3-brane and D5-brane on the left hand side of the NS5-brane give rise to fundamental chiral multiplets $N_F\mathbf{F}$, while the open strings connecting the D3-brane and D5-branes on the right hand side of NS5-brane give rise to anti-fundamental chiral multiplets $N_{AF}\mathbf{AF}$. Note that in this brane configuration, there is the freedom of putting D3-brane on any D5-branes on the left hand side of NS5-brane. These different positions of D3-branes compose the Higgs branch $\mathcal{M}_H$ determined by the vacua equation (3.13). In particular, the open string located at the D3-D5-brane intersection is of length zero, hence the corresponding $\mathbf{F}$ is massless; see e.g.[6]. From the gauge theory perspective, its real mass parameter is absorbed by shifting the kinetic term in (3.16).

The vortex partition function is interpreted as the open topological string amplitude. Hence implementing the topological vertex on the toric diagram shown in Figure 3.9, one can obtain its vortex partition function [80, 81, 10, 12, 82, 6], which in the unrefined limit $q = t$ takes form

$$Z^{\text{vortex}}_{U(1)_k+N_F\,\mathbf{F}+N_{AF}\,\mathbf{AF}}(z,\alpha,\beta) = \sum_{n=0}^{\infty} \frac{(-\sqrt{q})^{k^{\text{eff}}n^2} z^n}{(q,q)_n} \frac{(\alpha_1,q)_n\,(\alpha_2,q)_n \cdots (\alpha_{N_{AF}},q)_n}{(\beta_1,q)_n\,(\beta_2,q)_n \cdots (\beta_{N_F-1},q)_n}\,. \tag{3.109}$$

In chapter 5, we discuss its refined version.

Note that the mass parameter for fundamental chiral multiplet **F** is associated to β_i and for antifundamental chiral multiplet **AF** is associated to α_i. Real mass parameters are related to Kähler parameters by $\alpha_i = e^{im_i}$, $\beta_i = e^{i\tilde{m}_i}$. The Fayet-Iliopoulos parameter is encoded in z. We illustrate these parameters in Figure 3.9. The interpretation from M-theory perspective is that the open strings are given by M2-branes wrapping a chain of $\mathbb{P}^1$'s and a disk. The associated Kähler parameters are

$$z^n \prod_{i=1}^{N_{AF}} \prod_{j=1}^{N_F-1} \alpha_i^{d_i} \beta_j^{d_j} , \tag{3.110}$$

where (n, d_i, d_j) are degrees for (z, α_i, b_j), z is the open Kähler parameter, and α_i, β_j are closed Kähler parameters for **AF** and **F** respectively. The contributions of chiral multiplets **F** and **AF** to vortex partition functions are terms:

$$\mathbf{AF} \to (\alpha, q)_n , \quad \mathbf{F} \to \frac{1}{(\beta, q)_n} . \tag{3.111}$$

In particular, the term $(q, q)_n^{-1}$ in the vortex partition function (3.109) arises from the massless chiral multiplet **F** located at the D3-D5-brane intersection. In addition, one can decouple chiral multiplets by sending corresponding D5-branes to infinity.

3.2.9 Quiver generating series

It turns out that open topological string partition function can be written in the form of quiver motivic generating series. Originally this relation was found in the context of knot invariants that relate to open topological strings [83, 84]. It is then noticed that quivers also exist for open topological strings on strip Calabi-Yau threefolds in the presence of Lagrangian branes [10, 85, 86]. This subsection is based on [11].

In quiver representation theory, the motivic generating series associated to a symmetric quiver with $C_{ij} = C_{ji}$ takes form

$$P_{C_{ij}}(q; x_1, x_2, \ldots, x_N) = \sum_{d_1,\ldots,d_m=0}^{\infty} (-q^{1/2})^{\sum_{i,j=1}^N C_{ij} d_i d_j} \frac{x_1^{d_1} \cdots x_N^{d_N}}{(q, q)_{d_1} \cdots (q, q)_{d_N}}, \tag{3.112}$$

where x_i are variables. It is then shown that this generating series has the following product decomposition

$$P_{C_{ij}}(q; x_1, x_2, \ldots, x_N) = \prod_{d_1,\ldots,d_N=0} \prod_{j\in\mathbb{Z}} \prod_{n=0}^{\infty} \left(1 - q^{n+\frac{j-1}{2}} x_1^{d_1} \cdots x_m^{d_N}\right)^{(-1)^{j+1}\Omega_{d_1,\ldots,d_N;j}} , \tag{3.113}$$

where $\Omega_{d_1,\ldots,d_N;j}$ are integer motivic Donaldson-Thomas (DT) invariants [87, 88]. In some cases, motivic DT invariants can be refined. In particular, for the strip Calabi-Yau threefold with one Lagrangain brane, refined motivic DT invariants are equal to refined Ooguri-Vafa

invariants

$$\Omega^{(j,r)}_{d_1,\ldots,d_N} = N^{(j,r)}_{d_1,\ldots,d_N}\,, \tag{3.114}$$

For more details, see section 4.2.1 or [10].

The open partition function (3.109) can be written in terms of the form (3.112):

$$Z^{\text{vortex}}(z,\alpha,\beta) = Z_0 \cdot P_{C_{ij}}(x_1,\cdots,x_N)\,, \tag{3.115}$$

where Z_0 relates to one-loop contributions of chiral multiplets that we will discuss in chapter 5. Note that the product decomposition (3.113) is analogous to the product decomposition of the open topological string partition function (4.17). In chapter 4 we show that refined open string partition functions for strip Calabi-Yau threefolds can also be written in the quiver form with appropriate identification of x_i with closed and open Kähler parameters.

More explicitly, to write (3.109) in terms of quiver forms, we need to expand each Pochhammer product:

$$(\alpha_i,q)^{\pm}_n \sim \sum_{d_i=0}^{\infty}(-\sqrt{q})^{C_{0,0}[\alpha_i]n^2+2C_{0,i}[\alpha_i]nd_i+C_{ii}[\alpha_i]d_i^2}\frac{x_i^{d_i}}{(q,q)_n}\,, \tag{3.116}$$

where $C_{..}[\alpha_i]$ denotes the coefficients in front of the degrees n, d_i. There are two equivalent ways to expand Pochhammer products:

$$(\alpha_i;q)_n = \frac{(\alpha_i,q)_\infty}{(\alpha_i q^n,q)_\infty} = (\alpha_i,q)_\infty\sum_{d_i=0}^{\infty}(-\sqrt{q})^{2\,nd_i}\frac{\alpha_i^{d_i}}{(q;q)_{d_i}} \tag{3.117}$$

$$= (\alpha_i,q)_\infty\,(\alpha_i/\sqrt{q})^n\sum_{d_i=0}^{\infty}(-\sqrt{q})^{n^2-2\,nd_i+d_i^2}\frac{(\sqrt{q}\alpha_i^{-1})^{d_i}}{(q;q)_{d_i}}\,, \tag{3.118}$$

$$\frac{1}{(\beta_j;q)_n} = \frac{(\beta_j q^n,q)_\infty}{(\beta_j,q)_\infty} = \frac{1}{(\beta_j,q)_\infty}\sum_{d_j=0}^{\infty}(-\sqrt{q})^{2nd_j+d_j^2}\frac{\left(\frac{\beta_j}{\sqrt{q}}\right)^{d_j}}{(q;q)_{d_i}} \tag{3.119}$$

$$= \frac{1}{(\beta_j,q)_\infty}(\sqrt{q}/\beta_j)^n\sum_{d_j=0}^{\infty}(-\sqrt{q})^{-n^2-2nd_j}\frac{\left(q\,\beta_j^{-1}\right)^{d_j}}{(q;q)_{d_i}}\,. \tag{3.120}$$

To get the quiver generating series, we denote the contribution of each q-Pochhammer product by

$$(\alpha_i,q)^{\pm}_n \to \left(\begin{bmatrix} C_{0,0}[\alpha_i] & \ldots & C_{0,i}[\alpha_i] \\ \vdots & \ddots & \vdots \\ C_{i,0}[\alpha_i] & \ldots & C_{i,i}[\alpha_i] \end{bmatrix},\ x_i\right), \tag{3.121}$$

where all the elements denoted by "$\cdots$" in the above matrices are zero, and x_i are expansion

variables. The quiver C_{ij} is the combination of them

$$C_{ij} = C_{..}[z] + \sum_i C_{..}[\alpha_i] + \sum_j C_{..}[\beta_j]\,. \tag{3.122}$$

The contribution from each **F** is

$$(\alpha_i;q)_n \to \Big(\begin{bmatrix} 0 & \dots & 1 \\ \vdots & \ddots & \vdots \\ 1 & \cdots & 0 \end{bmatrix},\ \alpha_i\Big)\,, \quad \text{or} \quad \Big(\begin{bmatrix} 1 & \cdots & -1 \\ \vdots & \ddots & \vdots \\ -1 & \cdots & 1 \end{bmatrix},\ \sqrt{q}\,\alpha_i^{-1}\Big)\,, \tag{3.123}$$

and the contribution from each **AF** is

$$\frac{1}{(\beta_j;q)_n} \to \Big(\begin{bmatrix} 0 & \cdots & 1 \\ \vdots & \ddots & \vdots \\ 1 & \cdots & 1 \end{bmatrix},\ \frac{\beta_j}{\sqrt{q}}\Big)\,, \quad \text{or} \quad \Big(\begin{bmatrix} -1 & \cdots & -1 \\ \vdots & \ddots & \vdots \\ -1 & \cdots & 0 \end{bmatrix},\ \sqrt{q}\left(\frac{\beta_j}{\sqrt{q}}\right)^{-1}\Big)\,. \tag{3.124}$$

Therefore the quivers for (3.109) are not unique.

Chapter 4

Strip geometry with a Lagrangian brane

The computation of refined open topological string amplitudes is a challenging problem. Refined BPS invariants associated to the knots on the deformed conifold have been discussed in [89]. However the computation method of refined invariants has not been found for generic toric manifolds with Lagrangian branes. In literature, geometric transition is extensively used in gauge theories [6, 10, 81, 80, 90, 91, 34, 92], which usually gives rise to theories on surface defects. Inspired by this, we study refined open topological string amplitudes for a large class of strip Calabi-Yau threefolds, using refined geometric transition (Higgsing) and Nekrasov factors. More explicitly, we first use refined topological vertex [30, 37, 6] to compute refined closed partition functions of toric diagrams, and then apply Higgsing. The Higgsing procedure amounts to giving specific values to some Kähler parameters, so that refined closed amplitudes are reduced to refined open amplitudes associated to different types of refined open Lagrangian branes, from which one can extract refined invariants for open BPS states. We verify the integrality of these BPS invariants for some toric Calabi-Yau manifolds, and find different types of refined topological branes are equivalent under an exchange symmetry and flop transitions. Since refined geometric transitions introduce refined topological branes to toric diagrams, our methods can be considered as the generalization of the refined topological vertex formalism.

We focus on strip Calabi-Yau threefolds with nontrivial open topological string sector as well as non-toric strip Calabi-Yau threefolds that have some overlapped lines on corresponding toric diagrams. We show that for these manifolds refined open amplitudes take form of quiver generating series. The underlying quivers encode Donaldson-Thomas invariants [87, 88]. The existence of quivers in open topological strings was originally found in knot theories [83, 84]. Its relations with 3d gauge theories were conjectured in [93, 94], and (still in the unrefined case) were generalized to strip geometries with a Lagrangian brane in [85, 86]. We show that the refinement does not change the quiver structure. This implies some particular structure of refined BPS invariants. Namely, open BPS invariants can be expressed in terms of motivic Donaldson-Thomas invariants.

On the other hand, topological string theories relate to gauge theories, thanks to geometric

engineering. The open-closed topological string amplitudes encode the partition functions of 5d $\mathcal{N}=1$ gauge theories with surface defects [2, 95]. From this viewpoint one can perform Hanany-Witten transitions that involve the movement of 7-branes. The Hanany-Witten transitions create or annihilate 5-branes when 7-branes cross other 5-branes [71, 96, 40, 36]. Open topological string partition functions for brane webs related by Hanany-Witten transitions should be equivalent. We find that this argument is almost correct upon taking into account the fact that Hanany-Witten transitions introduce certain open string states, which is a new phenomenon that does not exist in closed topological strings.

This chapter is based on [10]. In section 4.1 we give an introduction to the refined geometric transition and discuss its connection to Nekrasov functions. We also discuss refined Ooguri-Vafa (OV) formulas. In section 4.2 we compute refined open amplitudes for strip geometries, and extract refined Ooguri-Vafa invariants and quivers. In section 4.3 we discuss Hanany-Witten transitions for non-toric strip geometries in the presence of an open topological brane. In section 4.4 we compute refined open amplitudes for toric diagrams with compact four-cycles and find that open BPS invariants are positive integers.

4.1 Refined geometric transitions and Lagrangian branes

Geometric transition is the open-closed duality in the A-model, connecting open and closed topological strings, which is accompanied by the transformation of local conifolds in Calabi-Yau manifolds [7]. As proposed in [6, 97], geometric transitions can be used to introduce surface defects engineered by Lagrangian branes in the A-model. In this context and from the viewpoint of 5d $\mathcal{N}=1$ gauge theories, geometric transitions play the role of Higgsing, which tune the 5d theories to some roots of the Higgs branch. The theory on the defect is the 3d $\mathcal{N}=2$ theory.

In the Ω-deformed background, rotations of complex coordinates z_1 and z_2 are parametrized respectively by $q=e^{-\epsilon_2}$ and $t=e^{\epsilon_1}$

$$(z_1,z_2)\to(qz_1,t^{-1}z_2), \tag{4.1}$$

and correspondingly there are four types of Lagrangian branes. The Lagrangian brane along z_1 is called a q-brane, and the Lagrangian brane along z_2 is called a $\bar{t}$-brane (anti-t-brane); there exist also their partner $\bar{q}$-brane and t-brane. In this section we show how to identify all these branes through analysis of geometric transitions and Nekrasov factors that arise in topological string partition functions, and discuss relations between them.

The crucial feature of the geometric transition is that closed topological string partition functions with certain Kähler parameters tuned to specific values Q^* can be identified as open topological string partition functions. The presence of a Lagrangian brane with open modulus z is identified with one Kähler parameter Q before the transition

$$Z^{\text{closed}}(Q,Q^*,t,q)=Z^{\text{open}}(z,t,q). \tag{4.2}$$

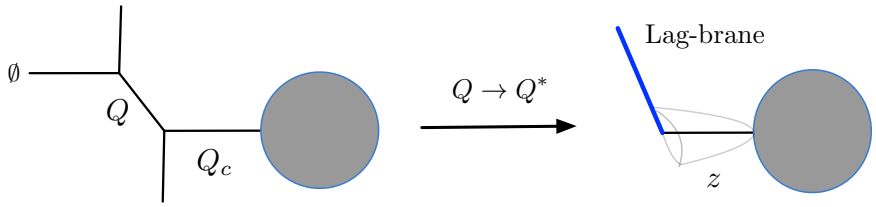

Figure 4.1: Geometric transition turns closed topological strings to open topological strings, which is interpreted as tuning the Kähler parameter Q of a resolved conifold to some specific value Q^*. Geometric transition (Higgsing) results in a simpler geometry with a Lagrangian brane with open Kähler parameter $Q_c = z$. The gray circle represents the remaining part of the toric diagram.

We illustrate this geometric transition in Figure 4.1, where one particular closed string Kähler parameter Q_c is identified as an open Kähler parameter z for a Lagrangian brane after the geometric transition (or, equivalently, as the FI parameter of vortex particles in the 3d $\mathcal{N} = 2$ gauge theory on the surface defect). In general, such specific values Q^* can be determined through constraints involving the half-Nekrasov factors $N_\nu^{\text{half},\pm}(Q^*, t^{-1}, q^{-1})$ that appear in closed topological string partition functions. If no Lagrangian brane is created during the geometric transition, the Kähler parameter $Q^* = (q/t)^{\pm 1/2}$ is fixed through the constraints

$$N_\nu^{\text{half},+}\left(\sqrt{\frac{q}{t}};\ t^{-1}, q^{-1}\right) = \begin{cases} 1 & \nu = \emptyset \\ 0 & \nu \neq \emptyset \end{cases}, \qquad N_{\nu^T}^{\text{half},-}\left(\sqrt{\frac{t}{q}};\ t^{-1}, q^{-1}\right) = \begin{cases} 1 & \nu = \emptyset \\ 0 & \nu \neq \emptyset \end{cases}. \tag{4.3}$$

If a single Lagrangian brane is created, the constraints on half-Nekrasov factors take form

$$\begin{aligned} N_\nu^{\text{half},+}\left(q\sqrt{\frac{q}{t}};\ \frac{1}{t}, \frac{1}{q}\right) &\neq 0 \qquad \text{only if} \quad \nu = \{n\}_A\,, \\ N_\nu^{\text{half},+}\left(\frac{1}{t}\sqrt{\frac{q}{t}};\ \frac{1}{t}, \frac{1}{q}\right) &\neq 0 \qquad \text{only if} \quad \nu = \{n\}_S\,, \\ N_\nu^{\text{half},-}\left(t\sqrt{\frac{t}{q}};\ \frac{1}{t}, \frac{1}{q}\right) &\neq 0 \qquad \text{only if} \quad \nu = \{n\}_S\,, \\ N_\nu^{\text{half},-}\left(\frac{1}{q}\sqrt{\frac{t}{q}};\ \frac{1}{t}, \frac{1}{q}\right) &\neq 0 \qquad \text{only if} \quad \nu = \{n\}_A\,, \end{aligned} \tag{4.4}$$

where $\nu = \{n\}_A$ and $\nu = \{n\}_S$ denote respectively antisymmetric and symmetric representations, whose Young diagrams are shown in (A.22). These conditions fix four possible values of Q^* which we identify with four types of Lagrangian branes mentioned above

$$\begin{aligned} q\text{-brane}: &\quad Q^* = q\sqrt{\frac{q}{t}}\,, \qquad t\text{-brane}: \quad Q^* = t\sqrt{\frac{t}{q}}\,, \\ \bar{q}\text{-brane}: &\quad Q^* = \frac{1}{q}\sqrt{\frac{t}{q}}\,, \qquad \bar{t}\text{-brane}: \quad Q^* = \frac{1}{t}\sqrt{\frac{q}{t}}\,. \end{aligned} \tag{4.5}$$

This identification is consistent with the Lagrangian branes in the refined Chern-Simon theory [34]. In fact, for these special values of Q^*, the above half-Nekrasov factors can be expressed

in terms of q-Pochhammers $(x;q)_n = \prod_{i=0}^{n-1}(1-xq^i)$:

$$\begin{aligned}
N^{\text{half},+}_{\{n\}_A}\left(q\sqrt{\frac{q}{t}};\ \frac{1}{t},\frac{1}{q}\right) &= (q;t)_n\,,\\
N^{\text{half},+}_{\{n\}_S}\left(\frac{1}{t}\sqrt{\frac{q}{t}};\ \frac{1}{t},\frac{1}{q}\right) &= \left(\frac{1}{t};\frac{1}{q}\right)_n\,,\\
N^{\text{half},-}_{\{n\}_S}\left(t\sqrt{\frac{t}{q}};\ \frac{1}{t},\frac{1}{q}\right) &= (t;q)_n\,,\\
N^{\text{half},-}_{\{n\}_A}\left(\frac{1}{q}\sqrt{\frac{t}{q}};\ \frac{1}{t},\frac{1}{q}\right) &= \left(\frac{1}{q};\frac{1}{t}\right)_n\,.
\end{aligned} \tag{4.6}$$

For future reference, we also note the following results for $\nu = \{n\}_A$:

$$\begin{aligned}
&|\nu| = n, \quad ||\nu||^2 = n, \quad ||\nu^T||^2 = n^2, \quad \tilde{Z}_\nu(t,q) = \frac{1}{(t;t)_n}, \quad \tilde{Z}_\nu(q,t) = \frac{1}{(q;q)_n},\\
&N^{\text{half},+}_\nu(Q,t^{-1},q^{-1}) = \left(Q\sqrt{\frac{t}{q}};t\right)_n, \quad N^{\text{half},-}_\nu(Q,t^{-1},q^{-1}) = \left(Q\sqrt{\frac{q}{t}};\frac{1}{t}\right)_n,
\end{aligned} \tag{4.7}$$

and analogous results for $\nu = \{n\}_S$:

$$\begin{aligned}
&|\nu| = n, \quad ||\nu||^2 = n^2, \quad ||\nu^T||^2 = n, \quad \tilde{Z}_\nu(t,q) = \frac{1}{(t;q)_n}, \quad \tilde{Z}_\nu(q,t) = \frac{1}{(q;t)_n},\\
&N^{\text{half},+}_\nu(Q,t^{-1},q^{-1}) = \left(Q\sqrt{\frac{t}{q}};\frac{1}{q}\right)_n, \quad N^{\text{half},-}_\nu(Q,t^{-1},q^{-1}) = \left(Q\sqrt{\frac{q}{t}};q\right)_n.
\end{aligned} \tag{4.8}$$

Some other useful identities involving Nekrasov factors are listed in appendix A.1.

Having identified four types of Lagrangian branes, we now show that they are related by two types of operations. First, there is an exchange symmetry $q \to t^{-1}$ that relates t-brane to $\bar{q}$-brane and q-brane to $\bar{t}$-brane. Second, q-brane and t-brane are related to their anti-branes by flop transitions. The flop transition turns out to be the shift of open Kähler parameters. We argue that the flop transition preserves for open topological strings, and open topological branes (Lagrangian branes) are equivalent to their anti-branes in our context. The relations are summarized in the following diagram:

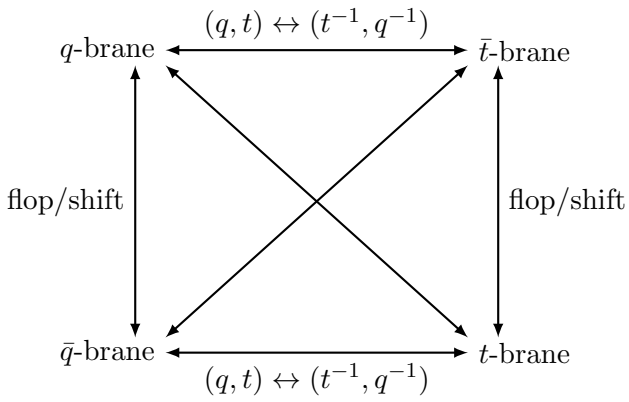

(4.9)

The exchange symmetry $q \leftrightarrow t^{-1}$ is a consequence of a relation between half-Nekrasov

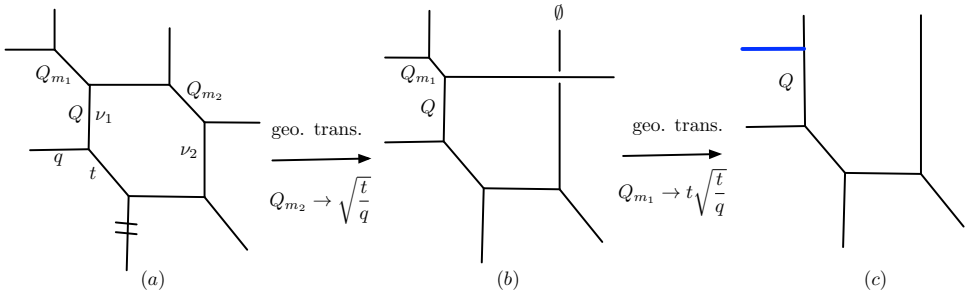

Figure 4.2: Geometric transitions can be used to engineer insertions of topological branes upon a specific choice of Kähler parameters Q^* that appear in Nekrasov factors. In this example, a toric Calabi-Yau manifold in (a) that engineers $SU(2)$ with three massive fundamental hypermultiples, which after two geometric transitions and the appropriate choice of Kähler parameters is reduced to a double-$\mathbb{P}^1$ strip geometry with an insertion of a Lagrangian brane in (c).

factors

$$N_{\nu}^{\text{half},+}\left(Q;t^{-1},q^{-1}\right) = N_{\nu^T}^{\text{half},-}\left(Q;q^{-1},t^{-1}\right), \tag{4.10}$$

which implies the equality of open partition functions

$$\begin{aligned} Z_{q\text{-brane}}(z,Q;t,q) &= Z_{\bar{t}\text{-brane}}\left(z,Q;q^{-1},t^{-1}\right), \\ Z_{t\text{-brane}}(z,Q;t,q) &= Z_{\bar{q}\text{-brane}}\left(z,Q;q^{-1},t^{-1}\right), \end{aligned} \tag{4.11}$$

where z is the open parameter and Q are closed Kähler parameters. We verified above relations in numerous examples. This exchange symmetry was found independently in [34] by the analysis of the partition function of refined Chern-Simon theory on S^3. On the other hand, the flop transition leads to the following relations between partition functions for topological branes and anti-branes that involve a shift of the open Kähler parameter z

$$\begin{aligned} Z_{q\text{-brane}}\Big(z\,\frac{1}{q}\sqrt{\frac{t}{q}},Q;t,q\Big) &= Z_{\bar{q}\text{-brane}}\left(z,Q;t,q\right), \\ Z_{t\text{-brane}}\Big(z\,\frac{1}{t}\sqrt{\frac{q}{t}},Q;t,q\Big) &= Z_{\bar{t}\text{-brane}}\left(z,Q;t,q\right). \end{aligned} \tag{4.12}$$

We can also combine the exchange symmetry and the flop transition, which yields the following relations

$$\begin{aligned} Z_{q\text{-brane}}\Big(z\;t\sqrt{\frac{t}{q}},Q;\frac{1}{q},\frac{1}{t}\Big) &= Z_{t\text{-brane}}\left(z,Q;t,q\right), \\ Z_{t\text{-brane}}\Big(z\;q\sqrt{\frac{q}{t}},Q;\frac{1}{q},\frac{1}{t}\Big) &= Z_{q\text{-brane}}(z,Q;t,q). \end{aligned} \tag{4.13}$$

Note that upon taking the unrefined limit $q = t$ we are left with two types of branes, q-brane and t-brane, which are related by $q \to 1/q$, and thus can be identified with a topological brane and its anti-brane.

Let us illustrate the above considerations in a more involved example, shown in Figure 4.2. In this case, there are terms $N_{\nu_1}^{\text{half},-}(Q_{m_1};t^{-1},q^{-1})$ and $N_{\nu_2}^{\text{half},-}(Q_{m_2};t^{-1},q^{-1})$ in the closed partition function. If we want to introduce a Lagrangian brane at the position where the local resolved conifold has the Kähler parameter Q_{m_1}, we have to set $Q_{m_1} = t\sqrt{\frac{t}{q}}$ or $\frac{1}{q}\sqrt{\frac{t}{q}}$ and $Q_{m_2} = \sqrt{\frac{t}{q}}$ because of constraints (4.3) and (4.4). This identifies the resulting brane as a t-brane or a $\bar{q}$-brane.

Finally, we stress that the above identification of q-branes or t-branes is defined in the assignment of q and t to toric legs presented in Figure 2.10. If one changes the assignment $(q,t) \leftrightarrow (t,q)$ then the the definition of open topological branes are changed.

For future reference, let us classify all possible choices of preferred directions in a local resolved conifold and the resulting identification of topological branes. First, for a horizontal preferred direction we get

(a) 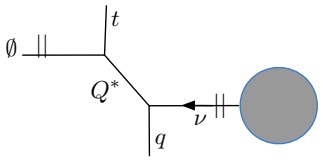

$N_{\nu}^{\text{half},+}(Q^*;t^{-1},q^{-1})\,, \quad Q^* = \begin{cases} q\sqrt{\frac{q}{t}} & q\text{-brane} \quad \nu = \{n\}_A \\ \frac{1}{t}\sqrt{\frac{q}{t}} & \bar{t}\text{-brane} \quad \nu = \{n\}_S \end{cases}$

(b) 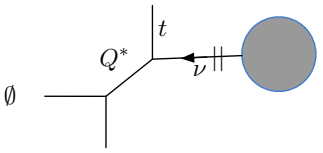

$N_{\nu}^{\text{half},-}(Q^*;t^{-1},q^{-1})\,, \quad Q^* = \begin{cases} t\sqrt{\frac{t}{q}} & t\text{-brane} \quad \nu = \{n\}_S \\ \frac{1}{q}\sqrt{\frac{t}{q}} & \bar{q}\text{-brane} \quad \nu = \{n\}_A \end{cases}$

. (4.14)

For vertical preferred direction we find

(c) 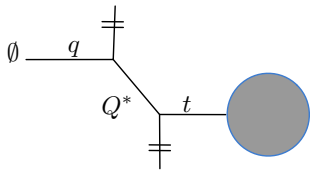

$Q^* = \begin{cases} q\sqrt{\frac{q}{t}} & q\text{-brane} \quad \nu = \{n\}_A \\ \frac{1}{t}\sqrt{\frac{q}{t}} & \bar{t}\text{-brane} \quad \nu = \{n\}_S \end{cases}$

(d) 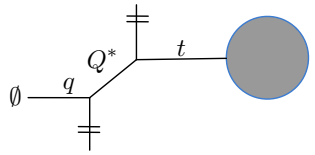

$Q^* = \begin{cases} t\sqrt{\frac{t}{q}} & t\text{-brane} \quad \nu = \{n\}_S \\ \frac{1}{q}\sqrt{\frac{t}{q}} & \bar{q}\text{-brane} \quad \nu = \{n\}_A \end{cases}$

. (4.15)

Finally, for the third choice of preferred direction, we get

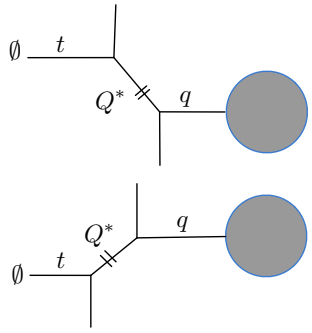

$$Q^* = \begin{cases} q\sqrt{\frac{q}{t}} & q\text{-brane} \quad \nu = \{n\}_A \\ \frac{1}{t}\sqrt{\frac{q}{t}} & \bar{t}\text{-brane} \quad \nu = \{n\}_S \end{cases} \qquad Q^* = \begin{cases} t\sqrt{\frac{t}{q}} & t\text{-brane} \quad \nu = \{n\}_S \\ \frac{1}{q}\sqrt{\frac{t}{q}} & \bar{q}\text{-brane} \quad \nu = \{n\}_A \end{cases} \tag{4.16}$$

.

Refined Ooguri-Vafa formula

M-theory interpretation of topological strings leads to integrality properties of open BPS invariants (Ooguri-Vafa invariants) encoded in refined open amplitudes, which however have not been systematically analyzed in literature. One goal of this chapter is to reveal that these invariants in M-theory realization also count appropriate BPS states for a wide class of Calabi-Yau manifolds; see also e.g. [6].

In our context, for a t-brane, the refined open amplitude takes form

$$\begin{aligned} Z_{t\text{-brane}}(z,Q,t,q) &= \prod_{\beta\in H_2(X,L,\mathbb{Z})}\prod_{s,r\in\mathbb{Z}/2}\prod_{n=0}^{\infty}\left(1-q^{-s+n+\frac{1}{2}}t^{r+\frac{1}{2}}\,Q_\beta\right)^{(-1)^{2s}N_\beta^{(s,r)}} \\ &= \exp\Big(\sum_{\beta\in H_2(X,L,\mathbb{Z})}\sum_{s,r\in\mathbb{Z}/2}\sum_{n=1}^{\infty}\frac{(-1)^{2s}N_\beta^{(s,r)}q^{-ns}t^{n\left(r+\frac{1}{2}\right)}}{n\left(q^{n/2}-q^{-n/2}\right)}Q_\beta^n\Big) \\ &= \prod_{\beta\in H_2(X,L,\mathbb{Z})}\prod_{s,r\in\mathbb{Z}/2}\mathrm{PE}\left[\frac{(-1)^{2s}N_\beta^{(s,r)}q^{-s}t^{r+\frac{1}{2}}}{q^{\frac{1}{2}}-q^{-\frac{1}{2}}}Q_\beta\right] \\ &\equiv \prod_{\beta\in H_2(X,L,\mathbb{Z})}\prod_{s,r\in\mathbb{Z}/2}\mathrm{PE}\Big[z^dQ_\beta,N_\beta^{(s,r)},s,r\Big]_{t\text{-brane}}, \end{aligned} \tag{4.17}$$

where Q^β are closed Kähler parameters of Calabi-Yau manifold X, z is the open parameter associated to the Lagrangian brane, and $N_\beta^{(s,r)}$ are refined open BPS invariants (refined Ooguri-Vafa invariants). We introduce a shorter notation $\mathrm{PE}\Big[z^dQ^\beta,N_\beta^{(s,r)},s,r\Big]_{*\text{-brane}}$ to denote plethystic exponents. Note that for a t-brane, the contribution from each open BPS state takes form

$$\mathrm{PE}\Big[z^dQ^\beta,N_\beta^{(s,r)},s,r\Big]_{t\text{-brane}} = \left(q^{-s+\frac{1}{2}}t^{r+\frac{1}{2}}Q_\beta,q\right)_\infty^{(-1)^{2s}N_\beta^{(s,r)}}. \tag{4.18}$$

Once we presented an integral expansion for a t-brane, we can use (4.11) and (4.12) to write down analogous expansions for other types of branes. Note that four types of Lagrangian branes have the same refined open BPS invariants.

For a $\bar{q}$-brane, using the exchange symmetry $q \to t^{-1}$ we get its refined formula

$$\begin{aligned} Z_{\bar{q}\text{-brane}} &= \prod_{\beta\in H_2(X,L,\mathbb{Z})} \prod_{s,r\in\mathbb{Z}/2} \prod_{n=0}^{\infty} \left(1 - t^{s-n-\frac{1}{2}} q^{-r-\frac{1}{2}}\, Q_\beta\right)^{(-1)^{2s} N_\beta^{(s,r)}} \\ &= \prod_{\beta\in H_2(X,L,\mathbb{Z})} \prod_{s,r\in\mathbb{Z}/2} \mathrm{PE}\left[\frac{(-1)^{2s+1} N_\beta^{(s,r)} t^s q^{-r-\frac{1}{2}}}{t^{\frac{1}{2}} - t^{-\frac{1}{2}}} Q_\beta\right] \\ &\equiv \prod_{\beta\in H_2(X,L,\mathbb{Z})} \prod_{s,r\in\mathbb{Z}/2} \mathrm{PE}\Big[z^d Q^\beta, N_\beta^{(s,r)}, s, r\Big]_{\bar{q}\text{-brane}}, \end{aligned} \tag{4.19}$$

where

$$\mathrm{PE}\Big[z^d Q^\beta, N_\beta^{(s,r)}, s, r\Big]_{\bar{q}\text{-brane}} = \Big(t^{s-\frac{1}{2}} q^{-r-\frac{1}{2}} Q_\beta, 1/t\Big)_\infty^{(-1)^{2s} N_\beta^{(s,r)}}. \tag{4.20}$$

We can reformulate the refined Ooguri-Vafa formula for $\bar{q}$-brane as follows

$$\begin{aligned} Z_{\bar{q}\text{-brane}} &= \exp\left[\sum_{\beta\in H_2(X,L,\mathbb{Z})} \sum_{s,r\in\mathbb{Z}/2} \sum_{n=1}^{\infty} -\frac{(-1)^{2s+2r} t^{-ns} \left(\frac{t}{q}\right)^{n\,r} N_\beta^{(s,r)}}{n\left(t^{\frac{n}{2}} - t^{-\frac{n}{2}}\right)}\, Q_\beta^n\right] \\ &= \mathrm{PE}\left[\sum_{\beta\in H_2(X,L,\mathbb{Z})} \sum_{s,r\in\mathbb{Z}/2} -\frac{(-1)^{2s+2r} t^{-s} \left(\frac{t}{q}\right)^{r} N_\beta^{(s,r)}}{\left(t^{\frac{1}{2}} - t^{-\frac{1}{2}}\right)}\, Q_\beta^n\right], \end{aligned} \tag{4.21}$$

where we have shifted s and r.

In what follows, we read off open BPS invariants $N_\beta^{(s,r)}$ from the above product expansions of open topological string partition functions; for example, a factor $(z\sqrt{qt}, q)_\infty$ encodes the open BPS invariant $N_z^{(0,0)} = 1$.

Finally, we stress that all formulas presented above are relevant in the assignment of q and t to the lines on toric diagrams presented in Figure 2.10. The alternative assignment is the opposite assignment of q and t, namely exchanging $q \leftrightarrow t$. The Ooguri-Vafa formula in the above should be modified. We consider first the formula (4.17). Exchanging the assignment of q and t changes the Higgsing value of a t-brane to $q\sqrt{\frac{q}{t}}$ and makes it natural to use $s' = -s, r' = -r-1$, so that (4.17) is transformed into

$$Z_{q\text{-brane}}(z,Q,t,q)^{\text{alt.}} = \prod_{\beta\in H_2(X,L,\mathbb{Z})} \prod_{s',r'\in\mathbb{Z}/2} \mathrm{PE}\left[-\frac{(-1)^{2s'+1} N_\beta^{(s',r')} t^{s'} q^{-r'-\frac{1}{2}}}{t^{\frac{1}{2}} - t^{-\frac{1}{2}}} Q_\beta\right], \tag{4.22}$$

which we identify with a partition functon of a q-brane in the alternative assignment (we stress that it is not equal to the partition function for a q-brane in the standard assignment). Similarly, after the exchange $q \leftrightarrow t$, the formula (4.19) is turned into the refined Ooguri-Vafa formula for $\bar{t}$-brane in the alternative assignment

$$Z_{\bar{t}\text{-brane}}(z,Q,t,q)^{\text{alt.}} = \prod_{\beta\in H_2(X,L,\mathbb{Z})} \prod_{s',r'\in\mathbb{Z}/2} \mathrm{PE}\left[-\frac{(-1)^{2s'} N_\beta^{(s',r')} q^{-s'} t^{r'+\frac{1}{2}}}{q^{\frac{1}{2}} - q^{-\frac{1}{2}}} Q_\beta\right], \tag{4.23}$$

where $s' = -s$, $r' = -r-1$. We emphasize that refined BPS invariants are always the same in both standard and alternative assignments, up to a shift of indices s and r. In what follows, to avoid confusion, we always choose the standard assignment presented in Figure 2.10.

4.2 Strip geometry with a Lagrangian brane

In this section we discuss toric manifolds without compact four-cycles, which are called strip geometries [98]. Strip geometries enable us to illustrate the Higgsing method that discussed in the last section. We compute open partition functions for several strip geometries and show that refined open BPS invariants are non-negative integers, thereby confirming the consistency of refined open topological string theory. We also represent refined open amplitudes in terms of quiver generating functions, generalizing the results of [85]. We also show that refined open BPS invariants for strip geometries have some interesting structures.

Recall that toric diagrams for strip geometries consist of a chain of finite segments that represent local $\mathbb{P}^1$'s, as well as some vertical and horizontal external lines extending to infinity. We consider the strip geometries that contain only one Lagrangian brane attached either to a vertical line see Figure 4.3, or to a horizontal line, see Figure 4.5. These two cases are qualitatively different. In what follows we discuss these two cases in general, and then present explicit results for some strip geometries. We stress that Figure 4.3 and 4.5 are not drown precisely, so keep in mind that (p, q)-charges should be conserved for each vertex.

In principle we could compute open amplitudes in the above setting directly using refined topological vertex. However, such computations are quite subtle because of the framing number and other issues. For this reason we compute refined open partition functions using the Higgsing method presented in section 4.1. The computations for strip geometries and also other manifolds are analyzed in subsequent sections, illustrating that this method is indeed powerful and can be effectively used in complicated diagrams. Moreover, we also extract refined open BPS invariants encoded in these partition functions and show that they are non-negative integers, which provides a non-trivial confirmation of correctness and consistency of the refined Higgsing method.

4.2.1 Refined open amplitudes for strip geometries

In this subsection, we compute refined open topological string amplitudes for strip geometries, and get the refined version in (3.109). To start with, we compute the diagram with a Lagrangian brane attached to a vertical leg, as shown in Figure 4.3. We denote the open Käahler parameter by z (which is identified with a closed Kähler parameter Q before the transition, as in Figure 4.2), and closed Kähler parameters of the strip geometry are denoted by Q_i for $i = 1, \ldots, \rho + \sigma$. We introduce more appropriate parameters $\alpha_i = Q_1 Q_2 \cdots Q_i$ where $i = 1, \ldots, \rho$ labels one of the legs pointing downwards, and $\beta_j = Q_1 Q_2 \cdots Q_j$ where $j = 1, \ldots, \sigma$ labels one of the legs pointing upwards.

As mentioned above, to determine open partition functions we use the method of geometric transition presented in section 4.1. To this end, we first need to engineer an appropriate mother

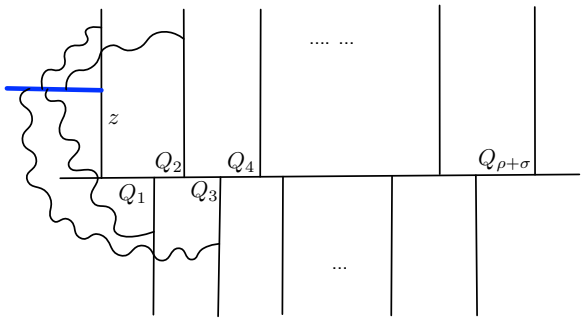

Figure 4.3: A Lagrangian brane (in blue) is attached to a vertical leg. Open topological strings stretched between this open topological brane and other branes are shown as wavy lines. This toric diagram is identical to the 3d brane web in Figure 3.9; here we rotate it by a 90 degree for convenience.

toric diagram, which will produce a Lagrangian brane of our interest after the geometric transition. We have illustrated this process in Figure 4.2. For a general strip geometry, we simply need to generalize this approach; see Figure 4.4. We first introduce a horizontal lines

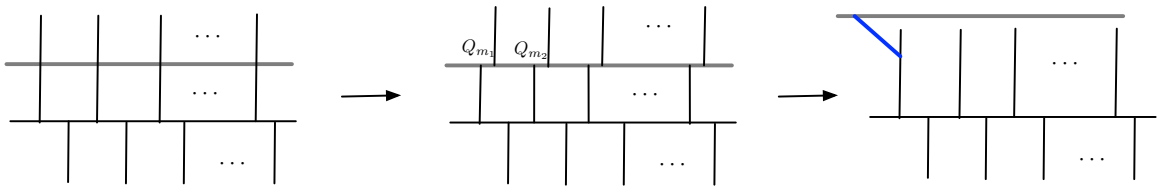

Figure 4.4: In the left diagram, we introduce a horizontal line, and then resolve intersections in the middle diagram. After giving appropriate values to Q_{m_i}, we end up with the strip geometry in the presence of a Lagrangian brane. Note that the gray line does not contribute to the open string partition functions, hence we can ignore it from the open topological string perspective.

intersecting all vertical lines pointing upwards. Each intersection is a local conifold that can be resolved with Kähler parameter denoted by Q_{m_i}, whose value is set to be $\sqrt{\frac{q}{t}}$ or $\sqrt{\frac{t}{q}}$ (which are equivalent upon flop transition) for $i > 1$, while the Q_{m_1} is given a value in (4.5), which results in an appropriate Lagrangian brane on which the Young diagram is either symmetric $\{n\}_S$ or antisymmetric representation $\{n\}_A$, depending on the arrow direction for the Young diagram we choose. This procedure is illustrated in Figure 4.4.

In particular, following (4.5) and setting $Q_{m_1} = \frac{1}{q}\sqrt{\frac{t}{q}}$, we obtain refined the open partition function for the $\bar{q}$-brane, which takes form

$$Z_{\bar{q}\text{-brane}}(z,\alpha_i,\beta_j) = \sum_{n=0}^{\infty} \frac{\left(z\sqrt{\frac{t}{q}}\right)^n}{(t,t)_n} \frac{\left(\alpha_1\sqrt{\frac{t}{q}},t\right)_n \left(\alpha_2\sqrt{\frac{t}{q}},t\right)_n \left(\alpha_3\sqrt{\frac{t}{q}},t\right)_n \cdots \left(\alpha_\rho\sqrt{\frac{t}{q}},t\right)_n}{\left(\beta_1\frac{t}{q},t\right)_n \left(\beta_2\frac{t}{q},t\right)_n \left(\beta_3\frac{t}{q},t\right)_n \cdots \left(\beta_\sigma\frac{t}{q},t\right)_n}\,. \tag{4.24}$$

Similarly, the t-brane partition function can be obtained by setting $Q_{m_1} = t\sqrt{\frac{t}{q}}$, or by using

equivalence relations in (4.9) and substituting $t \leftrightarrow q^{-1}$, which takes form

$$Z_{t\text{-brane}}(z,\alpha_i,\beta_j) = \sum_{n=0}^{\infty} \frac{\left(z\sqrt{\frac{t}{q}}\right)^n}{\left(\frac{1}{q},\frac{1}{q}\right)_n} \frac{\left(\alpha_1\sqrt{\frac{t}{q}},\frac{1}{q}\right)_n \left(\alpha_2\sqrt{\frac{t}{q}},\frac{1}{q}\right)_n \left(\alpha_3\sqrt{\frac{t}{q}},\frac{1}{q}\right)_n \cdots \left(\alpha_\rho\sqrt{\frac{t}{q}},\frac{1}{q}\right)_n}{\left(\beta_1\frac{t}{q},\frac{1}{q}\right)_n \left(\beta_2\frac{t}{q},\frac{1}{q}\right)_n \left(\beta_3\frac{t}{q},\frac{1}{q}\right)_n \cdots \left(\beta_\sigma\frac{t}{q},\frac{1}{q}\right)_n}. \tag{4.25}$$

Having found the above open topological partition functions (amplitudes), we can extract associated open BPS numbers using refined Ooguri-Vafa formulas. In the case of strip geometries we consider two perspectives: on one hand we analyze the refined Ooguri-Vafa decomposition, and on the other hand motivic Donaldson-Thomas invariants.

First, we consider refined Ooguri-Vafa forms of open partition function, and show that for refined Lagrangian branes the corresponding refined BPS invariants have some particular structures. Using refined Ooguri-Vafa formula, we write refined open amplitudes for strip geometry in the form

$$Z_{t\text{-brane}}(z,t,q) = \prod_{d=1}^{\infty} \prod_{\mathbf{l},\mathbf{k}=\mathbf{0}}^{\infty} \prod_{r\in\mathbb{Z}/2, j\in\mathbb{Z}} \prod_{n=0}^{\infty} \left(1 - q^{n+\frac{j-1}{2}} \left(\frac{t}{q}\right)^r z^d \alpha^{\mathbf{l}} \beta^{\mathbf{k}}\right)^{(-1)^{2r-j} \widetilde{N}^{(j,r)}_{d,\mathbf{l},\mathbf{k}}}, \tag{4.26}$$

where $\widetilde{N}^{(j,r)}_{d,\mathbf{l},\mathbf{k}}$ are refined Ooguri-Vafa invariants upon the shift of indices j and r. On the other hand, note that the dependence on q and t in (4.25) is equivalent to shifting parameters α_i and β_j:

$$\tilde{z} = z\sqrt{\frac{t}{q}}, \tilde{\alpha}_i = \alpha_i\sqrt{\frac{t}{q}}, \tilde{\beta}_j = \beta_j \frac{t}{q}. \tag{4.27}$$

Then the expression (4.25) takes form

$$Z_{t\text{-brane}}(z,t,q) = \sum_{n=0}^{\infty} \frac{\tilde{z}^n}{\left(\frac{1}{q},\frac{1}{q}\right)_n} \frac{\left(\tilde{\alpha}_1,\frac{1}{q}\right)_n \left(\tilde{\alpha}_2,\frac{1}{q}\right)_n \left(\tilde{\alpha}_3,\frac{1}{q}\right)_n \cdots \left(\tilde{\alpha}_\rho,\frac{1}{q}\right)_n}{\left(\tilde{\beta}_1,\frac{1}{q}\right)_n \left(\tilde{\beta}_2,\frac{1}{q}\right)_n \left(\tilde{\beta}_3,\frac{1}{q}\right)_n \cdots \left(\tilde{\beta}_\sigma,\frac{1}{q}\right)_n}, \tag{4.28}$$

which is the same as the unrefined open partition function for the strip geometry. Hence the refined open amplitudes has another decomposition

$$\begin{aligned} Z_{t\text{-brane}}(z,t,q) &= \prod_{d=1}^{\infty} \prod_{\mathbf{l},\mathbf{k}=\mathbf{0}}^{\infty} \prod_{j\in\mathbb{Z}} \prod_{n=0}^{\infty} \left(1 - q^{n+\frac{j-1}{2}} \tilde{z}^d \tilde{\alpha}^{\mathbf{l}} \tilde{\beta}^{\mathbf{k}}\right)^{(-1)^j N^j_{d,\mathbf{l},\mathbf{k}}} = \\ &= \prod_{d=1}^{\infty} \prod_{\mathbf{l},\mathbf{k}=\mathbf{0}}^{\infty} \prod_{j\in\mathbb{Z}} \prod_{n=0}^{\infty} \left(1 - q^{n+\frac{j-1}{2}} \left(\frac{t}{q}\right)^{(d+\sum_i l_i)/2+\sum_j k_j} z^d \alpha^{\mathbf{l}} \beta^{\mathbf{k}}\right)^{(-1)^j N^j_{d,\mathbf{l},\mathbf{k}}}. \end{aligned} \tag{4.29}$$

Note that (4.26) should be equal to the second line of (4.29). Hence we derive that for fixed d, $\mathbf{l}$, $\mathbf{k}$ and j, there is only one value of r

$$r = (n + \sum_i l_i)/2 + \sum_j k_j, \tag{4.30}$$

for which $\widetilde{N}^{(j,r)}_{d,\mathbf{l},\mathbf{k}}$ is non-zero, and we then get a relation between unrefined Ooguri-Vafa invariants and refined Ooguri-Vafa invariants

$$N^{j}_{n,\mathbf{l},\mathbf{k}} = (-1)^{2r}\widetilde{N}^{(j,r)}_{n,\mathbf{l},\mathbf{k}}\,. \tag{4.31}$$

Although it seems that the refinement for open topological strings on strip geometries is trivial, but explains the negative sign problem of unrefined Ooguri-Vafa invariants. Namely, the refined Ooguri-Vafa invariants extracted through refined Ooguri-Vafa formula are positive integers. We verified their positivity by examples in the next section.

In turn, we consider the relation to quivers. It arises from rewriting open partition functions in the form of quiver generating series (3.112); see also [85]. We can rewrite refined open partition functions in the quiver form using the identities (A.31) and (A.32). After rewriting, the $\bar{q}$-brane partition function (4.24) takes form

$$Z_{\bar{q}\text{-brane}}(z,\alpha_i,\beta_j) = Z_0\cdot P_{C_{ij}}\left(t; z\sqrt{\frac{t}{q}}, \alpha_1\sqrt{\frac{t}{q}},\cdots,\alpha_\rho\sqrt{\frac{t}{q}},\ \beta_1\frac{\sqrt{t}}{q},\cdots,\beta_\sigma\frac{\sqrt{t}}{q}\right), \tag{4.32}$$

where the z-independent prefactor reads

$$Z_0 = \frac{\left(\alpha_1\sqrt{\frac{t}{q}},t\right)_\infty\left(\alpha_2\sqrt{\frac{t}{q}},t\right)_\infty\left(\alpha_3\sqrt{\frac{t}{q}},t\right)_\infty\cdots\left(\alpha_\rho\sqrt{\frac{t}{q}},t\right)_\infty}{\left(\beta_1\frac{t}{q},t\right)_\infty\left(\beta_2\frac{t}{q},t\right)_\infty\left(\beta_3\frac{t}{q},t\right)_\infty\cdots\left(\beta_\sigma\frac{t}{q},t\right)_\infty}\,. \tag{4.33}$$

Note that the factor Z_0 does not satisfy refined Ooguri-Vafa formula. We ignore this factor Z_0 for a while, and in the next chapter we argue that Z_0 actually is the inverse of the one-loop partition function of the corresponding 3d $\mathcal{N}=2$ theory. The quiver matrix for strip geometry takes form

$$C_{ij} = \left[\begin{array}{c|ccc|ccc} 0 & 1 & \dots & 1 & 1 & \dots & 1 \\ \hline 1 & 0 & \dots & 0 & 0 & \dots & 0 \\ \vdots & & \ddots & & & \ddots & \\ 1 & 0 & \dots & 0 & 0 & \dots & 0 \\ \hline 1 & 0 & \dots & 0 & 1 & \dots & 0 \\ \vdots & & \ddots & & & \ddots & \\ 1 & 0 & \dots & 0 & 0 & \dots & 1 \end{array}\right].$$

Similarly, the partition function (4.25) for t-brane can be written in the quiver form (3.112) as

$$Z_{t\text{-brane}}(z,\alpha_i,\beta_j) = Z_0\cdot P_{C_{ij}}\left(q; z\sqrt{t},\alpha_1\sqrt{t},\cdots,\alpha_\rho\sqrt{t},\ \beta_1\,t,\cdots,\beta_\sigma\,t\right), \tag{4.34}$$

where the extra z-independent factor is

$$Z_0 = \frac{\left(\alpha_1\sqrt{\frac{t}{q}},\frac{1}{q}\right)_\infty\left(\alpha_2\sqrt{\frac{t}{q}},\frac{1}{q}\right)_\infty\left(\alpha_3\sqrt{\frac{t}{q}},\frac{1}{q}\right)_\infty\cdots\left(\alpha_\rho\sqrt{\frac{t}{q}},\frac{1}{q}\right)_\infty}{\left(\beta_1\frac{t}{q},\frac{1}{q}\right)_\infty\left(\beta_2\frac{t}{q},\frac{1}{q}\right)_\infty\left(\beta_3\frac{t}{q},\frac{1}{q}\right)_\infty\cdots\left(\beta_\sigma\frac{t}{q},\frac{1}{q}\right)_\infty} \tag{4.35}$$

and the quiver matrix takes form

$$C_{ij} = \left[\begin{array}{c|ccc|ccc} 1 & -1 & \dots & -1 & -1 & \dots & -1 \\ \hline -1 & 1 & \dots & 0 & 0 & \dots & 0 \\ \vdots & & \ddots & & & \ddots & \\ -1 & 0 & \dots & 1 & 0 & \dots & 0 \\ \hline -1 & 0 & \dots & 0 & 0 & \dots & 0 \\ \vdots & & \ddots & & & \ddots & \\ -1 & 0 & \dots & 0 & 0 & \dots & 0 \end{array}\right] . \tag{4.36}$$

Since there is the equivalence relation (4.9), we only need to consider one particular type of refined open topological branes and quiver matrices.

Having determined the above quivers, we can then identify Ooguri-Vafa (OV) invariants $\widetilde{N}^{j}_{n,\mathbf{l},\mathbf{k}}$ with motivic Donaldson-Thomas (DT) invariants $\Omega^{j}_{n,\mathbf{l},\mathbf{k}}$ defined via (3.113). Here we can define the refined motivic DT invariants $\Omega^{(j,r)}_{n,\mathbf{l},\mathbf{k}}$ as refined invariants $\widetilde{N}^{(j,r)}_{n,\mathbf{l},\mathbf{k}}$ in (4.26). The DT invariants should be non-negative integers [87, 88], which implies that all refined open BPS numbers for strip geometries must be non-negative integers too. Our statement is that for strip geometries with one Lagrangian brane, we have the equivalence between these two kinds of invariants

$$\text{OV} = \text{DT} . \tag{4.37}$$

The Lagrangian brane on a horizontal line

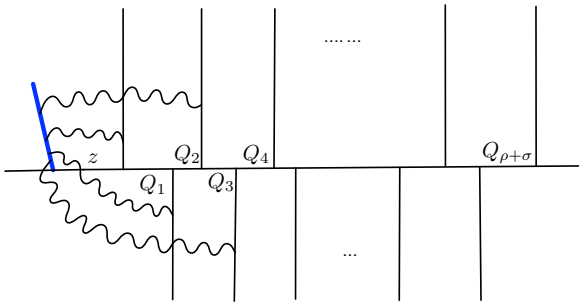

Figure 4.5: Open strings connect the Lagrangian brane and vertical lines (5-branes).

We now consider a different configuration with a Lagrangian brane attached to the horizontal line, as shown in Figure 4.5. Similarly, we first introduce a vertical line, and then resolve the local conifold. After Higgsing, we get the diagram in Figure 4.5. In this case the

partition function takes a form of q-Pochhammer products:

$$\begin{aligned} Z_{t\text{-brane}}(z,\alpha_i,\beta_j) &= \frac{\left(z\frac{t}{q},\frac{1}{q}\right)_\infty \left(z\beta_1\frac{t}{q},\frac{1}{q}\right)_\infty \left(z\beta_2\frac{t}{q},\frac{1}{q}\right)_\infty \cdots \left(z\beta_\sigma\frac{t}{q},\frac{1}{q}\right)_\infty}{\left(z\alpha_1\sqrt{\frac{t}{q}},\frac{1}{q}\right)_\infty \left(z\alpha_2\sqrt{\frac{t}{q}},\frac{1}{q}\right)_n \cdots \left(z\alpha_\rho\sqrt{\frac{t}{q}},\frac{1}{q}\right)_\infty} \\ &= \frac{(z\alpha_1\sqrt{qt},q)_\infty (z\alpha_2\sqrt{qt},q)_\infty \cdots (z\alpha_\rho\sqrt{qt},q)_\infty}{(zt,q)_\infty (z\beta_1 t,q)_\infty (z\beta_2 t,q)_\infty \cdots (z\beta_\sigma t,q)_\infty}, \\ Z_{\bar{q}\text{-brane}}(z,\alpha_i,\beta_j) &= \frac{\left(z\frac{t}{q},t\right)_\infty \left(z\beta_1\frac{t}{q},t\right)_\infty \left(z\beta_2\frac{t}{q},t\right)_\infty \cdots \left(z\beta_\sigma\frac{t}{q},t\right)_\infty}{\left(z\alpha_1\sqrt{\frac{t}{q}},t\right)_\infty \left(z\alpha_2\sqrt{\frac{t}{q}},t\right)_\infty \cdots \left(z\alpha_\rho\sqrt{\frac{t}{q}},t\right)_\infty}. \end{aligned} \tag{4.38}$$

Each q-Pochhammer product corresponds to a BPS invariant, and hence there are finite many open BPS invariants:

$$N_z^{(1/2,1/2)} = 1, \quad N_{z\alpha_i}^{(0,0)} = 1, \quad N_{z\beta_j}^{(1/2,1/2)} = 1. \tag{4.39}$$

Expanding all factors in (4.38), we can also determine the associated quivers, which consist of a finite number of disconnected nodes. Furthermore, open partition functions (4.38), from the viewpoint of 3d $\mathcal{N}=2$ theories, represent just a bunch of chiral multiplets.

4.2.2 $\mathbb{C}^3$ geometry

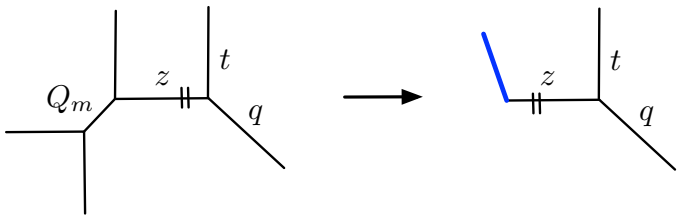

Figure 4.6: A geometric transition that transforms a double $\mathbb{P}^1$ strip geometry with Kähler parameters Q_m and z into $\mathbb{C}^3$ with a Lagrangian brane. After the transition, the closed Kähler parameter z becomes an open Kähler parameter, relating to the FI parameter in the 3d $\mathcal{N}=2$ theory. The assignment of q, t, and the preferred direction are shown in the diagram.

In what follows we illustrate the above analysis in specific examples, starting from $\mathbb{C}^3$ geometry. First, we compute the closed partition function for the left diagram in Figure 4.6, which takes form

$$Z^{\text{closed}}(z,Q_m) = \frac{M\left(zQ_m\sqrt{\frac{t}{q}},t,q\right)}{M\left(z\frac{t}{q},t,q\right)}, \tag{4.40}$$

where refined MacMahon function $M(z,q,t)$ is defined in (A.1). By comparing the diagram in Figure 4.6 (left) with (4.14) we find that the Lagrangian brane that can be introduced is t-brane or $\bar{q}$-brane. Imposing $Q_m = t\sqrt{\frac{t}{q}}$ and interpreting z as an open Kähler parameter we

get

$$Z_{t\text{-brane}} = Z^{\text{closed}}\left(z, Q_m = t\sqrt{\frac{t}{q}}\right) = \frac{1}{(zt,q)_\infty}. \tag{4.41}$$

Similarly, setting $Q_m = \frac{1}{q}\sqrt{\frac{t}{q}}$, we obtain

$$Z_{\bar{q}\text{-brane}} = Z^{\text{closed}}\left(z, Q_m = \frac{1}{q}\sqrt{\frac{t}{q}}\right) = \left(z\frac{t}{q}, t\right)_\infty . \tag{4.42}$$

Using identities for q-Pochhammer symbols in appendix we confirm that the exchange symmetry holds

$$Z_{t\text{-brane}} \xleftrightarrow{t\leftrightarrow q^{-1}} Z_{\bar{q}\text{-brane}}\,. \tag{4.43}$$

We can also write the above open partition functions in terms of the refined Ooguri-Vafa form, as well as the quiver form (3.112)

$$\begin{aligned} Z_{t\text{-brane}} &= \frac{1}{(zt,q)_\infty} = \text{PE}[z,1,1/2,1/2]_{t\text{-brane}} = P_{C_t}(q;zt)\,, \quad C_t = [0]\,, \\ Z_{\bar{q}\text{-brane}} &= \left(z\frac{t}{q}, t\right)_\infty = \text{PE}[z,1,1/2,1/2]_{\bar{q}\text{-brane}} = P_{C_{\bar{q}}}\left(q; z\frac{\sqrt{t}}{q}\right)\,, \quad C_{\bar{q}} = [1]\,. \end{aligned} \tag{4.44}$$

It follows from (4.17) and (4.19) that in these cases there is only one BPS number $N_z^{(1/2,1/2)} = 1$. Furthermore, open partition functions for $\bar{t}$-brane and q-brane can be obtained by using relations (4.12), which yield

$$Z_{\bar{t}\text{-brane}} = (z\sqrt{tq}, t)_\infty\,, \qquad Z_{q\text{-brane}} = \frac{1}{\left(z\sqrt{\frac{q}{t}}, q\right)_\infty}, \tag{4.45}$$

and encode the same BPS invariant.

4.2.3 Resolved conifold

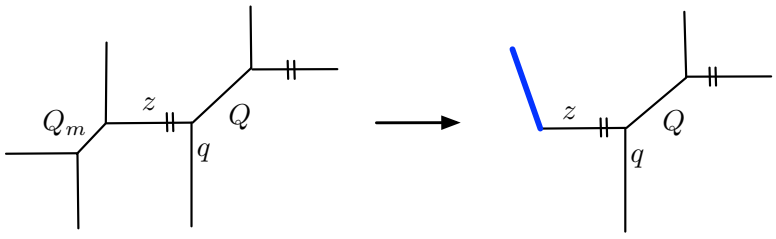

Figure 4.7: Implementing geometric transition (Higgsing) on a triple-$\mathbb{P}^1$ geometry leads to a resolved conifold with a Lagrangian brane. In this process the Q_m is given a value, and z becomes the open Kähler parameter.

Following the strategy presented in section 4.1, we first consider the geometry represented by the left diagram in Figure 4.7, whose closed partition function takes form of a product of

refined MacMahon functions

$$Z^{\text{closed}} \sim \frac{M\left(z\sqrt{\frac{t}{q}},t,q\right)M\left(zQQ_m\sqrt{\frac{t}{q}},t,q\right)}{M\left(zQ_m,t,q\right)M\left(zQ\frac{t}{q},t,q\right)}, \tag{4.46}$$

where $\sim$ means that we have ignored the closed string contributions that do not depend on Kähler parameter z. Geometric transition fixes $Q_m = t\sqrt{\frac{t}{q}}$, and gives rise to the t-brane open partition function

$$\begin{aligned} Z_{t\text{-brane}} &= Z^{\text{closed}}\left(z, Q_m = t\sqrt{\frac{t}{q}}\right) = \frac{(z\sqrt{tq},q)_\infty}{(zQt,q)_\infty} = \sum_{n=0}^{\infty}\frac{\left(z\sqrt{\frac{t}{q}}\right)^n\left(Q\sqrt{\frac{t}{q}},\frac{1}{q}\right)_n}{\left(\frac{1}{q},\frac{1}{q}\right)_n} \\ &= \text{PE}[z,1,0,0]_t\text{PE}[zQ,1/2,1/2]_t = P_{C_t}\left(q;z\sqrt{t},zQt\right). \end{aligned} \tag{4.47}$$

Similarly, we substitute $Q_m = \frac{1}{q}\sqrt{\frac{t}{q}}$ to get a $\bar{q}$-brane, which yields the open refined partition function

$$\begin{aligned} Z_{\bar{q}\text{-brane}} &= Z^{\text{closed}}\left(z, Q_m = \frac{1}{q}\sqrt{\frac{t}{q}}\right) = \frac{\left(zQ\frac{t}{q},t\right)_\infty}{\left(z\sqrt{\frac{t}{q}},t\right)_\infty} = \sum_{n=0}^{\infty}\frac{\left(z\sqrt{\frac{t}{q}}\right)^n\left(Q\sqrt{\frac{t}{q}},t\right)_n}{(t,t)_n} \\ &= \text{PE}[z,1,0,0]_{\bar{q}}\text{PE}[zQ,1/2,1/2]_{\bar{q}} = P_{C_{\bar{q}}}\left(t;z\frac{\sqrt{t}}{q},zQ\sqrt{\frac{t}{q}}\right). \end{aligned} \tag{4.48}$$

Above we have also provided quiver forms (3.112), in this example we get quiver matrices of the same form

$$C_{\bar{q}} = \begin{bmatrix} 1 & 0 \\ 0 & 0 \end{bmatrix}, \qquad C_t = \begin{bmatrix} 1 & 0 \\ 0 & 0 \end{bmatrix}. \tag{4.49}$$

Moreover, by comparing with (4.17) and (4.19), we read off refined Ooguri-Vafa invariants $N_z^{(0,0)} = 1$, $N_{zQ}^{(1/2,1/2)} = 1$.

4.2.4 Resolution of $\mathbb{C}^3/\mathbb{Z}_2$

Another example of a strip geometry with one local $\mathbb{P}^1$ is $\mathcal{O}(0)\oplus\mathcal{O}(-2)\to\mathbb{P}^1$, or equivalently the resolution of $\mathbb{C}^3/\mathbb{Z}_2$. We consider two topological brane locations, either on a horizontal or a vertical leg (in our earlier conventions), as shown in Figure 4.8. Partition functions for these two brane configurations can be obtained by two different geometric transitions. For the Lagrangian brane on a horizontal line the partition function takes form of a product of a finite number of quantum dilogarithms. We obtain open amplitudes for t-brane and $\bar{q}$-brane

$$Z^{(a)}_{t\text{-brane}} = \frac{1}{(zt,q)_\infty(zQt,q)_\infty}, \quad Z^{(a)}_{\bar{q}\text{-brane}} = \left(z\frac{t}{q},t\right)_\infty\left(zQ\frac{t}{q},t\right)_\infty. \tag{4.50}$$

The corresponding open BPS invariants are $N_z^{(1/2,1/2)} = 1$ and $N_{zQ}^{(1/2,1/2)} = 1$.

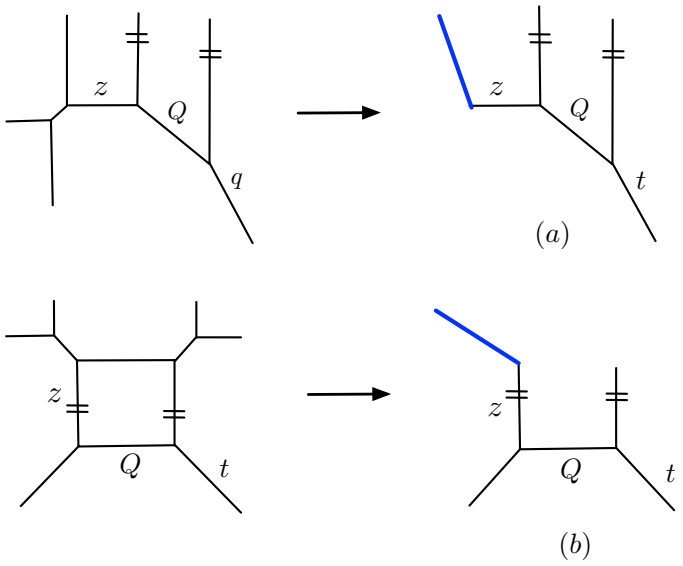

Figure 4.8: Geometric transitions that produce a Lagrangian brane on the horizontal line (a) or the vertical line (b) in the resolution of $\mathbb{C}^3/\mathbb{Z}_2$.

On the other hand, the partition function for t-brane in the configuration (b) in Figure 4.8 takes form

$$\begin{aligned} Z^{(b)}_{t\text{-brane}} &= \sum_{n=0}^{\infty} \frac{Q^n t^n}{(q,q)_n \left(Q_1 \frac{t}{q}, \frac{1}{q}\right)_n} = \frac{1}{(Q\frac{t}{q}, \frac{1}{q})_\infty} \sum_{n,d=0}^{\infty} (-\sqrt{q})^{-2nd} \frac{(Qt)^n (Q_1 t)^d}{(q,q)_n \, (q,q)_d} \\ &= \frac{1}{(Q_1 \frac{t}{q}, \frac{1}{q})_\infty} P_{C_t}(q; Qt, Q_1 t)\,. \end{aligned} \tag{4.51}$$

The quiver matrix in the representation (3.112) in this case reads

$$C_t = \begin{bmatrix} 0 & -1 \\ -1 & 0 \end{bmatrix}. \tag{4.52}$$

In this case there is an infinite number of open BPS invariants, see Table A.1. Note that for fixed d_0 and d_1, non-zero invariants arise only for one particular value of r, in agreement with our earlier prediction. As usual, the partition function for a $\bar{q}$-brane can be obtained by exchanging $q \to 1/t$ in (4.51)

$$Z^{(b)}_{\bar{q}\text{-brane}} = \sum_{n=0}^{\infty} \frac{(-\sqrt{t})^{n^2} \left(Q\sqrt{\frac{t}{q}}\right)^n}{(t,t)_n \left(Q_1 \frac{t}{q}, t\right)_n} = \frac{1}{(Q\frac{t}{q}, t)_\infty} P_{C_{\bar{q}}} \left(t; Q\sqrt{\frac{t}{q}}, Q_1 \frac{\sqrt{t}}{q}\right) \tag{4.53}$$

with quiver matrix in the representation (3.112)

$$C_{\bar{q}} = \begin{bmatrix} 1 & 1 \\ 1 & 1 \end{bmatrix}. \tag{4.54}$$

4.2.5 Double-$\mathbb{P}^1$

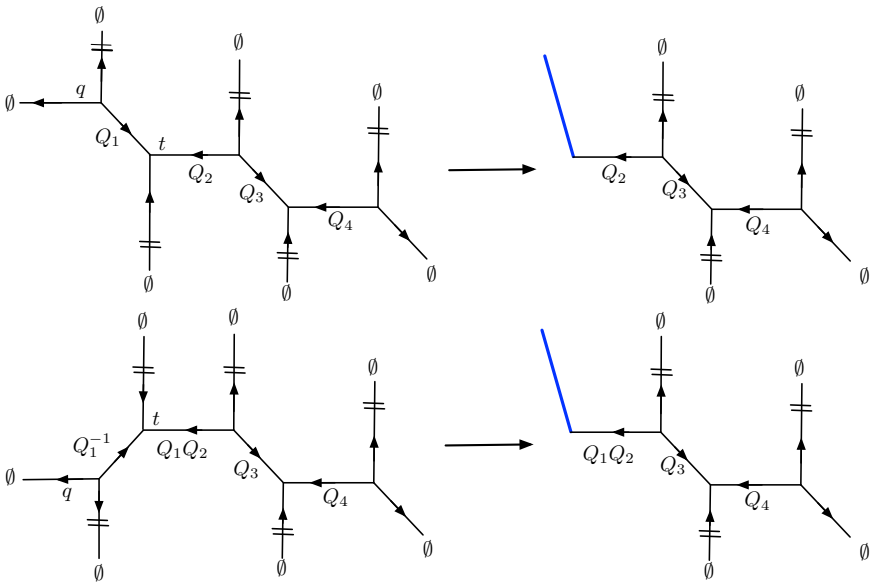

Figure 4.9: Two strip geometries related by a flop transition produces the same double-$\mathbb{P}^1$ geometry through Higgsing. However the introduced Lagrangian branes are different types.

In turn, we consider the Lagrangian brane in a double-$\mathbb{P}^1$ geometry (that involves two local $\mathbb{P}^1$'s), either on a horizontal or vertical line. First, by considering the Lagrangian brane attached to a horizontal line, as shown in Figure 4.9, we illustrate the effect of a flop transition on the resulting Lagrangian brane. Second, we consider the Lagrangian brane on a vertical line shown in Figure 4.11, and show that open BPS invariants are non-negative integers.

To start with, we consider the top left diagram in Figure 4.9. This is a strip geometry with a closed partition function expressed in terms of a finite number of refined MacMahon functions

$$\begin{aligned} Z^{\text{closed}} =& \frac{M\big(Q_1\sqrt{\frac{t}{q}},t,q\big)M\big(Q_2\sqrt{\frac{t}{q}},t,q\big)M\big(Q_3\sqrt{\frac{t}{q}},t,q\big)M\big(Q_4\sqrt{\frac{t}{q}},t,q\big)}{M\big(Q_1Q_2,q,t\big)M\big(Q_2Q_3,t,q\big)M\big(Q_3Q_4,q,t\big)M\big(Q_1Q_2Q_3Q_4,q,t\big)}\times \\ &\times M\Big(Q_1Q_2Q_3\sqrt{\frac{t}{q}},t,q\Big)M\Big(Q_2Q_3Q_4\sqrt{\frac{t}{q}},t,q\Big). \end{aligned} \tag{4.55}$$

In order to introduce a Lagrangian brane we perform a geometric transition at the two sphere Q_1. In this process we can ignore the terms $\frac{M(Q_3\sqrt{\frac{t}{q}},t,q)M(Q_4\sqrt{\frac{t}{q}},t,q)}{M(Q_3Q_4,q,t)}$ that capture only closed string contributions. Furthermore, following (4.15), we set $Q_1 = q\sqrt{\frac{q}{t}}$ or $\frac{1}{t}\sqrt{\frac{t}{q}}$ respectively to

obtain open partition functions for q-brane or $\bar{t}$-brane with the open Kähler parameter $z \equiv Q_2$

$$\begin{aligned} Z_{q\text{-brane}} &= \frac{M\left(Q_2\sqrt{\frac{t}{q}},t,q\right) M\left(Q_2Q_3q,t,q\right) M\left(Q_2Q_3Q_4\sqrt{\frac{t}{q}},t,q\right)}{M\left(Q_2\sqrt{qt},t,q\right) M\left(Q_2Q_3,t,q\right) M\left(Q_2Q_3Q_4\sqrt{qt},t,q\right)} \\ &= \frac{(Q_2\sqrt{tq},t)_\infty (Q_2Q_3Q_4\sqrt{tq},t)_\infty}{(Q_2Q_3q,t)_\infty} = P_{C_q}\left(t; Q_2\sqrt{q}, Q_2Q_3Q_4\sqrt{q}, Q_2Q_3q\right), \\ Z_{\bar{t}\text{-brane}} &= \frac{M\left(Q_2\sqrt{\frac{t}{q}},t,q\right) M\left(Q_2Q_3/t,t,q\right) M\left(Q_2Q_3Q_4\sqrt{\frac{t}{q}},t,q\right)}{M\left(Q_2/\sqrt{qt},t,q\right) M\left(Q_2Q_3,t,q\right) M\left(Q_2Q_3Q_4/\sqrt{qt},t,q\right)} \\ &= \frac{(Q_2Q_3\frac{q}{t},q)_\infty}{(Q_2\sqrt{\frac{q}{t}},q)_\infty (Q_2Q_3Q_4\sqrt{\frac{q}{t}},q)_\infty} = P_{C_{\bar{t}}}\left(q; Q_2Q_3\frac{\sqrt{q}}{t}, Q_2\sqrt{\frac{q}{t}}, Q_2Q_3Q_4\sqrt{\frac{q}{t}}\right), \end{aligned} \tag{4.56}$$

where

$$C_q = \begin{bmatrix} 1 & 0 & 0 \\ 0 & 1 & 0 \\ 0 & 0 & 0 \end{bmatrix}, \qquad C_{\bar{t}} = \begin{bmatrix} 1 & 0 & 0 \\ 0 & 0 & 0 \\ 0 & 0 & 0 \end{bmatrix}. \tag{4.57}$$

As a check, the above partition functions satisfy the relation (4.11).

On the other hand, we consider the geometry represented by the diagram in the bottom left in Figure 4.9, which is related to the previous geometry by a flop transition on the two sphere Q_1. Upon the geometric transition it leads to the same double-$\mathbb{P}^1$ geometry, however with different types of topological branes: substituting $Q_1^{-1} = t\sqrt{\frac{t}{q}}$ or $\frac{1}{q}\sqrt{\frac{q}{t}}$ respectively we obtain t-brane or $\bar{q}$-brane with open partition functions

$$Z_{t\text{-brane}} = \frac{M\left(Q_2t,q,t\right) M\left(Q_2Q_3\sqrt{\frac{t}{q}},t,q\right) M\left(Q_2Q_3Q_4t,q,t\right)}{M\left(Q_2,q,t\right) M\left(Q_2Q_3\sqrt{qt},q,t\right) M\left(Q_2Q_3Q_4,q,t\right)} \tag{4.58}$$

$$= \frac{(Q_2Q_3\sqrt{tq},q)_\infty}{(Q_2t,q)_\infty (Q_2Q_3Q_4t,q)_\infty} = P_{C_t}\left(q; Q_2Q_3\sqrt{t}, Q_2t, Q_2Q_3Q_4t\right), \tag{4.59}$$

$$Z_{\bar{q}\text{-brane}} = \frac{M\left(Q_2/q,q,t\right) M\left(Q_2Q_3\sqrt{\frac{t}{q}},t,q\right) M\left(Q_2Q_3Q_4/q,q,t\right)}{M\left(Q_2,q,t\right) M\left(Q_2Q_3/\sqrt{qt},q,t\right) M\left(Q_2Q_3Q_4,q,t\right)} \tag{4.60}$$

$$= \frac{(Q_2\frac{t}{q},t)_\infty (Q_2Q_3Q_4\frac{t}{q},t)_\infty}{(Q_2Q_3\sqrt{\frac{t}{q}},t)_\infty} = P_{C_{\bar{q}}}\left(t; Q_2\frac{\sqrt{t}}{q}, Q_2Q_3Q_4\sqrt{\frac{t}{q}}, Q_2Q_3\sqrt{\frac{t}{q}}\right), \tag{4.61}$$

where quiver matrices in the representation (3.112) are

$$C_t = \begin{bmatrix} 1 & 0 & 0 \\ 0 & 0 & 0 \\ 0 & 0 & 0 \end{bmatrix}, \qquad C_{\bar{q}} = \begin{bmatrix} 1 & 0 & 0 \\ 0 & 1 & 0 \\ 0 & 0 & 0 \end{bmatrix}. \tag{4.62}$$

There are just three open BPS numbers

$$N_{Q_2}^{(1/2,1/2)} = 1, \quad N_{Q_2Q_3}^{(0,0)} = 1, \quad N_{Q_2Q_3Q_4}^{(1/2,1/2)} = 1\,. \tag{4.63}$$

To sum up, the geometric transition may produce only two particular types of topological branes. A flop of the two-cycle that undergoes the geometric transition leads then to another two types of topological branes. As a check, all relations in (4.9) hold for the partition functions determined above.

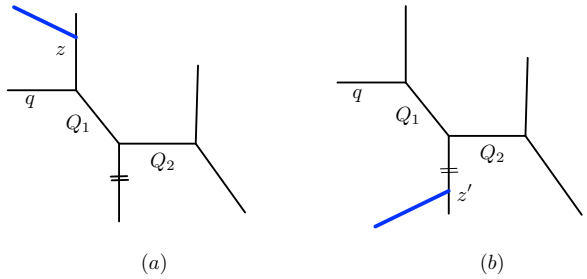

Figure 4.10: Branes on various vertical legs of a double-$\mathbb{P}^1$ geometry.

Furthermore, we consider the topological brane on vertical lines. Open partition functions for the $\bar{q}$-brane and t-brane in the diagram (a) in Figure 4.10 take form

$$\begin{aligned} Z^{(a)}_{\bar{q}\text{-brane}} &= \sum_{n=0}^{\infty} \frac{\left(z\sqrt{\frac{t}{q}}\right)^n \left(Q_1\sqrt{\frac{t}{q}},t\right)_n}{(t,t)_n \left(Q_1Q_2\frac{t}{q},t\right)_n} = \frac{\left(Q_1\sqrt{\frac{t}{q}},t\right)_\infty}{\left(Q_1Q_2\frac{t}{q},t\right)_\infty} P_{C_{\bar{q}}}\left(t; z\sqrt{\frac{t}{q}}, Q_1\sqrt{\frac{t}{q}}, Q_1Q_2\frac{\sqrt{t}}{q}\right), \\ Z^{(a)}_{t\text{-brane}} &= \sum_{n=0}^{\infty} \frac{(-z)^n q^{\frac{n^2}{2}} t^{\frac{n}{2}} \left(Q_1\sqrt{\frac{t}{q}},\frac{1}{q}\right)_n}{(q,q)_n \left(Q_1Q_2\frac{t}{q},\frac{1}{q}\right)_n} = \frac{\left(Q_1\sqrt{\frac{t}{q}},\frac{1}{q}\right)_\infty}{\left(Q_1Q_2\frac{t}{q},\frac{1}{q}\right)_\infty} P_{C_t}\left(q; z\sqrt{t}, Q_1Q_2t\right). \end{aligned} \tag{4.64}$$

The summation formulae above are special cases of (4.24) and (4.25), and quiver matrices read

$$C_{\bar{q}} = \begin{bmatrix} 0 & 1 & 1 \\ 1 & 0 & 0 \\ 1 & 0 & 1 \end{bmatrix}, \qquad C_t = \begin{bmatrix} 1 & -1 & -1 \\ -1 & 1 & 0 \\ -1 & 0 & 0 \end{bmatrix}. \tag{4.65}$$

We verify that corresponding refined open BPS invariants are indeed positive integers, as shown in Table A.2. Note that for fixed (d_0, d_1, d_2), non-zero BPS invariants arise only for one particular value of r, as predicted before.

On the other hand, open partition functions for the topological brane in the diagram (b) in Figure 4.10 can be obtained by performing geometric transitions and then blowing down the two-cycle $Q_3 \to 0$, as shown in Figure 4.11. In this way we obtain q-brane and $\bar{t}$-brane

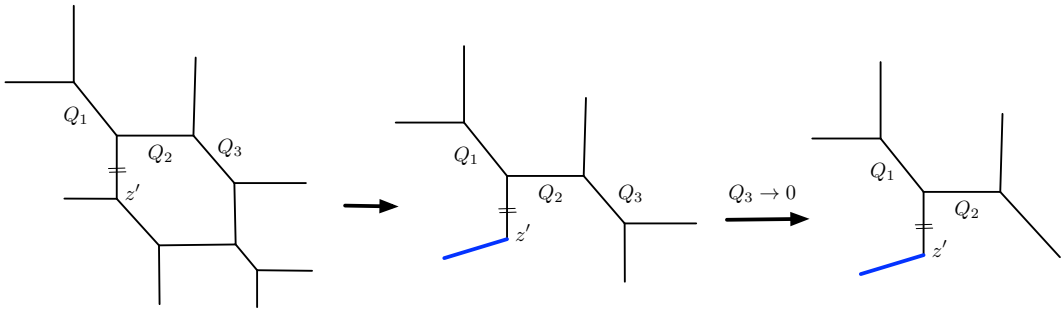

Figure 4.11: The geometric transition leads to the diagram (b) in Figure 4.10.

partition functions

$$\begin{aligned} Z^{(b)}_{q\text{-brane}} &= \sum_{n=0}^{\infty} \frac{q^n (z' Q_1)^n \left(\frac{1}{Q_1}\sqrt{\frac{t}{q}}, t\right)_n \left(Q_2\sqrt{\frac{t}{q}}, t\right)}{(t,t)_n}, \\ Z^{(b)}_{\bar{t}\text{-brane}} &= \sum_{n=0}^{\infty} \frac{(-z' Q_2)^n q^{\frac{n-n^2}{2}} \left(Q_1\sqrt{\frac{q}{t}}, q\right)_n \left(\frac{1}{Q_2}\sqrt{\frac{q}{t}}, q\right)_n}{(q,q)_n}. \end{aligned} \tag{4.66}$$

One can now apply the relations (4.12) to get $\bar{q}$-brane and t-brane partition functions

$$\begin{aligned} Z^{(b)}_{\bar{q}\text{-brane}} &= \sum_{n=0}^{\infty} \frac{\left(\tilde{z}\sqrt{\frac{t}{q}}\right)^n \left(\tilde{Q}_1\sqrt{\frac{t}{q}}, t\right)_n \left(Q_2\sqrt{\frac{t}{q}}, t\right)_n}{(t,t)_n} \\ &= \left(\tilde{Q}_1\sqrt{\frac{t}{q}}, t\right)_\infty \left(Q_2\sqrt{\frac{t}{q}}, t\right)_\infty P_{C_q}\left(t; \tilde{z}\sqrt{\frac{t}{q}}, \tilde{Q}_1\sqrt{\frac{t}{q}}, Q_2\sqrt{\frac{t}{q}}\right), \\ Z^{(b)}_{t\text{-brane}} &= \sum_{n=0}^{\infty} \frac{\left(\tilde{z}\sqrt{\frac{t}{q}}\right)^n \left(\tilde{Q}_1\sqrt{\frac{t}{q}}, \frac{1}{q}\right)_n \left(Q_2\sqrt{\frac{t}{q}}, \frac{1}{q}\right)_n}{\left(\frac{1}{q}, \frac{1}{q}\right)_n} = P_{C_{\bar{t}}}(q;\ \tilde{z}\sqrt{t}, \tilde{Q}_1\sqrt{t}, Q_2\sqrt{t}), \end{aligned} \tag{4.67}$$

where $\tilde{Q}_1 = 1/Q_1, \tilde{z} = z' Q_1 q\sqrt{\frac{q}{t}}$. These formulas have a standard form for open partition functions on a strip geometry, thus the corresponding open BPS invariants are non-negative integers. The corresponding quiver matrices are

$$C_q = \begin{bmatrix} 0 & 1 & 1 \\ 1 & 0 & 0 \\ 1 & 0 & 0 \end{bmatrix}, \qquad C_{\bar{t}} = \begin{bmatrix} 1 & -1 & -1 \\ -1 & 1 & 0 \\ -1 & 0 & 1 \end{bmatrix}. \tag{4.68}$$

4.2.6 Triple-$\mathbb{P}^1$

In turn, we consider the topological brane on the vertical line in a triple-$\mathbb{P}^1$ geometry, as shown in Figure 4.12. Similarly as before, the geometric transition gives rise to open partition

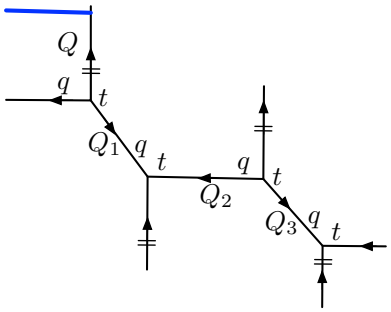

Figure 4.12: A topological brane on a vertical leg in a triple-$\mathbb{P}^1$.

functions for $\bar{q}$-brane and t-brane

$$\begin{aligned} Z_{\bar{q}\text{-brane}} &= \sum_{n=0}^{\infty} \frac{\left(Q\sqrt{\frac{t}{q}}\right)^n}{(t,t)_n} \frac{\left(Q_1\sqrt{\frac{t}{q}},t\right)_n \left(Q_1Q_2Q_3\sqrt{\frac{t}{q}},t\right)_n}{\left(Q_1Q_2\frac{t}{q},t\right)_n} \\ &= \frac{\left(Q_1\sqrt{\frac{t}{q}},t\right)_\infty \left(Q_1Q_2Q_3\sqrt{\frac{t}{q}},t\right)_\infty}{\left(Q_1Q_2\frac{t}{q},t\right)_\infty} P_{C_{\bar{q}}}\left(t; Q\sqrt{\frac{t}{q}}, Q_1\sqrt{\frac{t}{q}}, Q_1Q_2Q_3\frac{\sqrt{t}}{q}\right) , \end{aligned} \tag{4.69}$$

$$\begin{aligned} Z_{t\text{-brane}} &= \sum_{n=0}^{\infty} \frac{\left(Q\sqrt{\frac{t}{q}}\right)^n}{\left(\frac{1}{q},\frac{1}{q}\right)_n} \frac{\left(Q_1\sqrt{\frac{t}{q}},\frac{1}{q}\right)_n \left(Q_1Q_2Q_3\sqrt{\frac{t}{q}},\frac{1}{q}\right)_n}{\left(Q_1Q_2\frac{t}{q},\frac{1}{q}\right)_n} \\ &= \frac{\left(Q_1\sqrt{\frac{t}{q}},\frac{1}{q}\right)_\infty \left(Q_1Q_2Q_3\sqrt{\frac{t}{q}},\frac{1}{q}\right)_\infty}{\left(Q_1Q_2\frac{t}{q},\frac{1}{q}\right)_\infty} P_{C_t}\left(q; Q\sqrt{t}, Q_1\sqrt{t}, Q_1Q_2Q_3t\right) , \end{aligned} \tag{4.70}$$

where

$$C_{\bar{q}} = \begin{bmatrix} 0 & 1 & 1 & 1 \\ 1 & 0 & 0 & 0 \\ 1 & 0 & 0 & 0 \\ 1 & 0 & 0 & 1 \end{bmatrix} , \qquad C_t = \begin{bmatrix} 1 & -1 & -1 & -1 \\ -1 & 1 & 0 & 0 \\ -1 & 0 & 1 & 0 \\ -1 & 0 & 0 & 0 \end{bmatrix} . \tag{4.71}$$

We verify that refined open BPS invariants $N^{(s,r)}_{(d,d_1,d_2,d_3)}$ are non-negative integers as expected, as shown in Table A.3. Note that for fixed (d,d_1,d_2,d_3), non-zero invariants arise only for one particular value of r. We also conjecture that, for a given d, non-zero open BPS invariants arise for indices (s,r) that are in the range

$$r \le s \le d+1, \qquad \frac{1}{2}\left\lceil\frac{d}{2}\right\rceil \le r \le \frac{d-1}{2}, \tag{4.72}$$

and open BPS invariants with the maximal spin $s = d+1$ are equal to one.

4.3 Hanany-Witten transitions

In this section we consider Hanany-Witten (HW) transitions of 7-branes for brane webs (toric diagrams). Hanany-Witten transitions often lead to overlapped lines, which imply that there are some shrinking cycles in brane webs. These diagrams with overlapped lines are non-toric diagrams [96]. Non-toric diagrams in our context can be resolved by blowing up singular two-cycles, and finally we end up with toric diagrams that contain some local T_2-diagrams [99, 100, 82, 101]. T_2-diagram is a particular example of T_N-diagrams that engineer non-Lagrangian theories [96, 40]. We illustrated T_2-diagram in Figure 4.13.

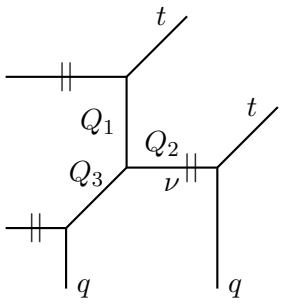

Figure 4.13: T_2-geometry includes three local $\mathbb{P}^1$'s that meet in one point.

One aim of this section is to confirm the consistency of refined open topological strings in processes of Hanany-Witten (HW) transitions. After reinterpreting toric diagrams as five-branes webs [71, 96], we introduce 7-branes at the end of semi-infinite 5-branes. These 7-brane can move around a given toric diagram. When such a 7-brane crosses 5-branes, some 5-branes may be created or annihilated, which is the process referred to as Hanany-Witten transition. On the level of topological strings, partition functions before and after such a transition should be equivalent. In this section we verify that this statement is correct for refined open partition functions for various strip Calabi-Yau threefolds that involve T_2-geometry. Furthermore, another interesting phenomenon that involves non-toric diagrams and T_2-geometry is T_2-tuning [36], which is a particular Higgsing that we use to obtain the refined open amplitudes for non-toric brane webs.

To start with, the geometric transitions in Figure 4.14 leads to the refined open amplitude for T_2-diagram and triple-$\mathbb{P}^1$ geometry. The HW transition of a 7-brane introduced at the infinity of a 5-brane relates these two geometries. More explicitly, the T_2-geometry with one Lagrangian brane is shown in diagram (c). This geometry can be obtained by Higgsing the toric diagram (a). Furthermore, we can make the Hanany-Witten transition of the 7-brane by moving it up. When applied to the T_2-geometry, HW transition produces a triple-$\mathbb{P}^1$ geometry up to an additional open string denoted by the wavy line in the diagram (d). In another way, this triple-$\mathbb{P}^1$ geometry can be obtained by Higgsing the diagram (b). In addition, the geometry in the diagram (b) itself can be obtained from the geometry (a) upon the Hanany-Witten transition. Therefore, geometric transition and HW transition compose a commute relation between these four diagrams, relating both open topological strings and closed topological strings.

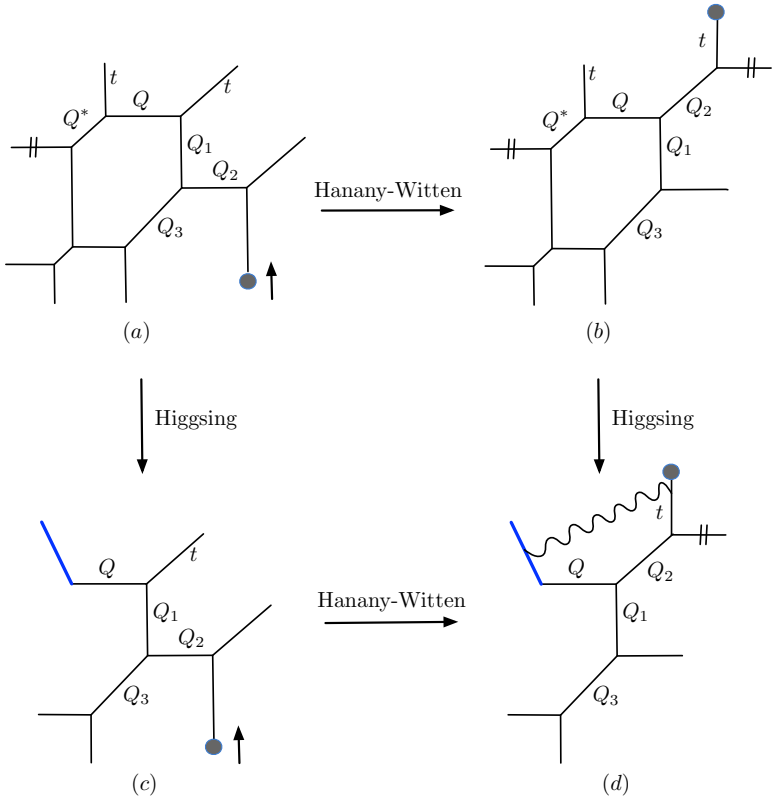

Figure 4.14: Geometric transition (Higgsing) and Hanany-Witten transition relate the T_2-geometry (diagram (c)) to a strip Calabi-Yau geometries in the presence of one Lagrangian brane. The 7-brane is denoted by a gray node.

We stress that geometric transitions and Hanany-Witten transitions have very different status. Geometric transitions enable us to determine explicitly open partition functions by giving specific values to certain Kähler parameters of the mother toric diagrams. For example, partition functions for diagram (c) and (d) in Figure 4.14 arise respectively from their mother diagram (a) and (b) upon geometric transitions. On the other hand, Hanany-Witten transitions change the brane webs significantly and predict that partition functions before and after the transition should be equivalent.

Let us compute the open partition functions for the diagrams in Figure 4.14 quantitatively. Closed partition function for the diagram (a) is given by [1]

$$\begin{aligned} Z^{T_2}_{(a)} = &\sum_{\mu,\nu}(-1)^{|\mu|+|\nu|}q^{\frac{||\mu||^2+||\nu||^2}{2}}Q^{|\mu|}Q_2^{|\nu|}||Z_\mu(q,t)||^2||Z_\nu(q,t)||^2 \\ &\times \frac{N_\mu^{\text{half},-}(Q^*,t^{-1},q^{-1})N_\nu^{\text{half},-}(Q_3,t^{-1},q^{-1})N_{\mu\nu}\left(Q_1\sqrt{\frac{t}{q}},t^{-1},q^{-1}\right)}{N_\mu^{\text{half},-}\left(Q_1Q_3\sqrt{\frac{q}{t}},t^{-1},q^{-1}\right)}, \end{aligned} \tag{4.73}$$

where the parameter Q plays the role of open Kähler modulus. Note that geometric transition tells us that fixing the values of Q^* in the term $N_\mu^{\text{half},-}(Q^*,t^{-1},q^{-1})$ by following the rules

[1] We ignore here the overall contributions of the form Z^M (2.131), as it does not depend on the open Kähler parameter Q.

from section 4.1, the $Z^{T_2}_{(a)}$ becomes the open amplitude for the diagram (c). For $Q^* = t\sqrt{\frac{t}{q}}$ we get a t-brane and for $Q^* = \frac{1}{q}\sqrt{\frac{t}{q}}$ we get $\bar{q}$-brane, whose open partition functions are denoted respectively by $Z^{T_2}_{t\text{-brane}}$ and $Z^{T_2}_{\bar{q}\text{-brane}}$.

On the other hand, the open amplitude for the diagram (d) in Figure 4.14 can be computed by Higgsing the closed amplitude for the diagram (b) analogously as in section 4.2.6. Again, 7-brane denoted by the dark node does not play a role as the associated external line are assigned with empty Young diagram. We get the open partition functions for t-brane and $\bar{q}$-brane respectively as follows:

$$\begin{aligned} Z^{3\mathbb{P}^1}_{t\text{-brane}} &= \sum_{n=0}^{\infty} \frac{(QQ_2t)^n \left(Q_1\sqrt{\frac{q}{t}},q\right)_n \left(\frac{1}{Q_2}\sqrt{\frac{q}{t}},q\right)_n}{(q,q)_n (Q_1Q_3q/t,q)_n} = P_{C_t}\left(q; QQ_2t, Q_1\sqrt{\frac{q}{t}}, Q_2^{-1}\sqrt{\frac{q}{t}}, Q_1Q_3\frac{\sqrt{q}}{t}\right), \\ Z^{3\mathbb{P}^1}_{\bar{q}\text{-brane}} &= \sum_{n=0}^{\infty} \frac{\left(\frac{Q}{Q_3q}\right)^n \left(\frac{1}{Q_1}\sqrt{\frac{t}{q}},t\right)_n \left(Q_2\sqrt{\frac{t}{q}},t\right)_n}{(t,t)_n \left(\frac{t}{Q_1Q_3q},t\right)_n} = P_{C_{\bar{q}}}\left(t; QQ_2\frac{\sqrt{t}}{q}, Q_1\sqrt{q}, Q_2^{-1}\sqrt{q}, Q_1Q_3q\right), \end{aligned} \tag{4.74}$$

where we also provide quiver forms (3.112) (ignoring Q-independent prefactors analogous to (4.33) and (4.35)) in the following

$$C_t = \begin{bmatrix} 0 & 1 & 1 & 1 \\ 1 & 0 & 0 & 0 \\ 1 & 0 & 0 & 0 \\ 1 & 0 & 0 & 1 \end{bmatrix}, \qquad C_{\bar{q}} = \begin{bmatrix} -1 & -1 & -1 & -1 \\ -1 & 1 & 0 & 0 \\ -1 & 0 & 1 & 0 \\ 1 & 0 & 0 & 0 \end{bmatrix}. \tag{4.75}$$

We can now compare partition functions in (4.73) with (4.74). We find that the HW transition does not change open amplitudes up to a simple factor

$$Z^{T_2}_{t\text{-brane}} = \frac{Z^{3\mathbb{P}^1}_{t\text{-brane}}}{(QQ_2t,q)^{-1}_\infty}, \qquad Z^{T_2}_{\bar{q}\text{-brane}} = \frac{Z^{3\mathbb{P}^1}_{\bar{q}\text{-brane}}}{(QQ_2\frac{t}{q},t)_\infty}. \tag{4.76}$$

The factor $(QQ_2t,q)^{-1}_\infty = (QQ_2\frac{t}{q},\frac{1}{q})_\infty = \mathrm{PE}[QQ_2,1,1/2,1/2]_{t\text{-brane}}$ in the denominator for the t-brane encodes a single open BPS invariant $N^{(1/2,1/2)}_{QQ_2} = 1$, and represents an open string of length QQ_2, denoted in the diagram (d) by a wavy line. The factor $(QQ_2\frac{t}{q},t)_\infty$ for the $\bar{q}$-brane has the same interpretation. We note that this additional open string can be easily identified, as it is not meaningful to have disconnected strings. This additional string with length QQ_2 is connected in the diagram (d), but is not connected in the diagram (c), so this string exist only in the right diagram (d). Altogether, the relations (4.76) confirm that refined open topological strings are consistent with Hanany-Witten transitions.

Furthermore, the relations (4.76) immediately imply that open partition functions for T_2-geometry can be also presented in the quiver form – in this case quivers look like the quivers for triple-$\mathbb{P}^1$ geometry in (4.75), and in addition have one extra node that represents the

denominators on the right side of (4.76). It follows that the quiver forms for T_2-geometry read

$$\begin{aligned} Z^{T_2}_{t\text{-brane}} &= P_{C_t}\left(q; QQ_2\frac{t}{\sqrt{q}}, QQ_2 t, Q_1\sqrt{\frac{q}{t}}, Q_2^{-1}\sqrt{\frac{q}{t}}, Q_1Q_3\frac{\sqrt{q}}{t}\right), \\ Z^{T_2}_{\bar{q}\text{-brane}} &= P_{C_{\bar{q}}}\left(t; QQ_2\frac{t}{q}, QQ_2\frac{\sqrt{t}}{q}, Q_1\sqrt{q}, Q_2^{-1}\sqrt{q}, Q_1Q_3 q\right), \end{aligned} \tag{4.77}$$

with quiver matrices

$$C_t = \begin{bmatrix} 1 & 0 & 0 & 0 & 0 \\ 0 & 0 & 1 & 1 & 1 \\ 0 & 1 & 0 & 0 & 0 \\ 0 & 1 & 0 & 0 & 0 \\ 0 & 1 & 0 & 0 & 1 \end{bmatrix}, \qquad C_{\bar{q}} = \begin{bmatrix} 0 & 0 & 0 & 0 & 0 \\ 0 & 1 & -1 & -1 & -1 \\ 0 & -1 & 1 & 0 & 0 \\ 0 & -1 & 0 & 1 & 0 \\ 0 & -1 & 0 & 0 & 0 \end{bmatrix}. \tag{4.78}$$

Having determined the open partition functions for T_2-geometry, let us discuss some of its properties. One of them is referred to as T_2-tuning found in [36]. In the context of closed strings this is the statement that after adjusting two of the three Kähler parameters of the T_2-geometry, either as $Q_1 = Q_3 = \sqrt{\frac{t}{q}}$ or $\sqrt{\frac{q}{t}}$, or $Q_2 = Q_3 = \sqrt{\frac{t}{q}}$, or $Q_1 = Q_2 = \sqrt{\frac{q}{t}}$, appropriate two parallel external lines of T_2-geometry overlap, and the geometry itself reduces effectively to two copies of $\mathbb{C}^3$ in a non-toric configuration. Such a process is shown in Figure 4.15. Note that for closed strings, in case (a), Q_1 and Q_3 can be fixed to two equivalent values

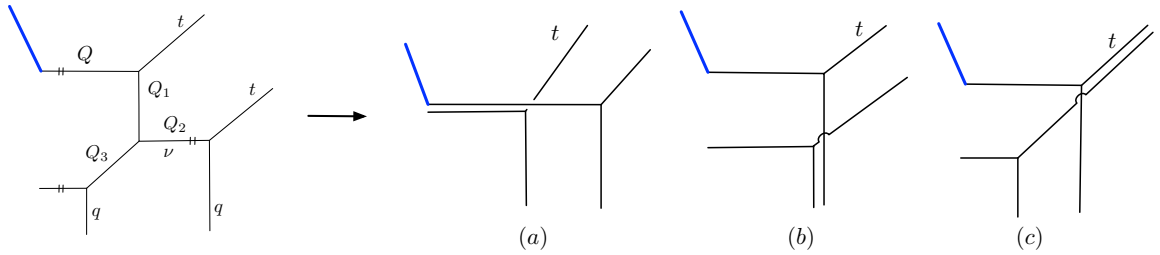

Figure 4.15: T_2-tuning with a Lagrangian brane: tuning appropriately Kähler parameters of T_2-geometry reduces it to two copies of $\mathbb{C}^3$, which are non-toric diagrams as some two-cycles have zero volume.

$\sqrt{\frac{t}{q}}$ or $\sqrt{\frac{q}{t}}$; this appears to be a feature of two lines overlapping along the preferred direction.

Note that now in the presence of a Lagrangian brane, the T_2-tuning is slightly broken. In case (a) the parameters Q_1 and Q_3 can be fixed to only one value $\sqrt{\frac{t}{q}}$. Similarly as in the closed string case, once we fix values of two Kähler parameters as above, the dependence on third parameter drops out. For example, fixing $Q_1 = Q_3 = \sqrt{\frac{t}{q}}$ in the partition function (4.73), it follows from (4.3) that $\nu = \emptyset$ and hence $Q_2^{|\nu|} = 1$. Ultimately, in all configurations $(a), (b)$ and (c) the t-brane partition function (4.73) reduces to $(Q\sqrt{qt}, q)_\infty$, which is indeed the same as t-brane partition function for the geometry $\mathbb{C}^3$.

Finally, let us consider more examples to illustrate the effects of Hanany-Witten transitions. First, consider the process in Figure 4.16, where moving a 7-brane from infinity to the T_2-geometry results in a non-toric structure that involves one additional open string. The open

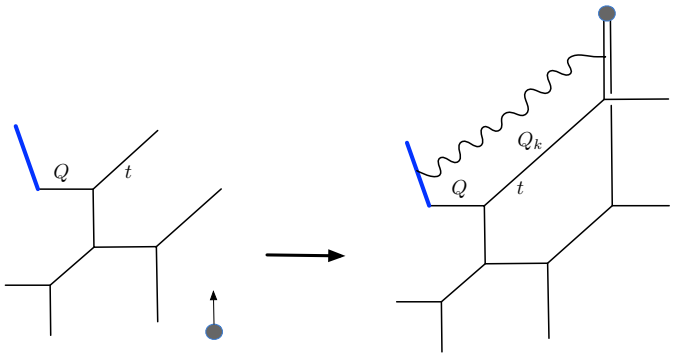

Figure 4.16: Hanany-Witten moving a 7-brane (dark node) from infinity to the T_2-geometry results in a non-toric diagram and one additional open string of length QQ_k.

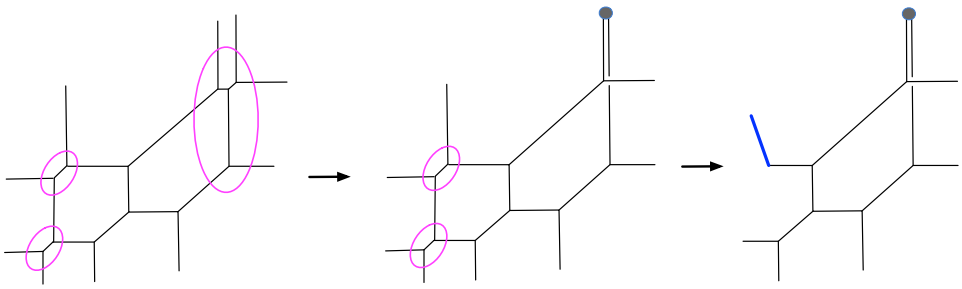

Figure 4.17: T_2-tuning followed by Higgsing two local $\mathbb{P}^1$'s (in the second step) gives to a non-toric diagram with a Lagrangian brane.

partition function for the T_2-geometry has been given in (4.74). To determine the open partition function after HW transition we engineer its mother toric diagram shown in Figure 4.17. We first compute its closed partition function using refined topological vertex, and then fix appropriate parameters according to the rules of T_2-tuning, and fix other Kähler parameters in the process of geometric transitions to produce a Lagrangian brane. This process finally gives rise to the geometry shown in Figure 4.17 (right), which is the same as in 4.16 (right), and we denote its open partition function by $Z^{\text{right}}_{t\text{-brane}}$. Then, comparing open partition functions of both geometries in Figure 4.16 we find

$$Z^{T_2}_{t\text{-brane}} = \frac{Z^{\text{right}}_{t\text{-brane}}}{(QQ_k t, q)^{-1}_\infty}, \tag{4.79}$$

where the factor $(QQ_k t, q)^{-1}_\infty = \text{PE}[QQ_k, 1, 1/2, 1/2]_{t\text{-brane}}$ represents the additional open string of length QQ_k that is produced by the Hanany-Witten transition.

An analogous example, however involving the triple-$\mathbb{P}^1$ geometry, is shown in Figure 4.18. We have computed the open partition function $Z^{3\mathbb{P}^1}_{t\text{-brane}}$ for a t-brane in triple-$\mathbb{P}^1$ geometry in (4.74). We determine the partition function $Z^{(b)}_{t\text{-brane}}$ for the geometry shown in 4.18 in diagram (b) following Figure 4.19, and again applying T_2-tuning and geometric transition to

an appropriately engineered more complicated geometry. We then find that

$$Z^{3\mathbb{P}^1}_{t\text{-brane}} = \frac{Z^{(b)}_{t\text{-brane}}}{(QQ_2Q_kt^2q^{-1},q)^{-1}_\infty}, \tag{4.80}$$

where the denominator $(QQ_2Q_kt^2q^{-1},q)^{-1}_\infty = \text{PE}[QQ_2Q_k,1,3/2,3/2]_{t\text{-brane}}$ represents the additional open string of length QQ_2Q_k introduced by the Hanany-Witten transition in Figure 4.18.

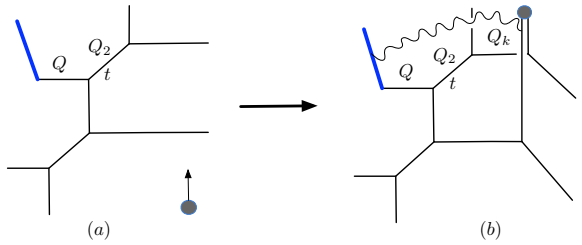

Figure 4.18: Hanany-Witten transition that moves a 7-brane (denoted by a blue dot) from infinity to the triple-$\mathbb{P}^1$ geometry results in a non-toric structure with one extra open strings of length QQ_2Q_k.

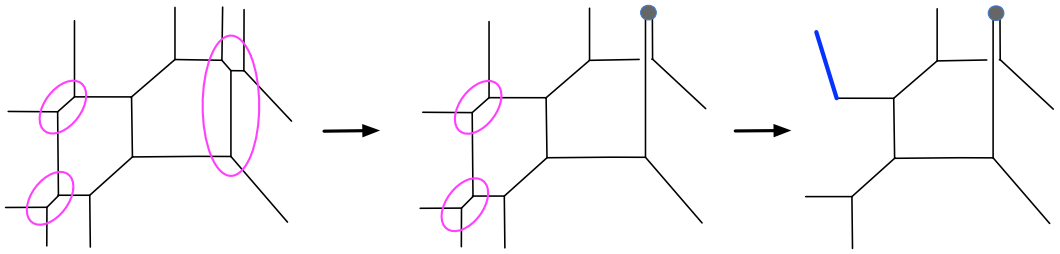

Figure 4.19: T_2-tuning (in the first step) followed by geometric transitions on two local $\mathbb{P}^1$'s (in the second step) gives the geometry with a Lagrangian brane shown in Figure 4.18 (right).

Furthermore, let us consider a more complicated process, where anti-fundamental chiral multiplets are introduced by sandwiching 7-branes between 5-branes, see Figure 4.20. We choose either to move one 7-brane down to infinity and another 7-brane up to infinity, see diagram (a) in Figure 4.20, or to move these 7-branes in opposite directions, see diagram (c). These operations result respectively in diagrams (b) and (d). We expect that their open partition functions should be equal, up to some factors representing additional open strings that arise in these different Hanany-Witten transitions. To verify this claim, we compute refined open partition functions for diagrams (b) and (d) following respectively Figure 4.21 and Figure 4.22. Denoting these open partition functions by $Z^{(b)}_{t\text{-brane}}$ and $Z^{(d)}_{t\text{-brane}}$, we then find

$$\frac{Z^{(b)}_{t\text{-brane}}}{(QQ_5t,q)^{-1}_\infty} = \frac{Z^{(d)}_{t\text{-brane}}}{(QQ_2t,q)^{-1}_\infty}. \tag{4.81}$$

This indeed the expected results, where additional open strings represented by $(QQ_5t,q)^{-1}_\infty = \text{PE}[QQ_5,1,1/2,1/2]_{t\text{-brane}}$ and $(QQ_2t,q)^{-1}_\infty = \text{PE}[QQ_2,1,1/2,1/2]_{t\text{-brane}}$. This result again

confirms the consistency of refined topological strings with Hanany-Witten transitions.

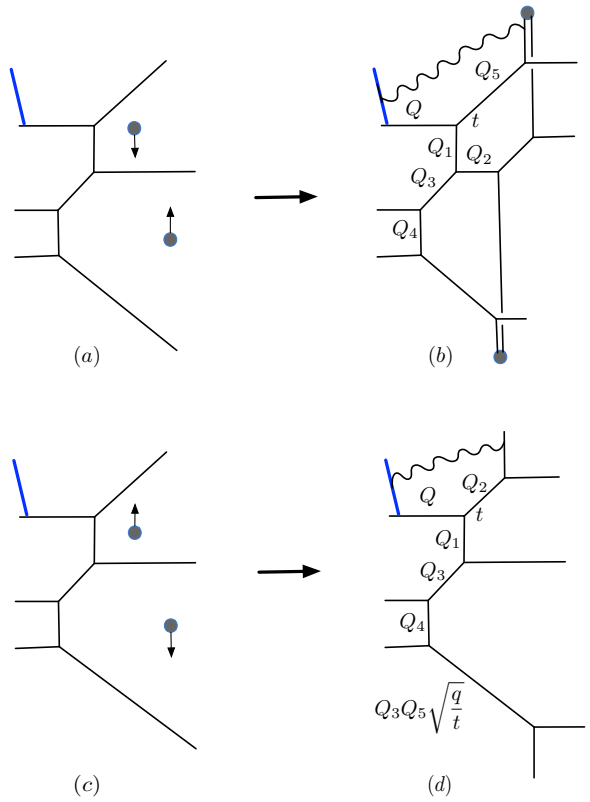

Figure 4.20: Hanany-Witten transition that involves moving two 7-branes to infinity, and produces additional open strings. Note that the shift $\sqrt{\frac{q}{t}}$ in $Q_3Q_5\sqrt{\frac{q}{t}}$ can be derived by T_2-tuning.

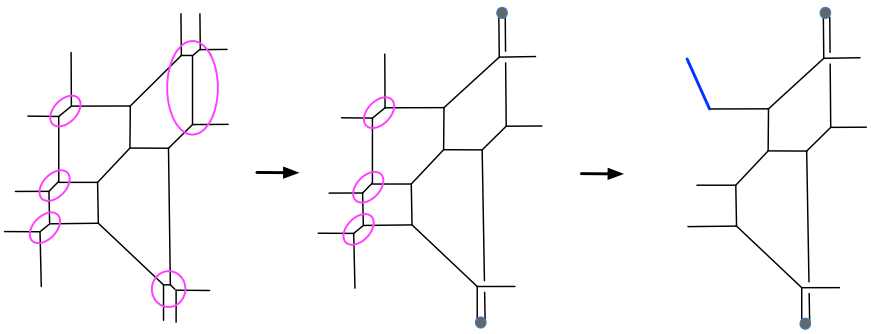

Figure 4.21: T_2-tuning on two pairs of lines (in the first step) followed by the geometric transition on three local $\mathbb{P}^1$'s (in the second step) engineers the geometry with a Lagrangian brane shown in Figure 4.20 (b).

4.4 Generic toric diagrams

In this section we consider examples of toric manifolds with compact four-cycles. We focus on Lagrangian branes in Hirzebruch surfaces and blow up some points. Let us first make the

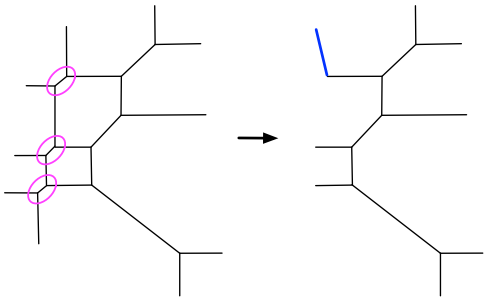

Figure 4.22: Geometric transitions on three local $\mathbb{P}^1$'s give rise to a Lagrangian brane shown in Figure 4.20 (d).

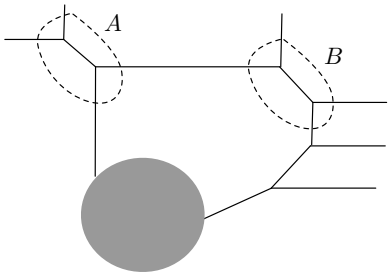

Figure 4.23: Introducing local $\mathbb{P}^1$'s may produce parallel external lines. In this example, Lagrangian branes can be engineered at positions A or B.

following remark. Our approach seems to work only for introducing Lagrangian branes on external parallel lines. In other situations one can blow up some points to produce more local $\mathbb{P}^1$'s, see Figure 4.23, which effectively changes the direction of external lines. Finally after decoupling these introduced lines, we obtain the original refined open partition functions.

The first example we consider is the Hirzebruch surface $\mathbb{F}_0^2$ with a Lagrangian brane. Its toric diagram is shown in Figure 4.24 (right) and can be obtained through Higgsing the geometry shown on the left. We just calculate the t-brane partition function, as other types of Lagrangian branes give rise to the same result upon the exchange symmetry (4.9). We set

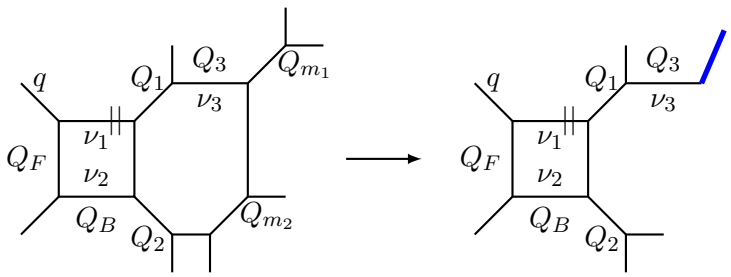

Figure 4.24: Geometric transitions at Q_{m_1} and Q_{m_2} introduce a Lagrangian brane at one external line of $\mathbb{F}_0^2$. One can also switch the values of Q_{m_1} and Q_{m_2} to introduce the Lagrangian brane on the bottom external line.

Kähler parameters $Q_{m_1} = t\sqrt{\frac{t}{q}}$ and $Q_{m_2} = \sqrt{\frac{t}{q}}$ in the left diagram in Figure 4.24, and obtain

$$\begin{aligned} Z^{\text{open-closed}}_{t\text{-brane}}(\mathbb{F}_0^2) = &\sum_{\nu_1,\nu_2,\nu_3} (-1)^{|\nu_3|} q^{\frac{||\nu_3||^T}{2}+||\nu_2^T||^2} t^{\frac{||\nu_3||^2}{2}+||\nu_1^T||^2} \times \\ &\times Q_3^{|\nu_3|} Q_B^{|\nu_1|+|\nu_2|} ||Z_{\nu_1}(q,t)||^2 ||Z_{\nu_2}(t,q)||^2 ||Z_{\nu_3}(t,q)||^2 \times \\ &\times \frac{N^{\text{half},-}_{\nu_3^T}\left(\frac{1}{q}\sqrt{\frac{t}{q}}\right) N^{\text{half},+}_{\nu_1}\left(Q_2 Q_F\right) N^{\text{half},+}_{\nu_2^T}\left(Q_2\right) N_{\nu_1,\nu_3^T}\left(Q_1\sqrt{\frac{t}{q}}\right) N_{\nu_2^T,\nu_3^T}\left(Q_1 Q_F\sqrt{\frac{t}{q}}\right)}{N^{\text{half},+}_{\nu_3^T}\left(Q_1 Q_2 Q_F\sqrt{\frac{t}{q}}\right) N_{\nu_2^T,\nu_1}\left(Q_F\right) N_{\nu_2^T,\nu_1}\left(Q_F\frac{t}{q}\right)}, \end{aligned} \tag{4.82}$$

where $N_{\mu,\nu}(Q)$ is a shorthand notation for $N_{\mu,\nu}(Q,t^{-1},q^{-1})$, and Q_3 represents the open Kähler parameter. Note that the partition function (4.82) contains also closed string contributions

$$\begin{aligned} Z^{\text{closed}}(\mathbb{F}_0^2) = &\sum_{\nu_1,\nu_2} q^{||\nu_2^T||^2} t^{||\nu_1^T||^2} Q_B^{|\nu_1|+|\nu_2|} ||Z_{\nu_1}(q,t)||^2 ||Z_{\nu_2}(t,q)||^2 \times \\ &\times \frac{N^{\text{half},-}_{\nu_1}\left(Q_1\right) N^{\text{half},-}_{\nu_2^T}\left(Q_1 Q_F\right) N^{\text{half},+}_{\nu_1}\left(Q_2 Q_F\right) N^{\text{half},+}_{\nu_2^T}\left(Q_2\right)}{N_{\nu_2^T,\nu_1}\left(Q_F\right) N_{\nu_2^T,\nu_1}\left(Q_F\frac{t}{q}\right)}. \end{aligned} \tag{4.83}$$

The t-brane open partition function of our interest therefore should be

$$Z_{t\text{-brane}}(\mathbb{F}_0^2) = \frac{Z^{\text{open-closed}}_{t\text{-brane}}(\mathbb{F}_0^2)}{Z^{\text{closed}}(\mathbb{F}_0^2)}\,. \tag{4.84}$$

We show the associated open refined BPS invariants in Table A.4. They are indeed non-negative integers, as expected.

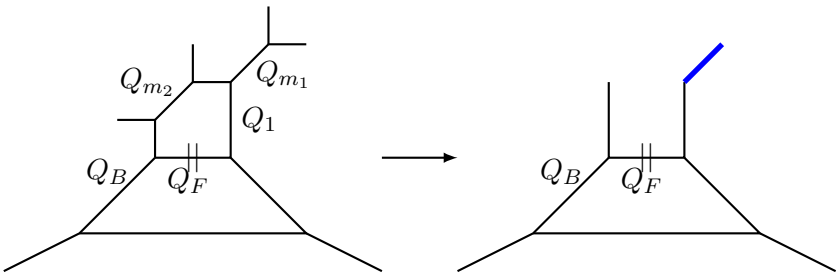

Figure 4.25: Geometric transitions at Q_{m_1} and Q_{m_2} (in the left diagram) produce the Hirzebruch surface $\mathbb{F}_2$ with a Lagrangian brane (right).

The second example we consider is the Hirzebruch surface $\mathbb{F}_2$ with a Lagrangian brane, illustrated in Figure 4.25 (right). This diagram can be obtained by Higgsing the left diagram in Figure 4.25, upon fixing Kähler parameters $Q_{m_1} = t\sqrt{\frac{t}{q}}$ and $Q_{m_2} = \sqrt{\frac{t}{q}}$. In this way we

obtain the open-closed partition function

$$Z^{\text{open-closed}}_{t\text{-brane}}(\mathbb{F}_2) = \sum_{\nu_1,\nu_2,\nu_3} q^{-||\nu_3||^2} t^{||\nu_2||^2+2||\nu_3^T||^2} Q_B^{2|\nu_3|} Q_F^{|\nu_2|+|\nu_3|} ||Z_{\nu_2}(t,q)||^2 ||Z_{\nu_3}(q,t)||^2 \times \\ \times \frac{N^{\text{half},+}_{\nu_2^T}\left(Q_1 t\sqrt{\frac{t}{q}}\right) N^{\text{half},+}_{\nu_3}\left(Q_1 Q_B t\sqrt{\frac{t}{q}}\right)}{N^{\text{half},+}_{\nu_3}\left(Q_1 Q_B\sqrt{\frac{t}{q}}\right) N^{\text{half},+}_{\nu_2^T}\left(Q_1\sqrt{\frac{t}{q}}\right) N_{\nu_2^T,\nu_3}\left(Q_B t\right) N_{\nu_2^T,\nu_3}\left(Q_B\frac{t}{q}\right)}, \tag{4.85}$$

which also contains closed string contributions

$$Z^{\text{closed}}(\mathbb{F}_2) = \sum_{\nu_2,\nu_3} \frac{q^{-||\nu_3||^2} t^{||\nu_3||^2+2||\nu_3^T||^2} Q_B^{2|\nu_3|} ||Z_{\nu_2}(t,q)||^2 ||Z_{\nu_3}(q,t)||^2}{N_{\nu_2^T,\nu_3}\left(Q_B t\right) N_{\nu_2^T,\nu_3}\left(Q_B\frac{t}{q}\right)}\,. \tag{4.86}$$

In this case Q_1 is the open Kähler parameter, which also appears in the prefactor (2.131)

$$Z^M(\mathbb{F}_2) = \frac{M(Q_1 t,q,t)M(Q_1Q_B t,q,t)}{M(Q_1,q,t)M(Q_1Q_B,q,t)}. \tag{4.87}$$

Therefore, the t-brane partition function of our interest should be

$$Z_{t\text{-brane}}(\mathbb{F}_2) = \frac{Z^M(\mathbb{F}_2)\cdot Z^{\text{open-closed}}_{t\text{-brane}}(\mathbb{F}_2)}{Z^{\text{closed}}(\mathbb{F}_2)}\,. \tag{4.88}$$

We show some refined open BPS invariants, in particular the curves wrapping the compact divisor, in Table A.5. They are non-negative integers, as expected.

Chapter 5

3d mirror symmetry and mixed Chern-Simons levels

We have discussed 3d mirror symmetry in section 3.1.4. The 3d mirror symmetry can be interpreted as a functional Fourier transformation on the path integral of partition functions [65]. A basic example is the duality between $U(1)+1\mathbf{F}$ and a free chiral multiplet. This mirror pair can be used to construct other mirror dual pairs such as SQED-XYZ model. Recently, using mirror dual pairs to construct mirror dual theories has been implemented in [67]. In this chapter, we are going to use this basic mirror pair as the building block to find the mirror dual theories of 3d abelian theories with a gauge group $U(1)$ and some fundamental or antifundamental chiral multiplets, denoted by $U(1)_k+N_F\mathbf{F}+N_{AF}\mathbf{AF}$. These abelian theories are interesting, as they are geometrically engineered by strip Calabi-Yau threefolds in the presence of a Lagrangian brane. For more details on 3d $\mathcal{N}=2$ theories, see e.g.[102, 6, 57, 103].

In order to perform mirror transformations on $U(1)_k+N_F\mathbf{F}+N_{AF}\mathbf{AF}$, we use a special type of theory denoted as $\mathcal{T}_{A,N}$ which consists of a bunch of building blocks $U(1)+1\mathbf{F}$ coupled together by mixed Chern-Simons levels (3.19). The abelian theories with mixed Chern-Simons levels has been discussed in [53]. We further discuss abelian theories with mixed Chern-Simons levels and their mirror symmetry transformations in this chapter.

Another motivation is to find a quiver representation. For a generic strip Calabi-Yau threefold, there is a corresponding quiver which is the same in both refined and unrefined cases; see chapter 4. These quivers are not very well understood and we need to physically understand it. It is conjectured in [93] that such quivers encoded in knot polynomials in Ooguri-Vafa construction [14] are mixed Chern-Simons levels for abelian 3d $\mathcal{N}=2$ theories. We find this conjecture is correct in another configuration, namely the 3d $\mathcal{N}=2$ theories engineered by strip Calabi-Yau threefolds, in which case the knot is trivial but the background geometry is much more complicated than the resolved conifold. By using mirror transformations, we find the quivers are actually the effective mixed Chern-Simons levels for mirror dual $\mathcal{T}_{A,N}$ theories. The interesting point is that mirror transformations can be implemented more than one time, and form a very nice group called mirror transformation group $\mathcal{H}(\mathcal{T}_{A,N})$. In particular, mirror transformations sometimes may not give rise to integer mixed Chern-Simons levels, which implies parity anomaly, hence we should throw away

these non-integer mixed Chern-Simons levels. We note that the mirror transformation group gives rise to several different effective mixed Chern-Simons levels, which are related by mirror transformations. We find that these integer mixed Chern-Simons levels are related by flipping the sign of effective FI parameters $\xi_i \to -\xi_i$ which can be interpreted as mirror maps. This flip has remarkable implication, as it changes positions of D5-branes as we discuss in the next chapter. In this chapter we focus on mirror transformations and mixed Chern-Simons levels. In the next chapter, we will discuss the influence of mirror symmetry on 3d brane webs.

This chapter is based on [11]. In section 5.1, we discuss partition functions and mirror transformations for $\mathcal{T}_{A,N}$ theories. In section 5.2, we perform mirror symmetry on abelian theories engineered by strip Calabi-Yau threefolds, and find mirror dual theories are $\mathcal{T}_{A,N}$ theories. The quivers are therefore interpreted as effective mixed Chern-Simons levels. In section 5.3, we discuss the application of mirror transformations on knot polynomials.

5.1 3d mirror symmetry and $\mathcal{T}_{A,N}$ theory

In order to implement mirror symmetry on 3d gauge theories, it is convenient to work with sphere partition functions. As we have discussed in subsection 3.1.4, mirror symmetry acts as functional Fourier transformations on the path integrals of partition functions. Hence we also refer to mirror symmetry as a mirror transformation. In this section, we first define $\mathcal{T}_{A,N}$ theories and then write down their sphere partition functions from which one can read off effective superpotentials encoding mixed Chern-Simons levels. In the second part of this section, we discuss that there is a mirror transformation group for the $\mathcal{T}_{A,N}$ theory.

5.1.1 $\mathcal{T}_{A,N}$ theory

We define the abelian quiver theories as follows:

$$\mathcal{T}_{A,N}: \quad (U(1)+1\mathbf{F})^{\otimes N}_{k_{ij},\,\xi_i}\,. \tag{5.1}$$

They consist of N copies of $U(1)+1\mathbf{F}$ theory with real symmetric bare Chern-Simons levels k_{ij} which couple gauge groups $U(1)\times U(1)\times\cdots\times U(1)$. In (5.1), ξ_i are Fayet-Iliopoulos parameters and u_i are real mass parameters for chiral multiplets. Note that there is no 3d superpotential for $\mathcal{T}_{A,N}$ theories. For other properties of this theory, see e.g. [104]. The sphere partition function for $\mathcal{T}_{A,N}$ theory reads

$$Z^{\mathcal{T}_{A,N}}_{S^3_b} = \int\prod_{i=1}^{N} dx_i\, e^{\sum_{i,j=1}^{N} -i\pi k_{ij}x_ix_j+2i\pi\xi_ix_i}\prod_{i=1}^{N} s_b\Big(\frac{iQ}{2}+x_i+\frac{u_i}{2}\Big)\,, \tag{5.2}$$

where $Q=b+1/b$. By shifting x_i, one can define shifted Fayet-Iliopoulos parameters $\tilde{\xi}_i$:

$$x_i\to -x_i-\frac{u_i}{2}\,,\quad \xi_i=-\tilde{\xi}_i-\frac{1}{2}\sum_{j=1}^{N}k_{ij}u_j\,, \tag{5.3}$$

which turn $\mathcal{T}_{A,N}$ theories into massless theories with sphere partition functions

$$Z_{S^3_b}^{\mathcal{T}_{A,N}} = \int \prod_{i=1}^{N} dx_i \, e^{\sum_{i,j=1}^{N} -i\pi k_{ij} x_i x_j + 2i\pi \tilde{\xi}_i x_i} \prod_{i=1}^{N} s_b\Big(\frac{iQ}{2} - x_i\Big)\,, \tag{5.4}$$

where real mass parameters u_i have been absorbed into $\tilde{\xi}_i$. We identify (5.4) as sphere partition functions of $\mathcal{T}_{A,N}$ theories. In this thesis we only consider symmetric Chern-Simons levels $k_{ij} = k_{ji}$. In addition, if we redefine parameters for each gauge node $U(1)_i$

$$x_i =: \frac{\log\big(-\frac{y_i}{\sqrt{q}}\big)}{-2\pi b}\,, \tag{5.5}$$

then the associated twisted effective superpotentials obtained by taking the semi-classical limit $\hbar \to 0$ and using (A.37), yield

$$\widetilde{\mathcal{W}}^{\text{eff}}_{\mathcal{T}_{A,N}}(k_{ij}, \xi, \mathbf{y}) = \sum_{i=1}^{N_f} \text{Li}_2(y_i) + \xi_i^{\text{eff}} \log y_i + \sum_{i,j=1}^{N_f} \frac{k_{ij}^{\text{eff}}}{2} \log y_i \log y_j\,, \tag{5.6}$$

where each polylogarithm functions $\text{Li}_2(y_i)$ is contributed by a chiral multiplets $\mathbf{F}$, k_{ij}^{eff} are effective Chern-Simons (CS) level matrices, and ξ_i^{eff} are effective Fayet-Iliopoulos (FI) parameters. More explicitly, these parameters are given by

$$k_{ij}^{\text{eff}} = k_{ij} + \frac{1}{2}\delta_{ij} \in \mathbb{Z}\,, \tag{5.7}$$

$$\xi_i^{\text{eff}} = 2\pi b\, \tilde{\xi}_i + i\pi(1 - bQ) \sum_{j=1}^{N_f} k_{ij} + \frac{i\pi}{2}\,. \tag{5.8}$$

We remind that for symmetric Chern-Simons terms

$$\sum_{i,j} \frac{k_{ij}^{\text{eff}}}{2} \log y_i \log y_j = \sum_i \frac{k_{ii}^{\text{eff}}}{2} (\log y_i)^2 + \sum_{i<j} k_{ij}^{\text{eff}} \log y_i \log y_j\,. \tag{5.9}$$

The effective superpotential plays a significant role. The vacua of 3d effective theories are given by the F-term [20, 63] as follows

$$\mathcal{M}_C: \quad e^{y_i \frac{d\,\widetilde{\mathcal{W}}^{\text{eff}}}{d\,y_i}} = 1\,, \text{ for } \forall\, i = 1, \cdots, N\,. \tag{5.10}$$

More explicitly,

$$\mathcal{M}_C: \quad e^{\xi_i^{\text{eff}}} \cdot \prod_{j=1}^{N} y_j^{k_{ij}^{\text{eff}}} + y_i - 1 = 0\,, \quad \forall\, i = 1, \cdots, N\,. \tag{5.11}$$

By comparing (5.6) with superpotentials in [85], we conjecture that vortex partition functions for $\mathcal{T}_{A,N}$ theories take form

$$Z^{\text{vortex}}_{\mathcal{T}_{A,N}}(x_i) = \sum_{d_1,\ldots,d_N=0}^{\infty} (-\sqrt{q})^{\sum_{i,j=1}^{N} k^{\text{eff}}_{ij} d_i d_j} \frac{x_1^{d_1}\cdots x_N^{d_N}}{(q,q)_{d_1}\cdots(q,q)_{d_N}}\,, \tag{5.12}$$

where $x_i := (-1)^{k^{\text{eff}}_{ii}} e^{\xi^{\text{eff}}_i}$, and d_i are magnetic flux numbers (vortex numbers) discussed in section 3.1.1. Vortex partition functions can also be obtained by the factorization property of sphere partition functions [80, 105].

5.1.2 Mirror transformations

Recall that 3d mirror symmetry can be interpreted as a functional Fourier transformation on partition functions [65], which is therefore called mirror transformation in this thesis. Here we discuss how it acts on $\mathcal{T}_{A,N}$ theories. We start from the most basic example, namely the dual pair between $U(1)_{1/2} + 1\mathbf{F}$ mirrors and a chiral singlet with Chern-Simons level $-1/2$:

$$U(1)_{1/2} + 1\mathbf{F} \quad \xleftrightarrow{\text{mirror symmetry}} \quad 1\mathbf{F}_{-\frac{1}{2}}\,. \tag{5.13}$$

Their partition functions are equivalent

$$\int dy\, e^{-\frac{i\pi}{2}y^2} e^{2\pi i\left(\frac{iQ}{4}-z\right)y} s_b\Big(\frac{iQ}{2}-y\Big) = e^{\frac{i\pi}{2}\left(\frac{iQ}{2}-z\right)^2} s_b\Big(\frac{iQ}{2}-z\Big)\,. \tag{5.14}$$

This is a mathematical identity discussed in [106, 107], which implies that any double-sine function $s_b(\cdots)$ can be replaced by an integral:

$$s_b\Big(\frac{iQ}{2}-z\Big) \xrightarrow{\text{mirror transformation}} e^{-\frac{i\pi}{2}\left(\frac{iQ}{2}-z\right)^2} \int dy\, e^{-\frac{i\pi}{2}y^2} e^{2\pi i\left(\frac{iQ}{4}-z\right)} s_b\Big(\frac{iQ}{2}-y\Big)\,. \tag{5.15}$$

Hence the double since function is the basic unit for mirror transformations.

On the other hand, mirror symmetry is interpreted as the ST operation in the $SL(2,\mathbb{Z})$ symmetry that acts on the Lagrangian of 3d Chern-Simons theory [66], so one can also use ST to denote the mirror transformation. We find an interesting property associated to mirror transformation. If we perform mirror symmetry on $U(1)_k + 1\mathbf{F}$ only once, we get a new theory $U(1)'_{k'} + 1\mathbf{F}$:

$$ST: \quad U(1)_k + 1\mathbf{F} \xrightarrow{ST} U(1) + \big(U(1)'_k + 1\mathbf{F}\big) \xrightarrow{\text{integrate out } U(1)_k} U(1)'_{k'} + 1\mathbf{F}\,, \tag{5.16}$$

where the old gauge group $U(1)_k$ was integrated out to get a new theory with Chern-Simons level k' and new FI parameters ξ'. Note that this transformation does not change sphere

partition functions. If we perform mirror symmetry twice we get another quiver $U(1)''_{k''}+1\mathbf{F}$:

$$(ST)^2: \quad U(1)_k+1\mathbf{F} \xrightarrow{ST} U(1)+\big(U(1)'+1\mathbf{F}\big) \xrightarrow{ST} U(1)+\big(U(1)'+\big(U(1)''+\mathbf{F}\big)\big) \xrightarrow{\text{integrate out } U(1) \text{ and } U(1)'} U(1)''_{k''}+1\mathbf{F}\,. \tag{5.17}$$

The corresponding partition functions are also equal. However, if we perform mirror transformation third time, we go back to the original theory

$$(ST)^3: \quad U(1)_k+1\mathbf{F} \xrightarrow{ST} U(1)'_{k'}+1\mathbf{F} \xrightarrow{ST} U(1)''_{k''}+1\mathbf{F} \xrightarrow{ST} U(1)_k+1\mathbf{F}\,, \tag{5.18}$$

which is consistent with a property of ST operator $(ST)^3=1$.

Analogously we can perform mirror transformations on each building block of $\mathcal{T}_{A,N}$ theories. For instance,

$$\begin{pmatrix} U(1)+1\mathbf{F} \\ U(1)+1\mathbf{F} \\ \cdots \\ U(1)+1\mathbf{F} \end{pmatrix}_{k_{ij},\ \xi_i} \xrightarrow{(ST,ST,\cdots,0)} \begin{pmatrix} U(1)+(U(1)'+1\mathbf{F}) \\ U(1)+(U(1)'+1\mathbf{F}) \\ \cdots \\ U(1)+1\mathbf{F} \end{pmatrix} \xrightarrow{\text{integrate out } U(1)} \begin{pmatrix} U(1)'+1\mathbf{F} \\ U(1)'+1\mathbf{F} \\ \cdots \\ U(1)+1\mathbf{F} \end{pmatrix}_{k'_{ij},\ \xi'_i}, \tag{5.19}$$

where we perform mirror transformations on the first two gauge nodes. After integrating out old gauge parameters, we get a seemingly different $\mathcal{T}'_{A,N}$ theory with Chern-Simons levels $k'_{i,j}$ and FI parameters ξ'_i. In addition, we find that mirror transformations are independent of each other, which implies the relation for each component

$$(\mathbf{n}_1,\mathbf{n}_2,\cdots\mathbf{n}_i,\cdots\mathbf{n}_N)\sim(\mathbf{n}_1,\mathbf{n}_2,\cdots\mathbf{n}_i+\mathbf{3},\cdots\mathbf{n}_N), \quad \forall\, i=1,\cdots,N \tag{5.20}$$

where we use a shorthand notation

$$(\mathbf{n}_1,\mathbf{n}_2,\cdots\mathbf{n}_i,\cdots\mathbf{n}_N):=\big((ST)^{n_1},(ST)^{n_2},\cdots,(ST)^{n_N}\big)\,. \tag{5.21}$$

Since k_{ij} is symmetric, one can exchange its rows and columns

$$k_{il}\leftrightarrow k_{jl}\,,\ k_{li}\leftrightarrow k_{lj},\ \text{for}\ \forall\ l=1,\cdots,N \tag{5.22}$$

by exchanging parameters $x_i\leftrightarrow x_j$ for gauge nodes $U(1)_i$ and $U(1)_j$. This yields another equivalence relation

$$\mathbf{n}_i\leftrightarrow\mathbf{n}_j\,. \tag{5.23}$$

Considering both equivalence relations (5.20) and (5.23), we find that mirror transformations

form a finite group

$$\begin{aligned}\mathcal{H}(\mathcal{T}_{A,N}) &:= \{(\mathbf{n}_1,\mathbf{n}_2,\cdots,\mathbf{n}_N) \mid \mathbf{n}_i \in \{0,1,2\},\ \mathbf{n}_i \geq \mathbf{n}_j \text{ if } i \leq j\,,\ \forall\, i,j=1,2,\cdots,N\} \\ &= \{(\mathbf{0},\mathbf{0},\cdots,\mathbf{0}),\ (\mathbf{1},\mathbf{0},\cdots,\mathbf{0}),\cdots,(\mathbf{2},\mathbf{2},\cdots,\mathbf{2})\}\,. \end{aligned} \tag{5.24}$$

The group addition is given by

$$(\mathbf{i}_1,\mathbf{i}_2,\cdots,\mathbf{i}_N)+(\mathbf{n}_1,\mathbf{n}_2,\cdots\mathbf{n}_i,\cdots\mathbf{n}_N)=(\mathbf{n}_1+\mathbf{i}_1,\mathbf{n}_2+\mathbf{i}_2,\cdots,\mathbf{n}_N+\mathbf{i}_N)\,. \tag{5.25}$$

Note that each element $(\mathbf{i}_1,\cdots,\mathbf{i}_N)$ can be regarded as a permutation on the finite group $\mathcal{H}(\mathcal{T}_{A,N})$. We comment that although mirror transformations produce many mirror dual theories with different Chern-Simons levels and FI parameters, the partition functions for these mirror dual theories are equivalent up to some irrelevant factors. In addition, mirror transformations often give rise to effective mixed Chern-Simons levels k_{ij}^{eff} that contains fractional (non-integer) numbers. In this case, the associated theories have parity anomaly and should be thrown away, and only $k_{ij}^{\text{eff}} \in \mathbb{Z}$ make sense [102, 45].

Let us denote the original theory by $\mathcal{T}[(\mathbf{0},\cdots,\mathbf{0})]$. Mirror transformation $(\mathbf{i}_1,\cdots,\mathbf{i}_N)$ acting on it leads to a mirror dual theory $\mathcal{T}[(\mathbf{i}_1,\cdots,\mathbf{i}_N)]$ with superpotential $\widetilde{\mathcal{W}}^{\text{eff},\,(\mathbf{i}_1,\cdots,\mathbf{i}_N)}$. Hence, this is a correspondence

$$(\mathbf{i}_1,\cdots,\mathbf{i}_N) \xleftrightarrow{\text{one to one}} \mathcal{T}[(\mathbf{i}_1,\cdots,\mathbf{i}_N)]\,. \tag{5.26}$$

Furthermore, based on (5.25), $(\mathbf{i}_1,\cdots,\mathbf{i}_N)$ gives rise to a map between $\mathcal{T}[(\mathbf{n_1},\cdots,\mathbf{n_N})]$ and $\mathcal{T}[(\mathbf{n}_1+\mathbf{i}_1,\cdots,\mathbf{n}_N+\mathbf{i}_N)]$:

$$(\mathbf{i}_1,\cdots,\mathbf{i}_N):\ \mathcal{T}[(\mathbf{n}_1,\cdots,\mathbf{n}_N)] \to \mathcal{T}[(\mathbf{n}_1+\mathbf{i}_1,\cdots,\mathbf{n}_N+\mathbf{i}_N)]\,. \tag{5.27}$$

Hence $(\mathbf{i}_1,\cdots,\mathbf{i}_N)$ can be viewed as the mirror map between two mirror dual theories. Since the mirror transformation group is finite, each $(\mathbf{i}_1,\cdots,\mathbf{i}_N)$ can be regarded as a permutation, and any $\mathcal{T}[(\mathbf{n_1},\cdots,\mathbf{n_N})]$ can be viewed as the original theory. By acting on the original theory with the whole group $\mathcal{H}(\mathcal{T}_{A,N})$, one can obtain a chain of mirror dual theories. Moreover the parity anomaly imposes constraints $k_{ij}^{\text{eff}} \in \mathbb{Z}$, hence only a subset of mirror dual theories are consistent. We denote these consistent subset as a class

$$\textbf{Class}(\mathcal{T}_{A,N}) := \{\mathcal{T}[(\mathbf{n}_1+\mathbf{i}_1,\cdots,\mathbf{n}_N+\mathbf{i}_N)] \text{ with } k_{ij}^{\text{eff}} \in \mathbb{Z}\ ,\ \forall\ (\mathbf{i}_1,\cdots,\mathbf{i}_N) \in \mathcal{H}(\mathcal{T}_{A,N})\}\,. \tag{5.28}$$

To summarize, we argue that there are the following correspondences for any $(\mathbf{i}_1,\cdots,\mathbf{i}_N)$:

$$(\mathbf{i}_1,\cdots,\mathbf{i}_N) \xleftrightarrow{\text{one to one}} \mathcal{T}[(\mathbf{i}_1,\cdots,\mathbf{i}_N)] \xleftrightarrow{\text{one to one}} \text{permutations} \xleftrightarrow{\text{one to one}} \text{miror maps}\,. \tag{5.29}$$

Each mirror dual theory $\mathcal{T}[(\mathbf{n}_1,\cdots,\mathbf{n}_N)]$ can be identified by its effective mixed Chern-Simons levels.

Example

We consider mirror transformations for the theory $\mathcal{T}_{A,2}:\ (U(1)+1\mathbf{F})^{\otimes 2}_{k_{ij}}$, whose sphere partition function is given by

$$Z^{\mathcal{T}_{A,2}}_{S^3_b} = \int dx_1 dx_2\, e^{2\pi\, i\,(\tilde{\xi}_1 x_1+\tilde{\xi}_2 x_2)-i\,\pi(k_{1,1}x_1^2+2k_{1,2}x_1x_2+k_{2,2}x_2^2)} s_b(\frac{iQ}{2}-x_1)s_b(\frac{iQ}{2}-x_2)\,. \tag{5.30}$$

According to (5.7), $\mathcal{T}_{A,2}$ theory has effective Chern-Simons levels and FI parameters

$$k^{\text{eff}}_{ij} = k_{ij}+\frac{1}{2}\delta_{ij}\,,\quad i,j=1,\,2\,, \tag{5.31}$$

$$\xi^{\text{eff}}_i = 2\,\pi b\,\tilde{\xi}_i + i\,\pi(1-b\,Q)\sum_{j=1}^{2} k_{ij}+\frac{i\pi}{2}\,. \tag{5.32}$$

We think of (5.30) as the sphere partition function for the original theory $\mathcal{T}[(\mathbf{0},\mathbf{0})]$. Following (5.24), we write down its mirror transformation group:

$$\mathcal{H}(\mathcal{T}_{A,2}) = \{(\mathbf{0},\mathbf{0}),(\mathbf{1},\mathbf{0}),(\mathbf{1},\mathbf{1}),(\mathbf{2},\mathbf{0}),(\mathbf{2},\mathbf{1}),(\mathbf{2},\mathbf{2})\}\,, \tag{5.33}$$

which corresponds to mirror dual theories $\{\ \mathcal{T}[\mathbf{0},\mathbf{0}],\mathcal{T}[\mathbf{1},\mathbf{0}],\mathcal{T}[\mathbf{2},\mathbf{0}],\mathcal{T}[\mathbf{1},\mathbf{1}],\mathcal{T}[\mathbf{2},\mathbf{1}],\mathcal{T}[\mathbf{2},\mathbf{2}]\ \}$. These theories are related by basic mirror transformations $(\mathbf{1},\mathbf{0})$ and $(\mathbf{0},\mathbf{1})$:

$$\begin{array}{ccccc}
\mathcal{T}[(\mathbf{2},\mathbf{0})] & \xrightarrow{(\mathbf{0},\mathbf{1})} & \mathcal{T}[(\mathbf{2},\mathbf{1})] & \xrightarrow{(\mathbf{0},\mathbf{1})} & \mathcal{T}[(\mathbf{2},\mathbf{2})] \\
\uparrow{\scriptstyle(\mathbf{1},\mathbf{0})} & & \uparrow{\scriptstyle(\mathbf{1},\mathbf{0})} & & \uparrow{\scriptstyle(\mathbf{1},\mathbf{0})} \\
\mathcal{T}[(\mathbf{1},\mathbf{0})] & \xrightarrow{(\mathbf{0},\mathbf{1})} & \mathcal{T}[(\mathbf{1},\mathbf{1})] & \xrightarrow{(\mathbf{0},\mathbf{1})} & \mathcal{T}[(\mathbf{1},\mathbf{2})] \\
\uparrow{\scriptstyle(\mathbf{1},\mathbf{0})} & & \uparrow{\scriptstyle(\mathbf{1},\mathbf{0})} & & \uparrow{\scriptstyle(\mathbf{1},\mathbf{0})} \\
\mathcal{T}[(\mathbf{0},\mathbf{0})] & \xrightarrow{(\mathbf{0},\mathbf{1})} & \mathcal{T}[(\mathbf{0},\mathbf{1})] & \xrightarrow{(\mathbf{0},\mathbf{1})} & \mathcal{T}[(\mathbf{0},\mathbf{2})]\,.
\end{array} \tag{5.34}$$

Each mirror dual theory has an associated effective twisted superpotential $\widetilde{\mathcal{W}}^{\text{eff, }(\mathbf{n}_1,\mathbf{n}_2)}$. We show effective mixed Chern-Simons levels for these theories in the following

$$
\begin{aligned}
\mathcal{T}[(\mathbf{0},\mathbf{0})] \;:\quad & \begin{bmatrix} k_{1,1}+\frac{1}{2} & k_{1,2} \\ k_{1,2} & k_{2,2}+\frac{1}{2} \end{bmatrix}, \\
\mathcal{T}[(\mathbf{1},\mathbf{0})] \;:\quad & \begin{bmatrix} \frac{2k_{1,1}-1}{2k_{1,1}+1} & -\frac{2k_{1,2}}{2k_{1,1}+1} \\ -\frac{2k_{1,2}}{2k_{1,1}+1} & \frac{-4k_{1,2}^2+2k_{2,2}+k_{1,1}(4k_{2,2}+2)+1}{4k_{1,1}+2} \end{bmatrix}, \\
\mathcal{T}[(\mathbf{0},\mathbf{1})] \;:\quad & \begin{bmatrix} \frac{-4k_{1,2}^2+2k_{2,2}+k_{1,1}(4k_{2,2}+2)+1}{4k_{2,2}+2} & -\frac{2k_{1,2}}{2k_{2,2}+1} \\ -\frac{2k_{1,2}}{2k_{2,2}+1} & \frac{2k_{2,2}-1}{2k_{2,2}+1} \end{bmatrix}, \\
\mathcal{T}[(\mathbf{2},\mathbf{0})] \;:\quad & \begin{bmatrix} \frac{2}{1-2k_{1,1}} & \frac{2k_{1,2}}{2k_{1,1}-1} \\ \frac{2k_{1,2}}{2k_{1,1}-1} & \frac{-4k_{1,2}^2-2k_{2,2}+k_{1,1}(4k_{2,2}+2)-1}{4k_{1,1}-2} \end{bmatrix}, \\
\mathcal{T}[(\mathbf{0},\mathbf{2})] \;:\quad & \begin{bmatrix} \frac{-4k_{1,2}^2+2k_{2,2}+k_{1,1}(4k_{2,2}-2)-1}{4k_{2,2}-2} & \frac{2k_{1,2}}{2k_{2,2}-1} \\ \frac{2k_{1,2}}{2k_{2,2}-1} & \frac{2}{1-2k_{2,2}} \end{bmatrix}, \\
\mathcal{T}[(\mathbf{1},\mathbf{1})] \;:\quad & \begin{bmatrix} \frac{2\left(-4k_{1,2}^2-2k_{2,2}+k_{1,1}(4k_{2,2}+2)-1\right)}{-8k_{1,2}^2+4k_{2,2}+k_{1,1}(8k_{2,2}+4)+2} & \frac{4k_{1,2}}{-4k_{1,2}^2+2k_{2,2}+k_{1,1}(4k_{2,2}+2)+1} \\ \frac{4k_{1,2}}{-4k_{1,2}^2+2k_{2,2}+k_{1,1}(4k_{2,2}+2)+1} & \frac{2\left(-4k_{1,2}^2+2k_{2,2}+k_{1,1}(4k_{2,2}-2)-1\right)}{-8k_{1,2}^2+4k_{2,2}+k_{1,1}(8k_{2,2}+4)+2} \end{bmatrix}, \\
\mathcal{T}[(\mathbf{2},\mathbf{1})] \;:\quad & \begin{bmatrix} \frac{2(2k_{2,2}+1)}{4k_{1,2}^2+2k_{2,2}-2k_{1,1}(2k_{2,2}+1)+1} & \frac{4k_{1,2}}{4k_{1,2}^2+2k_{2,2}-2k_{1,1}(2k_{2,2}+1)+1} \\ \frac{4k_{1,2}}{4k_{1,2}^2+2k_{2,2}-2k_{1,1}(2k_{2,2}+1)+1} & \frac{4k_{1,2}^2+k_{1,1}(2-4k_{2,2})+2k_{2,2}-1}{4k_{1,2}^2+2k_{2,2}-2k_{1,1}(2k_{2,2}+1)+1} \end{bmatrix}, \\
\mathcal{T}[(\mathbf{1},\mathbf{2})] \;:\quad & \begin{bmatrix} \frac{4k_{1,2}^2+k_{1,1}(2-4k_{2,2})+2k_{2,2}-1}{4k_{1,2}^2+k_{1,1}(2-4k_{2,2})-2k_{2,2}+1} & \frac{4k_{1,2}}{4k_{1,2}^2+k_{1,1}(2-4k_{2,2})-2k_{2,2}+1} \\ \frac{4k_{1,2}}{4k_{1,2}^2+k_{1,1}(2-4k_{2,2})-2k_{2,2}+1} & \frac{2(2k_{1,1}+1)}{4k_{1,2}^2+k_{1,1}(2-4k_{2,2})-2k_{2,2}+1} \end{bmatrix}, \\
\mathcal{T}[(\mathbf{2},\mathbf{2})] \;:\quad & \begin{bmatrix} \frac{2-4k_{2,2}}{-4k_{1,2}^2-2k_{2,2}+k_{1,1}(4k_{2,2}-2)+1} & \frac{4k_{1,2}}{-4k_{1,2}^2-2k_{2,2}+k_{1,1}(4k_{2,2}-2)+1} \\ \frac{4k_{1,2}}{-4k_{1,2}^2-2k_{2,2}+k_{1,1}(4k_{2,2}-2)+1} & \frac{2-4k_{1,1}}{-4k_{1,2}^2-2k_{2,2}+k_{1,1}(4k_{2,2}-2)+1} \end{bmatrix}.
\end{aligned}
\tag{5.35}
$$

One can see that equivalence relations (5.20) and (5.23) are satisfied, and parity anomaly puts strong constraints on the k_{ij} in (5.35).

Quiver reduction

Giving some specific values to Chern-Simons levels, k_{ij}^{eff} may be problematic. This is case when effective Chern-Simons levels have poles or vanishing determinant for some mirror dual $\mathcal{T}_{A,N}$ theories

$$
k_{ij}^{\text{eff}} = \begin{bmatrix} * & * & \cdots & * \\ * & \frac{a}{0} & \cdots & \frac{c}{0} \\ * & \frac{b}{0} & \cdots & \frac{d}{0} \end{bmatrix} \quad \text{or} \quad \det k_{ij} = 0\,. \tag{5.36}
$$

We call this phenomenon quiver reduction. For example, in (5.35), if we set $k_{1,1} = \pm 1/2$, $k_{2,2} = \pm 1/2$, etc., then the effective mixed Chern-Simons levels are problematic. It turns

out that when quiver reductions appear, the Gaussian formula (A.41) cannot be used as $\det \mathbf{A} = 0$. In this case the contour integrals of sphere partition functions contain some Dirac delta functions that reduce the rank (dimensions of the contour integral) of gauge groups. Therefore some gauge nodes are redundant and should be integrated out.

Chern-Simons level decomposition and charge vectors

In this section, we discuss the relations between Chern-Simons levels and charge vectors. We consider theories with chiral multiplets of arbitrary representations that are specified by their charges under gauge groups. We note that charge vectors and Chern-Simons level matrices are exchangeable.

The generic theories with gauge groups $U(1)_1 \times U(1)_2 \times \cdots \times U(1)_N$ and N chiral multiplets have partition functions

$$Z_{S^3_b}(\mathbf{K}, \mathbf{P}) = \int d\,\mathbf{x}\, e^{-i\,\pi\,\mathbf{x}^T\mathbf{K}\,\mathbf{x} + 2\,i\,\pi\,\tilde{\xi}^T\mathbf{x}} \prod_{i=1}^{N} s_b\Big(\frac{i\,Q}{2} - \mathbf{P}_i^T \cdot \mathbf{x}\Big)\,, \tag{5.37}$$

where $\mathbf{x} = (x_1; x_2; \cdots; x_N)$ is a $N \times 1$ matrix, and $\mathbf{P}_i^T$ are charge vectors for chiral multiples. We define

$$\mathbf{P} := (\mathbf{p}_1, \mathbf{p}_2, \cdots, \mathbf{p}_N)\,, \tag{5.38}$$

where $\mathbf{P}_i = \mathbf{p}_i$ and $\mathbf{y} := \mathbf{P}^T\,\mathbf{x}$.

We can change variables, ignore the Jacobian constant, and absorb charge vectors into a new mixed CS level and FI parameters. Then (5.37) is transformed into

$$Z_{S^3_b}(\mathbf{K}', \mathbf{1}) = \int d\,\mathbf{y}\, e^{-i\,\pi\,\mathbf{y}^T\mathbf{K}'\mathbf{y} + 2\,i\,\pi\,\tilde{\xi}'^T\mathbf{y}} \prod_{i=1}^{N} s_b\Big(\frac{i\,Q}{2} - y_i\Big)\,, \tag{5.39}$$

$$\mathbf{K}' = (\mathbf{P}^{-1}) \cdot \mathbf{K} \cdot (\mathbf{P}^{-1})^T\,, \tag{5.40}$$

$$\tilde{\xi}' = (\mathbf{P}^{-1}) \cdot \tilde{\xi}\,. \tag{5.41}$$

If $\mathbf{K}$ is symmetric, then $\mathbf{K}'$ is also symmetric. Both $\mathbf{K}$ and $\mathbf{K}'$ can be decomposed in the orthogonal basis and have the same eigenvalues $\mathbf{\Lambda}$

$$\mathbf{K} = \mathbf{Q}^{-1}\mathbf{\Lambda}\,(\mathbf{Q}^{-1})^T = \mathbf{Q}^T\mathbf{\Lambda}\,\mathbf{Q}\,, \tag{5.42}$$

$$\mathbf{K}' = (\mathbf{P}^{-1}) \cdot \mathbf{K} \cdot (\mathbf{P}^{-1})^T = \mathbf{Q}'^{-1}\mathbf{\Lambda}\,(\mathbf{Q}'^{-1})^T\,, \tag{5.43}$$

$$\mathbf{Q}' = \mathbf{Q}\,\mathbf{P}\,. \tag{5.44}$$

Moreover, using (5.42), one can transform (5.37) into theories with diagonal Chern-Simons levels but complicated charge vectors

$$Z_{S^3_b}(\mathbf{\Lambda}, \mathbf{Q}\,\mathbf{P}) = \int d\,\mathbf{z}\, e^{-i\,\pi\,\mathbf{z}^T\mathbf{\Lambda}\,\mathbf{z} + 2\,i\,\pi\,\left(\mathbf{Q}\,\tilde{\xi}\right)^T\mathbf{z}} \prod_{i=1}^{N} s_b\Big(\frac{i\,Q}{2} - (\mathbf{Q}\,\mathbf{P})_i^T \cdot \mathbf{z}\Big)\,, \tag{5.45}$$

where $\mathbf{x} = \mathbf{Q}^T \mathbf{z}$. We call it charge vector form.

To summarize, one can either transform generic theories (5.37) into $\mathcal{T}_{A,N}$ theories (5.39) with mixed CS level $\mathbf{K}'$ and simple charge vectors $\mathbf{1}$, or into the charge vector form (5.45) with diagonal CS level $\mathbf{\Lambda}$ and complicated charge vectors $\mathbf{Q}\,\mathbf{P}$

$$(\mathbf{K}, \mathbf{P}) \to (\mathbf{K}', \mathbf{1}) \text{ or } (\mathbf{\Lambda}, \mathbf{Q}\,\mathbf{P})\,. \tag{5.46}$$

The associated effective superpotentials for these three forms are equivalent. Hence these partition functions are supposed to describe the same mirror theory. In addition, we note that if $\mathbf{K}$ is real positive definite, then using Cholesky decomposition $\mathbf{K} = \mathbf{L}^T\mathbf{L}$, (5.37) takes another form

$$Z_{S^3_b}(\mathbf{1}, (\mathbf{L}^{-1})^T\mathbf{P}) = \int d\,\mathbf{x}'\, e^{-i\,\pi\,\mathbf{x}'^T\mathbf{x}' + 2\,i\,\pi\,\left((\mathbf{L}^{-1})^{\mathbf{T}}\tilde{\xi}\right)^T\mathbf{x}'} \prod_{i=1}^{N} s_b\Big(\frac{i\,Q}{2} - \big((\mathbf{L}^{-1})^T\mathbf{P}\big)_i^T \cdot \mathbf{x}'\Big)\,, \tag{5.47}$$

where $\mathbf{x}' = \mathbf{L}\,\mathbf{x}$.

5.2 Mirror transformations on chiral multiplets

In this section, we show that $U(1)_k + N_F\mathbf{F} + N_{AF}\mathbf{AF}$ can be transformed into certain $\mathcal{T}_{A,N}$ theory after implementing mirror transformation $(\mathbf{1}, \mathbf{1}, \cdots, \mathbf{1})$ and integrating out the original gauge node $U(1)_k$:

$$U(1)_k + N_F\mathbf{F} + N_{AF}\mathbf{AF} \xrightarrow{(\mathbf{1},\mathbf{1},\cdots,\mathbf{1})} \mathcal{T}_{A,\,N_F+N_{AF}}\,. \tag{5.48}$$

This gives rise to an indirect way to perform mirror transformations on chiral multiplets in $U(1)_k + N_F\mathbf{F} + N_{AF}\mathbf{AF}$.

We take $U(1) + N\mathbf{F}$ as an example. Applying mirror transformations on each chiral multiplet $N\mathbf{F}$, one can get a $\mathcal{T}_{A,N}$ theory. This process is illustrated in the following

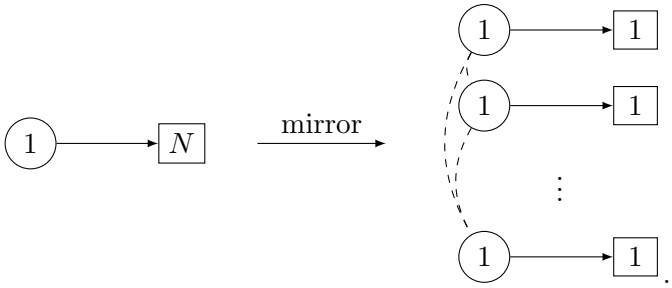

(5.49)

This is particularly interesting, as it implies that mixed Chern-Simons levels emerge from mirror transformations. In addition, if we act the mirror transformation group on this $\mathcal{T}_{A,N}$ theory, we get many others $\mathcal{T}_{A,N}$ theories with the same rank but different mixed Chern-Simons levels.

In this section, we analyze sphere partition functions of $U(1) + N_F\mathbf{F} + N_{AF}\mathbf{AF}$ and discuss the consequence of mirror transformations on FI parameters. It turns out that mirror transformations on chiral multiplets only flip the signs of real mass parameters. We verify this

conclusion by analyzing both sphere partition functions and vortex partition functions. We find that the vortex partition function of $U(1)+N\mathbf{F}$ can be written as the vortex partition function of $\mathcal{T}_{A,N}$ theory, from which effective Chern-Simons level matrices of the latter can be obtained by taking semi-classical limit $\hbar \to 1$. These mixed Chern-Simons levels are the same as what we obtain from analyzing sphere partition functions associated to various mirror dual $\mathcal{T}_{A,N}$ theories.

Sphere partition functions

We take $U(1)_k + N\mathbf{F}$ theory as an example. Its sphere partition function can be transformed into that of $\mathcal{T}_{A,N}$ theory

$$Z_{S^3_b}^{U(1)_k+N\mathbf{F}} \xrightarrow{(\mathbf{1},\mathbf{1},\cdots,\mathbf{1})} Z_{S^3_b}^{\mathcal{T}_{A,N}} . \tag{5.50}$$

The associated sphere partition function for $U(1)_k + N\mathbf{F}$ is

$$Z_{S^3_b}^{U(1)_k+N\mathbf{F}} = \int dx\, e^{-i\,\pi\, k x^2 + 2\,i\,\pi\xi x} \prod_{i=1}^{N} s_b\Big(\frac{i\,Q}{2} + x + \frac{u_i}{2}\Big) , \tag{5.51}$$

which in the semi-classical limit (5.51) gives the effective superpotential

$$\widetilde{\mathcal{W}}^{\text{eff}}_{U(1)_k+N\mathbf{F}} = \sum_{i=1}^{N} \mathrm{Li}_2(XY_i) + \xi^{eff}\log X + \frac{k^{\text{eff}}}{2}\big(\log X\big)^2 , \tag{5.52}$$

$$k^{\text{eff}} = k + \frac{N}{2} , \quad \xi^{\text{eff}} = \frac{1}{2}\big(i\,\pi N - 4b\pi\xi + \log\prod_{i=1}^{N} Y_i\big) , \tag{5.53}$$

$$X := e^{2b\pi x} , \qquad Y_i := -\sqrt{q}\, e^{b\pi u_i} . \tag{5.54}$$

The above superpotential is consistent with the fact that the one-loop contribution of each fundamental chiral multiplet $\mathbf{F}$ to k^{eff} is $1/2$, and anti-fundamental $\mathbf{AF}$ to k^{eff} is $-1/2$. Moreover, parity anomaly constrains effective Chern-Simons levels $k^{\text{eff}} \in \mathbb{Z}$. The mirror transformation $(\mathbf{1},\mathbf{1},\cdots,\mathbf{1})$ replaces each double sine function $s_b(\cdots)$ given by chiral multiplets into a contour integral via (5.15). Hence we get the sphere partition function for the dual $\mathcal{T}_{A,N}$ theory on the right hand side of (5.50):

$$Z_{S^3_b}^{\mathcal{T}_{A,N}} = \int \prod_{i=1}^{N} d\,y_i\, e^{\sum_{i,j=1}^{N} -\pi\,i\,\tilde{k}_{ij}\,y_i y_j + 2\pi\,i\,\tilde{\xi}_i y_i} \prod_{i=1}^{N} s_b\big(\frac{iQ}{2} - y_i\big) , \tag{5.55}$$

$$\tilde{k}_{ij} = \frac{1}{2}\delta_{ij} - \frac{2}{2k+N} , \quad \tilde{\xi}_i = \frac{iQ}{4} + \frac{u_i}{2} - \frac{2}{2k+N}\Big(\xi - \sum_{i=1}^{N}\big(\frac{iQ}{4} + \frac{u_i}{4}\big)\Big) ,$$

where mass parameters u_i can also be absorbed into new FI parameters $\tilde{\xi}_i$. When $k = -N/2$, (5.55) is ill defined because there is a pole in $\tilde{\xi}_i$. We will show in examples in section 5.2.1 that when $k = -N/2$, this pole can be bypassed and we end up with a mirror pair found by

Dorey and Tong in [53, 108].

Once a particular $\mathcal{T}_{A,N}$ theory with mixed Chern-Simons levels in (5.55) is constructed, one can get many equivalent mirror dual theories by implementing mirror transformations. After ruling out the theories with parity anomaly, many integer effective mixed Chern-Simons levels can be obtained, and each of them corresponds to a mirror dual $\mathcal{T}_{A,N}$ theory.

Vortex partition functions

As we have discussed in section 4.2, the open topological string partition function (3.109) can be written in a quiver generating series (quiver form); see e.g. [81, 85, 10]:

$$Z^{\text{vortex}}_{U(1)_k+N_F\mathbf{F}+N_{AF}\mathbf{AF}} = Z_0 \cdot P_{C_{ij}}(x_1, \cdots, x_m)\,, \tag{5.56}$$

with

$$Z_0 = \frac{(\alpha_1, q)_\infty (\alpha_2, q)_\infty \cdots (\alpha_{N_{AF}}, q)_\infty}{(\beta_1, q)_\infty (\beta_2, q)_\infty \cdots (\beta_{N_F-1}, q)_\infty}\,. \tag{5.57}$$

Here we show one particular quiver by choosing variables x_i as follows

$$P_{C_{ij}}(x_0, x_1, \cdots, x_m) = P_{C_{ij}}\left(q^{-\frac{f+1}{2}} z, \alpha_1, \cdots, \alpha_{N_{AF}}, \frac{\beta_1}{\sqrt{q}}, \cdots, \frac{\beta_{N_F-1}}{\sqrt{q}}\right)\,, \tag{5.58}$$

where the quiver matrix C_{ij} is

$$C_{ij}((5.56)) = \left[\begin{array}{c|ccc|ccc} f+1 & 1 & \dots & 1 & 1 & \dots & 1 \\ \hline 1 & 1 & \dots & 0 & 0 & \dots & 0 \\ \vdots & & \ddots & & & \ddots & \\ 1 & 0 & \dots & 1 & 0 & \dots & 0 \\ \hline 1 & 0 & \dots & 0 & 0 & \dots & 0 \\ \vdots & & \ddots & & & \ddots & \\ 1 & 0 & \dots & 0 & 0 & \dots & 0 \end{array}\right]\,, \tag{5.59}$$

which has size $(N_F + N_{AF}) \times (N_F + N_{AF})$. Based on various examples in section 4.2, it can be summarized that the framing number f in open topological strings is related to the Chern-Simons level

$$f + 1 = k^{\text{eff}} = k + \frac{N_F - N_{AF}}{2}\,. \tag{5.60}$$

Note that there are several ways to write vortex partition functions in term of quiver generating series, since there are two equivalent ways to choose variables in (3.123) and (3.124). We have the freedom of flipping any variable $x_i \to \sqrt{q}\, x_i^{-1}$; this leads to another matrix C'_{ij}. All variables x_i can be flipped one after another, and finally one can get a chain of $\{C_{ij}\}$.

Invoking the mirror symmetry, we find a physical interpretation for the quiver structure (3.115) and C_{ij}. Recall that (3.115) implies that the vortex partition functions of $U(1)_k +$

$N_F\mathbf{F}+N_{AF}\mathbf{AF}$ theories can be rewritten in the quiver form $P_{C_{ij}}(x_i)$. We note that Z_0 is actually related to the one-loop part $Z^{\text{1-loop}}=Z_0^{-1}$ on the Higgs branch

$$Z^{\text{1-loop}}_{U(1)_k+N_F\mathbf{F}+N_{AF}}=\frac{\prod_{j=1}^{N_F}(\beta_j,q)_\infty}{\prod_{i=1}^{N_{AF}}(\alpha_i,q)_\infty}\,, \tag{5.61}$$

and then (3.115) reads

$$Z^{\text{1-loop}}_{U(1)_k+N_F\mathbf{F}+N_{AF}\mathbf{AF}}\cdot Z^{\text{vortex}}_{U(1)_k+N_F\mathbf{F}+N_{AF}\mathbf{AF}}(z,\alpha_i,\beta_j)=P_{C_{ij}}(x_i)\,. \tag{5.62}$$

Moreover, vortex partition functions (5.12) of $\mathcal{T}_{A,N}$ theories also take a quiver form

$$Z^{\text{vortex}}_{\mathcal{T}_{A,N_F+N_{AF}}}(k^{\text{eff}}_{ij},x_i)=P_{C_{ij}}(x_i)\,, \tag{5.63}$$

hence we conjecture that $C_{ij}=k^{\text{eff}}_{ij}$ and $U(1)_k+N_F\,\mathbf{F}+N_{AF}\,\mathbf{AF}$ can be regarded as certain $\mathcal{T}_{A,N}$ theories. Then vortex partition functions of $U(1)_k+N_F\mathbf{F}+N_{AF}\mathbf{AF}$ theories are conjectured to be vortex partition functions of corresponding $\mathcal{T}_{A,N}$ theories

$$\boxed{Z^{\text{1-loop}}_{U(1)_k+N_F\mathbf{F}+N_{AF}\mathbf{AF}}(\alpha_i,\beta_j)\cdot Z^{\text{vortex}}_{U(1)_k+N_F\mathbf{F}+N_{AF}\mathbf{AF}}(z,\alpha_i,\beta_j)=Z_{\mathcal{T}_{A,N_F+N_{AF}}}(x_i).} \tag{5.64}$$

This is verified to be correct in various examples of the following section. We stress that the one-loop part of $\mathcal{T}_{A,N}$ theory on the Higgs branch is trivial, hence the vortex partition function involves the holomorphic block for $\mathcal{T}_{A,N}$ theories, see e.g. [105]. Note that by now the correspondence between $U(1)_k+N_F\mathbf{F}+N_{AF}\mathbf{AF}$ and $\mathcal{T}_{A,N}$ theories is a conjecture, based on the equivalence of vortex partition functions; we can prove this conjecture using sphere partition functions and mirror transformations (5.50).

There is still one problem left: what are the relations between these equivalent quivers? The answer is that each C_{ij} is the k^{eff}_{ij} of a mirror dual theory, and mirror transformations relate different quivers. Firstly, mirror transformations relate mirror dual theories

$$\mathcal{T}[(\mathbf{n}_1,\cdots,\mathbf{n}_{N_F+N_{AF}})]\xrightarrow{(\mathbf{i}_1,\cdots,\mathbf{i}_{N_F+N_{AF}})}\mathcal{T}[(\mathbf{n}_1+\mathbf{i}_1,\cdots,\mathbf{n}_{N_F+N_{AF}}+\mathbf{i}_{N_F+N_{AF}})]\,, \tag{5.65}$$

which relates effective mixed Chern-Simons levels

$$k^{\text{eff},(\mathbf{n}_1,\cdots,\mathbf{n}_{N_F+N_{AF}})}_{ij}\xrightarrow{\text{flipping some } x_i\to x_i^{-1}}k^{\text{eff},(\mathbf{n}_1+\mathbf{i}_1,\cdots,\mathbf{n}_{N_F+N_{AF}}+\mathbf{i}_{N_F+N_{AF}})}_{ij}\,, \tag{5.66}$$

where $x_i=\alpha_i$ or β_i. We will show in examples that these equivalent k^{eff}_{ij} can be obtained by performing mirror transformations on sphere partition functions. In terms of vortex partition function of corresponding $\mathcal{T}_{A,N_F+N_{AF}}$ theories, mirror symmetry acts as flipping closed Kähler parameters $\alpha_i\to\alpha_i^{-1}$ or $\beta_j\to\beta_j^{-1}$(or in other words, changing the sign of real mass parameters $u_i\to-u_i$, since the closed Kähler parameters equal to mass parameters and FI parameters $\alpha_i\,,\beta_i\sim e^{\pi b\,u_i}\,,z\sim e^{2b\pi\xi}$).

5.2.1 Examples

$U(1)_k + 1\,\mathbf{F}$

$\mathcal{T}_{k,1}$: $(1)_k - [1]$ theory is a basic example. Its sphere partition function is given by (3.73). We shift x and absorb the mass parameter in $\tilde{\xi}$ and obtain

$$Z^{\mathcal{T}_{k,1}} = \int dx\, e^{2\pi\, i\, \tilde{\xi} x - i\,\pi k x^2}\, s_b\big(\frac{iQ}{2} - x\big)\,. \tag{5.67}$$

The mirror transformation group $\mathcal{H}(\mathcal{T}_{A,1})$ in this case is

$$\mathcal{H}(\mathcal{T}_{A,1}) = \{(\mathbf{0}), (\mathbf{1}), (\mathbf{2})\}\,, \tag{5.68}$$

which leads to mirror dual theories

$$\{\ \mathcal{T}[(\mathbf{0})]\,,\ \mathcal{T}[(\mathbf{1})]\,,\ \mathcal{T}[(\mathbf{2})]\ \}\,. \tag{5.69}$$

Mirror transformation $(\mathbf{1})$ relates them as follows

$$\mathcal{T}[(\mathbf{0})] \xrightarrow{(\mathbf{1})} \mathcal{T}[(\mathbf{1})] \xrightarrow{(\mathbf{1})} \mathcal{T}[(\mathbf{2})]\,, \tag{5.70}$$

namely,

$$U(1) + 1\mathbf{F} \xrightarrow{(\mathbf{1})} U(1) + (U(1)' + 1\mathbf{F}) \xrightarrow{(\mathbf{1})} U(1) + (U(1)' + (U(1)' + 1\mathbf{F}))\,, \tag{5.71}$$

which are the following quivers after integrating out old gauge nodes

$$U(1)_k + 1\mathbf{F} \xrightarrow{(\mathbf{1})} U(1)'_{k'} + 1\mathbf{F} \xrightarrow{(\mathbf{1})} U(1)''_{k''} + 1\mathbf{F}\,. \tag{5.72}$$

Their sphere partition functions are

$$\begin{aligned}
Z^{\mathcal{T}[\mathbf{0}]}_{S^3_b} &= \int dx\, e^{2\pi\, i\, \tilde{\xi} x - k\pi\, i\, x^2}\, s_b\big(\frac{iQ}{2} - x\big)\,,\\
Z^{\mathcal{T}[\mathbf{1}]}_{S^3_b} &= \int dx\, e^{\frac{\pi(Q - 2kQ - 8i\tilde{\xi})x + i(3-2k)\pi x^2}{2+4k}}\, s_b\big(\frac{iQ}{2} - x\big)\,,\\
Z^{\mathcal{T}[\mathbf{2}]}_{S^3_b} &= \int dx\, e^{\frac{\pi(Q + 2kQ + 8i\tilde{\xi})x + i(3+2k)\pi x^2}{-2+4k}}\, s_b\big(\frac{iQ}{2} - x\big)\,.
\end{aligned} \tag{5.73}$$

It is obvious that mirror transformations change Chern-Simons levels and FI parameters significantly. By taking semi-classical limit and using formula (5.6), one can read off Chern-Simons levels

and FI parameters

$$\begin{aligned}
\mathcal{T}[\mathbf{0}]: &\ \left(k_{ij}^{\text{eff},(\mathbf{0})} = \frac{1}{2} + k\,, \quad \xi^{\text{eff},(\mathbf{0})} = 2b\pi\tilde{\xi} + i\pi(1-bQ)k + \frac{i\pi}{2} \right), \\
\mathcal{T}[\mathbf{1}]: &\ \left(k_{ij}^{\text{eff},(\mathbf{1})} = \frac{2k-1}{2k+1}\,, \ \xi^{\text{eff},(\mathbf{1})} = -\frac{4b\pi\tilde{\xi}}{1+2k} + \frac{i\pi(2k-1+bQ)}{1+2k} \right), \\
\mathcal{T}[\mathbf{2}]: &\ \left(k_{ij}^{\text{eff},(\mathbf{2})} = \frac{2}{1-2k}\,, \ \xi^{\text{eff},(\mathbf{2})} = \frac{i(-2\pi + b\pi Q - 4ib\pi\tilde{\xi})}{2k-1} \right).
\end{aligned} \tag{5.74}$$

As we discussed before, mirror transformations permute mirror dual theories. The permutation

$$\mathcal{T}[(\mathbf{0})] \to \mathcal{T}[(\mathbf{1})],\ \mathcal{T}[(\mathbf{1})] \to \mathcal{T}[(\mathbf{2})],\ \mathcal{T}[(\mathbf{2})] \to \mathcal{T}[(\mathbf{0})] \tag{5.75}$$

is given by mirror transformation $(\mathbf{1})$, and the mirror map is

$$(k,\tilde{\xi}) \to (k',\tilde{\xi}'):\ k' = \frac{3+2k}{2-4k},\ \tilde{\xi}' = \frac{i(Q+2kQ+8i\tilde{\xi})}{4-8k}\,. \tag{5.76}$$

The permutation given by mirror transformation $(\mathbf{2})$ is

$$\mathcal{T}[(\mathbf{0})] \to \mathcal{T}[(\mathbf{2})],\ \mathcal{T}[(\mathbf{2})] \to \mathcal{T}[(\mathbf{1})],\ \mathcal{T}[(\mathbf{1})] \to \mathcal{T}[(\mathbf{0})]\,, \tag{5.77}$$

whose corresponding mirror map is the reverse of (5.76)

$$(k,\tilde{\xi}) \to (k'',\tilde{\xi}''):\ k'' = \frac{-3+2k}{2+4k},\ \tilde{\xi}'' = \frac{i(-1+2k)Q - 8\tilde{\xi}}{4+8k}\,. \tag{5.78}$$

Similarly, one can analyze generic $\mathcal{T}_{A,N}$ theories.

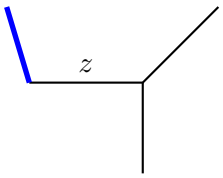

Figure 5.1: Calabi-Yau threefold $\mathbb{C}^3$ with a Lagrangian brane.

The toric diagram for the theory $U1)_k + 1\mathbf{F}$ is shown in Figure 5.1. By (3.109), the open Kähler parameter for the Lagrangian brane on Calabi-Yau threefold $\mathbb{C}^3$ is $q^{(f+1)/2}z$ where f is the framing number. To match it with the FI parameter in the vortex partition function (5.12), we identify

$$e^{\xi^{\text{eff},(\mathbf{0})}} = i\,(-1)^k q^{-\frac{k}{2}} e^{2b\pi\tilde{\xi}} = (-1)^{f+1} q^{-\frac{f+1}{2}} z\,, \tag{5.79}$$

which implies that the framing number f relates to the CS level k, and the open Kähler parameter relates to the FI parameter

$$f = k - 1/2\,, \quad z = q^{1/4}\, e^{2b\pi\tilde{\xi}}\,. \tag{5.80}$$

$U(1)_k + 2\,\mathbf{F}$

We turn this theory into a $\mathcal{T}_{A,N}$ theory

$$Z^{(1)_k+2\mathbf{F}}_{S^3_b} \xrightarrow{(\mathbf{1},\mathbf{1})} Z^{\mathcal{T}_{A,2}}_{S^3_b}\,, \tag{5.81}$$

where $Z^{\mathcal{T}_{A,2}}_{S^3_b}$ is given by (5.55) with $N=2$. We perform mirror transformations $(\mathbf{n}_1,\mathbf{n}_2)\in\mathcal{H}(\mathcal{T}_{A,2})$ and take the semi-classical limit to read off effective superpotentials. For simplicity, we denote mirror dual theories by $\mathcal{T}[(\mathbf{n}_1,\mathbf{n}_2)]:(k_{ij}^{\text{eff},(\mathbf{n}_1,\mathbf{n}_2)},\,\xi_i^{\text{eff},(\mathbf{n_1},\mathbf{n_2})})$ and find the following results

$$\begin{aligned}
\mathcal{T}[(\mathbf{0},\mathbf{0})]:&\ \left(\begin{bmatrix}\frac{k}{1+k} & -\frac{1}{1+k}\\ -\frac{1}{1+k} & \frac{k}{1+k}\end{bmatrix},\ \begin{bmatrix}\frac{\pi(2i(k-1+bQ-2ib\xi)+(b+2bk)u_1-bu_2)}{2(1+k)}\\ \frac{\pi(2i(k-1+bQ-2ib\xi)-bu_1+(b+2bk)u_2}{2(1+k)}\end{bmatrix}\right),\\
\mathcal{T}[(\mathbf{0},\mathbf{1})]:&\ \left(\begin{bmatrix}\frac{k-1}{k} & \frac{1}{k}\\ \frac{1}{k} & -\frac{1}{k}\end{bmatrix},\ \begin{bmatrix}\frac{\pi(2ik+4b\xi+b(2k-1)u_1+bu_2)}{2k}\\ -\frac{b\pi(4\xi-u_1+(1+2k)u_2)}{2k}\end{bmatrix}\right),\\
\mathcal{T}[(\mathbf{0},\mathbf{2})]:&\ \left(\begin{bmatrix}1 & 1\\ 1 & 1+k\end{bmatrix},\ \begin{bmatrix}\pi(2i-ibQ+bu_1-bu_2)\\ \frac{1}{2}\pi\left(-2i(bkQ-2ib\xi+bQ-k-2)-u_2(2bk+b)+bu_1\right)\end{bmatrix}\right),\\
\mathcal{T}[(\mathbf{1},\mathbf{0})]:&\ \left(\begin{bmatrix}-\frac{1}{k} & \frac{1}{k}\\ \frac{1}{k} & \frac{k-1}{k}\end{bmatrix},\ \begin{bmatrix}-\frac{\pi b((2k+1)u_1+4\xi-u_2)}{2k}\\ \frac{\pi(b(2k-1)u_2+4b\xi+bu_1+2ik)}{2k}\end{bmatrix}\right),\\
\mathcal{T}[(\mathbf{1},\mathbf{1})]:&\ \left(\begin{bmatrix}\frac{1}{1-k} & \frac{1}{1-k}\\ \frac{1}{1-k} & \frac{1}{1-k}\end{bmatrix},\ \begin{bmatrix}\frac{\pi(u_1(b-2bk)-4b\xi+2ibQ-bu_2-4i)}{2(k-1)}\\ -\frac{\pi(b(2k-1)u_2+4b\xi-2ibQ+bu_1+4i)}{2(k-1)}\end{bmatrix}\right),\\
\mathcal{T}[(\mathbf{1},\mathbf{2})]:&\ \left(\begin{bmatrix}0 & -1\\ -1 & k\end{bmatrix},\ \begin{bmatrix}\pi\left(i(bQ-1)-bu_1+bu_2\right)\\ \frac{1}{2}\pi\left(-2i(k(bQ-1)-b(Q+2i\xi)+1)+u_2(b-2bk)-bu_1\right)\end{bmatrix}\right),\\
\mathcal{T}[(\mathbf{2},\mathbf{0})]:&\ \left(\begin{bmatrix}k+1 & 1\\ 1 & 1\end{bmatrix},\ \begin{bmatrix}\frac{1}{2}\pi\left(-2i(bkQ-2ib\xi+bQ-k-2)-u_1(2bk+b)+bu_2\right)\\ \pi\left(-ibQ-bu_1+bu_2+2i\right)\end{bmatrix}\right),\\
\mathcal{T}[(\mathbf{2},\mathbf{1})]:&\ \left(\begin{bmatrix}k & -1\\ -1 & 0\end{bmatrix},\ \begin{bmatrix}\frac{1}{2}\pi\left(-2i(k(bQ-1)-b(Q+2i\xi)+1)+u_1(b-2bk)-bu_2\right)\\ \pi\left(ibQ+bu_1-bu_2-i\right)\end{bmatrix}\right).
\end{aligned} \tag{5.82}$$

Because of the exchange equivalence $\mathbf{n}_i\leftrightarrow\mathbf{n}_j$, there are only two independent theories. We choose $\{\,\mathcal{T}[(\mathbf{2},\mathbf{0})]\,,\ \mathcal{T}[(\mathbf{2},\mathbf{1})]\,\}$, which are related by the transformation $(\mathbf{0},\mathbf{1})$

$$\mathcal{T}[(\mathbf{2},\mathbf{0})] \xrightarrow{(\mathbf{0},\mathbf{1})} \mathcal{T}[(\mathbf{2},\mathbf{1})\,. \tag{5.83}$$

The toric diagram for $U(1)_k+2\mathbf{F}$ is shown in Figure 5.2. It follows from (3.109) that the vortex partition function takes form

$$Z^{\text{vortex}}_{U(1)_k+2\,\mathbf{F}} = \sum_{n=0}^{\infty}\frac{(-\sqrt{q})^{(f+1)\,n^2}(q^{-\frac{f+1}{2}}z)^n}{(q,q)_n}\frac{1}{(\beta,q)_n}\,, \tag{5.84}$$

which along with the one-loop part, takes form of the vortex partition function of a $\mathcal{T}_{A,2}$ theory. However, there are two equivalent forms of (5.84), as we discussed in section 5.2, and

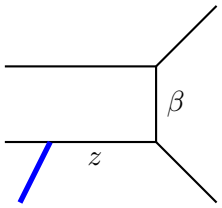

Figure 5.2: The toric Calabi-Yau threefold with a Lagrangian brane, which engineers $U(1)_k + 2\mathbf{F}$ theory.

each form corresponds to the vortex partition function of a particular $\mathcal{T}_{A,2}$ theory

$$Z^{\text{vortex}}_{\mathcal{T}_{A,2}} = Z^{\text{1-loop}}_{U(1)_k+2\,\mathbf{F}} \cdot Z^{\text{vortex}}_{U(1)_k+2\,\mathbf{F}} \tag{5.85}$$

$$= \sum_{d_1,d_2=0}^{\infty} (-\sqrt{q})^{\sum_{i,j=1}^{2} k_{ij}^{\text{eff},(\mathbf{2},\mathbf{0})} d_i d_j} \frac{z^{d_1}\,(\beta/\sqrt{q})^{d_2}}{(q,q)_{d_1}(q,q)_{d_2}} \tag{5.86}$$

$$= \sum_{d_1,d_2=0}^{\infty} (-\sqrt{q})^{\sum_{i,j=1}^{2} k_{ij}^{\text{eff},(\mathbf{2},\mathbf{1})} d_i d_j} \frac{z^{d_1}\,(q\beta^{-1})^{d_2}}{(q,q)_{d_1}(q,q)_{d_2}}\,, \tag{5.87}$$

where we have absorbed the framing number and some factors caused by flipping β into z. It can be noticed that (5.86) is the vortex partition function for theory $\mathcal{T}[(\mathbf{2},\mathbf{0})]$, and (5.87) is the vortex partition functions for theory $\mathcal{T}[(\mathbf{2},\mathbf{1})]$, and flipping mass parameter $\beta/\sqrt{q} \to q\beta^{-1}$ relates effective Chern-Simons levels

$$k_{ij}^{\text{eff},(\mathbf{2},\mathbf{0})} \xrightarrow{\text{flip } \beta} k_{ij}^{\text{eff},(\mathbf{2},\mathbf{1})}\,. \tag{5.88}$$

This flipping is interpreted as mirror transformation $(\mathbf{0},\mathbf{1})$, as $(\mathbf{2},\mathbf{0}) + (\mathbf{0},\mathbf{1}) = (\mathbf{2},\mathbf{1})$.

The relations between Kähler parameters $z\,, \alpha_i\,, \beta_j$ and gauge theory parameters u_i, ξ can be obtained by comparing with (5.12) where the variables x_i are defined to be $x_i := (-1)^{k_{ii}^{\text{eff}}} e^{\xi_i^{\text{eff}}}$. For $\mathcal{T}[(\mathbf{2},\mathbf{0})]$, the relations between Kähler parameters and gauge theory parameters are given by

$$\left(q^{-\frac{f+1}{2}} z,\, \beta/\sqrt{q}\right) = \left((-1)^{2k+1} q^{-\frac{k+1}{2}} e^{-b\pi u_1(\frac{1}{2}+k)} e^{b\pi u_2/2} e^{-2b\pi\xi}\,, -e^{b\pi(u_2-u_1)}/\sqrt{q}\right)\,, \tag{5.89}$$

while for $\mathcal{T}[(\mathbf{2},\mathbf{1})]$ the relations become

$$\left(q^{-\frac{f+1}{2}} z\,, q\beta^{-1}\right) = \left((-1)^{k+1} q^{-\frac{k-1}{2}} e^{b\pi u_1(\frac{1}{2}-k)} e^{-b\pi u_2/2} e^{-2b\pi\xi}\,, -\sqrt{q}\, e^{b\pi(u_1-u_2)}\right)\,. \tag{5.90}$$

If $u_1 = 0$, the relations between z, β and u_i, ξ simplify to $z \sim e^{2b\pi\xi}\,,\ \beta \sim e^{b\pi u_2}$.

$U(1)_k + 1\,\mathbf{F} + 1\,\mathbf{AF}$

The sphere partition function for this theory is

$$Z^{(1)_k+1\mathbf{F}+1\mathbf{AS}}_{S^3_b} = \int dx\, e^{2\pi\xi x - i\pi k x^2}\, s_b\Big(\frac{iQ}{2} + x + \frac{u_1}{2}\Big) s_b\Big(\frac{iQ}{2} - x + \frac{u_2}{2}\Big)\,, \tag{5.91}$$

which after the mirror transformation $(\mathbf{1},\mathbf{1})$ becomes that of $\mathcal{T}_{A,2}$ theories

$$Z^{(1)_k+1\mathbf{F}+1\mathbf{AS}}_{S^3_b} \xrightarrow{(\mathbf{1},\mathbf{1})} Z^{\mathcal{T}_{A,2}}_{S^3_b}\,, \tag{5.92}$$

where

$$\begin{aligned} Z^{\mathcal{T}_{A,2}}_{S^3_b} = \int dy_1 dy_2\, e^{-i\pi\frac{k-1}{k+1}\left(y_1^2+y_2^2\right)-\frac{i\pi(-ikQ-(2k+1)u_1-4\xi-iQ-u_2)}{2(k+1)}y_1-\frac{i\pi(-ikQ-(2k+1)u_2+4\xi-iQ-u_1)}{2(k+1)}y_2} \\ \times\, s_b\big(\frac{iQ}{2}-y_1\big)s_b\big(\frac{iQ}{2}-y_2\big)\,. \end{aligned} \tag{5.93}$$

Implementing mirror transformations in $\mathcal{H}(\mathcal{T}_{A,2})$, we obtain mirror dual theories as follows

$$\begin{aligned}
\mathcal{T}[(\mathbf{0},\mathbf{0})]&: \left(\begin{bmatrix} \frac{k}{1+k} & \frac{1}{1+k} \\ \frac{1}{1+k} & \frac{k}{1+k} \end{bmatrix}, \begin{bmatrix} \frac{\pi(u_1(2bk+b)+4b\xi+bu_2+2ik+2i)}{2(k+1)} \\ \frac{\pi(2i(2ib\xi+k+1)+u_2(2bk+b)+bu_1)}{2(k+1)} \end{bmatrix}\right), \\
\mathcal{T}[(\mathbf{0},\mathbf{1})]&: \left(\begin{bmatrix} \frac{k-1}{k} & -\frac{1}{k} \\ -\frac{1}{k} & -\frac{1}{k} \end{bmatrix}, \begin{bmatrix} \frac{\pi(2i(-2ib\xi+bQ+k-2)+b(2k-1)u_1-bu_2)}{2k} \\ -\frac{\pi(u_2(2bk+b)-4b\xi-2ibQ+bu_1+4i)}{2k} \end{bmatrix}\right), \\
\mathcal{T}[(\mathbf{0},\mathbf{2})]&: \left(\begin{bmatrix} 1 & -1 \\ -1 & 1+k \end{bmatrix}, \begin{bmatrix} \pi b\,(iQ+u_1+u_2) \\ \frac{1}{2}\pi\,(-2ibkQ-u_2(2bk+b)+4b\xi-bu_1+2ik) \end{bmatrix}\right), \\
\mathcal{T}[(\mathbf{1},\mathbf{0})]&: \left(\begin{bmatrix} -\frac{1}{k} & -\frac{1}{k} \\ -\frac{1}{k} & \frac{k-1}{k} \end{bmatrix}, \begin{bmatrix} \frac{\pi(u_1(2bk+b)+4b\xi-2ibQ+bu_2+4i)}{2k} \\ \frac{\pi(2i(2ib\xi+bQ+k-2)+b(2k-1)u_2-bu_1)}{2k} \end{bmatrix}\right), \\
\mathcal{T}[(\mathbf{1},\mathbf{1})]&: \left(\begin{bmatrix} \frac{1}{1-k} & \frac{1}{k-1} \\ \frac{1}{k-1} & \frac{1}{1-k} \end{bmatrix}, \begin{bmatrix} -\frac{\pi b((2k-1)u_1+4\xi-u_2)}{2(k-1)} \\ \frac{\pi b((1-2k)u_2+4\xi+u_1)}{2(k-1)} \end{bmatrix}\right), \\
\mathcal{T}[(\mathbf{1},\mathbf{2})]&: \left(\begin{bmatrix} 0 & 1 \\ 1 & k \end{bmatrix}, \begin{bmatrix} \pi\,(-ibQ-bu_1-bu_2+i) \\ \frac{1}{2}\pi\,(-2ibkQ+u_2(b-2bk)+4b\xi+bu_1+2ik+2i) \end{bmatrix}\right), \\
\mathcal{T}[(\mathbf{2},\mathbf{0})]&: \left(\begin{bmatrix} k+1 & -1 \\ -1 & 1 \end{bmatrix}, \begin{bmatrix} -\frac{1}{2}i\pi\,(2bkQ-iu_1(2bk+b)-4ib\xi-ibu_2-2k) \\ \pi b\,(iQ+u_1+u_2) \end{bmatrix}\right), \\
\mathcal{T}[(\mathbf{2},\mathbf{1})]&: \left(\begin{bmatrix} k & 1 \\ 1 & 0 \end{bmatrix}, \begin{bmatrix} \frac{1}{2}\pi\,(-2ibkQ+u_1(b-2bk)-4b\xi+bu_2+2ik+2i) \\ \pi\,(-ibQ-bu_1-bu_2+i) \end{bmatrix}\right).
\end{aligned} \tag{5.94}$$

Because of the exchange relation $\mathbf{n}_i \leftrightarrow \mathbf{n}_j$, there are only two independent mirror theories with integer effective Chern-Simons level matrices. We identify these theories as $\{\,\mathcal{T}[(\mathbf{2},\mathbf{1})]\,,\,\mathcal{T}[(\mathbf{2},\mathbf{0})]\,\}$, which are related by the mirror transformation $(\mathbf{0},\mathbf{2})$

$$\mathcal{T}[(\mathbf{2},\mathbf{1})] \xrightarrow{(\mathbf{0},\mathbf{2})} \mathcal{T}[(\mathbf{2},\mathbf{0})\,. \tag{5.95}$$

The corresponding toric diagram for $U(1)_k + 1\,\mathbf{F} + 1\,\mathbf{AF}$ is shown in Figure 5.3. Following (3.109), its vortex partition function reads

$$Z^{\text{vortex}}_{U(1)_k+1\,\mathbf{F}+1\,\mathbf{AF}} = \sum_{n=0}^{\infty} \frac{(-\sqrt{q})^{(f+1)\,n^2} z^n\,(\alpha,q)_n}{(q,q)_n}\,, \tag{5.96}$$

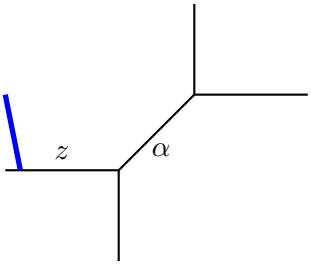

Figure 5.3: The toric diagram for the Calabi-Yau threefold engineering $U(1)_k + 1\mathbf{F} + 1\mathbf{AF}$.

which in combination with the one-loop part equals to the vortex partition functions of $\mathcal{T}[(\mathbf{2},\mathbf{1})]$ and $\mathcal{T}[(\mathbf{2},\mathbf{0})]$ theories

$$\begin{aligned} Z_{\mathcal{T}_{A,2}} &= Z^{\text{1-loop}}_{U(1)_k+1\,\mathbf{F}+1\,\mathbf{AF}} \cdot Z^{\text{vortex}}_{U(1)_k+1\,\mathbf{F}+1\,\mathbf{AF}} \\ &= \sum_{d_1,d_2=0}^{\infty} (-\sqrt{q})^{\sum_{i,j=1}^{2} k_{ij}^{\text{eff},(\mathbf{2},\mathbf{1})} d_i d_j} \frac{z^{d_1}\,\alpha^{d_2}}{(q,q)_{d_1}(q,q)_{d_2}} \qquad (5.97) \\ &= \sum_{d_1,d_2=0}^{\infty} (-\sqrt{q})^{\sum_{i,j=1}^{2} k_{ij}^{\text{eff},(\mathbf{2},\mathbf{0})} d_i d_j} \frac{z^{d_1}\,(\sqrt{q}\alpha^{-1})^{d_2}}{(q,q)_{d_1}(q,q)_{d_2}}\,, \qquad (5.98) \end{aligned}$$

where the second line is for $\mathcal{T}[(\mathbf{2},\mathbf{1})]$ theory and the third line is for $\mathcal{T}[(\mathbf{2},\mathbf{0})]$. One can see that flipping the expansion parameter $\alpha \to \sqrt{q}\,\alpha^{-1}$ relates two effective mixed Chern-Simons levels

$$k_{ij}^{\text{eff},(\mathbf{2},\mathbf{1})} \xrightarrow{\text{flip } \alpha} k_{ij}^{\text{eff},(\mathbf{2},\mathbf{0})}\,, \qquad (5.99)$$

and this flipping is caused by the mirror transformation $(\mathbf{0},\mathbf{2})$.

$U(1)_k + 3\,\mathbf{F}$

This theory can be turned into a particular $\mathcal{T}_{A,3}$ theory

$$Z^{(1)_k+3\mathbf{F}}_{S^3_b} \xrightarrow{(\mathbf{1},\mathbf{1},\mathbf{1})} Z^{\mathcal{T}_{A,3}}_{S^3_b}\,. \qquad (5.100)$$

Following (5.55), we get the sphere partition function of the corresponding $\mathcal{T}_{A,3}$ theory

$$Z^{\mathcal{T}_{A,3}}_{S^3_b} = \int \prod_{i,j=1}^{3} dy_i\, e^{2\pi\xi_i' y_i - i\pi k_{ij} y_i y_j}\, s_b\big(\frac{iQ}{2} - y_i\big)\,, \qquad (5.101)$$

$$k_{ij} = \begin{bmatrix} -\frac{i(2k-1)}{6+4k} & \frac{2i\pi}{3+2k} & \frac{2i\pi}{3+2k} \\ \frac{2i\pi}{3+2k} & -\frac{i(2k-1)}{6+4k} & \frac{2i\pi}{3+2k} \\ \frac{2i\pi}{3+2k} & \frac{2i\pi}{3+2k} & -\frac{i(2k-1)}{6+4k} \end{bmatrix}, \quad \xi_i' = \begin{bmatrix} -\frac{\pi(2kQ-4i(k+1)u_1-8i\xi-3Q+2iu_2+2iu_3)}{4k+6} \\ -\frac{\pi(2kQ-4i(k+1)u_2-8i\xi-3Q+2iu_1+2iu_3)}{4k+6} \\ -\frac{\pi(2kQ-4i(k+1)u_3-8i\xi-3Q+2iu_1+2iu_3)}{4k+6} \end{bmatrix}. \qquad (5.102)$$

By acting with mirror transformations on the sphere partition function, we get many mirror dual theories with integer effective Chern-Simons level matrices $k_{ij}^{\text{eff},(\mathbf{n}_1,\mathbf{n}_2,\mathbf{n}_3)}$

$$\begin{aligned}
&\mathcal{T}[(\mathbf{0},\mathbf{0},\mathbf{2})]: \begin{bmatrix} 1 & 0 & 1 \\ 0 & 1 & 1 \\ 1 & 1 & k+\frac{3}{2} \end{bmatrix}, \quad \mathcal{T}[(\mathbf{0},\mathbf{1},\mathbf{2})]: \begin{bmatrix} 1 & 0 & 1 \\ 0 & 0 & -1 \\ 1 & -1 & k+\frac{1}{2} \end{bmatrix}, \quad \mathcal{T}[(\mathbf{0},\mathbf{2},\mathbf{0})]: \begin{bmatrix} 1 & 1 & 0 \\ 1 & k+\frac{3}{2} & 1 \\ 0 & 1 & 1 \end{bmatrix}, \\
&\mathcal{T}[(\mathbf{0},\mathbf{2},\mathbf{1})]: \begin{bmatrix} 1 & 1 & 0 \\ 1 & k+\frac{1}{2} & -1 \\ 0 & -1 & 1 \end{bmatrix}, \quad \mathcal{T}[(\mathbf{2},\mathbf{0},\mathbf{0})]: \begin{bmatrix} k+\frac{3}{2} & 1 & 1 \\ 1 & 1 & 0 \\ 1 & 0 & 1 \end{bmatrix}, \quad \mathcal{T}[(\mathbf{2},\mathbf{0},\mathbf{1})]: \begin{bmatrix} k+\frac{1}{2} & 1 & -1 \\ 1 & 1 & 0 \\ -1 & 0 & 0 \end{bmatrix}, \\
&\mathcal{T}[(\mathbf{1},\mathbf{0},\mathbf{2})]: \begin{bmatrix} 0 & 0 & -1 \\ 0 & 1 & 1 \\ -1 & 1 & k+\frac{1}{2} \end{bmatrix}, \quad \mathcal{T}[(\mathbf{1},\mathbf{1},\mathbf{2})]: \begin{bmatrix} 0 & 0 & -1 \\ 0 & 0 & -1 \\ -1 & -1 & k-\frac{1}{2} \end{bmatrix}, \quad \mathcal{T}[(\mathbf{1},\mathbf{2},\mathbf{0})]: \begin{bmatrix} 0 & -1 & 0 \\ -1 & k+\frac{1}{2} & 1 \\ 0 & 1 & 1 \end{bmatrix}, \\
&\mathcal{T}[(\mathbf{1},\mathbf{2},\mathbf{1})]: \begin{bmatrix} 0 & -1 & 0 \\ -1 & k-\frac{1}{2} & -1 \\ 0 & -1 & 0 \end{bmatrix}, \quad \mathcal{T}[(\mathbf{2},\mathbf{1},\mathbf{0})]: \begin{bmatrix} k+\frac{1}{2} & -1 & 1 \\ -1 & 0 & 0 \\ 1 & 0 & 1 \end{bmatrix}, \quad \mathcal{T}[(\mathbf{2},\mathbf{1},\mathbf{1})]: \begin{bmatrix} k-\frac{1}{2} & -1 & -1 \\ -1 & 0 & 0 \\ -1 & 0 & 0 \end{bmatrix}.
\end{aligned} \tag{5.103}$$

Because of the exchange relation $\mathbf{n}_i \leftrightarrow \mathbf{n}_j$, there are only four independent theories. We choose $\{\mathcal{T}[(\mathbf{2},\mathbf{0},\mathbf{0})], \mathcal{T}[(\mathbf{2},\mathbf{0},\mathbf{1})], \mathcal{T}[(\mathbf{2},\mathbf{1},\mathbf{0})], \mathcal{T}[(\mathbf{2},\mathbf{1},\mathbf{1})]\}$. Their effective Chern-Simons levels matrices and effective FI parameters are

$$\begin{aligned}
&\mathcal{T}[(\mathbf{2},\mathbf{0},\mathbf{0})]: \left(\begin{bmatrix} k+\frac{3}{2} & 1 & 1 \\ 1 & 1 & 0 \\ 1 & 0 & 1 \end{bmatrix}, \begin{bmatrix} \frac{1}{2}\pi\left(-2ibkQ - 2b(k+1)u_1 - 4b\xi - 4ibQ + bu_2 + bu_3 + 2ik + 7i\right) \\ \pi\left(-ibQ - bu_1 + bu_2 + 2i\right) \\ \pi\left(-ibQ - bu_1 + bu_3 + 2i\right) \end{bmatrix} \right), \\
&\mathcal{T}[(\mathbf{2},\mathbf{0},\mathbf{1})]: \left(\begin{bmatrix} k+\frac{1}{2} & 1 & -1 \\ 1 & 1 & 0 \\ -1 & 0 & 0 \end{bmatrix}, \begin{bmatrix} \frac{1}{2}\pi\left(-2ibkQ - 2bku_1 - 4b\xi + bu_2 - bu_3 + 2ik + i\right) \\ \pi\left(-ibQ - bu_1 + bu_2 + 2i\right) \\ \pi\left(ibQ + bu_1 - bu_3 - i\right) \end{bmatrix} \right), \\
&\mathcal{T}[(\mathbf{2},\mathbf{1},\mathbf{0})]: \left(\begin{bmatrix} k+\frac{1}{2} & -1 & 1 \\ -1 & 0 & 0 \\ 1 & 0 & 1 \end{bmatrix}, \begin{bmatrix} \frac{1}{2}\pi\left(-2ibkQ - 2bku_1 - 4b\xi - bu_2 + bu_3 + 2ik + i\right) \\ \pi\left(ibQ + bu_1 - bu_2 - i\right) \\ \pi\left(-ibQ - bu_1 + bu_3 + 2i\right) \end{bmatrix} \right), \\
&\mathcal{T}[(\mathbf{2},\mathbf{1},\mathbf{1})]: \left(\begin{bmatrix} k-\frac{1}{2} & -1 & -1 \\ -1 & 0 & 0 \\ -1 & 0 & 0 \end{bmatrix}, \begin{bmatrix} \frac{1}{2}\pi\left(-2ibkQ - 2b(k-1)u_1 - 4b\xi + 4ibQ - bu_2 - bu_3 + 2ik - 5i\right) \\ \pi\left(ibQ + bu_1 - bu_2 - i\right) \\ \pi\left(ibQ + bu_1 - bu_3 - i\right) \end{bmatrix} \right).
\end{aligned} \tag{5.104}$$

These four mirror dual theories are related by

$$\begin{array}{ccc}
\mathcal{T}[(\mathbf{2},\mathbf{0},\mathbf{0})] & \xrightarrow{(\mathbf{0},\mathbf{1},\mathbf{0})} & \mathcal{T}[(\mathbf{2},\mathbf{1},\mathbf{0})] \\
\downarrow{\scriptstyle (\mathbf{0},\mathbf{0},\mathbf{1})} & & \downarrow{\scriptstyle (\mathbf{0},\mathbf{0},\mathbf{1})} \\
\mathcal{T}[(\mathbf{2},\mathbf{0},\mathbf{1})] & \xrightarrow{(\mathbf{0},\mathbf{1},\mathbf{0})} & \mathcal{T}[(\mathbf{2},\mathbf{1},\mathbf{1})]\,.
\end{array} \tag{5.105}$$

The toric diagram for $U(1)_k + 3\,\mathbf{F}$ is shown in Figure 5.4. Using (3.109), its vortex partition

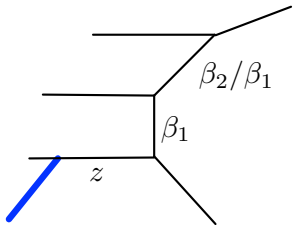

Figure 5.4: The toric diagram of the Calabi-Yau threefold engineering $U(1)_k + 3\,\mathbf{F}$ in the presence of a Lagrangian brane.

function is given by

$$Z^{\text{vortex}}_{U(1)_k+3\,\mathbf{F}} = \sum_{n=0}^{\infty} \frac{(-\sqrt{q})^{(f+1)\,n^2} z^n}{(q,q)_n} \frac{1}{(\beta_1,q)_n\,(\beta_2,q)_n}\,, \tag{5.106}$$

which can be written in terms of vortex partitions of the four dual theories in (5.105):

$$\begin{aligned}
Z_{\mathcal{T}_{A,3}} &= Z^{\text{1-loop}}_{U(1)_k+3\,\mathbf{F}} \cdot Z^{\text{vortex}}_{U(1)_k+3\,\mathbf{F}} && (5.107)\\
&= \sum_{d_1,d_2,d_3=0}^{\infty} (-\sqrt{q})^{\sum_{i,j=1}^{3} k_{ij}^{\text{eff},(\mathbf{2},\mathbf{0},\mathbf{0})} d_i d_j} \frac{z^{d_1} (\beta_1/\sqrt{q})^{d_2} (\beta_2/\sqrt{q})^{d_3}}{(q,q)_{d_1} (q,q)_{d_2} (q,q)_{d_3}} && (5.108)\\
&= \sum_{d_1,d_2,d_3=0}^{\infty} (-\sqrt{q})^{\sum_{i,j=1}^{3} k_{ij}^{\text{eff},(\mathbf{2},\mathbf{1},\mathbf{0})} d_i d_j} \frac{z^{d_1} (q\,\beta_1^{-1})^{d_2} (\beta_2/\sqrt{q})^{d_3}}{(q,q)_{d_1} (q,q)_{d_2} (q,q)_{d_3}} && (5.109)\\
&= \sum_{d_1,d_2,d_3=0}^{\infty} (-\sqrt{q})^{\sum_{i,j=1}^{3} k_{ij}^{\text{eff},(\mathbf{2},\mathbf{0},\mathbf{1})} d_i d_j} \frac{z^{d_1} (\beta_1/\sqrt{q})^{d_2} (q\,\beta_2^{-1})^{d_3}}{(q,q)_{d_1} (q,q)_{d_2} (q,q)_{d_3}} && (5.110)\\
&= \sum_{d_1,d_2,d_3=0}^{\infty} (-\sqrt{q})^{\sum_{i,j=1}^{3} k_{ij}^{\text{eff},(\mathbf{2},\mathbf{1},\mathbf{1})} d_i d_j} \frac{z^{d_1} (q\,\beta_1^{-1})^{d_2} (q\,\beta_2^{-1})^{d_3}}{(q,q)_{d_1} (q,q)_{d_2} (q,q)_{d_3}}\,. && (5.111)
\end{aligned}$$

It is obvious that mixed Chern-Simons level matrices for these mirror dual theories are related by flipping closed Kähler parameters β_i

$$\begin{array}{ccc}
k_{ij}^{\text{eff},(\mathbf{2},\mathbf{0},\mathbf{0})} & \xrightarrow{\text{flip } \beta_1} & k_{ij}^{\text{eff},(\mathbf{2},\mathbf{1},\mathbf{0})} \\
\Big\downarrow \text{flip } \beta_2 & & \Big\downarrow \text{flip } \beta_2 \\
k_{ij}^{\text{eff},(\mathbf{2},\mathbf{0},\mathbf{1})} & \xrightarrow{\text{flip } \beta_1} & k_{ij}^{\text{eff},(\mathbf{2},\mathbf{1},\mathbf{1})}\,.
\end{array} \tag{5.112}$$

Therefore, to match with (5.105) the flipping β_1 should correspond to mirror transformation $(\mathbf{0},\mathbf{1},\mathbf{0})$, and flipping β_2 corresponds to $(\mathbf{0},\mathbf{0},\mathbf{1})$. This confirms the fact that mirror transformations are interpreted as flipping Kähler parameter x_i of vortex partition functions of $\mathcal{T}_{A,N}$ theories.

Tong's mirror pair

When $k=-3/2$, the dual $\mathcal{T}_{A,3}$ theory given by (5.55) is problematic as there are poles in $\tilde{k}_{ij}$. Nevertheless, it is possible to bypass these poles and end up with a well defined $\mathcal{T}_{A,3}$ theory. The procedure of addressing this problem is as follows: firstly we do not give values to k and act with $(\mathbf{2},\mathbf{0},\mathbf{0})$ on the partition function, and in the end we set $k=-3/2$. This leads to a well defined partition function that can be viewed as that of the original theory. This new original theory $\mathcal{T}'_{A,3}$ is given by mirror transformation $(\mathbf{1},\mathbf{1},\mathbf{1})+(\mathbf{2},\mathbf{0},\mathbf{0})=(\mathbf{0},\mathbf{1},\mathbf{1})$. More explicitly, its sphere partition function is obtained in two steps

$$Z_{S^3_b}^{U(1)_{-3/2}+3\mathbf{F}} \xrightarrow{(\mathbf{1},\mathbf{1},\mathbf{1})} \bullet \xrightarrow{(\mathbf{2},\mathbf{0},\mathbf{0})} Z_{S^3_b}^{\mathcal{T}'_{A,3}}\,, \tag{5.113}$$

where

$$Z_{S^3_b}^{\mathcal{T}'_{A,3}} = \int dx_1 dx_2 dx_3\, e^{\mathbf{term}} s_b\big(\frac{iQ}{2}-x_1\big)s_b\big(\frac{iQ}{2}-x_2\big)s_b\big(\frac{iQ}{2}-x_3\big)\,, \tag{5.114}$$

$$\begin{aligned}\mathbf{term} :=& \frac{1}{2}\pi i\,(x_1^2-x_2^2-x_3^2)-\pi\left(\frac{Q}{2}+iu_1-iu_2\right)x_2-\pi\left(\frac{Q}{2}+iu_1-iu_3\right)\\ &-\pi\left(Q+2i\xi-\frac{i}{2}(u_1+u_2+u_3)\right)-2\pi i\,(x_2+x_3)x_1\,.\end{aligned} \tag{5.115}$$

Furthermore, when acting with the mirror transformation $(\mathbf{1},\mathbf{0},\mathbf{0})$ on this new original theory $\mathcal{T}'_{A,3}$, one gets $\mathcal{T}'_{A,3}[(\mathbf{1},\mathbf{0},\mathbf{0})]$

$$Z_{S^3_b}^{U(1)_{-3/2}+3\mathbf{F}} \xrightarrow{(\mathbf{1},\mathbf{1},\mathbf{1})} \bullet \xrightarrow{(\mathbf{2},\mathbf{0},\mathbf{0})} \bullet \xrightarrow{(\mathbf{1},\mathbf{0},\mathbf{0})} Z_{S^3_b}^{\mathcal{T}'_{A,3}[(\mathbf{1},\mathbf{0},\mathbf{0})]}\,. \tag{5.116}$$

Here, we encounter quiver reduction for $\mathcal{T}'_{A,3}[(\mathbf{1},\mathbf{0},\mathbf{0})]$ that turns out to have a reduced quiver. Its sphere partition function, after shifting $x_2\to -x_2,\ u_2\to -3iQ+4\xi-u_1-u_3$, is

$$Z_{S^3_b}^{\mathcal{T}'_{A,3}[(\mathbf{1},\mathbf{0},\mathbf{0})]} = \int dx_2 dx_3\, e^{\mathbf{CS\ terms}} s_b\big(\frac{iQ}{2}+x_2\big)s_b\big(\frac{iQ}{2}-x_3\big)s_b\big(\frac{iQ}{2}-x_2+x_3\big)\,, \tag{5.117}$$

$$\mathbf{CS\ terms} = -i\pi(x_2^2+x_3^2-x_2x_3)-i\pi(u_1-u_3)x_3-\pi(3Q+4i\,\xi-2iu_2-iu_3)x_2\,.$$

The integral dimension for this theory is two and hence the gauge group is $U(1)\times U(1)$. Since $(\mathbf{2},\mathbf{0},\mathbf{0})+(\mathbf{1},\mathbf{0},\mathbf{0})=(\mathbf{0},\mathbf{0},\mathbf{0})$, (5.117) is equivalent to the problematic sphere partition function given in (5.55) with $k=-3/2$. The associated bare CS level matrix for (5.117) is

$$k_{ij}=\begin{bmatrix}1 & -\frac{1}{2}\\ -\frac{1}{2} & 1\end{bmatrix}\,, \tag{5.118}$$

and the associated chiral multiplets have charges $(-1,0)$, $(1,-1)$, $(0,1)$ respectively. It is easy to draw its quiver diagram

$$1\mathbf{F}-U(1)-U(1)-1\mathbf{F}\,. \tag{5.119}$$

Interestingly, we obtain a mirror pair found by Dorey and Tong in [53]

$$\begin{array}{c} U(1)_{-3/2}+3\mathbf{F}\,, \\ \text{with } k=-3/2\,, \\ \text{and } \ k^{\text{eff}}=0 \end{array} \quad \xleftrightarrow{(\mathbf{1},\mathbf{1},\mathbf{1})} \quad \begin{array}{c} 1\mathbf{F}-U(1)-U(1)-1\mathbf{F} \quad \text{with} \quad k_{ij}=\begin{bmatrix} 1 & -\frac{1}{2} \\ -\frac{1}{2} & 1 \end{bmatrix}. \\ \text{and} \quad k_{ij}^{\text{eff}}=\begin{bmatrix} 2 & -1 \\ -1 & 2 \end{bmatrix} \end{array} \tag{5.120}$$

In this case the mirror transformation is $(\mathbf{1},\mathbf{1},\mathbf{1})$. This example illustrates that mirror transformations can be used to derive mirror dual pairs with the help of $\mathcal{T}_{A,N}$ theories.

$U(1)_k+2\,\mathbf{F}+1\,\mathbf{AF}$

The sphere partition function for this theory is

$$Z_{S_b^3}^{U(1)_k+2\,\mathbf{F}+1\,\mathbf{AF}}=\int dx\, e^{2\pi\xi x-i\pi k x^2}\, s_b\big(\frac{iQ}{2}+x+\frac{u_1}{2}\big)s_b\big(\frac{iQ}{2}-x+\frac{u_2}{2}\big)s_b\big(\frac{iQ}{2}+x+\frac{u_3}{2}\big)\,. \tag{5.121}$$

Due to parity anomaly, the bare CS level $k\in\mathbb{Z}+1/2$. Mirror transformation $(\mathbf{1},\mathbf{1},\mathbf{1})$ turns this theory into a $\mathcal{T}_{A,3}$

$$Z_{S_b^3}^{(1)_k+2\mathbf{F}+1\mathbf{AF}} \xrightarrow{(\mathbf{1},\mathbf{1},\mathbf{1})} Z_{S_b^3}^{\mathcal{T}_{A,3}}\,. \tag{5.122}$$

The open partition function for $\mathcal{T}_{A,3}$ is

$$Z_{S_b^3}^{\mathcal{T}_{A,3}}=\int\prod_{i,j=1}^{3} dy_i\, e^{2\pi\xi_i' y_i-i\pi k_{ij}y_iy_j}\, s_b\big(\frac{iQ}{2}-y_i\big)\,, \tag{5.123}$$

$$k_{ij}=\begin{bmatrix} -\frac{i(2k-1)}{6+4k} & -\frac{2i\pi}{3+2k} & \frac{2i\pi}{3+2k} \\ -\frac{2i\pi}{3+2k} & -\frac{i(2k-1)}{6+4k} & -\frac{2i\pi}{3+2k} \\ \frac{2i\pi}{3+2k} & -\frac{2i\pi}{3+2k} & -\frac{i(2k-1)}{6+4k} \end{bmatrix},\quad \xi_i'=\begin{bmatrix} -\frac{\pi((1+2k)Q-8i\xi-4i(1+k)u_1-2iu_2+2iu_3)}{6+4k} \\ -\frac{i\pi(-i(5+2k)Q+8\xi-2u_1-4(1+k)u_2-2u_3)}{6+4k} \\ -\frac{i\pi(-i(1+2k)Q-8\xi+2u_1-2u_2-4(1+k)u_3)}{6+4k} \end{bmatrix}. \tag{5.124}$$

We list all integer effective CS level matrices obtained by mirror transformations in the following

$$\begin{aligned}
&\mathcal{T}[(\mathbf{0},\mathbf{0},\mathbf{2})]:\begin{bmatrix}1&0&1\\0&1&-1\\1&-1&k+\frac{3}{2}\end{bmatrix},\quad \mathcal{T}[(\mathbf{0},\mathbf{1},\mathbf{2})]:\begin{bmatrix}1&0&1\\0&0&1\\1&1&k+\frac{1}{2}\end{bmatrix},\quad \mathcal{T}[(\mathbf{0},\mathbf{2},\mathbf{0})]:\begin{bmatrix}1&-1&0\\-1&k+\frac{3}{2}&-1\\0&-1&1\end{bmatrix},\\
&\mathcal{T}[(\mathbf{0},\mathbf{2},\mathbf{1})]:\begin{bmatrix}1&-1&0\\-1&k+\frac{1}{2}&1\\0&1&0\end{bmatrix},\quad \mathcal{T}[(\mathbf{1},\mathbf{0},\mathbf{2})]:\begin{bmatrix}0&0&-1\\0&1&-1\\-1&-1&k+\frac{1}{2}\end{bmatrix},\quad \mathcal{T}[(\mathbf{1},\mathbf{1},\mathbf{2})]:\begin{bmatrix}0&0&-1\\0&0&1\\-1&1&k-\frac{1}{2}\end{bmatrix},\\
&\mathcal{T}[(\mathbf{1},\mathbf{2},\mathbf{0})]:\begin{bmatrix}0&1&0\\1&k+\frac{1}{2}&-1\\0&-1&1\end{bmatrix},\quad \mathcal{T}[(\mathbf{1},\mathbf{2},\mathbf{1})]:\begin{bmatrix}0&1&0\\1&k-\frac{1}{2}&1\\0&1&0\end{bmatrix},\quad \mathcal{T}[(\mathbf{2},\mathbf{0},\mathbf{0})]:\begin{bmatrix}k+\frac{3}{2}&-1&1\\-1&1&0\\1&0&1\end{bmatrix},\\
&\mathcal{T}[(\mathbf{2},\mathbf{0},\mathbf{1})]:\begin{bmatrix}k+\frac{1}{2}&-1&-1\\-1&1&0\\-1&0&0\end{bmatrix},\quad \mathcal{T}[(\mathbf{2},\mathbf{1},\mathbf{0})]:\begin{bmatrix}k+\frac{1}{2}&1&1\\1&0&0\\1&0&1\end{bmatrix},\quad \mathcal{T}[(\mathbf{2},\mathbf{1},\mathbf{1})]:\begin{bmatrix}k-\frac{1}{2}&1&-1\\1&0&0\\-1&0&0\end{bmatrix}.
\end{aligned}\tag{5.125}$$

They satisfy exchange equivalence $\mathbf{n}_i \leftrightarrow \mathbf{n}_j$, so there are only four independent theories

$$\{\, T[(\mathbf{2},\mathbf{0},\mathbf{0})],\, \mathcal{T}[(\mathbf{2},\mathbf{0},\mathbf{1})],\, \mathcal{T}[(\mathbf{2},\mathbf{1},\mathbf{0})],\, \mathcal{T}[(\mathbf{2},\mathbf{1},\mathbf{1})]\,\}\,. \tag{5.126}$$

The associated effective Chern-Simons levels and effective FI parameters are

$$\mathcal{T}[(\mathbf{2},\mathbf{1},\mathbf{0})]:\left(\begin{bmatrix}\frac{1}{2}+k&1&1\\1&0&0\\1&0&1\end{bmatrix},\ \begin{bmatrix}\frac{1}{2}\pi\left(-2ibkQ-2bku_1-4b\xi-2ibQ+bu_2+bu_3+2ik+5i\right)\\ \pi\left(-ibQ-bu_1-bu_2+i\right)\\ \pi\left(-ibQ-bu_1+bu_3+2i\right)\end{bmatrix}\right), \tag{5.127}$$

$$\mathcal{T}[(\mathbf{2},\mathbf{0},\mathbf{0})]:\left(\begin{bmatrix}k+\frac{3}{2}&-1&1\\-1&1&0\\1&0&1\end{bmatrix},\ \begin{bmatrix}\frac{1}{2}\pi\left(-2ibkQ-2b(k+1)u_1-4b\xi-2ibQ-bu_2+bu_3+2ik+3i\right)\\ \pi b\left(iQ+u_1+u_2\right)\\ \pi\left(-ibQ-bu_1+bu_3+2i\right)\end{bmatrix}\right), \tag{5.128}$$

$$\mathcal{T}[(\mathbf{2},\mathbf{0},\mathbf{1})]:\left(\begin{bmatrix}k+\frac{1}{2}&-1&-1\\-1&1&0\\-1&0&0\end{bmatrix},\ \begin{bmatrix}-\frac{1}{2}i\pi\left(2bkQ-2ibku_1-4ib\xi-2bQ-ibu_2-ibu_3-2k+3\right)\\ \pi b\left(iQ+u_1+u_2\right)\\ \pi\left(ibQ+bu_1-bu_3-i\right)\end{bmatrix}\right), \tag{5.129}$$

$$\mathcal{T}[(\mathbf{2},\mathbf{1},\mathbf{1})]:\left(\begin{bmatrix}k-\frac{1}{2}&1&-1\\1&0&0\\-1&0&0\end{bmatrix},\ \begin{bmatrix}\frac{1}{2}\pi\left(-2ibkQ-2b(k-1)u_1-4b\xi+2ibQ+bu_2-bu_3+2ik-i\right)\\ \pi\left(-ibQ-bu_1-bu_2+i\right)\\ \pi\left(ibQ+bu_1-bu_3-i\right)\end{bmatrix}\right). \tag{5.130}$$

These four mirror dual theories are related by mirror transformations

$$\begin{array}{ccc}
\mathcal{T}[(\mathbf{2},\mathbf{1},\mathbf{0})] & \xrightarrow{(\mathbf{0},\mathbf{2},\mathbf{0})} & \mathcal{T}[(\mathbf{2},\mathbf{0},\mathbf{0})] \\
\downarrow{\scriptstyle(\mathbf{0},\mathbf{0},\mathbf{1})} & & \downarrow{\scriptstyle(\mathbf{0},\mathbf{0},\mathbf{1})} \\
\mathcal{T}[(\mathbf{2},\mathbf{1},\mathbf{1})] & \xrightarrow{(\mathbf{0},\mathbf{2},\mathbf{0})} & \mathcal{T}[(\mathbf{2},\mathbf{0},\mathbf{1})]\,.
\end{array} \tag{5.131}$$

The toric diagram for this example is shown in Figure 5.5 and its vortex partition function is

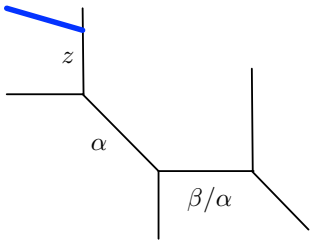

Figure 5.5: The toric diagram for $U(1)_k + 2\mathbf{F} + 1\mathbf{AF}$. Note that vortex partition function is invariant under the flop transition on the Kähler parameter α.

$$Z^{\text{vortex}}_{U(1)_k+2\,\mathbf{F}+1\,\mathbf{AF}} = \sum_{n=0}^{\infty} \frac{(-\sqrt{q})^{(f+1)\,n^2} z^n}{(q,q)_n} \frac{(\alpha,q)_n}{(\beta,q)_n}\,, \tag{5.132}$$

which along with one-loop part is equivalent to vortex partition functions of mirror dual theories mentioned in (5.126)

$$\begin{aligned}
Z_{\mathcal{T}_{A,3}} &= Z^{\text{1-loop}}_{U(1)_k+2\,\mathbf{F}+1\,\mathbf{AF}} \cdot Z^{\text{vortex}}_{U(1)_k+2\,\mathbf{F}+1\,\mathbf{AF}} && (5.133)\\
&= \sum_{d_1,d_2,d_3=0}^{\infty} (-\sqrt{q})^{\sum_{i,j=1}^{3} k_{ij}^{\text{eff},(\mathbf{2},\mathbf{1},\mathbf{0})} d_i d_j} \frac{z^{d_1} \alpha^{d_2} (\beta/\sqrt{q})^{d_3}}{(q,q)_{d_1}(q,q)_{d_2}(q,q)_{d_3}} && (5.134)\\
&= \sum_{d_1,d_2,d_3=0}^{\infty} (-\sqrt{q})^{\sum_{i,j=1}^{3} k_{ij}^{\text{eff},(\mathbf{2},\mathbf{0},\mathbf{0})} d_i d_j} \frac{z^{d_1} (\sqrt{q}\alpha^{-1})^{d_2} (\beta/\sqrt{q})^{d_3}}{(q,q)_{d_1}(q,q)_{d_2}(q,q)_{d_3}} && (5.135)\\
&= \sum_{d_1,d_2,d_3=0}^{\infty} (-\sqrt{q})^{\sum_{i,j=1}^{3} k_{ij}^{\text{eff},(\mathbf{2},\mathbf{0},\mathbf{1})} d_i d_j} \frac{z^{d_1} (\sqrt{q}\alpha^{-1})^{d_2} (q\,\beta^{-1})^{d_3}}{(q,q)_{d_1}(q,q)_{d_2}(q,q)_{d_3}} && (5.136)\\
&= \sum_{d_1,d_2,d_3=0}^{\infty} (-\sqrt{q})^{\sum_{i,j=1}^{3} k_{ij}^{\text{eff},(\mathbf{2},\mathbf{1},\mathbf{1})} d_i d_j} \frac{z^{d_1} \alpha^{d_2} (q\,\beta^{-1})^{d_3}}{(q,q)_{d_1}(q,q)_{d_2}(q,q)_{d_3}}\,. && (5.137)
\end{aligned}$$

It is obvious that flipping $\alpha \to \sqrt{q}\alpha^{-1}$ and $\beta \to \sqrt{q}\beta^{-1}$ relates their effective Chern-Simons levels

$$\begin{array}{ccc}
k_{ij}^{\text{eff},(\mathbf{2},\mathbf{1},\mathbf{0})} & \xrightarrow{\text{flip } \alpha} & k_{ij}^{\text{eff},(\mathbf{2},\mathbf{0},\mathbf{0})} \\
\Big\downarrow \text{flip } \beta & & \Big\downarrow \text{flip } \beta \\
k_{ij}^{\text{eff},(\mathbf{2},\mathbf{1},\mathbf{1})} & \xrightarrow{\text{flip } \alpha} & k_{ij}^{\text{eff},(\mathbf{2},\mathbf{0},\mathbf{1})}\,.
\end{array} \tag{5.138}$$

Once again, this confirms that mirror symmetry can be interpreted as flipping closed Kähler parameters in vortex partition functions.

$1\mathbf{F}-U(1)_{k_1}-U(1)_{k_2}-1\mathbf{F}$

This quiver theory has three chiral multiplets with charges $(1,0),(p_1,p_2),(0,1)$ respectively. The associated sphere partition function is given by

$$Z_{S^3_b}^{1\mathbf{F}-U(1)_{k_1}-U(1)_{k_2}-1\mathbf{F}}=\int dx_1dx_2\,e^{-ik_1\pi x_1^2-ik_2\pi x_2^2+2\pi i(\xi_1x_1+\xi_2x_2)}\times \\ s_b\big(\frac{iQ}{2}+x_1+\frac{u_1}{2}\big)s_b\big(\frac{iQ}{2}+x_2+\frac{u_2}{2}\big)s_b\big(\frac{iQ}{2}+p_1x_1+p_2x_2+\frac{u_1}{2}\big)\,. \tag{5.139}$$

After redefining parameters

$$u_1:=\frac{\log Y_1}{b\pi},\ u_2:=\frac{\log Y_2}{b\pi},\ u_3:=\frac{\log(-q^{(p_1+p_2-1)/2}\,Y_3-i\pi(p_1+p_2))}{b\pi}\,, \tag{5.140}$$

we get the associated effective superpotential in the semi-classical limit

$$\widetilde{\mathcal{W}}^{\text{eff}}_{1\mathbf{F}-U(1)_{k_1}-U(1)_{k_2}-1\mathbf{F}}=\mathrm{Li}_2(X_1Y_1)+\mathrm{Li}_2(X_2Y_2)+\mathrm{Li}_2(X_1^{p_1}X_2^{p_2}Y_3)+ \\ \frac{1}{2}\big(k_1+\frac{1+p_1^2}{2}\big)\log X_1^2+\frac{1}{2}\big(k_2+\frac{1+p_2^2}{2}\big)\log X_2^2+\frac{p_1p_2}{2}\log X_1\log X_2+ \\ \sum_{l=1}^{2}\big((1+p_l)\pi i+\log Y_1+p_l\log Y_3+2\pi i\,k_1-k_l\log q-4b\pi\xi_l\big)\log X_l\,. \tag{5.141}$$

The associated effective CS level matrix is

$$k_{ij}^{\text{eff}}=\begin{bmatrix}k_1+\frac{1+p_1^2}{2} & \frac{p_1p_2}{2}\\ \frac{p_1p_2}{2} & k_2+\frac{1+p_2^2}{2}\end{bmatrix}\,. \tag{5.142}$$

Similarly as before, mirror transformation $(\mathbf{1},\mathbf{1},\mathbf{1})$ turn this quiver theory into a particular $\mathcal{T}_{A,3}$ theory:

$$Z_{S^3_b}^{1\mathbf{F}-U(1)_{k_1}-U(1)_{k_2}-1\mathbf{F}}\xrightarrow{(\mathbf{1},\mathbf{1},\mathbf{1})}Z_{S^3_b}^{\mathcal{T}_{A,3}}\,. \tag{5.143}$$

We list some effective CS level matrices given by mirror transformations

$$\mathcal{T}[(\mathbf{0},\mathbf{2},\mathbf{2})]:\begin{bmatrix} 1 & \frac{1}{p_1} & -\frac{p_2}{p_1} \\ \frac{1}{p_1} & \frac{2k_1+p_1^2+1}{2p_1^2} & -\frac{2k_1p_2+p_2}{2p_1^2} \\ -\frac{p_2}{p_1} & -\frac{2k_1p_2+p_2}{2p_1^2} & \frac{k_1p_2^2}{p_1^2}+k_2+\frac{1}{2}\left(\frac{p_2^2}{p_1^2}+1\right) \end{bmatrix}, \tag{5.144}$$

$$\mathcal{T}[(\mathbf{1},\mathbf{2},\mathbf{2})]:\begin{bmatrix} 0 & -\frac{1}{p_1} & \frac{p_2}{p_1} \\ -\frac{1}{p_1} & \frac{2k_1+p_1^2-1}{2p_1^2} & \frac{p_2-2k_1p_2}{2p_1^2} \\ \frac{p_2}{p_1} & \frac{p_2-2k_1p_2}{2p_1^2} & \frac{k_1p_2^2}{p_1^2}+k_2-\frac{p_2^2}{2p_1^2}+\frac{1}{2} \end{bmatrix}, \tag{5.145}$$

$$\mathcal{T}[(\mathbf{2},\mathbf{0},\mathbf{2})]:\begin{bmatrix} \frac{1}{2}\left(2k_1+p_1^2+1\right) & p_1 & \frac{p_1p_2}{2} \\ p_2 & 1 & p_2 \\ \frac{p_1p_2}{2} & p_2 & \frac{1}{2}\left(2k_2+p_2^2+1\right) \end{bmatrix}, \tag{5.146}$$

$$\mathcal{T}[(\mathbf{2},\mathbf{1},\mathbf{2})]:\begin{bmatrix} k_1-\frac{p_1^2}{2}+\frac{1}{2} & -p_1 & -\frac{1}{2}p_1p_2 \\ -p_1 & 0 & -p_2 \\ -\frac{1}{2}p_1p_2 & -p_2 & k_2-\frac{p_2^2}{2}+\frac{1}{2} \end{bmatrix}, \tag{5.147}$$

$$\mathcal{T}[(\mathbf{2},\mathbf{2},\mathbf{0})]:\begin{bmatrix} \frac{2k_2p_1^2+p_1^2+p_2^2}{2p_2^2}+k_1 & -\frac{2k_2p_1+p_1}{2p_2^2} & -\frac{p_1}{p_2} \\ -\frac{2k_2p_1+p_1}{2p_2^2} & \frac{2k_2+p_2^2+1}{2p_2^2} & \frac{1}{p_2} \\ -\frac{p_1}{p_2} & \frac{1}{p_2} & 1 \end{bmatrix}, \tag{5.148}$$

$$\mathcal{T}[(\mathbf{2},\mathbf{2},\mathbf{1})]:\begin{bmatrix} \frac{2k_2p_1^2-p_1^2+p_2^2}{2p_2^2}+k_1 & \frac{p_1-2k_2p_1}{2p_2^2} & \frac{p_1}{p_2} \\ \frac{p_1-2k_2p_1}{2p_2^2} & \frac{2k_2+p_2^2-1}{2p_2^2} & -\frac{1}{p_2} \\ \frac{p_1}{p_2} & -\frac{1}{p_2} & 0 \end{bmatrix}. \tag{5.149}$$

It is obvious that if the charges p_1 and p_2 of the bifundamental multiplet are chosen properly, there could be many mirror dual theories with integer effective mixed Chern-Simons levels.

5.3 Knot polynomials

We can also apply 3d $\mathcal{N}=2$ mirror symmetry to knot theory. It is found in [83, 84] that the HOMFLY-PT polynomials of various knots K can be lifted to the form

$$P^K(a,x,q) \xrightarrow{\text{lift}} P^{Q_K}(\mathbf{x},q) := \sum_{d_1,\ldots,d_N=0}^{\infty} (-\sqrt{q})^{\sum_{i,j=1}^{N} C_{ij}d_id_j} \frac{x_1^{d_1}\cdots x_N^{d_N}}{(q,q)_{d_1}\cdots(q,q)_{d_N}}, \tag{5.150}$$

which implies that knots correspond to quivers encoded in matrices C_{ij}. This correspondence is called knots-quivers correspondence (KQ) in [84]. In addition, some relations need to be imposed on variables x_i, such that

$$P^K(a,x,q) = P^{Q_K}\left(x_i = x\, a^{a_i} q^{\frac{q_i-C_{ii}}{2}} (-\mathbf{t})^{\frac{C_{ii}}{2}}, q\right), \tag{5.151}$$

where the parameter $-\mathbf{t}=1$ in the unrefined limit $q=t$. On the other hand, 3d/3d correspondence conjectures that colored HOMFLY-PT polynomials are equivalent to the vortex

partition functions of some 3d $\mathcal{N}=2$ theories [6, 57]. Inspired by this and the quiver generating series (3.112), the authors in [93] conjecture that the lifted knot polynomial $P^{Q_K}(\mathbf{x},t)$ is also associated to certain 3d $\mathcal{N}=2$ theory $T[Q_K]$ with vortex partition functions, which in the semi-classical limit takes form

$$P^{Q_K}(\mathbf{x},q) \xrightarrow{\hbar\to 0} \int \prod_i \frac{dy_i}{y_i} \exp \frac{1}{\hbar}\Big(\widetilde{\mathcal{W}}_{T[Q_K]}(\mathbf{x},\mathbf{y})+O(\hbar)\Big)\,, \tag{5.152}$$

$$\widetilde{\mathcal{W}}_{\mathcal{T}[Q_K]}(\mathbf{x},\mathbf{y}) = \sum_i \mathrm{Li}_2(y_i) + \log\left((-1)^{C_{ii}}x_i\right)\log y_i + \sum_{i,j}\frac{C_{ij}}{2}\log y_i \log y_j\,. \tag{5.153}$$

By comparing (5.153) with (5.6), we note that the lifted HOMFLY-PT polynomials $P^{Q_K}(\mathbf{x},q)$ should be vortex partition functions of $\mathcal{T}_{A,N}$ theories denoted as

$$\mathcal{T}_{A,N}: \quad (U(1)+1\mathbf{F})^{\otimes N}_{k_{ij},\ \xi_i}\,. \tag{5.154}$$

Therefore C_{ij} play the role of effective Chern-Simons levels k_{ij}^{eff} and $\log\left((-1)^{C_{ii}}x_i\right)$ play the role of effective FI parameters ξ_i^{eff}. The mirror transformations of $\mathcal{T}_{A,N}$ theories enable us to obtain a chain of equivalent integer matrices $\{C_{ij}\}$.

Trefoil.

We take trefoil as an example, since it is one typical example in the knots-quivers correspondence [84, 93]. The associated knot-quiver matrix C_{ij} is

$$C_{ij} = \begin{bmatrix} 0 & 0 & 1 & 1 & 2 & 2 \\ 0 & 1 & 1 & 1 & 2 & 2 \\ 1 & 1 & 2 & 2 & 2 & 3 \\ 1 & 1 & 2 & 3 & 2 & 3 \\ 2 & 2 & 2 & 2 & 3 & 3 \\ 2 & 2 & 3 & 3 & 3 & 4 \end{bmatrix} + f \begin{bmatrix} 1 & 1 & 1 & 1 & 1 & 1 \\ 1 & 1 & 1 & 1 & 1 & 1 \\ 1 & 1 & 1 & 1 & 1 & 1 \\ 1 & 1 & 1 & 1 & 1 & 1 \\ 1 & 1 & 1 & 1 & 1 & 1 \\ 1 & 1 & 1 & 1 & 1 & 1 \end{bmatrix}, \tag{5.155}$$

where f is the framing number for trefoil. We assume the original theory $\mathcal{T}[(\mathbf{0},\mathbf{0},\mathbf{0},\mathbf{0},\mathbf{0},\mathbf{0})]$ for trefoil has effective Chern-Simons levels

$$C_{ij} = k_{ij}^{\text{eff},(\mathbf{0},\cdots,\mathbf{0})} = k_{ij} + \frac{1}{2}\delta_{ij}\,, \tag{5.156}$$

and real mass parameters have been absorbed into shifted FI parameters $\tilde{\xi}_i$. Implementing mirror transformations $\mathbf{H}(\mathcal{T}_{A,6})$ on its sphere partition function, one can get many integer effective CS level matrices.

Quiver reduction appears in this example as well. We find there is at least one gauge node left, and it cannot be integrated out. More explicitly, mirror transformation $(\mathbf{0},\mathbf{1},\mathbf{1},\mathbf{1},\mathbf{1},\mathbf{1})$

leads to the sphere partition function

$$
\begin{aligned}
&Z_{S^3_b}^{\mathcal{T}[(\mathbf{0},\mathbf{1},\mathbf{1},\mathbf{1},\mathbf{1})]} = \\
&\int dx\, e^{-\frac{1}{2}(9+14f+5f^2)\pi i\, x^2+\pi i\, x\left(-\frac{i(6+5f)}{4}Q+(2\tilde{\xi}_1+f\tilde{\xi}_2+(1+f)\tilde{\xi}_3+(1+f)\tilde{\xi}_4+(2+f)\tilde{\xi}_5+(2+f)\tilde{\xi}_6)\right)}\times \\
&s_b\big(\frac{iQ}{2}-x\big)s_b\big(\frac{iQ}{4}+f\,x-\tilde{\xi}_2\big)s_b\big(\frac{iQ}{4}+(1+f)\,x-\tilde{\xi}_3\big)s_b\big(\frac{iQ}{4}+(1+f)\,x-\tilde{\xi}_4\big)\times \\
&s_b\big(\frac{iQ}{4}+(2+f)\,x-\tilde{\xi}_5\big)s_b\big(\frac{iQ}{4}+(2+f)\,x-\tilde{\xi}_6\big)\,.
\end{aligned}
\tag{5.157}
$$

The corresponding theory has a star shape quiver shown in Figure 5.6, which has one gauge node $U(1)$ and six chiral multiplets with charges $\{-1, f, 1+f, 1+f, 2+f, 2+f\}$. The FI parameters $\tilde{\xi}_{2,3,4,5,6}$ have been turned into mass parameters while $\tilde{\xi}_1$ is still a FI parameter. When $f = 0, -1, -2$, some double sine functions from chiral multiplets can be moved out of

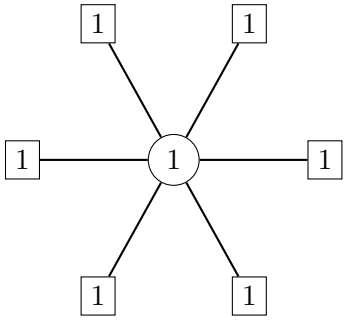

Figure 5.6: The star shape quiver for a 3d $\mathcal{N}=2$ theory given by trefoil.

integral, so framing f plays a subtle role here. Moreover, mirror transformation $(\mathbf{1},\mathbf{1},\mathbf{1},\mathbf{1},\mathbf{0},\mathbf{1})$ also leads to a star shape quiver with one gauge node $U(1)$ and six chiral multiplets with charges $\{2+f, 2+f, 2+f, 2+f, -1, 3+f\}$. The corresponding sphere partition function is

$$
\begin{aligned}
&Z_{S^3_b}^{\mathcal{T}[(\mathbf{1},\mathbf{1},\mathbf{1},\mathbf{1},\mathbf{0},\mathbf{1})]} = \\
&\int dx\, e^{-\frac{1}{2}(30+24f+5f^2)\pi i\, x^2+\pi i\, x\left(-\frac{11+5f}{4}iQ+(2\tilde{\xi}_1+2\tilde{\xi}_2+2\tilde{\xi}_3+2\tilde{\xi}_4+2\tilde{\xi}_5+3\tilde{\xi}_6)+f(\tilde{\xi}_1+\tilde{\xi}_2+\tilde{\xi}_3+\tilde{\xi}_4+\tilde{\xi}_6)\right)}\times \\
&s_b\big(\frac{iQ}{4}+(2+f)x-\tilde{\xi}_1\big)s_b\big(\frac{iQ}{4}+(2+f)\,x-\tilde{\xi}_2\big)s_b\big(\frac{iQ}{4}+(2+f)\,x-\tilde{\xi}_3\big)\times \\
&s_b\big(\frac{iQ}{4}+(2+f)\,x-\tilde{\xi}_4\big)s_b\big(\frac{iQ}{2}-x-\tilde{\xi}_5\big)s_b\big(\frac{iQ}{4}+(3+f)\,x-\tilde{\xi}_6\big)\,.
\end{aligned}
\tag{5.158}
$$

In this case, all FI parameters $\tilde{\xi}_{1,2,3,4,5,6}$ are turned into real mass parameters.

Chapter 6

3d brane webs and quivers

As we have discussed in chapter 4, some 3d $\mathcal{N} = 2$ theories have brane constructions that are given by Higgsing 5d theories, see e.g. [6, 48]. These 5d theories can be engineered in M-theory by Calabi-Yau three-manifolds that are dual to brane webs in type IIB string theory [27, 29, 49, 50, 51, 52]. In this chapter, we mainly discuss this Higgsing construction and 3d brane webs. This chapter is based on [12].

3d $\mathcal{N} = 2$ theories can be identified by some physical quantities, such as gauge groups, matter content, Chern-Simons levels, real mass parameters, etc. These physical quantities should be encoded in brane webs. For instance, the relative angle θ between NS5-brane and NS5'-brane is related to the Chern-Simons level [109, 110]. Turning on real mass parameters should separate overlapped D5-branes in 3d brane webs, and decoupling chiral multiplets should change effective Chern-Simons levels. Analogous to 5d $\mathcal{N} = 1$ theories discussed in e.g. [52], one can identify these physical quantities from 3d brane webs. In order to verify conclusions, we compute vortex partition functions using topological string vertex method. By computing various 3d brane webs and reading off Chern-Simons levels and real mass parameters from effective superpotentials, one can know how the brane webs encode data.

We show that there are many equivalent brane webs by turning on real mass parameters, namely, separating the overlapped D5-branes in 3d brane webs. These equivalent brane webs compose phases of 3d brane webs. A subset of these phases composes Higgs branch $\mathcal{M}_H$. These equivalent 3d brane webs are related by flipping the sign of real mass parameters. Moreover, flipping the sign of real mass parameters is equivalent to flipping the positions of D5-branes. The flipping of D5-branes can be interpreted in terms of 3d mirror symmetry for the mirror dual $\mathcal{T}_{A,N}$ theories, as we have discussed in chapter 5. Since each 3d brane web has associated mixed Chern-Simons levels, we conjecture that there is a correspondence between 3d brane webs and quiver matrices. Besides, we can also move flavor D5-branes in brane systems of 3d $\mathcal{N} = 2$ theories, which also leads to some equivalent brane webs.

In this chapter, we also discuss the nonabelian theories with a gauge group $U(N_c)$. By comparing with the vortex partition functions of nonabelian theories in [111, 112], we conjecture that 3d brane webs for nonabelian theories on Higgs branch also have quiver structure.

The organization of this chapter is as follows: in section 6.1, we discuss the relations between effective Chern-Simons levels and the relative angle between NS5-brane and NS5'-

brane. In section 6.2, we discus real mass deformations that lead to equivalent 3d brane webs. We also discuss the movement of D5-branes in this section. In section 6.3 we discuss 3d brane webs and quivers for nonabelian theories.

6.1 Effective Chern-Simons levels

In [109, 110], it is found that the relative angle θ between NS5-brane and NS5'-brane is related to Chern-Simons level

$$k = -\frac{p}{q} = -\tan\theta\,. \tag{6.1}$$

We note that this angle θ should relate to effective Chern-Simons levels, since there are one-loop corrections from chiral multiplets. In this chapter, we mainly discuss effective Chern-Simons levels for abelian theory, while the conclusion is also applicable to nonabelian theories.

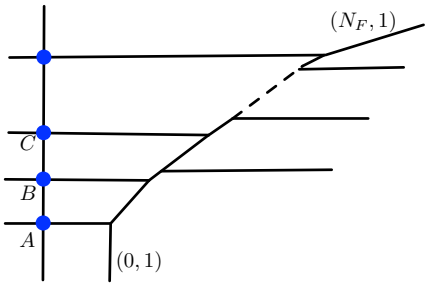

Figure 6.1: In this diagram, all possible locations of D3-branes are denoted by blue nodes. A D3-brane can be located on any fundamental D5-branes. Hence discrete points $\{A\,, B\,, C\,, \dots\}$ compose the Higgs branch $\mathcal{M}_H$. Note that each intersection point can be viewed as a local conifold singularity on the dual toric diagrams in M-duality [2].

For abelian theory $U(1)_k + N_F\mathbf{F} + N_{AF}\mathbf{AF}$, the Chern-Simons level receives quantum corrections from one-loop contributions, see e.g. [44, 45]:

$$k^{\text{eff}} = k + \frac{N_F}{2} - \frac{N_{AF}}{2}\,. \tag{6.2}$$

In particular, the effective Chern-Simons level is zero $k^{\text{eff}} = 0$ when the D3-brane is located on any point $\{A\,, B\,, C\,, \cdots\}$ on the brane web shown in Figure 6.1, since in this case the angle $\theta = 0$.

The range of the relative angle is important. If the angle is too large, there will be an intersection between NS5-brane and NS5'-brane, which often cause complications. We consider two cases $N_F \geqslant N_{AF}$ and $N_F < N_{AF}$ in the following.

$N_F \geqslant N_{AF}$

The 3d brane webs in this case are illustrated in Figure 6.2. Since N_F is larger than N_{AF}, the NS5-brane bends to the right. The range of the relative angle is shown in this figure. We get

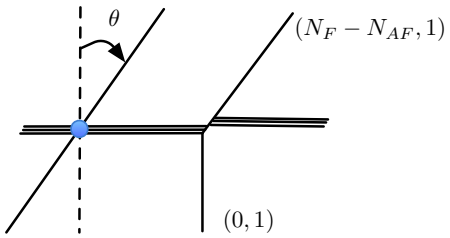

Figure 6.2: The range of the angle θ is shown in the web. In this web, the blue node stands for the D3-brane.

a bound

$$k^{\text{eff}} = \tan\theta \in [\,0\,, N_F - N_{AF}\,]\,, \tag{6.3}$$

which along with (6.2) leads to

$$k = \tan\theta + \frac{N_{AF} - N_F}{2} \in \Big[\, -\frac{N_F - N_{AF}}{2}\,, \frac{N_F - N_{AF}}{2}\,\Big]\,. \tag{6.4}$$

In particular, if $N_F = N_{AF}$, then $k^{\text{eff}} = k = 0$.

According to (6.4), the bare CS level can be $k = \pm\frac{1}{2}$ for the theory $U(1)_k + 1\,\mathbf{F}$. In Figure 6.3, we illustrate the values of Chern-Simons levels for the theory $U(1)_k + 2\,\mathbf{F}$, which has different relative angles. There are only three choices $k = \pm 1\,, 0$ in this case.

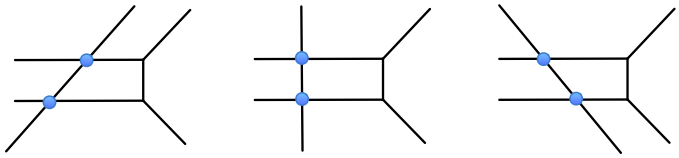

Figure 6.3: Note that the $SL(2,\mathbb{Z})$ symmetry of type IIB string theory is preserved in 3d brane webs, and hence only the relative angle matters.

$N_F < N_{AF}$ and decoupling

In this case, the NS5-brane bends to the left and always intersects with NS5'-brane. Note that intersections are allowed in 3d brane webs, as this kind of intersection can be also regarded as a local conifold singularity that can be resolved by a blow-up. Intersections can also be avoided by introducing additional fundamental D5-branes. Finally, one can decouple these additional fundamental multiplets by sending the associated real mass parameters to infinity.

For the case $N_F < N_{AF}$, we prefer to firstly introduce some fundamental multiplets $\mathbf{F}$ and finally decouple them. For simplicity, we add a particular number of fundamental chiral multiplets $\mathbf{F}$ such that the new effective Chern-Simons level vanishes. We note that there are two different cases, as illustrated in Figure 6.5. The first case (a) is that we introduce $n\mathbf{F}$ above the original line, while in the second case (b) we introduce $n\mathbf{F}$ below it, where $n = N_{AF} - N_F$.

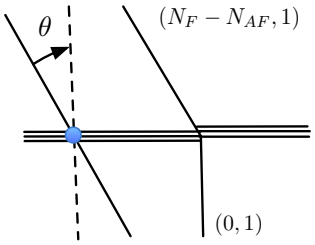

Figure 6.4: When $N_F < N_{AF}$, there is always an intersection between NS5'-brane and NS5-brane.

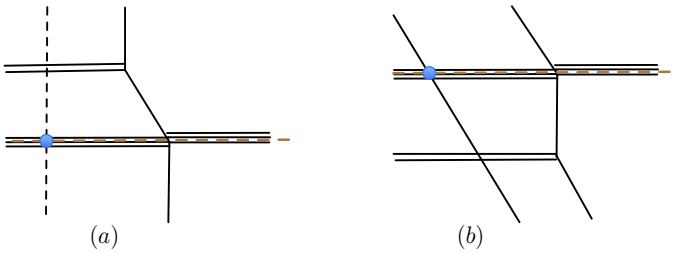

Figure 6.5: The original lines are denoted by dashed brown lines. In the left brane web (a), we add $(N_{AF} - N_F)\mathbf{F}$ to avoid an intersection above the original line, and in the right brane web (b), we add the same number of $\mathbf{F}$ below the original line to avoid intersection.

In both cases the new effective Chern-Simons level vanishes.

In this first case decoupling $n\mathbf{F}$ does not change the effective Chern-Simons level, because if we decouple a fundamental multiplet $\mathbf{F}$ by sending the real mass parameter $\beta \to 0$, its contribution becomes trivial $\left(\beta\sqrt{\frac{t}{q}}, t\right)_n^{-1} \to 1$. The corresponding 3d brane web in this case is shown in diagram (a) in Figure 6.4 with the Chern-Simons level $k^{\text{eff}} = 0$.

In order to decouple a fundamental multiplet in the second case we need to flip Kähler parameter β, namely

$$\left(\beta\frac{t}{q}, t\right)_n^{-1} \simeq \left(\beta^{-1}\frac{q}{t}, t^{-1}\right)_n^{-1} (-\sqrt{t})^{-n^2}\,, \tag{6.5}$$

and then send $\beta^{-1} \to 0$. This operation leaves a factor $(-\sqrt{t})^{-n^2}$ that reduces the effective Chern-Simons level by one. In this case, we can at most decouple $N_{AF} - N_F$ number of $\mathbf{F}$ and get a effective CS level

$$k^{\text{eff}} \geq 0 - (N_{AF} - N_F) = N_F - N_{AF}\,. \tag{6.6}$$

This Chern-Simons level corresponds to the diagram (b) in Figure 6.4. Therefore, when $N_{AF} > N_F$, the range of k^{eff} is

$$k^{\text{eff}} \in [N_F - N_{AF}, 0]\,, \tag{6.7}$$

and the associated bare Chern-Simons level

$$k = \tan\theta + \frac{N_{AF} - N_F}{2} \in \left[-\frac{N_{AF} - N_F}{2}, \frac{N_{AF} - N_F}{2}\right]. \tag{6.8}$$

We summarize that for both cases $N_F \geqslant N_{AF}$ and $N_F < N_{AF}$, the Chern-Simons level falls in the bound

$$k = \tan\theta - \frac{N_F - N_{AF}}{2} \in \Big[-\frac{|N_F - N_{AF}|}{2}, \frac{|N_F - N_{AF}|}{2} \Big], \tag{6.9}$$

which agrees with the bound found by localization methods [112, 113]. This bound is also the constraint on Chern-Simons levels for Aharony duality [46].

6.2 Real mass deformations

3d $\mathcal{N} = 2$ theories without superpotentials have two kinds of free parameters: real mass parameters and FI parameters. In this section, we discuss the 3d brane webs obtained by turning on real mass parameters.

Phases of brane webs

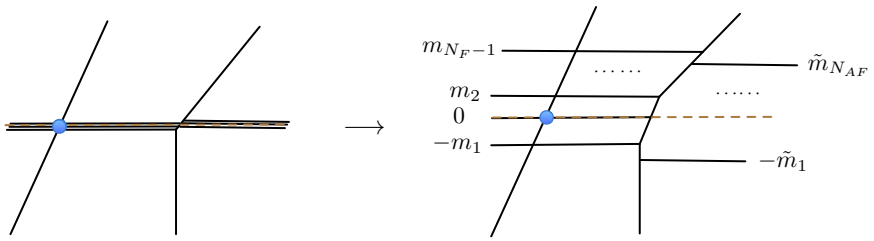

Figure 6.6: The real mass deformation for $U(1)_k + N_F\mathbf{F} + N_{AF}\mathbf{AF}$ is illustrated in this figure. We have assigned the real mass parameters to each D5-brane on the right brane web. The D3-brane can be located on any fundamental D5-brane.

The procedure of turning on real mass parameters is illustrated in Figure 6.6. Firstly, we need to pick up a fundamental D5-brane and locate the D3-brane on it. Then we separate all D5-branes by turning on the real masses. These are various configurations to separate D5-branes, since some mass parameters are larger than others. We could get many equivalent 3d brane webs. In particular, possible locations of D3-brane compose the Higgs branch $\mathcal{M}_H$ defined by $\{\sigma + m_i = 0\,, \forall i\}$. The real mass deformations for **AF** do not belong to the Higgs branch. These equivalent brane webs obtained by real mass deformations can be considered as the phases of 3d abelian theories. Since these phases are physically equivalent, the corresponding vortex partition functions should be equivalent.

Based on computations, we note that the assignment rule for real mass parameters is the following: D5-branes below the original line should be assigned with negative masses, and D5-brane above the original line should be assigned with positive masses. The mass parameter for the original line where D3-brane is located, is zero. If we locate the D3-brane on other fundamental D5-branes or change the positions of antifundamental D5-branes, then the assignment of mass parameters will be changed but will still follow the same assignment rule.

Note that different phases correspond to the same theory and hence have the same effective CS level, and the relative angle θ between NS5-brane and NS5'-brane is independent of the real mass deformations. Generically, different phases of 3d brane webs cannot be related by Hanany-Witten transitions or flop transitions. In the following part of this chapter, we compute the vortex partition functions associated to some brane webs and verify the assignment rule for real mass parameters [1].

Examples

In this section, we compute vortex partition functions for $U(1)_k + 2\,\mathbf{F}$ and $U(1)_k + 2\,\mathbf{F} + 1\,\mathbf{AF}$. We use the refined topological vertex and the Higgsing method (geometric transitions) that we have discussed in chapter 4 to produce D3-branes, see also e.g. [6, 10, 81, 80, 11, 90, 91, 34, 92].

$U(1)_k + 2\,\mathbf{F}$

The Higgs branch of this theory contains two discrete points A and B as shown in the brane web in Figure 6.7. If we introduce one D3-brane (denoted by the blue node) at phase point

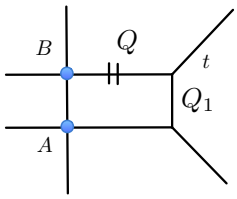

$k = 0$

Figure 6.7: The bare Chern-Simons level for this web is zero. The assignment of refined parameter t is shown in the web. The short double line || is a notation in topological vertex method, denoting that the preferred direction.

A, the corresponding vortex partition function obtained by Higgsing (geometric transition) method is

$$Z^A_{\bar{q}\text{-brane}} = \sum_{n=0}^{\infty} \frac{(-\sqrt{t})^{n^2} \left(\frac{\sqrt{t}}{q} Q\right)^n}{(t,t)_n (Q_1 \frac{t}{q}, t)_n} \,. \tag{6.10}$$

Here we only show its $\bar{q}$-brane partition function for simplicity. Similarly, we can introduce D3-brane at phase point B and obtain the vortex partition function

$$Z^B_{\bar{q}\text{-brane}} = \sum_{n=0}^{\infty} \frac{(-\sqrt{t})^{n^2} \left(\sqrt{t} Q_1^{-1} Q\right)^n}{(t,t)_n \left(Q_1^{-1} \frac{t}{q}, t\right)_n} \,, \tag{6.11}$$

where we can absorb Kähler parameter Q_1^{-1} to Q which plays the role of FI parameter.

We note that these two partition functions are equal upon the identification of the mass

[1] The one-loop contribution (5.61) can also be added.

parameter

$$Z^{A}_{\bar{q}\text{-brane}} \overset{Q\to Q^{-1}}{=\!=\!=} Z^{B}_{\bar{q}\text{-brane}}\,. \tag{6.12}$$

For $Z^{A}_{\bar{q}\text{-brane}}$, the real mass parameter is Q_1, while for $Z^{B}_{\bar{q}\text{-brane}}$, mass parameter is Q_1^{-1}. This verifies the argument rule that the real mass parameter above the original line is positive, and the real mass parameter below the original line is negative. Note that the effective CS levels for both phase A and phase B are the same $k^{\text{eff}} = 0 + \frac{2}{2} = 1$, using the formula discussed in section 6.1.

$U(1)_k + 2\,\mathbf{F} + 1\,\mathbf{AF}$

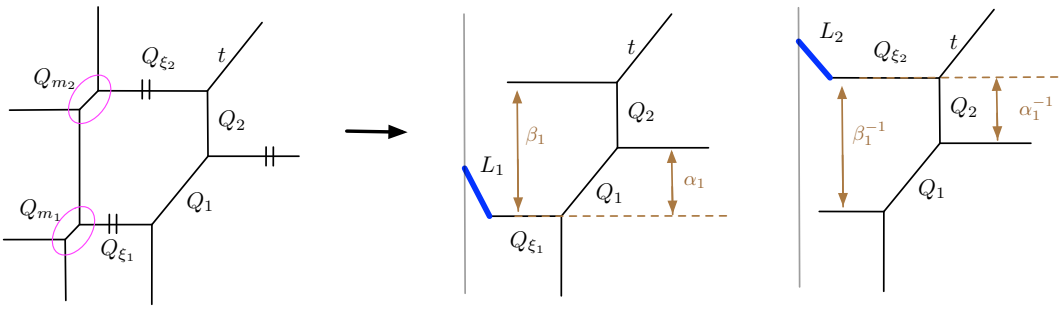

Figure 6.8: We denote the D3-brane introduced by Higgsing Q_{m_1} as L_1, and the one given by Higgsing Q_{m_2} as L_2. The Kähler parameters for mass parameters have been denoted on the brane webs.

We draw brane webs for this theory in Figure 6.8, where the D3-brane is introduced by Higgsing Q_{m_1} and Q_{m_2}. We first introduce a D3-brane at Q_{m_1} by setting $Q_{m_1} = \frac{1}{q}\sqrt{\frac{t}{q}}$ and $Q_{m_2} = \sqrt{\frac{t}{q}}$. This is a $\bar{q}$-brane whose vortex partition function is

$$Z^{L_1}_{\bar{q}\text{-brane}}(Q_i) = \sum_{n=0}^{\infty} \frac{\left(Q_{\xi_1}\sqrt{\frac{t}{q}}\right)^n \left(Q_1\sqrt{\frac{t}{q}}, t\right)_n}{(t,t)_n \left(Q_1 Q_2 \frac{t}{q}, t\right)_n}\,. \tag{6.13}$$

The relations between gauge theory parameters and Kähler parameters are $\alpha_1 = Q_1\,,\ \ \beta_1 = Q_1 Q_2\,,\ \ z = Q_{\xi_1}$. Then this partition function can be written as

$$Z^{L_1}_{\bar{q}\text{-brane}}(z,\alpha,\beta) = \sum_{n=0}^{\infty} \frac{\left(z\sqrt{\frac{t}{q}}\right)^n \left(\alpha_1\sqrt{\frac{t}{q}}, t\right)_n}{(t,t)_n \left(\beta_1 \frac{t}{q}, t\right)_n}\,. \tag{6.14}$$

The D3-brane L_2 is introduced by Higgsing $Q_{m_1} = \sqrt{\frac{t}{q}}$ and $Q_{m_2} = \frac{1}{q}\sqrt{\frac{t}{q}}$, whose partition function is

$$Z^{L_2}_{\bar{q}\text{-brane}}(Q_i) = \sum_{n=0}^{\infty} \frac{\left(Q_{\xi_2}\sqrt{\frac{t}{q}}\right)^n \left(Q_2\sqrt{\frac{q}{t}}, \frac{1}{t}\right)_n}{(t,t)_n \left(Q_1 Q_2 \frac{q}{t}, \frac{1}{t}\right)_n} = \sum_{n=0}^{\infty} \frac{\left(\frac{Q_{\xi_2}}{Q_1}\frac{t}{q}\right)^n \left(Q_2^{-1}\sqrt{\frac{t}{q}}, t\right)_n}{(t,t)_n \left(Q_1^{-1} Q_2^{-1} \frac{t}{q}, t\right)_n}\,. \tag{6.15}$$

The relations between gauge theory parameters and Kähler parameters are given by $\alpha_1 = Q_2^{-1}$, $\beta_1 = Q_1^{-1}Q_2^{-1}$, $z = \frac{Q_{\xi_2}}{Q_1}\sqrt{\frac{t}{q}}$. Then the partition function can be written as

$$Z^{L_2}_{\bar{q}\text{-brane}}(z,\alpha,\beta) = \sum_{n=0}^{\infty} \frac{\left(z\sqrt{\frac{t}{q}}\right)^n \left(\alpha_1\sqrt{\frac{t}{q}},t\right)_n}{(t,t)_n \left(\beta_1\frac{t}{q},t\right)_n}\,. \tag{6.16}$$

Therefore, upon the redefinition of parameters α_1 and β_1, these two partition functions take the same form

$$Z^{L_1}_{\bar{q}\text{-brane}}(z,\alpha,\beta) = Z^{L_2}_{\bar{q}\text{-brane}}(z,\alpha,\beta)\,, \tag{6.17}$$

which implies that these two brane web configurations L_1 and L_2 in Figure 6.8 are equivalent. We remind that the effective CS level k^{eff} for these two brane webs is zero, which is known by comparing (6.14) with the generic form (3.109). We confirm again that mass parameters m_i and $\tilde{m}_i$ below the original line are negative and above the original line are positive.

6.2.1 Flipping D5-branes

Recall that in 5d $\mathcal{N} = 1$ theories, there are many equivalent 5d brane webs that can be related by Hanany-Witten transitions and flop transitions. For example, the 5d theory with gauge group $SU(2)$ and two fundamental hypermultiplets has some equivalent 5d brane webs as illustrated in Figure 6.9. These 5d brane webs can be related by Hanany-Witten transitions, which could move the flavor D5-branes up and down. One would expect that there

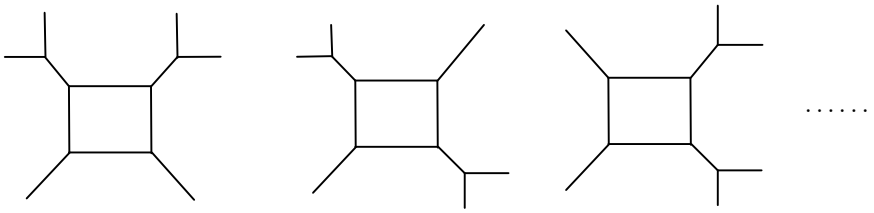

Figure 6.9: Some 5d brane webs for the 5d $\mathcal{N} = 1$ theory with a gauge group $SU(2)$ and two fundamental hypermultiplets.

may also be certain physical operations to relate equivalent 3d brane webs given by various real mass deformations. However, it turns out that Hanany-Witten transitions cannot relate these equivalent 3d brane webs, even for very simple theory $U(1) + 2\mathbf{F}$ shown in Figure 6.10. Moreover, we cannot directly Hanany-Witten move the D5-branes in 3d brane webs without causing problems. We should return to their mother 5d brane webs which are the brane webs before the Higgsing, and then perform Hanany-Witten transition then. However, this operation makes the brane webs more complicated, and seems difficult to relate equivalent 3d brane webs given by real mass deformations. Fortunately, there is a particular type of Hanany-Witten transition that can be implemented without complication, which is discussed in section 4.3; see also [91, 10].

By looking at the vortex partition functions for 3d $U(1) + N_F\mathbf{F} + N_{AF}\mathbf{AF}$ theories, one

could find that equivalent 3d brane webs differ only by the assignment of real mass parameters. For example, the partition functions for the 3d brane webs shown in Figure 6.8 are related by the operation

$$Z^{L_1}_{\tilde{q}\text{-brane}}(Q_i) \xrightarrow{Q_1\to Q_1^{-1}\,,\; Q_1Q_2\to Q_1^{-1}Q_2^{-1}} Z^{L_2}_{\tilde{q}\text{-brane}}(Q_i)\,, \tag{6.18}$$

The operation

$$\{Q_1 \to Q_1^{-1}\,,\; Q_1Q_2 \to Q_1^{-1}Q_2^{-1}\} \tag{6.19}$$

relates 3d brane webs L_1 and L_2. We can express (6.19) in terms of real mass parameters

$$\{\tilde{m}_1 \to -\tilde{m}_1\,,\quad m_1 \to -m_1\}\,. \tag{6.20}$$

This implies that flipping the sign of real mass parameters relate two equivalent 3d brane webs. This can be verified in more examples.

Then, what is a physical interpretation of this flipping from gauge theory perspective? The answer is that this flipping is caused by mirror symmetry transformation discussed in chapter 5; see also [11]. The mirror symmetry is a duality between theories, which does not change their partition functions. One can perform mirror symmetry several times and get a chain of mirror dual theories. We have discussed in chapter 5 that 3d mirror transformations only flip the sign of some mass parameters for the mirror dual $\mathcal{T}_{A,N}$ theories.

For a generic abelian theory $U(1) + N_F\mathbf{F} + N_{AF}\mathbf{AF}$, there are many mass parameters, and one can flip the sign of any mass parameter. This on the side of brane webs acts as reflecting the positions of D5-branes up and down the original line, since the positions of D5-branes correspond to real mass parameters. By flipping mass parameters in a sequence, one can obtain all equivalent 3d brane webs. Moreover, flipping parameters $\alpha \to \alpha^{-1}$ and $\beta \to \beta^{-1}$ changes the quiver matrix C_{ij} in the quiver generating series (3.112). Hence there is the correspondence

$$\text{3d brane webs} \leftrightarrow \text{quiver matrices}\,. \tag{6.21}$$

Let us look at brane webs for some simple theories and show their quiver matrices to verify this correspondence. $U(1)_k + 1\mathbf{F}$ is a trivial theory since it only has one brane web. The first

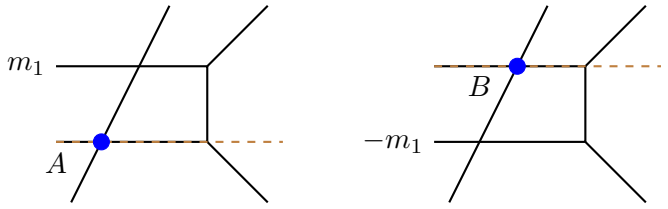

Figure 6.10: Flipping the D5-brane relates equivalent brane webs.

example we discuss is $U(1) + 2\mathbf{F}$, which has two equivalent brane webs as illustrated in Figure 6.10, corresponding to discrete points on Higgs branch. The corresponding quiver matrices

(effective mixed Chern-Simons levels) are

$$C_{ij}^{A} = k_{A}^{\text{eff}} = \begin{bmatrix} k+1 & 1 \\ 1 & 1 \end{bmatrix}, \quad C_{ij}^{B} = k_{B}^{\text{eff}} = \begin{bmatrix} k & -1 \\ -1 & 0 \end{bmatrix}. \tag{6.22}$$

The next example is $U(1)_k + 3\mathbf{F}$, whose brane webs are shown in Figure 6.11. There are in

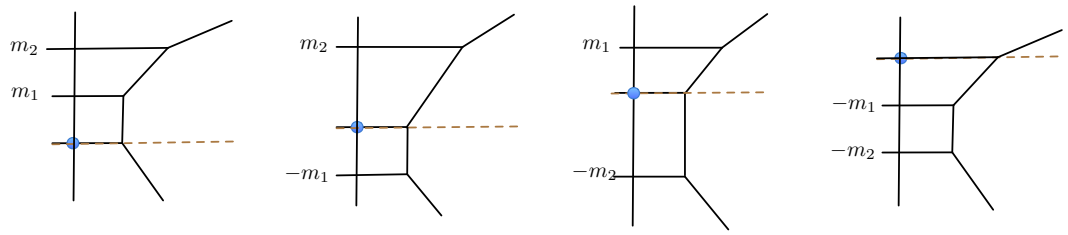

Figure 6.11: The brane webs for the theory $U(1) + 3\mathbf{F}$ are associated with the same effective CS level $k^{\text{eff}} = 1$.

total four brane webs, which are given by flips:

$$\text{flip 0: } \{m_1, m_2\}, \quad \text{flip 1: } \{-m_1, m_2\}, \ \{m_1, -m_2\}, \quad \text{flip 2: } \{-m_1, -m_2\}. \tag{6.23}$$

The corresponding quivers are the following:

$$\begin{bmatrix} k+\frac{3}{2} & 1 & 1 \\ 1 & 1 & 0 \\ 1 & 0 & 1 \end{bmatrix}, \quad \begin{bmatrix} k+\frac{1}{2} & -1 & 1 \\ -1 & 0 & 0 \\ 1 & 0 & 1 \end{bmatrix}, \quad \begin{bmatrix} k+\frac{1}{2} & 1 & -1 \\ 1 & 1 & 0 \\ -1 & 0 & 0 \end{bmatrix}, \quad \begin{bmatrix} k-\frac{1}{2} & -1 & -1 \\ -1 & 0 & 0 \\ -1 & 0 & 0 \end{bmatrix}. \tag{6.24}$$

The first element $C_{0,0}$ is the effective Chern-Simons level for the fundamental D5-brane where D3-brane is located; each row or column corresponds to a different D5-brane. We summarize the quiver components associated to D5-branes and classified by their mass parameters as follows:

$$m_i > 0, \quad C_{ij}(\beta_i) = \begin{bmatrix} 0 & 1 \\ 1 & 0 \end{bmatrix}, \qquad m_i < 0, \quad C_{ij}(\beta_i) = \begin{bmatrix} 1 & -1 \\ -1 & 1 \end{bmatrix}, \tag{6.25}$$

$$\tilde{m}_i > 0, \quad C_{ij}(\alpha_i) = \begin{bmatrix} 0 & 1 \\ 1 & 1 \end{bmatrix}, \qquad \tilde{m}_i < 0, \quad C_{ij}(\alpha_i) = \begin{bmatrix} -1 & -1 \\ -1 & 0 \end{bmatrix}, \tag{6.26}$$

which are obtained from q-Pochhammer products (3.123) and (3.124).

The last example is $U(1)_0 + 2\mathbf{F} + 2\mathbf{AF}$. There are eight equivalent brane denoted by flips:

$$\begin{aligned} &\text{flip 0: } \{m_1, \tilde{m}_1, \tilde{m}_2\}, \\ &\text{flip 1: } \{-m_1, \tilde{m}_1, \tilde{m}_2\}, \ \{m_1, -\tilde{m}_1, \tilde{m}_2\}, \ \{m_1, \tilde{m}_1, -\tilde{m}_2\}, \\ &\text{flip 2: } \{-m_1, -\tilde{m}_1, \tilde{m}_2\}, \{m_1, -\tilde{m}_1, -\tilde{m}_2\}, \{-m_1, \tilde{m}_1, -\tilde{m}_2\}, \\ &\text{flip 3: } \{-m_1, -\tilde{m}_1, -\tilde{m}_2\}. \end{aligned} \tag{6.27}$$

We show a few of them in Figure 6.12.

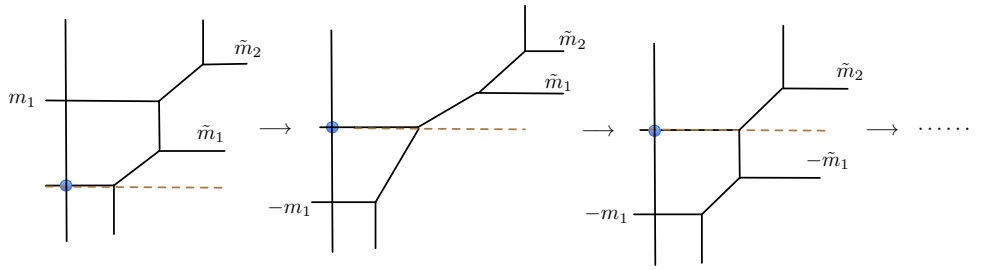

Figure 6.12: Flipping D5-branes leads to a chain of equivalent 3d brane webs.

6.2.2 Moving D5-branes

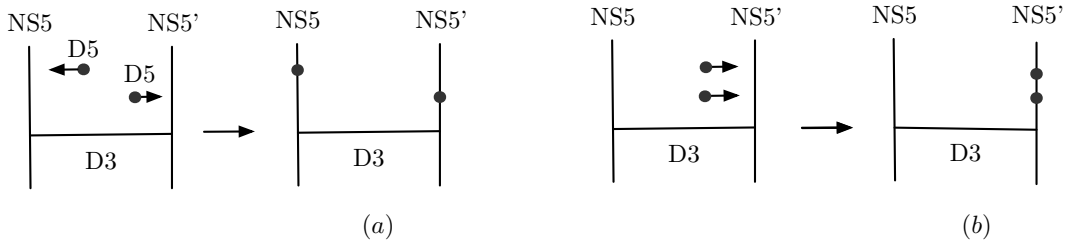

Figure 6.13: There is some freedom in moving flavor D5-branes. In the brane configuration (a), we move two D5-branes in opposite directions and attach them to NS5-brane and NS5'-brane separately, while in the brane configuration (b), we attach both flavor D5-branes to the NS5'-brane.

Moving D5-branes also gives rise to equivalent 3d brane webs. For details about this movement, see e.g. [47]. In brane construction of 3d $\mathcal{N} = 2$ theories, the matter arises from D5-branes located between NS5-brane and NS5'-brane. Each D5-brane gives rise to one **F** and one **AF**. These flavor D5-branes can move to either left or right, leading to different brane webs. We illustrate this by considering brane systems in Figure 6.13. If we move one D5-brane to the left and another D5-brane to the right, then we get a theory represented by $\boxed{1+1} - \textcircled{1} - \boxed{1+1}$[2]. On the other hand, if we move both D5-branes to the right, then we get a theory denoted by $\textcircled{1} - \boxed{2+2}$. Since these two diagrams describe the same theory $U(1) + 2\mathbf{F} + 2\mathbf{AF}$, we have

$$\boxed{1+1} - \textcircled{1} - \boxed{1+1} \quad = \quad \textcircled{1} - \boxed{2+2}. \tag{6.28}$$

The corresponding brane systems are actually brane web (a) and web (b) respectively in Figure 6.13, which can be drawn more precisely as brane web (d) and web (e) in Figure 6.14. The

[2]Here we use circle and box diagrams to denote gauge theories, which are well known as quiver diagrams in literature. In this notation, the circle with a number N denotes the gauge group $U(N)$, and the box with number $N_F + N_{AF}$ denotes $N_F\mathbf{F}$ and $N_{AF}\mathbf{AF}$.

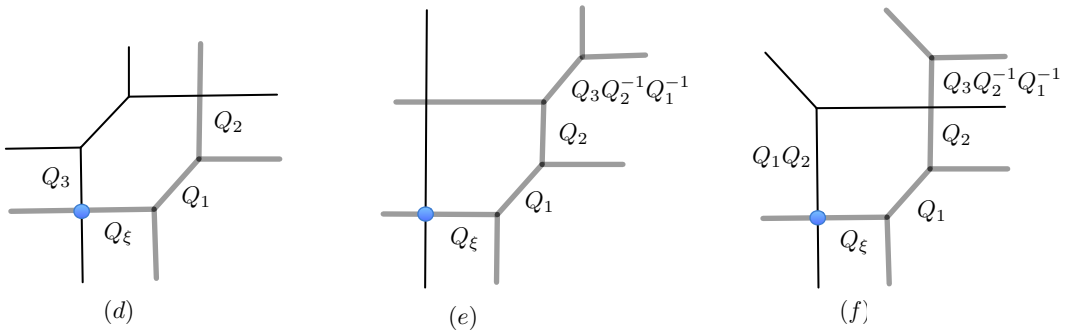

Figure 6.14: Some equivalent brane webs for $U(2) + 2\mathbf{F} + 2\mathbf{AF}$.

vortex partition functions of these brane webs are the same

$$Z^{\text{vortex}}_{\bar{q}\text{-brane}} = \sum_{n=0}^{\infty} \frac{\left(Q_\xi \sqrt{\frac{t}{q}}\right)^n \left(Q_1\sqrt{\frac{t}{q}}, t\right)_n \left(Q_3\sqrt{\frac{t}{q}}, t\right)_n}{(t,t)_n \left(Q_1 Q_2 \frac{t}{q}, t\right)_n}, \tag{6.29}$$

where the effective Chern-Simons level is zero. The open strings connecting D3-brane and D5-branes can be identified from q-Pochhammer products following (3.111). Similarly, we can flop a Kähler parameter and perform the Hanany-Witten transition to get the brane web (the diagram (f) in Figure 6.14) for $\boxed{1+0} - \textcircled{1} - \boxed{1+2}$.

6.3 Nonabelian theories and quivers

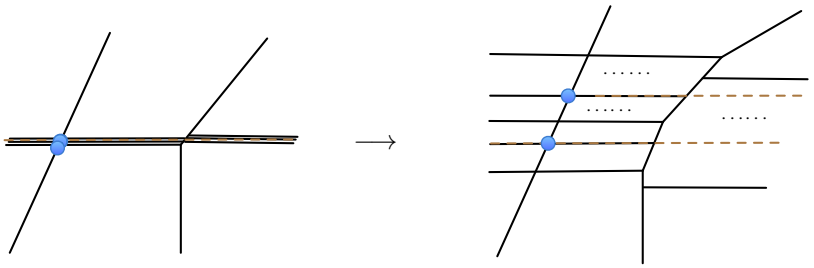

Figure 6.15: We illustrate the real mass deformations of the nonabelian theory $U(2) + N\mathbf{F} + N_{AF}\mathbf{AF}$ in this figure. The mass deformations for higher rank $U(N)$ theories are similar.

We can turn on the real mass parameters for nonabelian theories. As illustrated in Figure 6.15, the overlapped flavor D5-branes for $U(2) + N_F\mathbf{F} + N_{AF}\mathbf{AF}$ are separated by real mass deformations. Two D3-branes are located on a pair of D5-branes, corresponding to a vacuum on the Higgs branch.

Vortex partition function and brane webs

In [111, 112], vortex partition functions of $U(N)_k+N_F\mathbf{F}+N_{AF}\mathbf{AF}$ have been computed using the factorization property of superconformal indices, taking the form

$$Z^{\text{vortex}}(\sigma(t))=\sum_{\vec{n}=0}^{\infty}(-\omega)^{|n|}Z_{\{n_j\}}(q,\sigma(t),\tilde{t},\tau,k)\,, \tag{6.30}$$

$$Z_{\{n_j\}}(q,\sigma(t),\tilde{t},\tau,k)=(-1)^{\left(k+\frac{N_F-N_{AF}}{2}\right)\left(\sum_{i=1}^{N}n_i\right)}e^{ik\sum\limits_{j=1}^{N}\left(M_jn_j+\mu n_j+i\gamma n_j^2\right)} \tag{6.31}$$

$$\cdot\frac{\prod\limits_{a=1}^{N_{AF}}\prod\limits_{j=1}^{N}\prod\limits_{k=0}^{n_j-1}2\sinh\frac{-i\tilde{M}_a-iM_j-2i\mu+2\gamma k}{2}}{\prod\limits_{i=1}^{N}\prod\limits_{j=1}^{N}\prod\limits_{k=0}^{n_j-1}2\sinh\frac{iM_i-iM_j+2\gamma(k-n_i)}{2}\cdot\prod\limits_{a=N+1}^{N_F}\prod\limits_{j=1}^{N}\prod\limits_{k=0}^{n_j-1}2\sinh\frac{iM_a-iM_j+2\gamma(k+1)}{2}}\,, \tag{6.32}$$

where we did not sum up all vortex partition functions on the Higgs branch moduli space, and (6.30) is just the vortex partition function on a particular vacuum $\sigma(t)$. According to the discussion before, the vortex partition functions for all vacua are equivalent upon redefinitions of real mass parameters. If we define $q=e^{-2\gamma}\,,t=e^{iM},\tilde{t}=e^{i\tilde{M}}\,,\tau=e^{i\mu}$, then the partition function takes form

$$\begin{aligned}Z_{\{n_j\}}(q,\sigma(t),\tilde{t},\tau,\kappa)=&(-\sqrt{q})^{||n||^2k^{\text{eff}}}q^{-\sum\limits_{i,j=1}^{N}n_in_j}\cdot\tau^{|n|(k-N_{AF})}(\sqrt{q})^{\frac{|n|(N_{AF}+N_F-2N)}{2}}\\&\cdot\frac{\left(\prod\limits_{j=1}^{N}t_j^{n_j}\right)^{k^{\text{eff}}}}{\left(\prod\limits_{i=1}^{N_F}t_i\prod\limits_{a=1}^{N_{AF}}\tilde{t}_a\right)^{\frac{|n|}{2}}}\cdot\frac{\prod\limits_{a=1}^{N_{AF}}\prod\limits_{j=1}^{N}(\tau t_j\tilde{t}_a,\ q)_{n_j}}{\prod\limits_{i,j=1}^{N}\left(\frac{t_j}{t_i}q^{-n_i},\ q\right)_{n_j}\cdot\prod\limits_{a=N+1}^{N_F}\prod\limits_{j=1}^{N}\left(\frac{t_j}{t_a}q,\ q\right)_{n_j}}\,,\end{aligned} \tag{6.33}$$

where we use the shorthand notation $|n|=\sum_{i=1}^{N}n_i$ and $||n||^2=\sum_{i=1}^{N}n_i^2$. Here $k^{\text{eff}}=k+\frac{N_F-N_{AF}}{2}$ is the effective CS level for non-abelian theories, and $t_i,\tilde{t}_i$ are associated to real mass parameters.

We note that the vortex partition functions for non-abelian theories are themselves abelianized as (6.33) can be expressed in terms of q-Pochhammer products. Therefore, there should be corresponding quiver structure. We verify this in the following subsection.

$U(2)+2\mathbf{F}+2\mathbf{AF}$

We firstly consider $U(2)+2\mathbf{F}+2\mathbf{AF}$. We implement refined topological vertex and Higgsing (geometric transition) method discussed in chapter 4 to obtain vortex partition function. The brane web for this theory is shown in Figure 6.16. We note that in order to agree with (6.33), the internal line associated to NS5'-brane should be cut, or in other words, the Young diagrams on these internal lines should be empty. This implies that the we should introduce two NS5'-branes rather than one. Its 3d brane web is illustrated in Figure 6.17. Since we consider vortex partition functions on the Higgs branch, the gauge group is broken to $U(1)^2$.

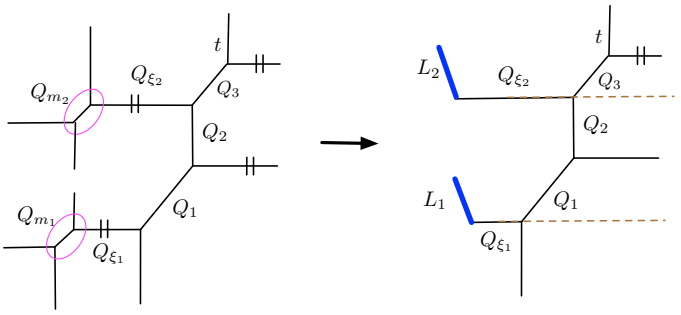

Figure 6.16: We introduce two D3-branes L_1 and L_2 by Higgsing. In topological vertex method, cutting lines means the associated Young diagrams on internal lines are empty.

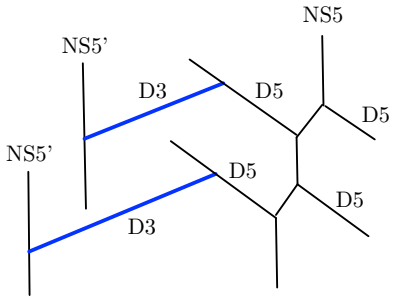

Figure 6.17: The new brane web has a partition function matching with (6.33).

The new brane web that we get also confirms this point.

Using refined topological vertex method, we compute the refined open topological string amplitude for the toric diagram in Figure 6.16; the more precise web is shown in Figure 6.17. We implement geometric transitions by setting $Q_{m_1} = \frac{1}{q}\sqrt{\frac{t}{q}}, Q_{m_2} = \frac{1}{q}\sqrt{\frac{t}{q}}$ to obtain the $(\bar{q},\bar{q})$-brane amplitude. In this case, Young diagrams on the open topological brane L_1 and L_2 are antisymmetric, denoted by $\{n_1\}_V$ and $\{n_2\}_V$ respectively[3]. By using (A.20) and other identities in Appendix, we find

$$
\begin{aligned}
&Z^{(\bar{q},\bar{q})\text{-brane}}(Q_1,Q_2) \\
&= \sum_{n_1,n_2=0}^{\infty} \frac{\left(Q_{\xi_1}\sqrt{\frac{t}{q}}\right)^{n_1}\left(Q_{\xi_2}\sqrt{\frac{t}{q}}\right)^{n_2}}{(t,t)_{n_1}(t,t)_{n_2}} \cdot \frac{(Q_1\sqrt{\frac{t}{q}},t)_{n_1}(Q_2\sqrt{\frac{q}{t}},t^{-1})_{n_2}(Q_3\sqrt{\frac{t}{q}},t)_{n_2}(Q_1Q_2Q_3\sqrt{\frac{t}{q}},t)_{n_1}}{(Q_1Q_2t^{n_1},t^{-1})_{n_2}(Q_1Q_2\frac{t}{q}\cdot t^{-n_2},t)_{n_1}} \\
&= \sum_{n_1,n_2=0}^{\infty} \frac{(-\sqrt{t})^{-2n_1n_2}\left(Q_{\xi_1}\sqrt{\frac{t}{q}}\right)^{n_1}\left(Q_1^{-1}Q_{\xi_2}\right)^{n_2}}{(t,t)_{n_1}(t,t)_{n_2}} \cdot \frac{(Q_1\sqrt{\frac{t}{q}},t)_{n_1}(Q_1Q_2Q_3\sqrt{\frac{t}{q}},t)_{n_1}(Q_2^{-1}\sqrt{\frac{t}{q}},t)_{n_2}(Q_3\sqrt{\frac{t}{q}},t)_{n_2}}{(Q_1Q_2\frac{t}{q}\cdot t^{-n_2},t)_{n_1}(Q_1^{-1}Q_2^{-1}t^{-n_1},t)_{n_2}},
\end{aligned}
\tag{6.34}
$$

[3]Here we draw the arrows for Young diagrams towards Lagrangian branes (D3-branes). If we reverse the directions of arrows, then Young diagrams are transposed.

which in the unrefined limit $q = t$ takes form

$$Z^{(\bar{q},\bar{q})\text{-brane}}(Q_1,Q_2)|_{q=t} = \sum_{n_1,n_2=0}^{\infty} \frac{q^{-n_1 n_2} Q_{\xi_1}^{n_1} (Q_1^{-1}Q_{\xi_2})^{n_2} (Q_1,q)_{n_1} (Q_1Q_2Q_3,q)_{n_1} (Q_2^{-1},q)_{n_2} (Q_3,q)_{n_2}}{(q,q)_{n_1}(q,q)_{n_2}(Q_1Q_2q^{-n_2},q)_{n_1}(Q_1^{-1}Q_2^{-1}q^{-n_1},q)_{n_2}}\,, \tag{6.35}$$

which is consistent with (6.33). We note that the Kähler parameters above the original lines have positive powers of $Q_iQ_j\cdots$ associated with positive masses, and the Kähler parameters below the corresponding original lines are given by negative power $Q_i^{-1}Q_j^{-1}\cdots$ with negative masses. Therefore, the assignment rule found in abelian theories discussed in section 6.2 is also applicable to nonabelian theories. For nonabelian theories, we need to draw more original lines.

The strings connecting two separate D3-branes give rise to the term

$$N_{\{n_j\}_A,\{n_i\}_A}\Big(\beta\frac{t}{q},t^{-1},q^{-1}\Big) = \Big(\beta t^{n_i},\frac{1}{t}\Big)_{n_j}\Big(\beta\frac{t}{q}\,q^{-n_j},\ t\Big)_{n_i}\,, \tag{6.36}$$

which in our context comes from $W_\pm$-bosons in 3d $\mathcal{N}=2$ nonabelian theories. Using the identity

$$(\alpha q^{-m},q)_n = \begin{cases} (\alpha,q)_{n-m}(\alpha q^{-1},q^{-1})_n & \text{if } n \geqslant m \\ (\alpha q^{-1},q^{-1})_n(\alpha q^{-1},q^{-1})_{m-n}^{-1} & \text{if } n < m \end{cases}\,, \tag{6.37}$$

we can split $W_\pm$ contributions into two parts

$$(\alpha q^{-m},q)_n(\alpha^{-1}q^{-n},q)_m \tag{6.38}$$

$$= \begin{cases} (\alpha^{-1}q^{-1},q^{-1})_m(\alpha q^{-1},q^{-1})_n \cdot (\alpha^{-1},q)_{m-n}(\alpha q^{-1},q^{-1})_{m-n}^{-1} & \text{if } m \geqslant n \\ (\alpha^{-1}q^{-1},q^{-1})_m(\alpha q^{-1},q^{-1})_n \cdot (\alpha,q)_{n-m}(\alpha^{-1}q^{-1},q^{-1})_{n-m} & \text{if } n > m \end{cases} \tag{6.39}$$

$$= \begin{cases} (\alpha^{-1}q^{-1},q^{-1})_m(\alpha q^{-1},q^{-1})_n \cdot \frac{(-\sqrt{q})^{(m-n)^2}(\sqrt{q}\alpha)^{n-m}(1-\alpha)}{1-\alpha q^{n-m}} & \text{if } m \geqslant n \\ (\alpha^{-1}q^{-1},q^{-1})_m(\alpha q^{-1},q^{-1})_n \cdot \frac{(-\sqrt{q})^{(m-n)^2}(\sqrt{q}\alpha^{-1})^{m-n}(1-\alpha^{-1})}{1-\alpha^{-1}q^{m-n}} & \text{if } n > m \end{cases}\,. \tag{6.40}$$

We can also set $Q_{m_1} = t\sqrt{\frac{t}{q}}\,, Q_{m_2} = t\sqrt{\frac{t}{q}}$ to obtain (t,t)-multiple brane amplitude, which is equivalent to the $(\bar{q},\bar{q})$-brane amplitude through discrete symmetry $q \to 1/t\,, t \to 1/q$ preserved in open topological strings. Therefore,

$$Z^{(\bar{q},\bar{q})\text{-brane}}(Q_1,Q_2) \xleftrightarrow{q\to 1/t\,,\ t\to 1/q} Z^{(t,t)\text{-brane}}(Q_1,Q_2)\,. \tag{6.41}$$

This discrete symmetry transposes the Young diagrams on open topological branes, hence we have symmetric Young tableaux $\{n_1\}_S$ and $\{n_2\}_S$ for (t,t)-brane. In (A.22), we show Young diagrams in this notation.

Now, we go to the quiver structure of this nonabelian theory. The terms from $W_\pm$-boson

can be expressed as follows in a shorthand notation

$$\frac{1}{(\beta q^{-n_1},q)_{n_2}} \to \left(\begin{array}{c|cccc} & n_1 & n_2 & d_i & d_j \\ \hline n_1 & & & -1 & -1 \\ n_2 & & & 1 & \\ d_i & -1 & 1 & 1 & \\ d_j & -1 & & & \end{array} , \left(\frac{\beta}{\sqrt{q}},\ \beta\right)\right), \tag{6.42}$$

which enables us to write (6.35) in a quiver form

$$Z^{(\bar{q},\bar{q})\text{-brane}}(Q_1,Q_2)|_{q=t} \simeq P_{C_{ij}}\left(Q_{\xi_1}, Q_1^{-1}Q_{\xi_2}, \frac{Q_1Q_2}{\sqrt{q}}, Q_1Q_2, \frac{Q_1^{-1}Q_2^{-1}}{\sqrt{q}}, Q_1^{-1}Q_2^{-1}, Q_1, Q_1Q_2Q_3, Q_2^{-1}, Q_3\right), \tag{6.43}$$

where quiver matrix C_{ij} reads

$$C_{ij} = \begin{array}{c|cccccccccc} & n_1 & n_2 & d_1 & d_2 & d_3 & d_4 & d_5 & d_6 & d_7 & d_8 \\ \hline n_1 & & -1 & -1 & -1 & 1 & & 1 & 1 & & \\ n_2 & -1 & & 1 & & -1 & -1 & & & 1 & 1 \\ \hline d_1 & -1 & 1 & 1 & & & & & & & \\ d_2 & -1 & & & & & & & & & \\ \hline d_3 & 1 & -1 & & & 1 & & & & & \\ d_4 & & -1 & & & & & & & & \\ \hline d_5 & 1 & & & & & & & & & \\ d_6 & 1 & & & & & & & & & \\ d_7 & & 1 & & & & & & & & \\ d_8 & & 1 & & & & & & & & \end{array} . \tag{6.44, 6.45}$$

The missing elements in C_{ij} are zero.

$U(2) + 3\mathbf{F} + 2\mathbf{AF}$

We illustrate the brane web of this theory in Figure 6.18. This web has three fundamental D5-branes, two antifundamental D5-branes and two D3-branes. These D3-branes can be located at any pair of fundamental D5-branes.

We locate D3-branes on the first and the third fundamental D5-branes as an example. The corresponding 3d brane web is shown in Figure 6.18. Note that in the 3d brane web, there is the freedom of flipping D5-branes up and down the original lines; which relates other phases of 3d brane webs. The effective CS level k^{eff} for the 3d brane web in Figure 6.18 is zero. We set

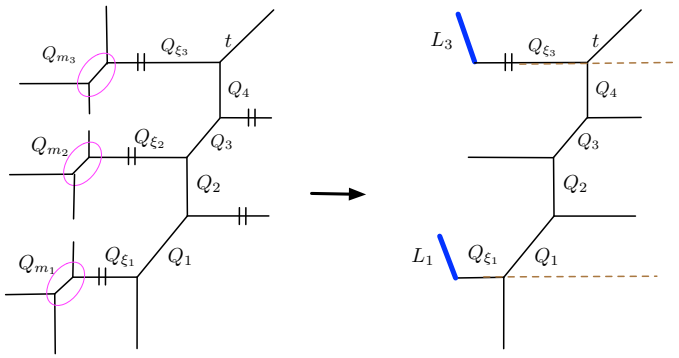

Figure 6.18: There are two original lines for two D3-branes. On the Higgs branch $\mathcal{M}_H$, we need to cut some internal lines in the 5d brane web. The effective Chern-Simons level for this brane web vanishes $k^{\text{eff}} = 0$, since the relative angle between NS5-brane and NS5'-brane is zero.

$Q_{m_1} = \frac{1}{q}\sqrt{\frac{t}{q}}, Q_{m_2} = \sqrt{\frac{t}{q}}, Q_{m_3} = \frac{1}{q}\sqrt{\frac{t}{q}}$ to obtain the $(\bar{q},\emptyset,\bar{q})$-multiple brane open amplitude

$$Z^{(\bar{q},\emptyset,\bar{q})\text{-brane}} = \sum_{n_1,n_3=0}^{\infty} \frac{(-\sqrt{t})^{-2n_1n_3}\left(\frac{Q_{\xi_1}}{Q_1}\sqrt{\frac{t}{q}}\right)^{n_1}\left(\frac{Q_{\xi_3}}{Q_3}\sqrt{\frac{q}{t}}\right)^{n_3}}{(t,t)_{n_1}(t,t)_{n_3}} \cdot \frac{\left(Q_1\sqrt{\frac{t}{q}},\ t\right)_{n_1}\left(Q_1Q_2Q_3\sqrt{\frac{t}{q}},\ t\right)_{n_1}\left(Q_4^{-1}\sqrt{\frac{t}{q}},\ t\right)_{n_3}\left(Q_2^{-1}Q_3^{-1}Q_4^{-1}\sqrt{\frac{t}{q}},\ t\right)_{n_3}}{\left(Q_1Q_2\frac{t}{q},\ t\right)_{n_1}\left(Q_3^{-1}Q_4^{-1}\frac{t}{q},\ t\right)_{n_3}\left(Q_1Q_2Q_3Q_4\frac{t}{q}\cdot t^{-n_3},\ t\right)_{n_1}\left(Q_1^{-1}Q_2^{-1}Q_3^{-1}Q_4^{-1}t^{-n_1},\ t\right)_{n_3}}. \tag{6.46}$$

It is more convenient to extract the corresponding quiver from its unrefined version by setting $q = t$

$$Z^{(\bar{q},\emptyset,\bar{q})\text{-brane}}|_{q=t} = \sum_{n_1,n_3=0}^{\infty} \frac{(-\sqrt{q})^{-2n_1n_3}\left(\frac{Q_{\xi_1}}{Q_1}\right)^{n_1}\left(\frac{Q_{\xi_3}}{Q_3}\right)^{n_3}}{(q,q)_{n_1}(q,q)_{n_3}} \cdot \frac{(Q_1,\ q)_{n_1}\left(Q_1Q_2Q_3,\ q\right)_{n_1}\left(Q_4^{-1},\ q\right)_{n_3}\left(Q_2^{-1}Q_3^{-1}Q_4^{-1},\ q\right)_{n_3}}{(Q_1Q_2,\ q)_{n_1}\left(Q_3^{-1}Q_4^{-1},\ q\right)_{n_3}\left(Q_1Q_2Q_3Q_4\cdot q^{-n_3},\ q\right)_{n_1}\left(Q_1^{-1}Q_2^{-1}Q_3^{-1}Q_4^{-1}t^{-n_1},\ q\right)_{n_3}}. \tag{6.47}$$

We can see there is already a mixed effective Chern-Simons level $-\delta_{1,3}$. Once again, one can see that the assignment rule for real mass parameters in section 6.2 also works in this example.

This partition function can be written in the form

$$Z^{(\bar{q},\emptyset,\bar{q})\text{-brane}}|_{q=t} \simeq P_{C_{ij}}\left(\frac{Q_{\xi_1}}{Q_1}, \frac{Q_{\xi_3}}{Q_3}, \frac{Q_{1,2,3}}{\sqrt{q}}, Q_{1,2,3}, \frac{Q_{1,2,3,4}^{-1}}{\sqrt{q}}, Q_{1,2,3,4}^{-1}, Q_1, Q_{1,2,3}, Q_4^{-1}, Q_{2,3,4}^{-1}, Q_{1,2}, Q_{3,4}^{-1}\right), \tag{6.48}$$

where we use shorthand notation $Q_{1,2,3,\dots} = Q_1 Q_2 Q_3 \cdots$, and the quiver matrix C_{ij} is

$$C_{ij} = \begin{array}{c} \\ n_1 \\ n_3 \\ d_1 \\ d_2 \\ d_3 \\ d_4 \\ d_5 \\ d_6 \\ d_7 \\ d_8 \\ d_9 \\ d_{10} \end{array} \begin{array}{c} \begin{array}{cccccccccccc} n_1 & n_3 & d_1 & d_2 & d_3 & d_4 & d_5 & d_6 & d_7 & d_8 & d_9 & d_{10} \end{array} \\ \left[\begin{array}{cccccccccccc} & -1 & -1 & -1 & 1 & & 1 & 1 & & & 1 & \\ -1 & & 1 & & -1 & -1 & & & 1 & 1 & & 1 \\ \hline -1 & 1 & 1 & & & & & & & & & \\ -1 & & & & & & & & & & & \\ \hline 1 & -1 & & & 1 & & & & & & & \\ & -1 & & & & & & & & & & \\ \hline 1 & & & & & & & & & & & \\ 1 & & & & & & & & & & & \\ & 1 & & & & & & & & & & \\ & 1 & & & & & & & & & & \\ \hline 1 & & & & & & & & & & 1 & \\ & 1 & & & & & & & & & & 1 \end{array}\right] \end{array} . \tag{6.50}$$

Here $n_1, n_3, d_1, \cdots d_{10}$ are degrees for variables $x_i^{d_i}$ in the quiver form $P_{C_{ij}}(x_i)$.

Ooguri-Vafa invariants

Recall that vortex partition functions for the abelian theory $U(1)_k + N_F \mathbf{F} + N_{AF} \mathbf{AF}$ can be written in terms of quiver generating series, and refined Ooguri-Vafa (OV) invariants are actually Donaldson-Thomas (DT) invariants

$$N_{Q_\beta}^{(j,r)} = \Omega_{d_1,\dots,d_m}^{(j,r)} , \tag{6.51}$$

where $Q_\beta = x_1^{d_1} \cdots x_m^{d_m}$, and $(d_1, \dots, d_m)$ is unique for each Q_β. However, for nonabelian theories the expansion variables in the quiver generating series (3.112) are not independent, for instance (6.43) and (6.48). In this case, Ooguri-Vafa invariants are linear combinations of DT-invariants

$$N_{Q_\beta}^{(j,r)} = \sum_{\{(d_1,\dots,d_m)\}} \Omega_{d_1,\dots,d_m}^{(j',r')} , \tag{6.52}$$

where $Q_\beta = x_1^{d_1} \cdots x_m^{d_m}$, and $(d_1, \dots, d_m)$ is not unique for each Q_β. One can use the refined formula (4.17) to extract refined DT invariants $\Omega_{d_1,\dots,d_m}^{(j,r)}$ encoded in $P_{C_{ij}}(x_i)$ and then impose the relations between variables x_i to obtain refined OV invariants $N_{Q_\beta}^{(j,r)}$.

Appendix A

Identities

A.1 Various identities

Refined MacMahon function can be written as

$$M(Q,t,q)=\prod_{i,j=1}^{\infty}(1-Q\ q^{i}t^{j-1})=\exp\left(-\sum_{n=1}^{\infty}\frac{Q^{n}\left(\frac{q}{t}\right)^{\frac{n}{2}}}{n(q^{\frac{n}{2}}-q^{-\frac{n}{2}})(t^{\frac{n}{2}}-t^{-\frac{n}{2}})}\right) \tag{A.1}$$

and satisfies relations

$$M(Q,q,t)=M(Q^{-1},t,q)=M\left(Q,t^{-1},q^{-1}\right)=M\Big(Qtq^{-1},t,q\Big)\,. \tag{A.2}$$

The plethystic exponent is very useful to extract BPS invariants through Gopakumar-Vafa formula and Ooguri-Vafa formula. It is defined as

$$\mathrm{PE}\big[f(a)\big]=\exp\left[\sum_{n=1}^{\infty}\frac{f(a^{n})}{n}\right] \tag{A.3}$$

and satisfies $\mathrm{PE}[f(a)]\cdot\mathrm{PE}[f(b)]=\mathrm{PE}[f(a)+f(b)]$.

Schur function has some useful properties:

$$s_{\mu}(q^{\rho})=q^{\frac{||\mu||^{2}-||\mu^{T}||^{2}}{2}}s_{\mu^{T}}(q^{\rho})\,,\quad s_{\nu/\lambda}(z)=\begin{cases}z^{|\nu|-|\lambda|} & \nu>\lambda\\ 0 & \text{others}\,.\end{cases} \tag{A.4}$$

Besides, there is a factor $\tilde{Z}_{\nu}(t,q)$ in topological partition functions, defined as follows

$$\tilde{Z}_{\nu}(t,q):=\prod_{(i,j)\in\nu}\left(1-q^{\nu_{i}-j}t^{\nu_{j}^{T}-i+1}\right)^{-1}\,, \tag{A.5}$$

$$||\tilde{Z}_{\mu}(t,q)||^{2}=||\tilde{Z}_{\mu^{T}}(q,t)||^{2}\,,\quad ||\tilde{Z}_{\mu}(t,q)||^{2}:=\tilde{Z}_{\mu^{T}}(t,q)\tilde{Z}_{\mu}(q,t)\,. \tag{A.6}$$

Nekrasov factors often appear in topological string partition functions. We summarize their

definitions and some formulas below

$$N_{\mu\nu}(Q;t,q) := \prod_{i,j=1}^{\infty} \frac{1-Q\ q^{\nu_i-j}\ t^{\mu_j^T-i+1}}{1-Q\ q^{-j}\ t^{-i+1}} \tag{A.7}$$

$$N_{\mu\nu}(Q;t,q) = \prod_{(i,j)\in\nu} \left(1-Q\ q^{\nu_i-j}\ t^{\mu_j^T-i+1}\right) \prod_{(i,j)\in\mu} \left(1-Q\ q^{-\mu_i+j-1}\ t^{-\nu_j^T+i}\right), \tag{A.8}$$

$$N_{\nu}^{\text{half},+}(Q;t,q) := N_{\emptyset\nu}(Q\sqrt{\frac{q}{t}},t,q), \tag{A.9}$$

$$N_{\nu}^{\text{half},-}(Q;t,q) := N_{\nu\emptyset}(Q\sqrt{\frac{q}{t}},t,q), \tag{A.10}$$

$$N_{\nu}^{\text{half},+}\left(Q;t^{-1},q^{-1}\right) = N_{\nu^T}^{\text{half},-}\left(Q;q^{-1},t^{-1}\right), \tag{A.11}$$

$$N_{\nu}^{\text{half},+}\left(Q;t^{-1},q^{-1}\right) = N_{\emptyset\nu}\left(Q\sqrt{\frac{t}{q}},t^{-1},q^{-1}\right), \tag{A.12}$$

$$N_{\nu}^{\text{half},-}\left(Q;t^{-1},q^{-1}\right) = N_{\nu\emptyset}\left(Q\sqrt{\frac{t}{q}},t^{-1},q^{-1}\right), \tag{A.13}$$

$$N_{\nu}^{\text{half},+}(Q,t^{-1},q^{-1}) = (-Q)^{|\nu|}t^{\frac{||\nu^T||^2}{2}}q^{\frac{-||\nu||^2}{2}}N_{\nu}^{\text{half},-}(Q^{-1},t^{-1},q^{-1}) \tag{A.14}$$

$$N_{\mu\nu}\left(Q;t,q\right) = N_{\nu^T\mu^T}\left(Q\frac{t}{q};q,t\right), \tag{A.15}$$

$$N_{\mu\nu}\left(Q;t^{-1},q^{-1}\right) = N_{\nu^T\mu^T}\left(Q\frac{q}{t};q^{-1},t^{-1}\right), \tag{A.16}$$

$$N_{\mu\nu}\left(Q\sqrt{\frac{t}{q}};t^{-1},q^{-1}\right) = N_{\nu^T\mu^T}\left(Q\sqrt{\frac{q}{t}};q^{-1},t^{-1}\right), \tag{A.17}$$

$$N_{\mu\nu}\left(Q^{-1}\sqrt{\frac{t}{q}};\frac{1}{t},\frac{1}{q}\right) = (-Q)^{-|\mu|-|\nu|}t^{-\frac{||\mu^T||^2}{2}+\frac{||\nu^T||^2}{2}}q^{\frac{||\mu||^2}{2}-\frac{||\nu||^2}{2}}N_{\nu^T\mu^T}\left(Q\sqrt{\frac{t}{q}};\frac{1}{t},\frac{1}{q}\right). \tag{A.18}$$

In particular, when Young diagrams are symmetric or antisymmetric, Nekrasov factors can be written in terms of q-Pochhammer products as follows:

$$N_{\{n_1\}_A,\{n_2\}_A}\left(Q;t^{-1},q^{-1}\right) = (Q\ t^{-n_1},t)_{n_2}(Qqt^{-1}\ t^{n_2},t^{-1})_{n_1}, \tag{A.19}$$

$$N_{\{n_1\}_S,\{n_2\}_S}\left(Q;t^{-1},q^{-1}\right) = (Qqt^{-1}q^{-n_2},q)_{n_1}(Q\ q^{n_1},q^{-1})_{n_2}, \tag{A.20}$$

$$N_{\{n\}_S,\{n\}_S}(Q,t,q) = (Qt,q)_n(Qq^{-n},q)_n, \tag{A.21}$$

where $\{n\}_S$ and and $\{n\}_A$ denote symmetric and anti-symmetric Young diagrams respectively

$$\{n\}_S := \quad \underbrace{\square\square\square\cdots\square}_{n}, \qquad \{n\}_A := \quad \begin{array}{|c|}\hline \\ \hline \\ \hline \vdots \\ \hline \\ \hline \end{array}\ . \tag{A.22}$$

For more details and notations, see e.g. [10, 36].

The q-Pochhammer product is extensively used in deriving quivers. It is defined as

$$(Q,q)_n := \prod_{k=0}^{n-1}(1-Qq^k)\,, \quad (q,q)_0 = 1\,, \quad (q,q)_1 = 1-q\,. \tag{A.23}$$

One can also define $(Q,q)_\infty = \prod_{k=0}^{\infty}(1-Qq^k)$. We summarize some useful identities below

$$(Q^{-1},q)_n = (Q,q^{-1})_n\ (-\sqrt{q})^{n^2}(\sqrt{q}Q)^{-n}\,, \tag{A.24}$$

$$(Qq^{-n},q)_n = (Qq^{-1},q^{-1})_n\,, \tag{A.25}$$

$$(Q,q)_{-n} = (Q\ q^{-n},q)_n{}^{-1} = (Q\ q^{-1},q^{-1})_n{}^{-1} = \frac{(-qQ^{-1})^n(\sqrt{q})^{n^2-n}}{(qQ^{-1},q)_n}\,, \tag{A.26}$$

$$\left(t^{-1},q^{-1}\right)_n = (-1)^n t^{-n} q^{\frac{n-n^2}{2}}(t;q)_n\,, \quad \left(q^{-1},q^{-1}\right)_n{}^{-1} = \frac{(-1)^n(\sqrt{q})^{n^2+n}}{(q,q)_n}\,, \tag{A.27}$$

$$\left(Qt^{-1},t^{-1}\right)_\infty = (Q,t)_\infty^{-1}\,, \tag{A.28}$$

$$\frac{1}{(Q,q)_\infty} = \sum_{n=0}^{\infty}\frac{Q^n}{(q,q)_n} = \exp\Big[\sum_{n=1}^{\infty}\frac{1}{n}\frac{Q^n}{1-q^n}\Big] =: \mathrm{PE}\Big[\frac{Q}{1-q}\Big]\,, \tag{A.29}$$

$$(Q,q)_\infty = \sum_{n=0}^{\infty}\frac{(-\sqrt{q})^{n^2}\left(\frac{Q}{\sqrt{q}}\right)^n}{(q,q)_n} = \exp\Big[-\sum_{n=1}^{\infty}\frac{1}{n}\frac{Q^n}{1-q^n}\Big] =: \mathrm{PE}\Big[-\frac{Q}{1-q}\Big]\,, \tag{A.30}$$

$$(\alpha,q)_n = \frac{(\alpha,q)_\infty}{(\alpha q^n,q)_\infty} = (\alpha,q)_\infty\sum_{d=0}^{\infty}(-\sqrt{q})^{2nd}\frac{\alpha^d}{(q,q)_d}\,, \tag{A.31}$$

$$\frac{1}{(\beta,q)_n} = \frac{(\beta q^n,q)_\infty}{(\beta,q)_\infty} = \frac{1}{(\beta,q)_\infty}\sum_{d=0}^{\infty}(-\sqrt{q})^{2nd+d^2}\frac{\beta^d}{(q,q)_d}\,, \tag{A.32}$$

$$\frac{1}{(\beta q^{-n_1},q)_{n_2}} = \frac{(\beta q^{n_2-n_1},q)_\infty}{(\beta q^{-n_1},q)_\infty} = \sum_{d_i,d_j=0}^{\infty}(-\sqrt{q})^{d_i^2+2(n_2-n_1)d_i-2n_1d_j}\frac{\left(\frac{\beta}{\sqrt{q}}\right)^{d_i}\beta^{d_j}}{(q,q)_{d_i}(q,q)_{d_j}}\,, \tag{A.33}$$

$$\frac{M(Q;t,q)}{M(tQ;t,q)} = \prod_{i=0}^{\infty}(1-Qq\ q^i) = (Qq;q)_\infty\,, \quad \frac{M(Q;t,q)}{M(qQ;t,q)} = \prod_{i=0}^{\infty}(1-Qq\ t^i) = (Qq;t)_\infty\,. \tag{A.34}$$

A.2 Double-sine function

The double-sine function is defined as

$$s_b(x) = \prod_{m,n\geq 0}\frac{m\,b+n/b+Q/2-i\,x}{m\,b+n/b+Q/2+i\,x}\,, \qquad Q = b+\frac{1}{b}\,, \tag{A.35}$$

and it satisfies $s_b(x)\,s_b(-x) = 1$. The equivariant parameter q in localization is defined as

$$q = e^{\hbar} = e^{2\pi\,i\,b^2} = e^{2\pi\,i\,b\,Q}\,, \quad \hbar = 2\pi\,i\,b^2 = 2\pi\,i\,b\,Q\,. \tag{A.36}$$

In the asymptotic limit $b \to 0$ the double-sine function is

$$s_b(z) \to e^{-i\,\pi\,z^2/2} e^{i\,\pi(2-Q^2)/24} \exp\left(\frac{1}{2\pi\,i\,b^2}\mathrm{Li}_2(e^{2\pi b z})\right)\,, \tag{A.37}$$

where $\mathrm{Li}_2(z)$ is the polylogarithm function defined by a power series

$$\mathrm{Li}_s(z) := \sum_{k=1}^{\infty} \frac{z^k}{k^s}\,. \tag{A.38}$$

In the decompactification limit $R \to +\infty$, the effective superpotentials of 3d $\mathcal{N} = 2$ gauge theories on spacetime $\mathbb{R}^2 \times S^1_R$ involve

$$\lim_{R\to+\infty} \frac{\mathrm{Li}_2\big(e^{-R\,x}\big)}{R^2} = \frac{[\![x]\!]^2}{2}\,, \qquad [\![x]\!]^2 := \theta(-x)\cdot x = \begin{cases} 0 & x > 0\,, \\ x & x < 0\,, \end{cases} \tag{A.39}$$

where $[\![x]\!]^2$ is defined in [64] and $\theta(x)$ is Heaviside step function. The derivative of $\mathrm{Li}_2(y)$ is

$$\exp\left(y\frac{d\,\mathrm{Li}_2(y)}{d\,y}\right) = \frac{1}{1-y}\,. \tag{A.40}$$

A.3 Integral formula

When performing mirror transformations, we use the higher dimensional Gaussian integral formula

$$\int \mathrm{d}\,\mathbf{x}\,\exp\Big(-\frac{1}{2}\,\mathbf{x}\cdot\mathbf{A}\cdot\mathbf{x} + \mathbf{J}\cdot\mathbf{x}\Big) = \sqrt{\frac{(2\pi)^n}{\det\mathbf{A}}}\,\exp\Big(\frac{1}{2}\,\mathbf{J}\cdot\mathbf{A}^{-1}\cdot\mathbf{J}\Big)\,,\quad \text{only if}\ \ \det\mathbf{A} \neq 0\,. \tag{A.41}$$

In addition, the Dirac delta function $\delta(k) = \frac{1}{2\pi}\int dx\, e^{i\,kx}$ is also useful.

A.4 Open BPS invariants

In this section, we show the refined Ooguri-Vafa invariants for several strip Calabi-Yau threefolds.

$d=1,\ (d_0,d_1)$	$2r$	$2s=1$
$(1,0)$	1	1

$d=2,\ (d_0,d_1)$	$2r$	$2s=3$
$(1,1)$	3	1

$d=3,\ (d_0,d_1)$	$2r$	$2s=5$
$(2,1),(1,2)$	5	1

$d=4,\ (d_0,d_1)$	$2r$	$2s=7$	9
$(3,1),(1,3)$	7	1	
$(2,2)$	7	1	1

$d=5,\ (d_0,d_1)$	$2r$	$2s=9$	11	13
$(4,1),(1,4)$	9	1		
$(2,3),(3,2)$	9	1	1	1

$d=6,\ (d_0,d_1)$	$2r$	$2s=11$	13	15	17	19
$(5,1),(1,5)$	11	1				
$(4,2),(2,4)$	11	2	2	1	1	
$(3,3)$	11	3	3	3	1	1

$d=7,\ (d_0,d_1)$	$2r$	$2s=13$	15	17	19	21	23	25
$(6,1),(1,6)$	13	1						
$(5,2),(2,5)$	13	2	2	1	1			
$(4,3),(3,4)$	13	5	5	6	4	3	1	1

$d=8,\ (d_0,d_1)$	$2r$	$2s=15$	17	19	21	23	25	27	29	31	33
$(7,1),(1,7)$	15	1									
$(6,2),(2,6)$	15	3	3	2	2	1	1				
$(5,3),(3,5)$	15	7	8	10	8	7	4	3	1	1	
$(4,4)$	15	8	12	14	14	10	8	5	3	1	1

$d=9,\ (d_0,d_1)$	$2r$	$2s=17$	19	21	23	25	27	29	31	33	35	37	39	41
$(8,1),(1,8)$	17	1												
$(7,2),(2,7)$	17	4	3	3	2	2	1	1						
$(6,3),(3,6)$	17	9	12	15	13	13	9	7	4	3	1	1		
$(5,4),(4,5)$	17	14	21	30	30	29	22	19	12	9	5	3	1	1

Table A.1: Refined open BPS invariants for the geometry $\mathbb{C}^3/\mathbb{Z}_2$ in Figure. 4.8 (b). (d_0,d_1) are degrees for the term $Q^{d_0}Q_1^{d_1}$.

$d=1,\ (d_0,d_1,d_2)$	$2r$	$2s=0$
$(1,0,0)$	0	1

$d=2,\ (d_0,d_1,d_2)$	$2r$	$2s=1$
$(1,1,0)$	1	1

$d=3,\ (d_0,d_1,d_2)$	$2r$	$2s=2$
$(1,1,1)$	2	1

$d=4,\ (d_0,d_1,d_2)$	$2r$	$2s=3$
$(1,2,1)$	3	1

$d=5,\ (d_0,d_1,d_2)$	$2r$	$2s=4$
$(2,2,1),(1,2,2)$	4	1

$d=6,\ (d_0,d_1,d_2)$	$2r$	$2s=5$
$(2,3,1),(2,2,2),(1,3,2)$	5	1

$d=7,\ (d_0,d_1,d_2)$	$2r$	$2s=6$	8
$(3,3,1),(1,3,3)$	6	1	
$(2,3,2)$	6	2	1

$d=8,\ (d_0,d_1,d_2)$	$2r$	$2s=7$	9
$(3,4,1),(1,4,3)$	7	1	
$(3,3,2),(2,4,2),(2,3,3)$	7	1	1

$d=9,\ (d_0,d_1,d_2)$	$2r$	$2s=8$	10	12
$(4,4,1),(1,4,4)$	8	1		
$(3,3,3)$	8		1	
$(3,4,2),(2,4,3)$	8	3	2	1

$d=10,\ (d_0,d_1,d_2)$	$2r$	$2s=9$	11	13	15
$(4,5,1),(1,5,4)$	9	1			
$(4,4,2),(3,5,2),(2,5,3),(2,4,4)$	9	2	1	1	
$(3,4,3)$	9	3	4	2	1

$d=11,\ (d_0,d_1,d_2)$	$2r$	$2s=10$	12	14	16	18
$(5,5,1),(1,5,5)$	10	1				
$(4,4,3),(3,4,4)$	10	1	2	1	1	
$(4,5,2),(2,5,4)$	10	4	3	2	1	
$(3,5,3)$	10	6	6	5	2	1

$d=12,\ (d_0,d_1,d_2)$	$2r$	$2s=11$	13	15	17	19	21
$(5,5,1),(1,5,5)$	11	1					
$(4,4,4)$	11		1		1		
$(5,5,2),(4,6,2),(2,6,4),(2,5,5)$	11	2	2	1	1		
$(3,6,3)$	11	3	3	3	1	1	
$(4,5,3),(3,5,4)$	11	6	9	7	5	2	1

Table A.2: Refined open BPS invariants for a double-$\mathbb{P}^1$ strip geometry in Figure. 4.10 (a). (d_0,d_1,d_2) are degrees corresponding to the term $z^{d_0}Q_1^{d_1}Q_2^{d_2}$.

$d=1,\ (d_0,d_1,d_2,d_3)$	$2r$	$2s=0$
$(1,0,0,0)$	0	1

$d=2,\ (d_0,d_1,d_2,d_3)$	$2r$	$2s=1$
$(1,1,0,0)$	1	1

$d=3,\ (d_0,d_1,d_2,d_3)$	$2r$	$2s=2$
$(1,1,1,0)$	2	1

$d=4,\ (d_0,d_1,d_2,d_3)$	$2r$	$2s=1$	3
$(1,1,1,1)$	1	1	
$(1,2,1,0)$	3		1

$d=5,\ (d_0,d_1,d_2,d_3)$	$2r$	$2s=2$	4
$(1,2,1,1)$	2	1	
$(2,2,1,0),(1,2,2,0)$	4		1

$d=6,\ (d_0,d_1,d_2,d_3)$	$2r$	$2s=3$	5
$(2,2,1,1),(1,2,2,1)$	1	1	
$(2,3,2,0),(2,2,2,0),(1,3,2,0)$	1		1

$d=7,\ (d_0,d_1,d_2,d_3)$	$2r$	$2s=4$	6	8
$(2,3,1,1),(2,2,2,1),(1,3,2,1)$	4	1		
$(3,3,1,0),(1,3,3,0)$	6		1	
$(2,3,2,0)$	6		1	1

$d=8,\ (d_0,d_1,d_2,d_3)$	$2r$	$2s=5$	7	9
$(1,3,3,1),(3,3,1,1)$	5	1		
$(2,3,2,1)$	5	3	1	
$(1,4,3,0),(3,4,1,0)$	7		1	
$(2,3,3,0),(2,4,2,0),(3,3,2,0)$	7		1	1

$d=9,\ (d_0,d_1,d_2,d_3)$	$2r$	$2s=4$	6	8	10	12
$(2,3,2,2)$	4	1				
$(1,4,3,1),(3,4,1,1)$	6		1			
$(2,3,3,1),(2,4,2,1),(3,3,2,1)$	6		2	1		
$(1,4,4,0),(4,4,1,0)$	8			1		
$(3,3,3,0)$	8				1	
$(2,4,3,0),(3,4,2,0)$	8			3	2	1

$d=10,\ (d_0,d_1,d_2,d_3)$	$2r$	$2s=5$	7	9	11	13	15
$(2,3,3,2),(2,4,2,2),(3,3,2,2)$	5	1					
$(1,4,4,1),(4,4,1,1)$	7		1				
$(3,3,3,1)$	7		1	1			
$(2,4,3,1),(3,4,2,1)$	7		5	3	1		
$(1,5,4,0),(4,5,1,0)$	9			1			
$(2,4,4,0),(2,5,3,0),(3,5,2,0),(4,4,2,0)$	9			2	1	1	
$(3,4,3,0)$	9			3	4	2	1

$d=11,\ (d_0,d_1,d_2,d_3)$	$2r$	$2s=6$	8	10	12	14	16	18
$(3,3,3,2)$	6	1						
$(2,4,3,2),(3,4,2,2)$	6	2	1					
$(1,5,4,1),(4,5,1,1)$	8		1					
$(2,4,4,1),(2,5,3,1),(3,5,2,1),(4,4,2,1)$	8		3	2	1			
$(3,4,3,1)$	8		7	7	3	1		
$(1,5,5,0),(5,5,1,0)$	10			1				
$(3,4,4,0),(4,4,3,0)$	10			1	2	1	1	
$(2,5,4,0),(4,5,2,0)$	10			4	3	2	1	
$(3,5,2,0)$	10			6	6	5	2	1

Table A.3: Open refined BPS invariants for the triple-$\mathbb{P}^1$ strip geometry in Figure. 4.12.

(d_1, d_3, d_B, d_F)	$2r \setminus 2s$	0
$(0, 1, 0, 0)$	0	1

(d_1, d_3, d_B, d_F)	$2r \setminus 2s$	1
$(1, 1, 0, 0)$	1	1

(d_1, d_3, d_B, d_F)	$2r \setminus 2s$	1
$(1, 1, 1, 0), (1, 1, 0, 1)$	1	1

$(d_1, d_2, d_3, d_B, d_F)$	$2r \setminus 2s$	-1	1	3
$(2, 0, 1, 0, 1)$	1		1	
$(1, 0, 1, 1, 1)$	-1	1		
	1		1	
	3			1

$(d_1, d_2, d_3, d_B, d_F)$	$2r \setminus 2s$	-3	-1	0	1	3	5
$(2, 0, 1, 1, 1)$	0			1			
	1				1		
$(2, 1, 1, 0, 1), (2, 0, 2, 1, 0)$	3					1	
$(1, 1, 1, 1, 1)$	0			1			
	1				1		
$(1, 0, 1, 1, 2), (1, 0, 1, 2, 1)$	-3	1					
	-1		1				
	1				1		
	3					1	
	5						1

$(d_1, d_2, d_3, d_B, d_F)$	$2r \setminus 2s$	-7	-6	-5	-4	-3	-2	-1	0	1	2	3	4	5	6	7	8	9
$(2, 1, 1, 1, 1)$	1									1								
$(2, 0, 2, 1, 1)$	3											1						
$(2, 1, 1, 0, 2)$	3											1						
$(3, 0, 2, 0, 1)$	4												1					
$(2, 1, 2, 0, 1)$																		
$(2, 0, 1, 1, 2)$	-2						1											
$(2, 0, 1, 2, 1)$	0								1									
$(1, 1, 1, 1, 2)$	2										1							
$(1, 1, 1, 2, 1)$	4												1					
$(1, 0, 1, 1, 3)$	-5			1														
$(1, 0, 1, 3, 1)$	-3					1												
	-1							1										
	1									1								
	3											1						
	5													1				
	7															1		
$(1, 0, 1, 2, 2)$	-7			1														
	-5	1		2		1												
	-3			1		3		1										
	-1					1		3		1								
	1							1		3		1						
	3									1		3		1				
	5											1		3		1		
	7													1		2		1
	9															1		

Table A.4: Refined open BPS invariants for Hirzebruch surface $\mathbb{F}_0^2$ with a Lagrangian brane. d_3 is the degree for open Kähler parameter Q_3.

(d_1, d_B, d_F)	$2r\backslash 2s$	-7	-5	-3	-1	1	3	5	7	9
$(1,4,2)$	-7		1							
	-5	1	2	1						
	-3		1	4	1					
	-1			1	4	1				
	1				1	4	1			
	3					1	4	1		
	5						1	4	1	
	7							1	3	1
	9								1	1

(d_1, d_B, d_F)	$2r\backslash 2s$	-5	-3	-1	1	3	5	7	9	11
$(2,4,2)$	-5		1							
	-3	1	2	1						
	-1			5	2					
	1				6	2				
	3					6	2			
	5						6	2		
	7							5	2	
	9								3	1
	11									1

(d_1, d_B, d_F)	$2r\backslash 2s$	-5	-3	-1	1	3	5	7	9	11
$(1,4,3)$	-5	1	1							
	-3	1	3	1						
	-1		1	5	1					
	1			1	5	1				
	3				1	5	1			
	5					1	5	1		
	7						1	5	1	
	9							1	3	1
	11								1	1

(d_1, d_B, d_F)	$2r\backslash 2s$	-11	-9	-7	-5	-3	-1	1	3	5	7	9	11	13
$(1,5,2)$	-11			1										
	-9		1	2	1									
	-7	1	2	4	3	1								
	-5		1	3	7	3	1							
	-3			1	3	8	3	1						
	-1				1	3	8	3	1					
	1					1	3	8	3	1				
	3						1	3	8	3	1			
	5							1	3	8	3	1		
	7								1	3	7	3	1	
	9									1	3	5	2	1
	11										1	2	2	
	13											1		

Table A.5: Open BPS invariants for Hirzebruch surface $\mathbb{F}_2$, with Q_1 playing the role of open Kähler parameter. The open strings winding around the compact divisor(with the length $Q_1 Q_B^4 Q_F^2$), have degrees at least $(1,4,2)$.

Bibliography

[1] S. H. Katz, A. Klemm, and C. Vafa, *Geometric engineering of quantum field theories*, *Nucl. Phys. B* **497** (1997) 173–195, [hep-th/9609239].

[2] N. C. Leung and C. Vafa, *Branes and toric geometry*, *Adv.Theor.Math.Phys.* **2** (1998) 91–118, [hep-th/9711013].

[3] R. Gopakumar and C. Vafa, *M theory and topological strings. 1.*, hep-th/9809187.

[4] R. Gopakumar and C. Vafa, *M theory and topological strings. 2.*, hep-th/9812127.

[5] A. Iqbal, *All genus topological string amplitudes and five-brane webs as Feynman diagrams*, hep-th/0207114.

[6] T. Dimofte, S. Gukov, and L. Hollands, *Vortex Counting and Lagrangian 3-manifolds*, *Lett. Math. Phys.* **98** (2011) 225–287, [arXiv:1006.0977].

[7] R. Gopakumar and C. Vafa, *On the gauge theory / geometry correspondence*, *AMS/IP Stud. Adv. Math.* **23** (2001) 45–63, [hep-th/9811131].

[8] M. Aganagic, M. Marino, and C. Vafa, *All loop topological string amplitudes from Chern-Simons theory*, *Commun.Math.Phys.* **247** (2004) 467–512, [hep-th/0206164].

[9] M. Aganagic, A. Klemm, M. Marino, and C. Vafa, *The Topological vertex*, *Commun.Math.Phys.* **254** (2005) 425–478, [hep-th/0305132].

[10] S. Cheng and P. Sułkowski, *Refined open topological strings revisited*, arXiv:2104.00713.

[11] S. Cheng, *Mirror symmetry and mixed Chern-Simons levels for Abelian 3D N=2 theories*, *Phys. Rev. D* **104** (2021), no. 4 046011, [arXiv:2010.15074].

[12] S. Cheng, *3d $\mathcal{N} = 2$ Brane Webs and Quivers*, arXiv:2108.03696.

[13] E. Witten, *Mirror manifolds and topological field theory*, *AMS/IP Stud. Adv. Math.* **9** (1998) 121–160, [hep-th/9112056].

[14] H. Ooguri and C. Vafa, *Knot invariants and topological strings*, *Nucl. Phys.* **B577** (2000) 419–438, [hep-th/9912123].

[15] E. Witten, *Phases of N=2 theories in two-dimensions*, *Nucl. Phys. B* **403** (1993) 159–222, [hep-th/9301042].

[16] A. Neitzke and C. Vafa, *Topological strings and their physical applications*, hep-th/0410178.

[17] M. Vonk, *A Mini-course on topological strings*, hep-th/0504147.

[18] K. Hori and C. Vafa, *Mirror symmetry*, hep-th/0002222.

[19] K. Hori, S. Katz, A. Klemm, R. Pandharipande, R. Thomas, C. Vafa, R. Vakil, and E. Zaslow, *Mirror Symmetry*. Clay Mathematics Monographs. American Mathematical Society, United States, 2003. With a preface by Vafa.

[20] N. A. Nekrasov and S. L. Shatashvili, *Supersymmetric vacua and Bethe ansatz*, *Nucl. Phys. Proc. Suppl.* **192-193** (2009) 91–112, [arXiv:0901.4744].

[21] P. Candelas, X. C. De La Ossa, P. S. Green, and L. Parkes, *A pair of calabi-yau manifolds as an exactly soluble superconformal theory*, *Nuclear Physics B* **359** (1991), no. 1 21–74.

[22] H. Ooguri, Y. Oz, and Z. Yin, *D-branes on Calabi-Yau spaces and their mirrors*, *Nucl. Phys. B* **477** (1996) 407–430, [hep-th/9606112].

[23] K. Hori, A. Iqbal, and C. Vafa, *D-branes and mirror symmetry*, hep-th/0005247.

[24] M. Aganagic and C. Vafa, *Mirror symmetry, D-branes and counting holomorphic discs*, hep-th/0012041.

[25] M. Bershadsky, S. Cecotti, H. Ooguri, and C. Vafa, *Kodaira-Spencer theory of gravity and exact results for quantum string amplitudes*, *Commun. Math. Phys.* **165** (1994) 311–428, [hep-th/9309140].

[26] C. Closset, *Toric geometry and local Calabi-Yau varieties: An Introduction to toric geometry (for physicists)*, arXiv:0901.3695.

[27] O. Aharony, A. Hanany, and B. Kol, *Webs of (p,q) five-branes, five-dimensional field theories and grid diagrams*, *JHEP* **01** (1998) 002, [hep-th/9710116].

[28] M. Aganagic, A. Klemm, and C. Vafa, *Disk instantons, mirror symmetry and the duality web*, *Z. Naturforsch.* **A57** (2002) 1–28, [hep-th/0105045].

[29] O. Aharony and A. Hanany, *Branes, superpotentials and superconformal fixed points*, *Nucl.Phys.B* **504** (1997) 239–271, [hep-th/9704170].

[30] A. Iqbal, C. Kozcaz, and C. Vafa, *The Refined topological vertex*, *JHEP* **10** (2009) 069, [hep-th/0701156].

[31] E. Witten, *Chern-Simons gauge theory as a string theory*, *Prog. Math.* **133** (1995) 637–678, [hep-th/9207094].

[32] N. A. Nekrasov, *Seiberg-Witten prepotential from instanton counting*, *Adv. Theor. Math. Phys.* **7** (2003), no. 5 831–864.

[33] N. Nekrasov and A. Okounkov, *Seiberg-Witten theory and random partitions*, *Prog. Math.* **244** (2006) 525–596, [hep-th/0306238].

[34] M. Aganagic and S. Shakirov, *Refined Chern-Simons Theory and Topological String*, arXiv:1210.2733.

[35] S.-S. Kim and F. Yagi, *Topological vertex formalism with O5-plane*, *Phys. Rev.* **D97** (2018) 026011, [arXiv:1709.01928].

[36] S. Cheng and S.-S. Kim, *Refined topological vertex for a 5d $Sp(N)$ gauge theories with antisymmetric matter*, *Phys. Rev. D* **104** (2021), no. 086004 [arXiv:1809.00629].

[37] H. Awata and H. Kanno, *Instanton counting, Macdonald functions and the moduli space of D-branes*, *JHEP* **0505** (2005) 039, [hep-th/0502061].

[38] L. Bao, V. Mitev, E. Pomoni, M. Taki, and F. Yagi, *Non-Lagrangian Theories from Brane Junctions*, *JHEP* **1401** (2014) 175, [arXiv:1310.3841].

[39] H.-C. Kim, S.-S. Kim, and K. Lee, *5-dim Superconformal Index with Enhanced En Global Symmetry*, *JHEP* **1210** (2012) 142, [arXiv:1206.6781].

[40] H. Hayashi, H.-C. Kim, and T. Nishinaka, *Topological strings and 5d T_N partition functions*, *JHEP* **1406** (2014) 014, [arXiv:1310.3854].

[41] S.-S. Kim, M. Taki, and F. Yagi, *Tao Probing the End of the World*, *PTEP* **2015** (2015), no. 8 083B02, [arXiv:1504.03672].

[42] https://github.com/ShiChengUW/schurcancellation.

[43] K. A. Intriligator and N. Seiberg, *Mirror symmetry in three-dimensional gauge theories*, *Phys. Lett.* **B387** (1996) 513–519, [hep-th/9607207].

[44] O. Aharony, A. Hanany, K. Intriligator, N. Seiberg, and M. J. Strassler, *Aspects of n=2 supersymmetric gauge theories in three dimensions*, *Nucl.Phys.B* **499** (1997) 67–99, [hep-th/9703110].

[45] K. Intriligator and N. Seiberg, *Aspects of 3d N=2 Chern-Simons-Matter Theories*, *JHEP* **07** (2013) 079, [arXiv:1305.1633].

[46] O. Aharony, *IR duality in d = 3 N=2 supersymmetric USp(2N(c)) and U(N(c)) gauge theories*, *Phys. Lett. B* **404** (1997) 71–76, [hep-th/9703215].

[47] A. Giveon and D. Kutasov, *Seiberg Duality in Chern-Simons Theory*, *Nucl. Phys. B* **812** (2009) 1–11, [arXiv:0808.0360].

[48] L. F. Alday, D. Gaiotto, S. Gukov, Y. Tachikawa, and H. Verlinde, *Loop and surface operators in N=2 gauge theory and Liouville modular geometry*, *JHEP* **01** (2010) 113, [arXiv:0909.0945].

[49] D. R. Morrison and N. Seiberg, *Extremal transitions and five-dimensional supersymmetric field theories*, *Nucl.Phys.* **B483** (1997) 229–247, [hep-th/9609070].

[50] M. R. Douglas, S. H. Katz, and C. Vafa, *Small instantons, Del Pezzo surfaces and type I-prime theory*, *Nucl.Phys.* **B497** (1997) 155–172, [hep-th/9609071].

[51] O. J. Ganor, D. R. Morrison, and N. Seiberg, *Branes, Calabi-Yau spaces, and toroidal compactification of the N=1 six-dimensional E(8) theory*, *Nucl. Phys.* **B487** (1997) 93–127, [hep-th/9610251].

[52] K. A. Intriligator, D. R. Morrison, and N. Seiberg, *Five-dimensional supersymmetric gauge theories and degenerations of Calabi-Yau spaces*, *Nucl.Phys.* **B497** (1997) 56–100, [hep-th/9702198].

[53] N. Dorey and D. Tong, *Mirror symmetry and toric geometry in three-dimensional gauge theories*, *JHEP* **05** (2000) 018, [hep-th/9911094].

[54] N. Nekrasov, *Five dimensional gauge theories and relativistic integrable systems*, *Nucl. Phys.* **B531** (1998) 323–344, [hep-th/9609219].

[55] N. A. Nekrasov, *Seiberg-Witten prepotential from instanton counting*, *Adv.Theor.Math.Phys.* **7** (2004) 831–864, [hep-th/0206161].

[56] N. A. Nekrasov and S. L. Shatashvili, *Quantization of Integrable Systems and Four Dimensional Gauge Theories*, in *Proceedings, 16th International Congress on Mathematical Physics (ICMP09): Prague, Czech Republic, August 3-8, 2009*, pp. 265–289, 2009. arXiv:0908.4052.

[57] T. Dimofte, D. Gaiotto, and S. Gukov, *Gauge Theories Labelled by Three-Manifolds*, *Commun. Math. Phys.* **325** (2014) 367–419, [arXiv:1108.4389].

[58] T. Dimofte, D. Gaiotto, and S. Gukov, *3-manifolds and 3d indices*, arXiv:1112.5179.

[59] A. Gadde, S. Gukov, and P. Putrov, *Walls, lines, and spectral dualities in 3d gauge theories*, *Journal of High Energy Physics* **2014** (May, 2014).

[60] M. Yamazaki, *Quivers, YBE and 3-manifolds*, *JHEP* **1205** (2012) 147, [arXiv:1203.5784].

[61] S. Shadchin, *On F-term contribution to effective action*, *Journal of High Energy Physics* **2007** (Aug, 2007) 052–052, [hep-th/0611278].

[62] H. Nakajima and K. Yoshioka, *Instanton counting on blowup. i. 4-dimensional pure gauge theory*, *Inventiones mathematicae* **162** (Jun, 2005) 313–355, [math/0306198].

[63] N. A. Nekrasov and S. L. Shatashvili, *Quantum integrability and supersymmetric vacua*, *Prog. Theor. Phys. Suppl.* **177** (2009) 105–119, [arXiv:0901.4748].

[64] H. Hayashi, S.-S. Kim, K. Lee, and F. Yagi, *Complete prepotential for 5d $\mathcal{N} = 1$ superconformal field theories*, *JHEP02(2020)074* (12, 2019) [arXiv:1912.10301].

[65] A. Kapustin and M. J. Strassler, *On mirror symmetry in three-dimensional Abelian gauge theories*, *JHEP* **04** (1999) 021, [hep-th/9902033].

[66] E. Witten, *SL(2,Z) action on three-dimensional conformal field theories with Abelian symmetry*, hep-th/0307041.

[67] S. Benvenuti and S. Pasquetti, *3d $\mathcal{N} = 2$ mirror symmetry, pq-webs and monopole superpotentials*, *JHEP* **08** (2016) 136, [arXiv:1605.02675].

[68] V. Pestun, *Localization of gauge theory on a four-sphere and supersymmetric Wilson loops*, *Commun. Math. Phys.* **313** (2012) 71–129, [arXiv:0712.2824].

[69] N. Hama, K. Hosomichi, and S. Lee, *SUSY Gauge Theories on Squashed Three-Spheres*, *JHEP* **05** (2011) 014, [arXiv:1102.4716].

[70] A. Kapustin, B. Willett, and I. Yaakov, *Exact Results for Wilson Loops in Superconformal Chern-Simons Theories with Matter*, *JHEP* **03** (2010) 089, [arXiv:0909.4559].

[71] A. Hanany and E. Witten, *Type IIB superstrings, BPS monopoles, and three-dimensional gauge dynamics*, *Nucl.Phys.* **B492** (1997) 152–190, [hep-th/9611230].

[72] J. Polchinski, *Tasi lectures on D-branes*, in *Theoretical Advanced Study Institute in Elementary Particle Physics (TASI 96): Fields, Strings, and Duality*, pp. 293–356, 11, 1996. hep-th/9611050.

[73] A. Giveon and D. Kutasov, *Brane Dynamics and Gauge Theory*, *Rev. Mod. Phys.* **71** (1999) 983–1084, [hep-th/9802067].

[74] R. Blumenhagen, D. Lüst, and S. Theisen, *Basic concepts of string theory*. Theoretical and Mathematical Physics. Springer, Heidelberg, Germany, 2013.

[75] R.-K. Seong, *Brane dynamics and supersymmetric gauge theories*, *a spring course in YMSC* (2018).

[76] C. Vafa, *Evidence for F theory*, *Nucl. Phys. B* **469** (1996) 403–418, [hep-th/9602022].

[77] D. R. Morrison and C. Vafa, *Compactifications of F theory on Calabi-Yau threefolds. 1*, *Nucl. Phys. B* **473** (1996) 74–92, [hep-th/9602114].

[78] D. R. Morrison and C. Vafa, *Compactifications of F theory on Calabi-Yau threefolds. 2.*, *Nucl.Phys.* **B476** (1996) 437–469, [hep-th/9603161].

[79] J. de Boer, K. Hori, Y. Oz, and Z. Yin, *Branes and mirror symmetry in n=2 supersymmetric gauge theories in three dimensions*, *Nucl.Phys.B* **502** (1997) 107–124, [hep-th/9702154].

[80] S. Pasquetti, *Factorisation of N = 2 Theories on the Squashed 3-Sphere*, *JHEP* **04** (2012) 120, [arXiv:1111.6905].

[81] C. Kozçaz, S. Pasquetti, and N. Wyllard, *A& b model approaches to surface operators and toda thoeries*, *Journal of High Energy Physics* **2010** (aug, 2010).

[82] C. Kozcaz, S. Pasquetti, and N. Wyllard, *A \& B model approaches to surface operators and Toda theories*, *JHEP* **08** (2010) 042, [arXiv:1004.2025].

[83] P. Kucharski, M. Reineke, M. Stosic, and P. Sułkowski, *BPS states, knots and quivers*, *Phys. Rev.* **D96** (2017), no. 12 121902, [arXiv:1707.02991].

[84] P. Kucharski, M. Reineke, M. Stosic, and P. Sułkowski, *Knots-quivers correspondence*, *Adv. Theor. Math. Phys.* **23** (2019) 1849–1902, [arXiv:1707.04017].

[85] M. Panfil and P. Sułkowski, *Topological strings, strips and quivers*, *JHEP* **01** (2019) 124, [arXiv:1811.03556].

[86] T. Kimura, M. Panfil, Y. Sugimoto, and P. Sułkowski, *Branes, quivers and wave-functions*, *SciPost Phys.* **10** (11, 2021) 51, [arXiv:2011.06783].

[87] M. Kontsevich and Y. Soibelman, *Cohomological Hall algebra, exponential Hodge structures and motivic Donaldson-Thomas invariants*, *Commun. Num. Theor. Phys.* **5** (2011) 231–352, [arXiv:1006.2706].

[88] A. I. Efimov, *Cohomological Hall algebra of a symmetric quiver*, *Compositio Mathematica* **148** (2012), no. 4 1133–1146, [arXiv:1103.2736].

[89] M. Kameyama and S. Nawata, *Refined large N duality for torus knots*, arXiv:1703.05408.

[90] A. Nedelin, S. Pasquetti, and Y. Zenkevich, *T[SU(N)] duality webs: mirror symmetry, spectral duality and gauge/CFT correspondences*, *JHEP* **02** (2019) 176, [arXiv:1712.08140].

[91] S.-S. Kim, Y. Sugimoto, and F. Yagi, *Surface defects on E-string from 5-brane webs*, *JHEP* **12** (2020) 183, [arXiv:2008.06428].

[92] T. Kimura and F. Nieri, *Intersecting Defects and Supergroup Gauge Theory*, arXiv:2105.02776.

[93] T. Ekholm, P. Kucharski, and P. Longhi, *Physics and geometry of knots-quivers correspondence*, arXiv:1811.03110.

[94] T. Ekholm, P. Kucharski, and P. Longhi, *Multi-cover skeins, quivers, and 3d $\mathcal{N} = 2$ dualities*, *JHEP* **02** (2020) 018, [arXiv:1910.06193].

[95] D. Gaiotto and H.-C. Kim, *Surface defects and instanton partition functions*, *JHEP* **10** (2016) 012, [arXiv:1412.2781].

[96] F. Benini, S. Benvenuti, and Y. Tachikawa, *Webs of five-branes and N=2 superconformal field theories*, *JHEP* **0909** (2009) 052, [arXiv:0906.0359].

[97] M. Taki, *Surface Operator, Bubbling Calabi-Yau and AGT Relation*, *JHEP* **1107** (2011) 047, [arXiv:1007.2524].

[98] A. Iqbal and A.-K. Kashani-Poor, *The Vertex on a strip*, *Adv.Theor.Math.Phys.* **10** (2006) 317–343, [hep-th/0410174].

[99] J. Bryan and D. Karp, *The closed topological vertex via the Cremona transform*, math/0311208.

[100] P. Sułkowski, *Crystal model for the closed topological vertex geometry*, *JHEP* **12** (2006) 030, [hep-th/0606055].

[101] A. Brini and R. Cavalieri, *Crepant resolutions and open strings II*, arXiv:1407.2571.

[102] O. Aharony, A. Hanany, K. A. Intriligator, N. Seiberg, and M. J. Strassler, *Aspects of N=2 supersymmetric gauge theories in three-dimensions*, *Nucl. Phys.* **B499** (1997) 67–99, [hep-th/9703110].

[103] Y. Terashima and M. Yamazaki, *SL(2,R) Chern-Simons, Liouville, and Gauge Theory on Duality Walls*, *JHEP* **08** (2011) 135, [arXiv:1103.5748].

[104] Y. Terashima and M. Yamazaki, *3d N=2 theories from cluster algebras*, *Prog.Theor.Exp.Phys.* **023** (2014) B01, [arXiv:1301.5902].

[105] C. Beem, T. Dimofte, and S. Pasquetti, *Holomorphic Blocks in Three Dimensions*, *JHEP* **12** (2014) 177, [arXiv:1211.1986].

[106] L. D. Faddeev, *Discrete heisenberg-weyl group and modular group*, *Letters in Mathematical Physics* **34** (Jul, 1995) 249–254.

[107] L. D. Faddeev, R. M. Kashaev, and A. Y. Volkov, *Strongly coupled quantum discrete liouville theory. 1: Algebraic approach and duality*, *Communications in Mathematical Physics* **219** (May, 2001) 199–219.

[108] D. Tong, *Dynamics of N=2 supersymmetric Chern-Simons theories*, *JHEP* **07** (2000) 019, [hep-th/0005186].

[109] O. Bergman, A. Hanany, A. Karch, and B. Kol, *Branes and supersymmetry breaking in three-dimensional gauge theories*, *JHEP* **10** (1999) 036, [hep-th/9908075].

[110] T. Kitao, K. Ohta, and N. Ohta, *Three-dimensional gauge dynamics from brane configurations with (p,q)-fivebrane*, *Nucl.Phys.* **B539** (1999) 79–106, [hep-th/9808111].

[111] C. Hwang, H.-C. Kim, and J. Park, *Factorization of the 3d superconformal index*, *JHEP* **08** (2014) 018, [arXiv:1211.6023].

[112] F. Benini and W. Peelaers, *Higgs branch localization in three dimensions*, *JHEP* **1405** (2014) 030, [arXiv:1312.6078].

[113] F. Benini, C. Closset, and S. Cremonesi, *Comments on 3d seiberg-like dualities*, *JHEP* **1110** (2011) 075, [arXiv:1108.5373].